Studies of novel perfluoroalkyl derivatives of azobenzene in solution and on surfaces

Studies of novel perfluoroalkyl derivatives of azobenzene in solution and on surfaces.

By

James R Fletcher

Supervisor: Dr. D.R.Worrall

Doctoral Thesis

Submitted in partial fulfilment of the requirements

for the award of

Doctor of Philosophy of Loughborough University

(April 2011)

Abstract

Azobenzene based photochromics have been studied widely since the development of the first azo dye, Mauvine, by Perkin in 1856. Azo based dyes have been widely used in industry for over a century. The desire to study them arose from their ease of synthesis and the wide availability of colours which can be tuned by manipulation of the chromophores on the azo molecule itself.

The ability of azobenzene to photoisomerise between *trans* and *cis* states is widely known. The change in dipole moment affords the ability to fine-tune surfaces via photoisomerisation of the azo molecule. The objective of this investigation was to alter the surface properties of a variety of substrates via the photoisomerisation reaction of several perfluoroalkyl derived azobenzene compounds. These compounds are novel and are based on the idea of the fluoroalkyl chain creating a superhydrophobic surface, similar to Teflon, which would change surface energy upon isomerisation of the azobenzene molecule to give a more hydrophilic surface. This would ultimately then be utilised to coat a fabric surface to provide a photosensitive coating.

The compounds used in this work (Admat 1 and 2 and Cfam derivatives) were synthesised in order for their photochemistry in solution and on surfaces to be investigated. The studies began with the photoisomerisation investigations in solution and the calculation of the rate constant and finally the activation energies of these compounds in a variety of common solvents. Interesting results were observed in polar protic solvents which were investigated further. The discovery that aggregation occurred in polar protic solvents due to solubility issues, which in turn led to a fast rate constant was a key finding of the solution work.

The surface studies began with the investigation of cellulose as a substrate due to the structural similarity it has with cotton. The azo compounds were derivatised using cyanuric chloride to afford a triazinyl group which was able to attach to the surface of the cellulose via the hydroxyl groups on the surface. The samples produced were found to photoisomerise and the rate constants and activation energies were then calculated for the thermal isomerisation reaction on the surface and found to be 2-4 kJ mol^{-1} with azo compounds adsorbed to the surface and 4-10 kJ mol^{-1} for azo compounds coupled to the surface of cellulose.

Following on from that work, silica was chosen as a substrate to investigate, as the ease of coupling to the surface would be useful as a comparison to cellulose. The triazinyl group was attached to the surface of silica and, along with adsorbed azo compounds, the rate constants of the thermal *cis/trans* isomerisation reaction were measured and the activation energies were calculated to be between 4-13 kJ mol^{-1} for adsorbed azo compounds on silica and between 5-16 kJ mol^{-1} for coupled compounds on silica surfaces. The values of the activation energies on silica were found to be larger than on cellulose surfaces.

The measurement of contact angles on a flat surface was then undertaken. The flat surface used here was chitosan, a derivative of chitin found in crab shells. The coupling of the azobenzene to the surface allowed for the photoisomerisation reaction to be measured and the subsequent changes in contact angles were obtained. The contact angles obtained were very promising; changes observed were between 40° and 60° and were a key outcome of this work.

The study of polymers containing azo derivatives was then undertaken. The polymers were prepared with different amounts of azobenzene on the polymer backbone. The photoisomerisation of the polymers was investigated in solution and the rate constants were obtained. The rate of thermal relaxation from *cis* to *trans* azobenzene was found to be around 20 times slower with azobenzene based polymers than for the azobenzene monomers in solution.

Keywords: Azobenzene, photochromic, surfaces, silica, chitosan, contact angles, polymers cellulose, photoisomerisation.

Acknowledgements

Firstly I would like to thank Dr David Worrall for the opportunity to work in the photochemistry group at Loughborough and for his excellent guidance over the past three years. I would also like to thank Dr Sian Williams-Worrall for her input and help with my work over the last three years. Secondly I would like to thank Defence Science and Technology Laboratory (DSTL) and Loughborough University for funding this research programme. Particular thanks are due to Dr Colin Willis, Dr Corinne Stone and Dr Cheryl Fish at DSTL for their advice, useful discussions and help in synthesising the compounds.

I would also like to thank the research group at Loughborough, particularly Dr. Nadya Muhammed, Dr Iain Kirkpatrick and Mrs Anisoara Vancea for their help and company in the lab over the years. A big thank you must also go to the technicians, Mr David Wilson, Mr Trevor Brown and Mr Stuart Pinkney for their technical support throughout my work. Thanks also to Dr Mark Edgar for the NMR studies conducted in this thesis and Dr George Weaver for useful synthesis discussions. Also to the electrochemistry section both past and present, Professor Stephen Fletcher, Professor Roger Mortimer, Nooshin, Tom, Vicky, Russell and Zee for letting me borrow equipment. A big thank you also to Chris, Martin, Jack, Matt, Shimi and Natalie for their friendship over the years. Not to forget all of the Loughborough crowd, Ruth McGhee, George, Steve and everyone at Kingfisher Hall at Loughborough University for providing plenty of entertainment for me whilst living here in Loughborough.

Of course, I probably would not have gone on to study science had it not been for the encouragement of several excellent teachers at my former school, particularly Miss Fitzmaurice, Mrs Ainsworth and Mr Matthews who also deserve thanks.

Last, but by no means least, thank you to my family, particularly my parents for financial help and support throughout my higher education endeavours. Thank you for all the support you have given me over the years and the knowledge that whatever I attempt to do, you will always be behind me all the way. To all my extended family, grandparents, aunties, uncles and cousins, thank you for your support.

James Fletcher September 2010

Index

List of abbreviations

UV = Ultra Violet

DCM = Dichloromethane

THF = Tetrahydrofuran

DSTL = Defence Science and Technology Laboratory

APTS = Aminopropyltriethoxysilane

°C = Degrees Celsius

MPa = Mega Pascals

PVA = Polyvinylalchol

DMF = Dimethylformamide

MeOH = methanol

CH_3CN = acetonitrile

DMA = Dimethylaniline

nm = nanometres

m = meters

mmol = millimole

M = moles

s = seconds

t = time

λ = wavelength

K = Kelvin

TEOS = tetraethylorthosilicate

CA = contact angles

PolyHEMA = polyhydroxylethylmethacrylate

µm = micrometers

HPLC = high performance liquid chromatography.

Research Objectives

The main aim of this research is to develop a novel photoswitchable surface which upon irradiation the isomerisation of the azobenzene moiety changes a property of the surface, namely the wettability. The compounds studied here are azobenzene systems with fluoroalkyl chains on the surface. The main areas of study over three years of this research were:

Solution photochemistry: ground state absorbance, fluorescence studies and activation energies of the thermal relaxation rate in solution.

Surface photochemistry: The coupling and adsorbing of the compounds to surfaces, such as cellulose and chitosan, measuring activation energies of thermal relaxation on surfaces, for comparison to solution photochemistry and the measurements of the contact angles for wettability properties.

The completion of the above areas of study should provide a photoswitchable surface with controllable wettability. The use of cellulose as a model for fabric is an area that will be covered within this project. The prospect of clothing which is photoswitchable clothing for resistance to substances is the main drive behind this project

Chapter 1.0: Introduction to photochemistry

1.1 The principles of photochemistry

Photochemistry is, by definition, the study of chemical processes that occur upon absorption of light. Light exists as a form of electromagnetic radiation, which can be described as an oscillating electric field and an oscillating magnetic field, which operate in planes perpendicular to one another and to the direction of propagation. Photochemists are usually concerned with the visible and ultra violet (UV) region of the electromagnetic spectrum.

The velocity and wavelength of light are related to each other by the equation

$v\lambda = c$ (Eqn. 1.1) [1]

Where λ is defined as the wavelength (the distance travelled during one complete cycle), ν is the frequency (the number of complete cycles in one second) and c as the speed of light in a vacuum (2.99×10^8 m s^{-1}).

A molecule may be promoted from its ground state to form an electronically excited state via the absorption of light of an appropriate frequency, usually from the ultra-violet or the visible region. This may result in the molecule possessing different nuclear and electronic properties to the ground state, and thus the reaction products may be very different from those obtained via thermal reactions, which is the basis of the Woodward Hoffman rules. [1]

1.2 Quantisation of Energy

The idea of discrete energy levels, which was first proposed by Boltzmann, shows the overall energy of a molecule could only be changed via a jump in energy between these levels.

Stark and Einstein formulated a law, which states that a molecule undergoing a photochemical change does so through the absorption of a single quantum of light. The molecule, which has absorbed a quantum of radiation, has then become excited in the absorption process, increasing the amount of energy in the molecule. The exact nature of the

excitation is governed by the energy of the adsorbed photon. Light of a given energy can be absorbed by the molecule to produce an electronically excited state; the energy of this quantum of light will be equal to the excitation energy of each of the excited molecules, as shown by the following equation. (Eqn 1.2) [1]

$$E = h\nu \qquad \text{(Eqn 1.2)}$$

Where h = Planck Constant (6.63×10^{-34} J s)

ν = Frequency of radiation

E = Energy

The energy per mole of photons can be obtained via Equation 1.3. This is known as the Einstein Equivalence law.

$$E/\text{mol} = Nhc/\lambda = N_A h\nu \qquad \text{(Eqn 1.3)}$$

Where N_A = Avogadro Number (6.023×10^{23} mol^{-1}), c = Velocity of light in a vacuum, λ = Wavelength

1.3 Absorption of radiation

When a photon is absorbed by a molecule, photophysical processes may occur, changing its electronic structure. The molecule must absorb a quantum of energy which is equal to the energy transition within that molecule. This results in a change in the occupation patterns within the orbitals.

If the energy of a photon does not match the energy difference between the lowest vibrational level in the ground state and the lowest vibrational level in the excited state, the promotion of the photon between the vibrational states cannot occur, and therefore no emission will result.[1]

1.3.1 Beer-Lambert Law

A crucial relationship between the fraction of light absorbed by a light absorbing solution and the concentration of the absorbing species at a given wavelength is shown via the Beer-Lambert Law;

$$A = log\left(\frac{Io}{I}\right) = \varepsilon cl \quad \text{(Eqn 1.4)}$$

Where A = Absorbance

I_o = Incident light intensity

I = Transmitted light intensity

c = concentration

l = Path length through the solution

ε = Molar absorption coefficient

1.4 Electronic structures of molecules

The electrons found in a molecule are arranged in molecular orbitals. The excitation from one molecular orbital to another and the absorption and emission of radiation by a chemical species falls within the realm of quantum mechanics, the complex mathematical theory which replaces the classical ideas of position and trajectory, with the concepts of wavefunction and amplitude. The theory gives rise to quantum numbers that define the electronic state of a species, with the tools for obtaining the quantum numbers based on various forms of the Schrödinger Equation.

The molecular orbitals are referred to as bonding, non-bonding and antibonding orbitals. Antibonding orbitals are of higher energy than both bonding and non-bonding orbitals. According to the Aufbau principle, the orbitals are filled from the lowest energy level to the highest. Molecular orbitals are often notated as σ and π, which are bonding orbitals, and π* and σ*, which are antibonding orbitals, and n, which is called a non-bonding orbital. (Figure 1)

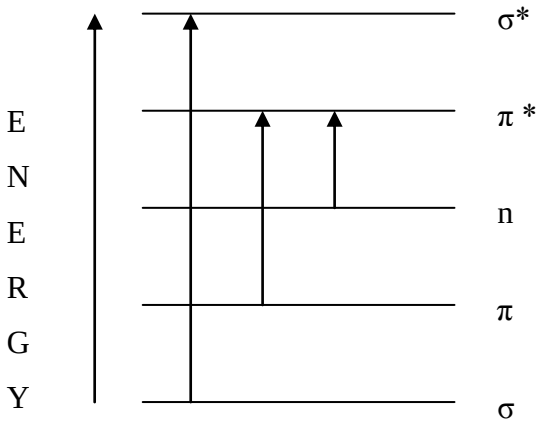

Figure 1: Energy levels within a molecule

1.5 Franck Condon Principle

The Franck Condon principle states that in an electronic transition, the change from one vibrational energy level in a molecule to another is more likely to happen if there is significant overlap between the two vibrational wave functions. The resulting state is called a Franck Condon state and involves vertical transitions (see Figure 2), in the same way that a species has a spectrum resulting from electronic transitions, (Figure 1), there are spectra resulting from transitions between vibrational and rotational energy levels. These levels are described by their own quantum numbers v =1 v =2 etc (see Figure 2)

Given a general diatomic molecule, the most likely transition will occur from the lowest vibrational energy level of the ground state to a vibrational level of a higher electronic state. The largest vibrational overlap, in this particular diagram, occurs from v" = 0 to v' = 2 which affords the highest absorption intensity. The Franck Condon principle also states that the intensity of the vibrational transition is proportional to the square of the overlap integral of the two states involved in the transition.

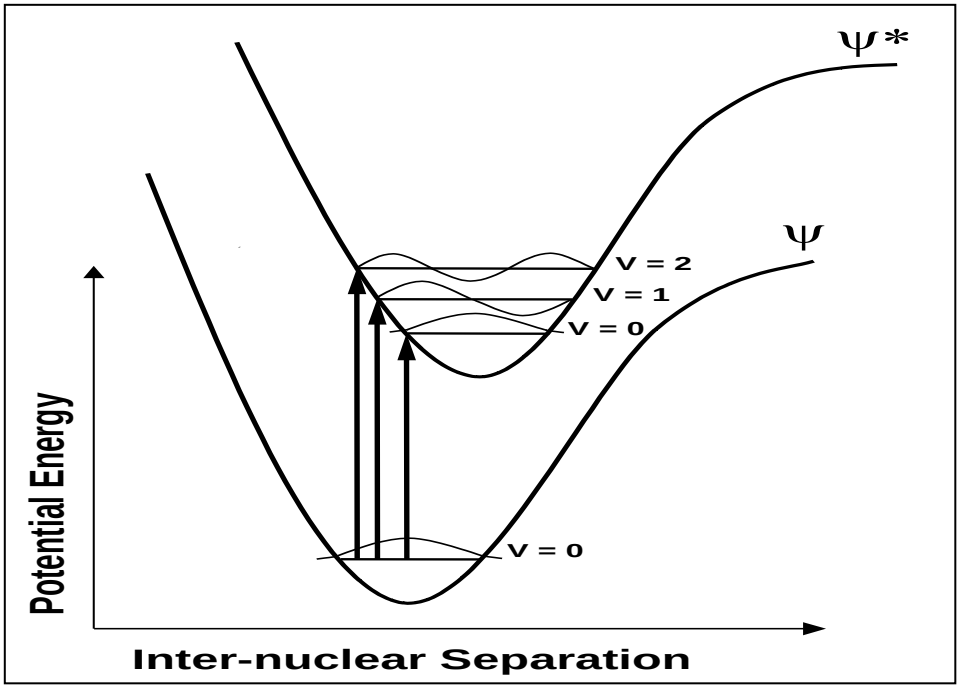

Figure 2: Franck Condon Principle

1.6 Spin Multiplicity

Electrons within a molecule possess a spin quantum number of 1/2 , which possess two different orientations, either 'up' or 'down' (see Figure 3) as a result of position of the electron on the specified axis, which results in spin magnetic quantum numbers (m_s) of either +1/2 or –1/2. The total spin angular momentum for a molecule is S, the vector sum of all the contributions for each electron. The spin multiplicity gives the number of states expected in the presence of an applied magnetic field and is given by the following equation.

Spin multiplicity $m_s = 2S + 1$ (Eqn 1.5)

Molecules with parallel spin electrons have S = n and a spin multiplicity of n, where n is an integer. If the spins are anti-parallel then S = 0 and the spin multiplicity is 1 so this results in a singlet state (See Figure 3). The two states are common in photochemistry and possess different chemical and physical properties. S_0 is, the symbol use to represent the ground singlet state, and S_1, S_2 and S_3 are the designation assigned to the higher states, the numbers increasing in energy. Similarly, T_1, T_2 etc are triplet states.

The Pauli Exclusion Principle states: If two electrons occupy the same orbital they must have opposite spins $m_s = +1/2$ or $-1/2$.

Further to this, Hunds rule states,

"Every orbital within a subshell is occupied before any one orbital is doubly occupied and all electrons in singly occupied orbitals have the same spin."[(1)]

The triplet state has a lower energy than the singlet state, due to the repulsive nature of the spin-spin interaction between electrons of the same spin. Promotion of an electron from the ground state can give rise to either an excited singlet state or a triplet state, which reverses the spin orientation.

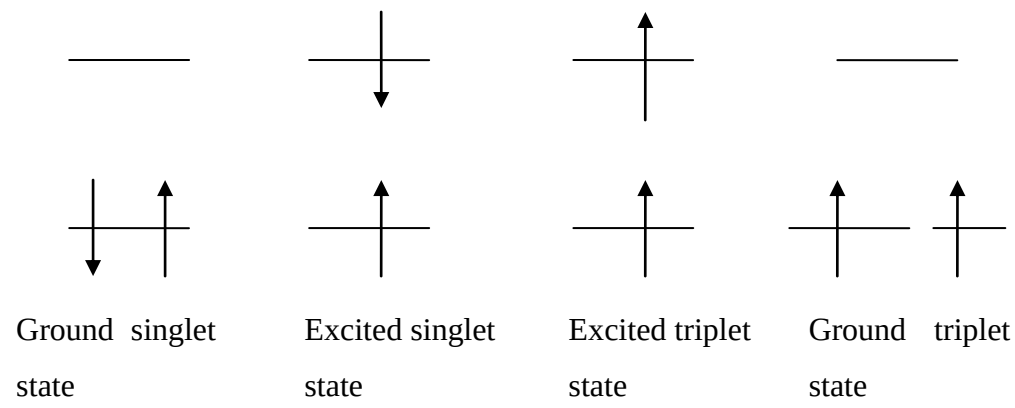

Figure 3: Singlet state and excited state electron arrangements

1.7 Selection Rules

The selection rules are used to establish if a transition between two states is likely to occur. The transitions are named as allowed (high probability) or forbidden (low probability). The spin selection rule states that the radiative transitions should occur with no change in total electron spin. i.e. $\Delta S = 0$. Orbital symmetry selection rules state that transitions involving large change in the orbital angular momentum are forbidden, the electron should occupy the same region of space after the absorption of light has occurred. For a transition to be allowed

there must be good spatial overlap between the orbitals of the state involved. Thus a π to π^* transition is allowed, whereas an n to π^* is of low probability.

There must be no overall change in spin angular momentum for an allowed transition. Therefore S_0 to S_1 transitions afford the most intense absorptions. S_1 to T_1 transitions do occur via intersystem crossing, providing the spin orbit coupling is large enough, smaller spin orbit coupling means a less likely chance of intersystem crossing occurring, but are overall spin forbidden. Total angular momentum remains unchanged. The first orbital and the final orbital must possess good spatial overlap.

In the case of azobenzenes, the low n- π^* absorption coefficients are a result of the fact that the n- π^* states in the molecule are closer together reducing the energy gap and overlap, and therefore lowering the absorption coefficient of that transition, hence the absorption coefficients are between 20-200 $dm^3\ mol^{-1}\ cm^{-1}$, whereas in π-π^* transitions, the absorption coefficients vary from 0 to 100000 $dm^3\ mol^{-1}\ cm^{-1}$.[3]

1.8 The relaxation of excited states

Once a molecule has become excited, the excited state relaxes. This can occur via many processes, such as spontaneous decay, or interaction with other species. Spontaneous decay of the excited state, known as an intramolecular process, occurs without the presence of another species in the system. If another species is present and interaction occurs, the excited state can lose energy via interaction with this species, called an intermolecular process. Furthermore, the processes can be categorised as radiative or non-radiative in nature. Radiative decay results in the emission of a photon to lose the excess energy. Non-radiative processes convert electronic energy to vibrational energy.

1.9 Intramolecular processes

The following diagram represents the electronic states of a molecule (Figure. 4)

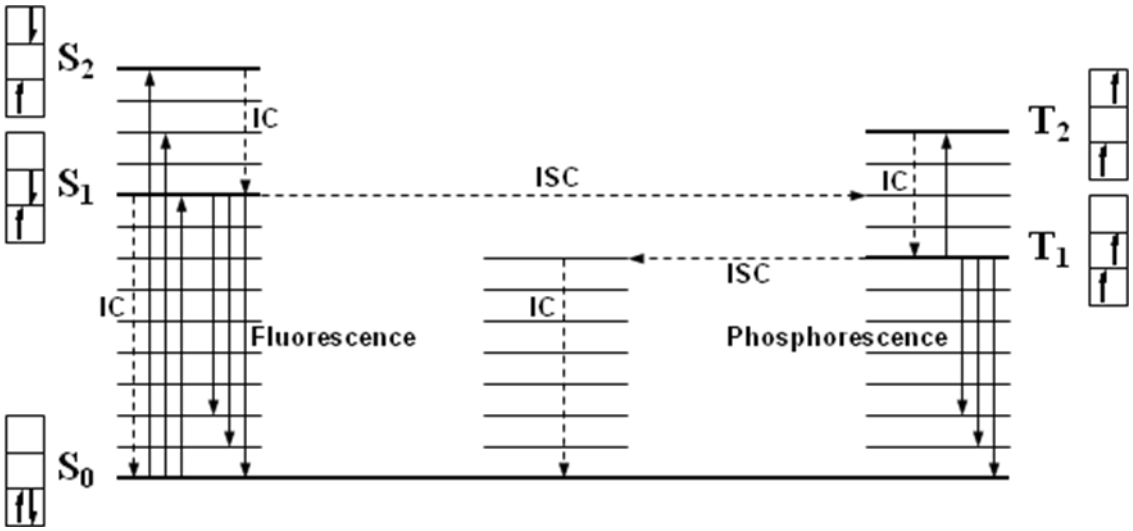

An explanation into the occurrence of the processes shown in the diagram above is given below.

1.10 Fluorescence -

$^1A^* \rightarrow {}^1A + h\nu$

Fluorescence occurs as the excited singlet state loses its energy via the emission of a photon of light. Fluorescence is a spin allowed process which occurs between two states with the same spin multiplicity. The energy gap between the excited and ground states is the same as the energy of the emitted photon.

Further, Kasha's rule states that photon emission occurs only from the lowest excited state of a given multiplicity.(2)

The smaller the energy gap present, the larger the rate of non-radiative transitions. As the energy gap increases, the radiationless transition from state 1 will be to an increasingly higher vibrational level in state 2, with reducing vibrational overlap and a reduced rate constant.

As upper excited states are densely packed, i.e. there are smaller energy gaps between them, then rapid internal conversions will occur, so that the rate constant for internal conversions is much greater than the rate constant for fluorescence, therefore, due to the proximity of the

excited states to one another, the ability for fluorescence is reduced, however, delayed fluorescence can be observed as the triplet state crosses back to the singlet state via intersystem crossing, and fluorescence from S_1 to S_0 is observed.

1.11 Phosphorescence

Phosphorescence occurs when, due to intersystem crossing from a singlet state to a triplet state (see Figure 4), the triplet state then decays to the ground state, of a different multiplicity, as the ground state is a singlet ground state, releasing radiation. Hence phosphorescence is defined as a radiative transition.

This process occurs between two states with different spin multiplicities. The longer lifespan of the triplet state occurs as the process of phosphorescence is slower, due to the spin forbidden nature of the transition. Temperature can also affect the rate of phosphorescence via the thermal deactivation process, i.e. decay of the triplet state via intersystem crossing conversion, competing with decay of the triplet state via phosphorescence, and also diffusional quenching via solvent molecules, which have more energy at higher temperatures.

1.12 Triplet triplet annihilation and thermally activated delayed fluorescence

$$^3A^* + {}^3A^* \rightarrow {}^1A^* + A$$

The formation of the triplet state can lead to the observance of phosphorescence or other processes can occur. One of these processes is called triplet-triplet annihilation. For triplet-triplet annihilation to occur, two molecules in a triplet state must interact upon collision to produce an excited singlet state. This molecule can then decay via fluorescence to the ground singlet state.

Triplet-triplet annihilation is a mechanism for delayed fluorescence. For example, in anthracene, the fluorescence decay consists of two components, one with normal fluorescent lifetimes and one with a slower lifetime, although the spectral distribution of both components is identical. This is often called P type fluorescence, as it is also seen in solutions of pyrene.

Another mechanism for delayed fluorescence is the E-type delayed fluorescence, named as such because it is observed in the dye Eosin. E-type delayed fluorescence shows spectral features which are characteristic of the normal, short lived fluorescence, however the emission decays at the same rate as phosphorescence, which is much slower, hence this E type fluorescence can be distinguished from other types.

This kind of delayed fluorescence arises from the promotion of T_1 to S_1 via intersystem crossing. The rate of this activation is slow compared to the rate of decay of T_1 to S_1 so the decay of delayed fluorescence is related to the depopulation of T_1 as T_1 populates S_1, and if T_1 does not depopulate, then S_1 cannot therefore be populated, therefore no delayed fluorescence can occur. The activation energy for the emission, (which is calculated from the temperature dependence of the intensity) should be identical to ΔE (S_1-T_1). The P-type fluorescence does not display the same dependence on temperature as thermally activated E-type delayed fluorescence, and it may be distinguished from it by this means. Another diagnostic feature is the relationship between emitted and absorbed intensities, which is linear in E-type delayed fluorescence, but squared in the P-type triplet triplet annihilation process. E-type fluorescence has the same lifetime as that of the triplet–singlet phosphorescence in the same solution, delayed fluorescence excited by the triplet annihilation mechanism should have a lifetime equal to the square root of that of the phosphorescence, due to the second order dependence on triplet concentration.

1.13 Non radiative energy transfer: Internal conversion (IC) and vibrational relaxation

Electronic energy is also converted into other forms of energy without the emission of light, these processes are known as *non-radiative* processes.

The process of internal conversion involves the relaxation of a molecule into a lower electronic state without the loss of energy. This process occurs via the conversion of electronic energy in one state to vibrational energy in another lower energy state. Both states have the same spin multiplicity and the process is spin allowed and non radiative. The vibrational energy is soon lost as heat in collisions with other molecules (vibrational relaxation).

1.14 Intersystem crossing (ISC)

$^1A^* \rightarrow {}^3A^*$

Intersystem crossing only occurs if the excited states have differing spin multiplicities, hence, it is a spin forbidden, non-radiative process. As it is a spin forbidden process, intersystem crossing generally takes longer to occur than internal conversion and the efficiency of the process relies partially on the size of the energy gap between the states and on spin orbit coupling.

1.15 Intermolecular processes.

An excited molecule can also lose its energy by transferring it to neighbouring molecules. This transfer process occurs via a different mechanism, which is either radiative or non-radiative. The energy levels in both molecules must be close in energy for this transfer to occur. The difference in energy, provided it is small can be accommodated by rotational and translational motion within the solvent. Energy can be transferred from a donor molecule (X) to an acceptor molecule (Y) if the excited state X* has a higher energy than the excited state of Y*

$X^* + Y \rightarrow X + Y^*$

The transfer of energy from X* to Y will lead to quenching of X* by Y.

1.16 Radiative energy transfer

Radiative transfer involves the emission of a photon by the excited molecule. The photon does not exit the system; it is absorbed by another molecule within the system to form a new excited state. In order for this process to occur, the emission spectrum of the donor molecule and the absorption spectrum of the acceptor molecule should overlap.

Non-radiative energy transfer does not involve the emission of a photon from the excited molecule. This can occur via the two methods outlined below, collisional/exchange energy transfer and the induced dipole mechanism.

1.17 Collisional/ Exchange energy transfer

For a collisional transfer to occur the molecules need to be close enough for their electron clouds to overlap, to allow the exchange of electrons between the donor and acceptor molecules. This type of transfer is limited by the rate of diffusion reaction; the more frequent the collisions, the faster the energy transfer. Another consideration is the energy gap between the donor and acceptor molecule. The energy gap between the ground state and excited state of the donor molecule should be equal or larger than the energy gap between the states of the acceptor molecule. If these conditions are satisfied, the electrons will move. The low extinction coefficient of the S_0 to T_1 transitions on which the coulombic mechanism is dependent means that triplet-triplet energy transfer usually occurs via the collisional mechanism (See Fig. 5)

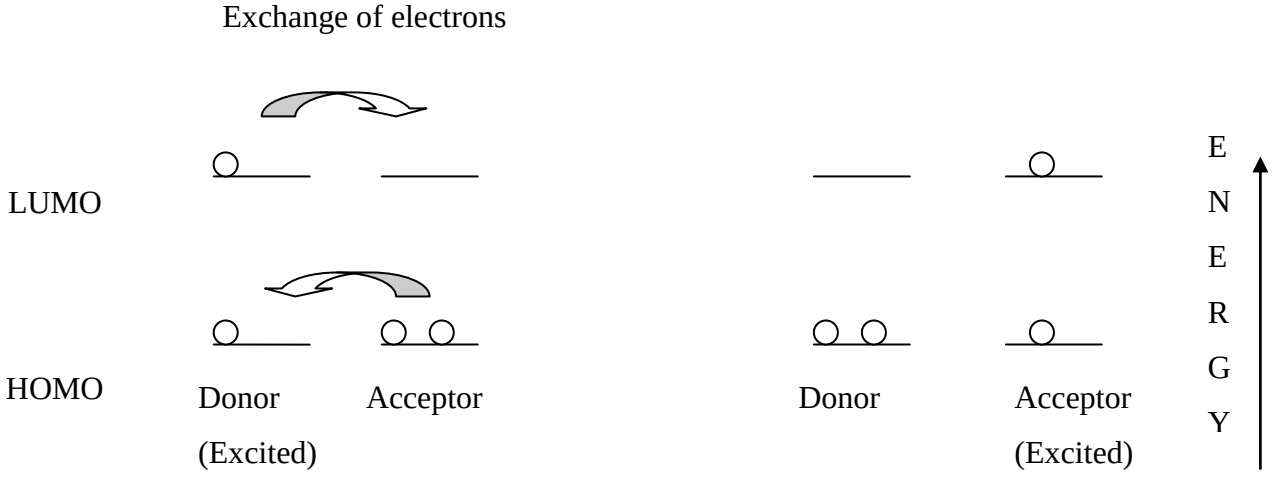

Figure 5: Electron exchange energy transfer schematic representation.

1.18 Induced dipole mechanism

The Förster exchange mechanism depends on the electronic interactions between the charge clouds on donor and acceptor molecules, versus the coulombic (exchange) mechanism depends on electrostatic interactions. The Förster exchange mechanism does not require physical contact of the interacting molecules. Förster exchange occurs via the induction of a dipole oscillation in the acceptor (A) by the donor (D*). No electron exchange occurs (unlike the exchange mechanism) from the donor to the acceptor molecule. For the Forster exchange mechanism to occur, the emission spectrum of the donor and the absorption spectrum of the acceptor molecules must overlap.

Electron oscillation within the donor molecule induces oscillation in the electron with the highest energy in the acceptor, resulting in relaxation of the excited electron in the donor and excitation of the electron in the acceptor (see Figure 6).

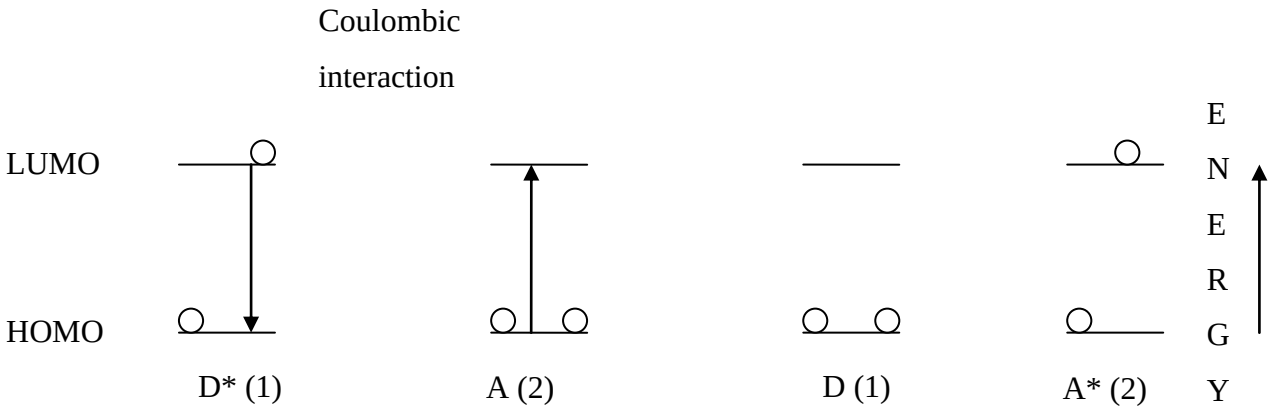

Figure 6 : Förster (Coulombic) energy transfer schematic representation

2.0 Literature Survey

2.1 Overview of azo-compounds

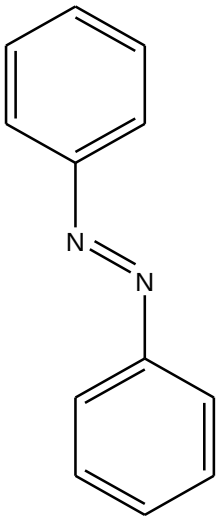

Figure 7: Azobenzene (trans form)

Azobenzene consists of two phenyl rings separated by an azo (–N=N–) bond. It serves as the parent molecule for a large range of aromatic 'azo' compounds. These versatile molecules have been the focus of attention in research areas both fundamental and applied. Azobenzene itself possesses a strong electronic absorption maximum, which can be shifted by ring substitution to absorb from the ultraviolet to visible regions, allowing for the fine-tuning of the colour via chemical modification. This fact, combined with the fact that these azo groups are relatively robust and chemically stable, has prompted extensive study of azobenzene-based structures as possible dyes.[3] There has also been much focus of research into polymers which have been functionalised or doped with azobenzene moieties, and hence they are commonly found in liquid crystal media.[4]

The most interesting property of azobenzene chromophores, and the subject of this work, is the photochemically induced and reversible isomerisation about the azo bond between the *trans* and the *cis* geometric isomers. This photochemical conversion allows systems incorporating azobenzenes to be used as photoswitches, effecting rapid and reversible control over a variety of chemical, mechanical, electronic, and optical properties. The azo group itself is isosteric with the ethylene group, thus, two configurations can exist, which are the *trans* and the *cis* form. The *cis* isomer of azobenzene was isolated and characterised by

Hartley in 1937[5] and the first recorded preparation of the *cis* compound was reported in 1964 by Hutton *et. al.*[6]

Another interesting aspect of azobenzene molecules is the variety of molecular systems into which it is possible to incorporate them. They have been successfully incorporated into LC media,[4,7] monolayers, superlattices,[8] sol-gel silica glasses,[9] and biological material.[10]

The photoswitchable properties of azobenzenes can also be used to control the properties of small molecules which incorporate an azo group. Molecules of this type include azobenzenes attached to crown-ethers,[11] cyclodextrins,[12,13] organometallic ferrocene polymers,[14] dendrimers,[15,16] 3-D polycyclics such as cubane[17] or adamantine,[18] proteins such as bacteriorhodopsin,[19] and azo-functionalized C_{60} buckminsterfullerenes.[20]

Azobenzene type molecules were reviewed by H. Rau in 1990[21] who concluded that there are three main points which are of vital importance to the classification and use of azobenzene molecules. The first point of consideration is the classification by molecular structure, of which three main classes of molecules have been defined, azobenzene molecules, aminoazobenzene molecules, and pseudo-stilbene type molecules on the basis of their order of (n-π*) and (π-π*) states. The second point of interest is the mechanistic aspects of isomerisation and the third is the use of these materials for the control of material properties.[21]

2.2 Azobenzene type molecules

The azobenzene ranges of compounds are usually red to yellow in colour. The main spectral feature of these compounds is a weak long wavelength absorption band well separated from the shorter wavelength systems.[21] Azobenzene molecules are characterised by the low lying (n-π*) states and a large energy gap between this and the next higher (π-π*) state. The energy activation energy barrier between the *cis* and *trans* conformation is around 50 kJ mol^{-1}.[21]

For *cis* azobenzene in benzene solution ε at 449 nm = 404 mol^{-1} dm^3 cm^{-1}, for *trans*, ε at 440 nm = 1250 mol^{-1} dm^3 cm^{-1}.[22] The molar absorption coefficient for the π-π* transition is around 22000 mol^{-1} dm^3 cm^{-1}. The difference in intensity for the n-π* band for *cis* and *trans*

isomers is due to spin selection rules. In the planar C_{2h} and C_{2v} symmetry, the n-π* transition is forbidden for the *cis* but allowed for the *trans*, hence the large difference in intensity of the n-π* and π-π* bands.[23]

Excitation into the π-π* absorption (excitation to S_2) of the *trans* form results in population of the *cis* isomer with a quantum yield of about 0.4, whilst excitation into the n-π* transition (excitation to S_1) of the *cis* form at about 450 nm populates the *trans* isomer with a quantum yield of about 0.25.[24]

2.3 Aminoazobenzene type molecules

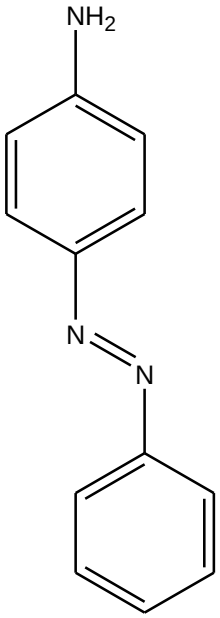

Figure 8 Aminoazobenzene (trans form)

The effect of ortho or para amino group substitution on an azobenzene group is dramatic. The result is a shift in the spectrum, the π-π* band being shifted by anything up to 50 nm. The compounds of the aminoazobenzene group are characterised by the close proximity of the n-π* states and the π-π* states.

The absorption bands are very sensitive to solvent polarity, as the azo group in an aminoazobenzene will interact with hydrogen bonding solvents more readily than the amino group,[23] which can result in the re-ordering of relative energies of the states, meaning that

this compound may display pseudo-stilbene like behaviour in alcohols, protic solvents and acid solutions. Fluorescence of aminoazobenzene compounds was reported by Bisle *et. al*.[25] and Rau[26] at low temperature in glassy solvents. Aminoazobenzenes do not phosphoresce; however, the lowest triplet state can be located via energy transfer experiments. Monti *et. al.* [27] concluded that in triplet state molecules, the energies of the lowest triplet states of the azo derivatives investigated do not depend very much on the substituent and are in the range 30 – 35 kcal mol^{-1} (125 – 145 kJ mol^{-1}).

2.4 Pseudostilbene type molecules

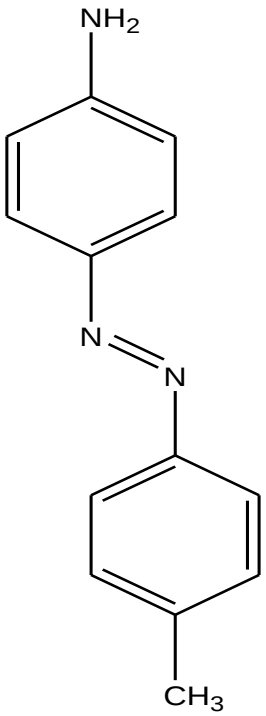

Figure 9: Pseudostilbene (trans form)

Pseudostilbenes are characterised by a low-lying π-π* state. Rearrangement of the electronic states of azobenzene can result in the formation of a pseudostilbene. This is accomplished via raising the energy of the n-π* state, via protonation of the azobenzene, or by lowering the π-π* state of the azobenzene via substitution with electron donating or accepting groups.[28,29]

The substitution of azobenzene with electron donating and withdrawing groups shifts the π-π* band to longer wavelengths than aminoazobenzenes. This is due to charge transfer in the

transition. Solvents can influence band position in the spectrum of donor/acceptor substituted compounds.

Fluorescence of pseudostilbene compounds has been reported, though fluorescence does not occur at room temperature. Fluorescence of protonated azo derivatives has been found to occur at 77K in a rigid sulphuric acid, however, even at low temperatures in rigid sulphuric acid the fluorescence is weak.[30]

2.5 Isomerisation Mechanism

The *cis-trans* thermal isomerisation of azobenzene was investigated Magee and Eyring.[31] They proposed a rotation mechanism, with a planar transition state where the double bond in the azo bond is broken.

The inversion mechanism was proposed by Curtin and McCarthy[32] in 1966 which is analogous to the inversion state of imines. The calculations conducted by Curtin and McCarthy and by Magee show that via inversion and rotation mechanisms, the ground state and the excited state are not far apart which favours fast radiationless deactivation via internal conversion from the excited state to the ground state without emission occurring. Ross and Blanc conducted experiments which assumed that intersystem crossing and its deactivation to the ground state should be the reason that fluorescence is not observed for azobenzene at room temperature.[33]

Rau developed the concept of different isomerisation mechanisms in the excited state.[34,35] The equality of the observed quantum yields for *trans* to *cis* conversion for the n- π^* and the π - π^* excited molecules of these compounds indicate that all of the molecules initially reach the lowest electronic state and isomerise via the inversion mechanism. The fact that the *trans* to *cis* yield of these molecules and of azobenzene are the same indicate that the inversion mechanism is active in the n-π^* state.

The exact mechanism of isomerisation of azobenzenes remains unclear, however, earlier suggestions of a rotating N=N bond were a contradiction to later work suggesting an inversion mechanism via a transition state was involved in the isomerisation process. The

range of results displayed suggests that there is not one single mechanism, but competition between the two, depending on the spectral class of the molecule, chromophore and the environment. Work in the area of thin films suggests the dominant pathway for rotation to be an in-plane inversion of the phenyl ring most distant to the polymer backbone, which is in agreement with *ab initio* and density functional theoretical studies.[36]

The photo-isomerisation of azobenzene is extremely rapid, occurring on picosecond timescales.[37] A summary of the isomerisation pathways is presented below.

1) Rotation about the N-N bond

2) Inversion, via a transition state. It has been suggested that the *trans*-to-*cis* conversion occurs via rotation into the S_2 state, whereas inversion mechanism could possibly give rise to the *cis*-to-*trans* conversion.

3*)* Concerted inversion, as π-π^* ($S_2 \leftarrow S_0$) excitation occurs, there is the possibility that sufficient energy is available to create an additional pathway (concerted-inversion) as proposed by Diau.[38]

4) A further study also proposed a "Hula Twist" mechanism in which an out of plane movement of the N atoms results in the same orientation of the phenyl rings as in a planar inversion. [38] It has also been suggested that the S_2 state undergoes internal conversion to the S_1 state, and then the *trans*-to-*cis* isomerisation occurs.[37]

To contrast this, speculation that a tunnelling mechanism from the excited to the ground state occurs has been proposed as an intersection was found to occur between the ground and first excited states along the rotation pathway for each of azo molecules that were studied.[38]

2.6 Introduction to photochromics

The photoisomerisation reaction of azobenzene described in the last section is the main focus of this work on photochromic azobenzene molecules. Light has been used as a stimulus to

control a wide variety of chemical reactions, via control of the wavelength, intensity, area of illumination and direction of the light source.[40-52]

The illumination of a photoresponsive material with light can reversibly change its geometric or electronic structure in solution, on surfaces and in gels and colloids. This change can then induce changes to the materials physical properties, such as polarity, fluorescence and refractive index. In the past decade, a series of photoresponsive chemical and physical properties have been explored, including photoswitching, electrical conductivity, dipoles, and biocatalysis.

In addition to photoresponsive magnetic and mechanical properties, biological photoresponsive materials have been investigated. Azobenzene was chemically attached to papain, which exhibited reversible biocatalytic activity under stimulation with light.[53]

Photoisomerisation of films and surfaces therefore can prove a desirable property for smart devices, coatings, and optical devices. Recent work in the area of surface wettability has shown that the ability to control the wettability of a surface is an exciting topic for surface scientists.[54] Superhydrophobic surfaces are present in nature which contain contact angles of greater than 150°, such as that of a lotus leaf.[55]

This is commonly referred to in the literature as the Lotus Effect, from a waxy coating present on the leaf surface, which is the inspiration for the production of novel nature-inspired superhydrophobic surfaces.[56]

Numerous methods have been used to prepare superhydrophobic surfaces by controlling the surface chemistry and roughness. These include cast-coating,[57] one step immersion (Langmuir Blogett)[58] and electrohydrodynamic techniques.[59]

Attention is being paid to the development of smart surfaces that respond to an external stimulus, e.g. light,[60,61] temperature,[62] electricity,[63] pH,[64] and solvent.[65] Organic complexes based on photoactive groups are widely known. Azobenzenes, spiropyrans and cinnamates change configuration under irradiation. Under photoirradiation, the chemical configuration of these groups change between two states, with the molecular polarity and

surface free energy changing accordingly, which in turn leads to a change in surface wettability. This change of chemical composition is the key to responsive surface switching with controlled wettability.

Organic materials possess many useful advantages in terms of chemical modification and diversity of photochemical reactions. Organic photoresponsive compounds possess a reversible photoinduced transformation between two states. The photoinduced transformation causes a variety of physical changes to occur, such as changes in surface energy, absorption spectra, refractive index, dielectric constant and redox potential and structural geometry.

Immobilisation of organic molecules onto substrates determines whether a uniform responsive surface can be stabilised and many techniques have been utilised to modify solid surfaces, such as ion beam techniques,[66] self-assembly processes,[67,68] and the chemical attachment of long-chain molecules to a surface.[69]

Most photochromic based photoresponsive materials are based around three core photoisomerisation reactions. The *cis-trans* isomerisation of azobenzene, the photochemical cleavage of the C-O bond in a spiropyran, to form the polar open form from the non-polar closed form, and the opening of the diarylethene ring from its closed form to the open form. These reactions are among the most common photochemical reactions studied and the main focus of current investigations into surface functionalisation using photochromic materials.

2.7 Azobenzene based photochromics

Recent studies outlined below on organic photoresponsive surfaces with controllable wettability can be classified according to the functional group present in the molecule, which is this case, the photoresponsive functional group used is azobenzene (Figure 10).

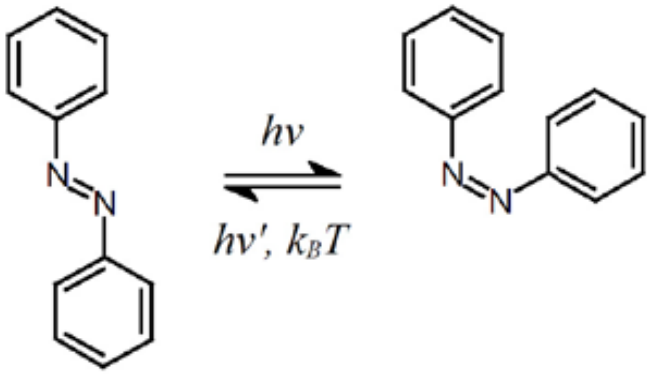

Figure 10: Trans-cis isomerisation of azobenzene

By using a chemisorption self-assembly technique, an azobenzene monolayer surface on a flat substrate was prepared, on which a small contact angle change (less than 10°) was observed via UV irradiation.[70] An azobenzene monolayer was grafted onto a smooth silicon surface covalently and a subsequent contact angle change of 5° was observed after UV irradiation.[71] Subsequent work by Feng *et. al.* has led to the fabrication of an azobenzene polymer film by the Langmuir Blodgett technique, giving a contact angle change of 11° after UV irradiation.[72]

The *trans* isomer possesses a smaller dipole moment than the *cis* isomer, as in the *trans* isomer, the resultant dipole moments cancel each other out, resulting in a dipole moment of zero, therefore a lower surface energy, whereas the *cis* isomer possesses a larger dipole moment and higher surface energy. Thus the isomerisation of azobenzene from *trans* to *cis* results in the change in wettability from a larger contact angle to a smaller contact angle.[73] (The aspect of contact angles is discussed in much more detail in section 3).

Recent work by Jiang *et. al.*[74] produced a photoswitchable azobenzene monolayer through electrostatic assembly on a flat silicon substrate. The contact angle change during irradiation was 1.8° during the alternation of visible (494 nm) and UV (365nm) irradiation. An interesting observation encountered is that transfer of the monolayer of azobenzenes on to a rough substrate results in a variation in the contact angle due to the change in the surface of the substrate. This results in a very small contact angle change on the smooth surface (1.8°) which is altered to a large extent to 66°, or in other words is essentially from hydrophobicity

to hydrophilicity. This study demonstrates that surface roughness can be an effective tool to control the contact angle and therefore wettability of a photoresponsive surface.

2.8 Spiropyran based photochromics

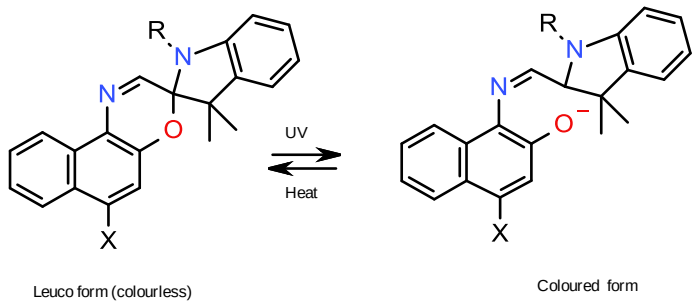

Figure 11: Spiropyran photoisomerisation.

Study of spiropyran molecules, which rely on the reversible photochemical cleavage of a C-O bond within the ring which leads to a reversible transition between the closed non-polar and the open polar form (merocyanine) (Figure 11)[75] Spiropyran based photoresponsive surfaces have attracted much attention in the exploration of stimuli responsive surface wettability.

Early work by Rosario *et. al.* employed a spiropyran monolayer to coat a silicon nanowire surface on which the light induced contact angle change, from UV irradiation (366 nm) to visible irradiation (450 nm) increased to 23° from 12° on a flat surface. Under visible irradiation, a superhydrophobic surface is observed on the nanowire substrate, reducing the contact angle hysteresis. This is an example of the lotus effect amplifying the photoresponsive contact angle switching.[76]

Recently, Athanassiou *et. al.* prepared a spiropyran doped polymer surface and observed the impact of surface roughness on surface wettability by alternation of UV and green light irradiation. On the patterned grating surface, the contact angle changes were amplified and the hydrophilicity and hydrophobicity were enhanced.[77,78]

Belfort *et. al.* grafted a spiropyran containing responsive polymer onto a synthetic membrane by photograft-induced polymerisation leading to an optically reversible switching of wettability and protein adsorption.[79]

Smirnov *et. al.* produced a photoresponsive membrane which switched to allow membrane transport of water and ions. A nanoporous alumina membrane was modified with spiropyran moieties which are non-polar. The spiropyran molecule itself is not wet by an aqueous solution, however, upon irradiation, the cleavage of the C-O bond, which forms the merocyanine and allows water to penetrate the membrane.[80]

The use of a photodimerisation reaction to produce a change in wettability was accomplished by Roston *et.al.* via the utilisation of pyrimidine terminated spiropyran molecules which were attached to solid substrates, and were then irradiated with UV light between 240 and 280nm. The thymine terminated groups on a gold surface gave the largest reversible contact angle change (26°), as a result of a photodimerisation which induces a surface change from an ionised monomer form to a non-ionised dimer form. In comparison with other pyrimidine groups instead of thymine, uracil self-assembly monolayers photodimerise but do not photocleave leading to an irreversible contact angle change.[81,82]

2.9 Diarylethenes

The study of diarylethenes on microcrystalline surfaces by Irie *et. al.* resulted in the formation of a photoinduced reversible surface switch. The photoisomerisation of a diarylethene molecule between open ring and closed ring isomers is the foundation of the switchable wettability. Upon irradiation with UV light, microfibrils form upon the surface, which lead to a contact angle of 163°, which is superhydrophobic. Further irradiation with visible light, the surface becomes flat again and returns to the original contact angle of around 120°.[83]

Irie *et. al.* produced conductive polymers containing diarylethene moieties. Under illumination with light, a photoresponsive change occurred where a change in the π conjugated system bought about a change in conductivity.[84] Photoswitchable magnetism was also found in diarylethene derivatives.[85] Recent work by Einaga *et. al.* demonstrated the combination of photochromic molecules with magnetic nanoparticles to create photoswitchable magnetism.[86,87] These studies may provide candidates for photo-recording

media and optical switches in molecular devices. The above changes in conductivity etc. can be adapted in order to form molecular machines.

2.10 Molecular machines: Photoisomerisable chromophores as targets for molecular machines.

The term for large clusters of functional molecules together is known as a molecular machine. This term was coined by Richard Feynman in an address to the American Physical Society in 1959.[88] A molecular machine can be defined as " an assembly of a distinct number of molecular components that are designed to perform machine like movements (output) as a result of an appropriate external stimuli (input)". These 'machines' can be further characterised by

- The kind of energy input supplied to make it work, i.e. photochemical (light) electrochemical, (electricity).
- The nature of the movements of the component parts
- The purpose of the operation
- Timescale of motion
- Reversibility

The most successful energy inputs used here are photons (light) or electrons (electricity), hence the interest in photochemical isomerisation reactions, or on the other hand electrochemically-induced isomerisation reactions. Fundamental to any molecular machine is the ability to self assemble and self organise, a process which has led to increased understanding of the areas of non-covalent synthesis and the emergence of the term supramolecular chemistry, which is the chemistry of molecular assemblies via intermolecular interactions, which culminated in the Nobel Prize being awarded to Jean Marie Lehn for the discovery of cryptands and his work in the supra-molecular chemistry field in 1987.[89]

The focus of this thesis is photochemistry therefore the literature surveyed will be of a photochemical rather than electrochemical nature, however, molecular machines are also present in nature, which is an important source of inspiration for some of the most recent work on molecular machines. The formation of artificial molecular machines based on biomolecules and interfacing them with surface and solid supports constitutes some of the

most exciting work conducted in this field to date, and of course our bodies can be regarded as complex assemblies of molecular machines which convert energy in one form into energy in another, as in assemblies of proteins in the body.

The earliest examples of synthetic molecular machines however, were based upon the phtoisomerisation of azobenzene based molecules, therefore it would be pertinent to review developments in this area.

2.11 Photochemically induced conformational motion.

Several donor-bridge-acceptor compounds have been shown to undergo conformational folding upon exposure to light in non-polar solvents. Excitation of the compounds in solution cause them to form an excited state, on the acceptor unit, which in this case is azobenzene, which can then decay to a charge separated state. The donor and acceptor units carry a positive and a negative charge respectively and are separated from each other by free space. The N=N bond in azobenzene can adopt two configurations, *cis* and *trans*. This is a photoinduced conversion which occurs upon irradiation at different wavelengths. Hence, the geometries of the molecule can be altered by controlling the photoisomerisation. The changes in the structure can modulate physical chemical properties of these molecules.(90)

This fact has been used to control the geometries and functions of several biomolecules, materials and supramolecular complexes. This process can be used to adapt crown ethers with *trans* azobenzenes which upon irradiation the conformational change that occurs is sufficient to change the polyether linkage which causes the macrocyclic cavity to open up and expand in order to trap inorganic ions, such as metal ions and anions such as chloride.(91)

Thus, the *trans* isomer causes a retraction in the cavity, and as such it cannot bind alkali metal ions, whereas photoisomerisation causes an expansion, which allows the binding of alkali metal ions. In the same fashion, the opposite reaction (*cis*/*trans*) has been developed to shrink the cavity of cyclophanes and to shorten and elongate the recognition sites of receptors and induce intramolecular complexation in self complementary molecules, in other words, a photochemical controllable complexation reaction.(92)

2.12 Photochemically controllable complexes.

Complex formation via light stimulation of photosensitive compounds is by far the most interesting and most promising way to control molecular self assembly. Photoisomerisations, such as the *trans*/*cis* isomerisation of the azobenzene molecule has been utilised for a long time to exert photocontrol on a system.[93,94,95]

For example, an azobenzene capped cyclodextrin cannot fit a 4-4-bipyridine molecule into the cavity when all of the azobenzene moieties are in their *trans* form, however, when isomerisation to the *cis* form occurs upon irradiation with UV light, the resulting expansion of the cavity enables the bipyridine molecule to fit into the cavity with ease. The reversibility of the reaction enables the bipyridine molecule to be ejected, either by allowing for thermal relaxation in the dark, or by irradiation of the complex using the correct wavelength of light. This method has also been used to cause dethreading of rotaxanes and other complex supramolecular structures.[96,97]

Another area in which photochemistry is used to control molecules is with complexes which are stabilised using π electron donor/acceptor interactions. The result of these interactions is the formation of a new energy level which causes the appearance of charge transfer bands in the visible region of the spectrum. Excitation within these bands by irradiation with photons of light, cause the transfer of an electron from the donor to the acceptor, which can destabilise the charge transfer required for self assembly of the molecules in the first place, which leads to the structure falling apart.

The main drawback for this method is that back electron transfer is much faster than the separation of the molecular components. This can be overcome using an external electron transfer photosensitiser and a reductant scavenger species. Suitable molecules for the photosensitiser role have been found to be based on ruthenium tris(bipy) [$Ru(bpy)_3$] , whilst triethanolamine serves as a good reductant scavenger.[98,99,100,101]

The relatively fast back electron transfer from the reduced component, such as a cyclophane or other cage self assembly structure, to the oxidised photosensitiser is reduced by the reductant which intercepts the oxidised photosensitiser and regenerates it. The topic of

photocontrol over molecular assembly has been extensively review by Balzani and others. The core of this work is the "top down approach" to the creation of intrinsic effects over a large surface using external stimuli.[105-110] The so called 'top down' approach, which leads to the manipulation of many small molecules in order to create an intrinsic effect, in the case of this thesis, contact angle change and surface wettability, is fundamental, as to create changes upon a large surface for example, you first need to understand what happens at a molecular level. This key idea which is crucial to this work can be summed up by Professor Richard Feynman "When we have some control over the arrangement of things on a molecular scale, we will get an enormous range of possible properties which a substance can have, and these new properties will lead most certainly to a wide variety of applications which we cannot even begin to envisage today".[111,112]

2.13 Cellulose

Cellulose is a long chain polymer of β-glucose. It is the primary structural component of all green plant cells. (Figure 12)

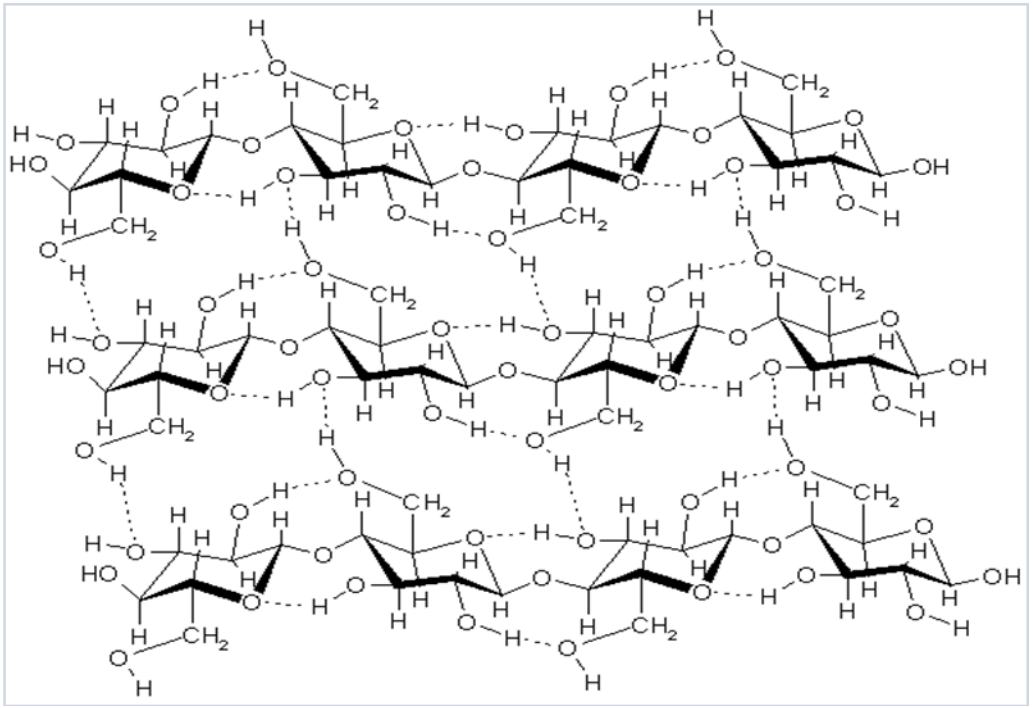

Figure 12: Chemical Structure of cellulose

Cellulose consists of β-glucose monomers which are linked together via β 1- 4 glycosidic bonds, which are formed via a condensation reaction whereas in other carbohydrates, the monomers are linked together via α 1→4 glycosidic bond. Cellulose is a straight chain polymer, which implies that no coiling occurs as in starch. The molecules of cellulose adopt a rod like conformation, often referred to a microfibril. In these microfibrils, the many hydroxyl (-OH) groups that occur on the β-glucose residues undergo hydrogen bonding to each other which in turn holds the chains firmly together and is responsible for their high strength. Cellulose is also a major component in cell walls, where cellulose fibrils are meshed together to form a carbohydrate matrix, which keeps the plant cells rigid. This is known as the cell wall.[113]

Cellulose is the major constituent of paper and textiles such as cotton and linen. Cellulose can be further processed to produce cellophane and rayon. Cellulose is widely used in laboratories for thin layer chromatography, and cotton linters. Cellulose is also more crystalline than starch. Starch possesses a crystalline to amorphous phase transition at 60 -70 °C in water; however, it takes 320°C and 25 MPa for cellulose to become amorphous in water.[114]

Cellulose can be separated into the α and β forms by the addition of sodium hydroxide solution. The portion that does not dissolve at 20°C is α cellulose, the portion that can dissolve but is precipitated from acid is known as β-cellulose and the portion that dissolves in sodium hydroxide and is not precipitated via the addition of acid is called γ cellulose. Further refining of the α form of cellulose creates a form of cellulose known as microcrystalline cellulose.[115]

2.14 Microcrystalline Cellulose

Microcrystalline Cellulose is cellulose derived from high quality wood pulp. Whilst cellulose is the most abundant organic material, microcrystalline cellulose can only be produced from α-cellulose.

It is a naturally occurring polymer consisting of glucose units connected by 1-4 β glycosidic bonds. The linear cellulose chains are bundled together as microfibrils spiralled together in

the walls of a plant cell. Each microfibril exhibits a high degree of three-dimensional internal bonding resulting in a crystalline structure that is insoluble in water and resistant to reagents. There are relatively weak segments of the microfibril present which have weaker internal bonding, known as amorphous regions but are more accurately referred to as dislocations. The crystalline region is isolated to produce microcrystalline cellulose.[116]

Processing of the cellulose microfibrils is achieved by shredding the sheets of high purity α grade pulp. The shredded pulp is immersed in a hot bath of hydrochloric acid that dissolves the amorphous regions of the microfibrils while leaving the microcrystalline segments intact. The objective is to break down the long polymer chains.[117] After hydrolysis, chemicals and impurities are removed through a washing step, followed by spray drying. The slurry is sprayed through hot air jets to evaporate the water. This process produces particles of the desired size and moisture content.[118]

While the process of producing microcrystalline cellulose appears to be relatively straightforward, the product quality can be directly linked to a variety of parameters of the process in terms of time, temperature, pressure, purity of materials and the manufacturing environment.[119]

Microcrystalline cellulose also is highly absorptive due to the capillary action of its surface porosity, making it possible to act as a carrier for liquids and yet retain free flowing and compression properties.[120]

The use of cellulose as a substrate in photochemistry has been explored by many researchers. The study of dyes on cellulose has been undertaken as it is of great interest to the clothing industry.[120] The study of cyanine dyes on surfaces via diffuse reflectance ground state absorbance show the formation of aggregates on the surface of microcrystalline cellulose. Two dyes were studied 1,1, diethyl 2,2, cyanine iodide and 1,1,diethyl 2,2, carbocyanine iodide adsorbed onto microcrystalline cellulose. For the first dye, H and J aggregates were formed on the surface, whereas with the latter dye, only H aggregates were formed. Emission was observed from excited molecular aggregates at high laser fluencies, but only from concentrated samples, where monomers and aggregates can co-exist in the ground state.[121]

Further investigations utilising oxacarbocyanine dyes DOCI and DODCI were conducted on microcrystalline cellulose at a range of concentrations. DOCI shows both H and J aggregation on the surface, whereas DODCI shows only H aggregation. The aggregation is found to be hydration dependent , increasing with decreasing hydration, which gives decreasing hydration giving decreasing sample aggregation, therefore more molecules are in the monomeric form, hence greater fluorescence from the monomer. A photoisomer is produced in the excited state, and the intensity of the emission band of this isomer is proportional to the square of the laser fluence.[122]

Energy transfer on microcrystalline surfaces has been investigated, alongside the excited state lifetimes of dyes on cellulose as well as in solution. Triplet-triplet energy transfer has been studied between benzophenone and an oxazine dye (2,7-bis(diethyl-amino)-phenazoxonium chloride) co-adsorbed on the surface of microcrystalline cellulose. Ground state absorption and fluorescence measurements provide evidence for dimer formation of the oxazine dye when adsorbed on cellulose in contrast to the behaviour in ethanol solution where no dimerisation is observed. The equilibrium constant for dimerisation, which is found to be 1.0×10^{6} mol per gram for oxazine alone on cellulose decreases in the presence of co-adsorbed benzophenone.[123]

Fluorescence is detected from excited monomeric but not from excited dimeric oxazine. The absorption spectrum of the triplet state of oxazine adsorbed on cellulose was obtained and its extinction coefficient evaluated relative to that of triplet benzophenone which was used as a sensitizer. The lifetime of adsorbed triplet oxazine is 4.3 ms which is 300 times longer than that in acetonitrile solution.[124]

Rose Bengal adsorbed on microcrystalline cellulose at concentrations up to 4×10^{-7} mol g^{-1} was studied in the solid phase by total and diffuse reflectance and steady-state emission spectroscopy and a simple monomer–dimer equilibrium was fitted to the reflectance data which allowed the calculation of monomer and dimer spectra. Increases in the dye loading resulted in the formation of higher aggregates. Observed emission and excitation spectra and quantum yields were corrected for re-absorption and re-emission of luminescence, using a previously developed model, within the assumption that only monomers are luminescent.[125]

The relationship between photodegradation rates and dye concentrations were determined by extraction, reflectance, and visual methods. Polyester and cellulose ester fabrics dyed with 4-[N-(2-cyanoethyl)-N-(ethylamino)]-4'-nitroazo benzene at various concentrations were exposed to an arc lamp, and the amount of dye disintegration, as a function of time, was determined by diffuse reflectance.

Correlations were found between visual light fastness ratings on the fabrics, dye loss determined by reflectance methods, and concentration of dye in the fabric. Extraction methods were useful for determination of dye content of dyed fabrics before and after extensive photodegradation, but they lacked the sensitivity required for determination of small dye losses resulting from photolysis. Neither the fading kinetics nor the reflectance spectra indicated extensive aggregation of dye in the fabrics.[126] The use of cellulose as a model for fabric is an area that will be covered within this project. The prospect of clothing which is photoswitchable clothing for resistance to substances is the main drive behind this project.

2.16 Morphological structure of cellulose

The morphology of cellulose exists as a well organised aggregation of fibrilar elements. Natural and regenerated types of cellulose have different structures, for example, microfibrils have a diameter in the range of 2-20 nm and the macrofibrils in the range of 10-50 nm. The aggregation of microfibrils leads to the formation of larger fibrils macrofibrils, which are aligned parallel and densely packed to form a helical spiral in the case of cotton, the fibre is composed of layers of different thickness.

In addition to the arrangements of the fibrils, there is also a system of pores and capillaries which are of random shape and size. The total pore volume and the average pore size can be determined, but the distribution or the shape of the pores varies immensely. The only way to gather information on the size of the pores is by using small angle X-ray scattering for small pores and mercury porosimetry for larger pores.

Total pore volume and pore size distribution are affected by swelling and drying the samples of cellulose. Drying of cellulose can lead to irreversible narrowing of pore size, versus interfibrillar swelling in liquid such as water and methanol, which can lead to an increase in

pore volume, which can be preserved by drying techniques, such as freeze drying the sample using a freeze pump thaw cycle, but this requires special apparatus and is time consuming.

The volume of pores as a percentage of the volume of cellulose differs depending on the source and the treatment of the cellulose samples themselves. The surface area of those pores can be determined either by sorption of inert gases or water, which has led to findings that the pores in the amorphous region of cellulose have a larger internal surface area than in the crystalline regions of the cellulose sample.

Also, other natural forms of cellulose can be mixed in with other polysaccharides, as trace components of iron and of calcium can be found in the raw cellulose product. The presence of these cations can cause problems when machine processing the fibres, however, they can be leached out of the fibrils using solutions of EDTA, which is a complexing agent, which complexes the cations and removes them from the cellulose.

The adsorption of species to the surface of cellulose can often depend on the availability of groups on the inner surface. Water can also penetrate into the amorphous regions of the cellulose and destroy weak hydrogen bonds between the water and hydroxyl groups on the cellulose backbone. The affinity leads to cellulose readily absorbing moisture from the atmosphere and readily becoming wet. The fibres of cellulose undergo swelling upon saturation with water, which can lead to the fibrils becoming shorter and fatter and having increased strength, hence dry cotton cloth is easier to tear than when it is wet.[127]

2.17 Cellulose radical formation.

As mentioned in the previous section the backbone of cellulose possesses many hydroxyl groups and radicals may be formed on the backbone of cellulose by abstraction of a hydrogen atom. The site of the abstraction of this hydrogen atom will vary depending upon the strength of the bond which links the hydrogen atom to the backbone of the cellulose structure.

For a single glucose unit within a polymer chain, the weaker C-H bonds would be expected to be those α to a hydroxyl group. The abstractions of so called α hydrogens leads to the

formation of α hydroxyl radicals. In the case of cellulose, as it consists of the α form of glucose, α hydroxyl radicals would be formed.

In comparison to other α hydrogen bonds in, for example, isopropanol and propane, in propanol to remove the α hydrogen from the hydroxyl group requires 401 kJ mol $^{-1}$ whereas to move the α hydrogen from 2 propanol required 381 kJ mol^{-1}.[128] The bond strength between the carbon atom to which the hydroxyl groups present in cellulose are attached is also reduced as the C-OH groups have weaker bonds than the C-H bonds in propanol.

2.18 Irradiation of cellulose.

The irradiation of cellulose can lead to the degradation of the polymer and this can be characterised via a change in the light absorption properties of the polymer, which in the case of cellulose is known as yellowing. The photo-oxidation of cellulose is thought to be photoinitiated, which can explain the degradation of cellulose samples over many years, however, the yellowing is much more pronounced in the presence of oxygen.[129]

The radiolysis and photolysis of sugars results in the formation of radicals, and ESR studies have been carried out on irradiated cellulose which found that there was evidence for the formation of a number of radicals on irradiation.[130] Addition of dyes to the system results in a wider spectral range that may cause yellowing of the cellulose. However, with most azo-dyes being of yellow-orange in colour, the photo-oxidation would be extremely hard to detect. Also, the perceived problem of the radicals produced reacting with the azo dyes which are on the surface of the cellulose is a consideration if the samples will be exposed to light for long enough in order for radicals to form.[131,132]

There have also been several studies into the role of singlet oxygen in cellulose photo-oxidation, which has lead to the inference that singlet oxygen is the main cause of the photo-oxidation of cellulose. Singlet oxygen is produced when oxygen is excited with enough energy to undergo photoexcitation from the ground triplet state to the excited singlet state (one of the very few molecules which has a ground triplet state), however, as the energy required to do this is large, and a laser is required, it is not perceived as a big problem for the photochemical studies of compounds anchored to the surface of cellulose.[133]

2.19 Dyes and pigments

Fabric colourants can be divided into two main categories, dyes and pigments. Pigments tend to be insoluble in the medium in which they are applied, whereas dyes are soluble. The most important property of a colourant is that it can absorb visible light, but other properties, such as colourfastness are also desirable. Fastness to both light and water are very important properties of the dye, if the system to which they are applied will come into contact with light and water.

Dyes can be classified by their chemical structure or their method of application to fabric. Lay people working in the dye industry use the latter classification, whereas the former is used by trained dye and pigment chemists. There are many classes of dyes, and azo dyes are just one group that are examined here.

2.20 Application of dyes to fibres

There are several methods in which a dye can be applied to a fibre. The method chosen depends upon the properties, such as resistance to solvents etc of the fabric and also the final method of use of the dyed product.[134]

2.21 Disperse ionic and vat dyeing

Disperse and ionic dyes are usually used on fibres other than cellulose, so they are not used in this work, but a brief overview is given for comparison. The most common substrate for the dye to be applied to is polyester. This is carried out at high pressure in a specially adapted pressurised container at high temperature. Under these conditions, it is possible for the dye to enter the structure of the polyester and once this has been achieved, the wet fastness of the dyed polyester is high due to the hydrophobic structure of the polyester polymer. Ionic dyes react with the charged groups on the surface of the material to which they are applied, and are most often applied to wool, nylons, acrylics and other synthetic fibres.

Vat dyeing can be applied to cellulose based materials, which is useful if the dye is not soluble in water, as most azobenzene related compounds are not. The azo compounds can be

solubilised via the addition of sodium sulphite, which then makes it possible for the dye to enter the polymer, which can then be precipitated to form its insoluble state, therefore giving it a high water fastness.[135]

2.22 Direct and reactive dyeing

Direct dyes have a high affinity for cellulosic polymers and attach themselves to the fibre via hydrogen bonding. Direct dyes are usually long polyazo dyes containing sulphonic acid groups which facilitate dissolution into water. They are applied in an aqueous solution with no need for the addition of extra reagents as in the case of other dyes.

Whilst this method of dyeing is cheaper, it presents several problems, one of which is the wash fastness of the fibres which have been dyed with direct dyeing often have very poor wash fastness and are therefore discarded after 1- 2 washes as the colour begins to fade. This has been found to be a problem in fake goods imported from other countries, such as replica t-shirts which have been dyed using inferior dyeing methods and therefore fade with washing. Direct dyes can however be improved by adding finishers to the dyeing process. These finishers are chemicals which slow down the diffusion of the dye in the fibres, but they do not stop it from happening altogether, they just hinder the process for a while. The finishers themselves have been implicated in having an effect on the light fastness of the fibre as well, so the fibres can be faded not only via washing, but via light also.[136]

2.23 Reactive dyeing

Reactive dyes have groups in their structure that are capable of reacting with the OH groups on the cellulose surface. The chemical bonds are formed between the dye and the fibre. The most common reactive dyeing group used for cellulose is the chlorotriazinyl group.

2.24 Chemical structure of dyes

Many synthetic dyes have similar structures to naturally occurring dyes. For example, phthalocyanines have a related structure to porphyrins e.g. haemoglobin and chlorophyll. Alizarin is a neutral dye with an anthraquinone structure. Indigo, which is naturally occurring

is still used as a dye to this day, but is manufactured synthetically. Also, the first synthetic dye to be synthesised by Perkin in 1856 is an azo dye, given the name Mauvine,[137] on account of its mauve colour. The most common types of dye used are azo dyes, and these have no natural counterparts and are purely synthetically produced.

2.25 Azo dyes and their reactivity on cellulose

Organic azo dyes absorb in the visible part of the spectrum due to the presence of the low lying n-π* state as discussed earlier. The spectral position of this state is dependent on the moieties attached to the molecule. The ability to select colours and spectral properties make the azo dyes attractive candidates for dyeing fabric, and as such substituted aromatics are widely used as dyes.

Emission from azo compounds is not observed, unless the molecule is highly substituted. There has been slight emission observed from azo dyes when they have been set highly substituted.[138,139] The ability to photoisomerise as discussed before makes these molecules both useful and versatile.

2.26 Azo Hydrazones

The ability of an azobenzene molecule containing a hydroxyl group to exist as two tautomers has been investigated.[140,141] The tautomers are both the azo and hydrazone forms of the molecule which occur on surfaces and in solution. The nature of the medium and the substitution pattern also play a large role in determining the position of the equilibrium of the azo-hydrazone forms.[142,143]

The hydrazone form is dominant where the azo molecule contains electron withdrawing substituents, and also in solutions made with most common solvents.[145,146] The hydrazone tautomer is known to be an intermediate in the thermal relaxation reaction from *cis* to *trans* of a hydroxyl-azo compound.[146] This hydrazone tautomer can also react readily with singlet oxygen. Studies of this phenomenon can be found in the literature.[144]

2.27 Photodegradation of dyes

The understanding of how photodegradation occurs in any dye molecule is important in order to understand how the surface itself can affect the azo molecule. Azo dyes have been found to undergo permanent discolouration via both oxidation and reduction and the mechanism for fading has been studied extensively, but the mechanism of fading on cotton and cellulose based surfaces is not well understood. The overriding factor appears to be the environment in which the dye exists and this seems to be the key to determining how dyes fade on surfaces. (147)

Investigations conducted on the photodegrdation of dyes on substrates with similar structures to cotton have been carried out, i.e. on cellulose acetate, or on substrates used to model other fibres. The use of films as a model for fibres is often used due to their transparency which can facilitate optical measurements such as absorption and reflectance and in the case of fluorescent dyes, fluorescence measurements can be observed.(148,149)

Many workers have investigated the effect a substrate can have on the photodegradation of dyes and overall the conclusion seems to be that the presence of a substrate itself can affect the overall rate of photodegradation of an azo molecule. A detailed review has been compiled by Tennent *et. al*. in which the mechanisms for photodegradation are also postulated.(148,150)

The environmental factors have also been investigated as possible contributors to the rate of photodegradation on surfaces. The presence of water has been found to increase the rate of fading of dyes on cottons. Even amino acids, such as histidine have been found to increase the rate of photodegradation. Another cause of photodegradation on surfaces is exposure to the atmosphere in general, as polluted atmospheres contain gases such as sulphur dioxide, which acts as a bleach towards any dye present.(151)

Both chemical(152) and physical(153) properties of dyes have been found to affect the photodegradation rate on surfaces. The general consensus on this issue is that dyes tend to have higher stabilities at higher concentrations,(154) which is when aggregation can be observed. Aggregation is also a problem for photoisomerisable dyes, as the reverse reaction

can be prevented from occurring due to aggregation as the molecules are hindered, which precludes any free isomerisation back to the original form.

The fading of non azo dyes has been studied [155,156] but is not considered in this thesis, as the main focus is on azobenzene containing molecules. As mentioned earlier, the ability of dyes to quench singlet oxygen can be considered as both interesting and as a hindrance. Studies carried out indicate that dyes can quench singlet oxygen easily and therefore make useful tools in singlet oxygen research.[157]

The quenching of singlet oxygen has been observed both in solution and on the surface of microcrystalline cellulose,[158] which is used in this work, however oxygen in its natural state is in the triplet state, therefore this should not pose a problem. Storage of the material in airtight containers and in the dark should preclude this problem, if not eliminate this factor all together.[157,158]

The part that radicals play in the photodegradation of dyes on cotton has been investigated and it can be shown that simple ketyl radials can reduce azo dyes, resulting in the production of hydrazyl radicals which have been detected by flash photolysis. Furthermore, these hydrazyl radicals can break down further via N-N fission to form amines, which have been found following irradiation of azo molecules and analysis of the products formed.[159,160]

2.28 Azobenzene on the surface of silica

To expand the range of applications as well as create new properties, various organic functional groups have been attached to the surfaces of mesoporous materials such as silica. The main groups that have been incorporated are phenyl, octyl, vinyl and epoxide groups.
Stimuli responsive devices have been around a long time but Brinker *et.al.* [161] proposed that incorporating a pendent group on the porous framework would allow the surface to be controlled via external stimuli.

Azobenzenes provide ideal opportunities for surface modification, as the isomerisation can be controlled via irradiation with light of the correct wavelength. To best utilise the ability of

azobenzenes to photoisomerise, they need to be anchored to a surface where they can freely move and anchored to a pore structure with uniform pore sizes.

The incorporation of azobenzene into silica both in a sol–gel formation and as a Langmuir Blogett self assembly on surfaces has been well documented. The incorporation of azobenzenes into silica gel matrices has been investigated by Brinker *et. al*.[161] and they have been photochemically characterised. The post grafting method involves fuctionalising sol gel materials with reactive azo moieties to tether them to the surface. This can be accomplished via co-hydrolysis and condensation of the azobenzene containing organosilanes with other organic silica precursors such a tetraethylorthosilicate (TEOS).

Delorme *et. al*. used the surface of silicon, which contains OH moieties, as a substrate to couple an azobenzene based molecule to using a coupling reaction between the azobenzene molecule, which was modified using an isocyanate (NCO) group and the OH group on the silica surface. This was conducted with dendrons, which are azo groups in large linked polymers, but the modification of the surface before grafting is a principle which has been widely used.[162]

In 2006 Meada *et. al*. grafted alkyl chained azobenzenes to the surface of silica using aminopropylsilane groups as linkers, which relies on the reaction of the OH groups on the silica with the organosilane reagent which then can react with halogenated derivatives of the azobenzenes in order to link the molecules to the surface of the silica gel. This method appears to be simpler than creating sol gels from other chemicals and reacting them with azobenzenes. This also required air free techniques and a lot of time, which is a slight disadvantage of this method.[163]

The use of linkers to attach azobenzenes to the surface of silica has been widely investigated as other groups have an interest in this method also. Yongqiang Wen *et. al*. discovered that azobenzene-containing compounds covalently attached onto Si surfaces via Si−O linkages using a two-step procedure. The modified Si surfaces were characterized by X-ray photoelectron spectroscopy (XPS) and Fourier transform infrared (FT-IR) spectroscopy measurements. The monolayer surface showed chemical stability. Reversible photoisomerisation of azobenzene molecules on these modified surfaces was observed in response to alternating UV and visible light exposure. The measured conductivity showed

distinct difference with *trans* and *cis* forms of azobenzene compounds on modified Si surfaces.[164]

Aside from macroscopic switchable wettability on noncurved surfaces, recently Smirnov *et al.* modified the surface of nanoporous alumina membranes using mixtures of spiropyran and hydrophobic molecule.[165] The freshly modified membrane with the non-polar spiropyran form is not wetted by an aqueous solution, while after UV exposure, the polar merocyanine form occupies the surface, outside and in the nanopores, allowing water or ions to enter the pores and cross the membrane. Thus, the membrane acts as a photosensitive valve that not only switches the transport of water and ions across the membrane, but also switches the conductance.

Moreover, a reversible photodimerisation reaction has also been used in an attempt to perform a wettability conversion. Ralston *et. al.* [166,167] reported a wettability change on thin coatings of photoresponsive, pyrimidine-terminated molecules attached to solid substrates when irradiated with UV light at 280 and 240 nm. The thymine-terminated self-assembled monolayers on gold gave a large reversible photoinduced contact angle change (26°), originating from a photodimerization that induces a change in surface charge from ionised monomer to non-ionised dimer. In comparison to thymine, uracil self assembled monolayers photodimerise but do not photocleave, and there is an irreversible contact angle change.

By virtue of the photoresponsive characteristics of malachite green carbinol base, Sasaki *et. al.* proposed an alternative means to construct a photoresponsive surface by preparing a composite film made up of malachite green carbinol base and fluoride on silicon dioxide particles. [168] Upon exposure to UV light, the malachite green carbinol base changes into a less hydrophobic conformation when the hydroxide anion is detached. As a result, on the composite surface, where silicon dioxide particles can tune the surface roughness, light induces a surface wettability transition from hydrophobic to hydrophilic.

2.29 Chitosan

Chitin is one of the most abundant natural aminopolysaccarides, with estimated production nearing that of cellulose annually. It consists of 20-acetamido-2-deoxy-β-D-glucose via a β 1-

4 linkage. It is very insoluble and resembles cellulose in physical charaterisitics, with low chemical reactivity. Structurally, cellulose can be compared to chitosan, as cellulose is chitosan with the hydroxyl at the C2 position replaced by an acetamido group. Chitin is mainly a structural polysaccharide, found in crab and shrimp shells. The deacetylated derivative of chitin is known as chitosan.

Most polymers present today, such as polyethene are synthetic materials and therefore do not biodegrade, unlike natural polymers, such as cellulose and chitin. Chitin and chitosan are recommended as functional materials as they possess desirable properties such as biocompatibility, biodegradation, non-toxicity, and adsorption properties.

Chemically modified functional derivatives have been prepared, although very few have been found to be soluble in organic solvents.(169) Modifications to chitin and chitosan structure have also been reported.(170) Unlike cellulose, chitin is highly hydrophobic and is insoluble in water and most organic solvents. It is however soluble in certain fluorinated solvents, dilute mineral acids and dimethylacetamide.(171)

The ratio of the acetylated to deacetylated compound has an effect on solubility. Deacetylation of chitin enables the formation of chitosan, which is soluble in dilute aqueous acids. The molecular weight of chitosan has been determined via HPLC methods.(172)

Viscometry was used to determine the molecular weight via the Mark Houwink equation.

$[\eta] = KM^{\alpha}$ (173)

Chitosan is charged in acidic solvents and may form aggregates; therefore care is required when applying the constants derived.

The constants a and K in the Mark Houwink equation have been determined using 0.1 M acetic acid and 0.1 M sodium chloride. The weight average of the deacetylated product, chitin, is 100kD to 500 kDa which upon acetylation increases to 1003 kDa to 2500 kDa.(174)

Cellulose and chitosan are crystalline materials, of which only a limited number of solvents can be used as solvents for reactions. Due to extensive hydrogen bonding, chitin and chitosan degrade before melting, hence the requirement to dissolve the chitin and chitosan in a suitable solvent to allow for functionality. A coagulant (such as PVA) is required for solidification. The nature of the coagulant is highly dependent on the solvent and solution properties as well as the type of polymer used.[175]

The uses of chitosan range from photography,[176] cosmetics,[177] artificial skin,[178] and drug delivery systems.[179] The formation of films of chitosan can be accomplished easily and films of Chitosan and PVA have been prepared and investigated for biomedical applications.

Study of the photochemistry of chitosan is a relatively recent phenomenon, with a majority of the studies having been conducted over the last ten years. Chitosan has been investigated as a possible natural approach to wound healing, as a possible pharmaceutical delivery agent and as a scaffold for novel biopolymers and an anticoagulant agent for blood.[180]

Due to the ease of forming transparent films of chitosan, the measurement of contact angle changes on the surface would be made possible, as the azobenzene on the surface could be photoisomerised using UV light. Recent work on the contact angles of chitosan films by Wisinewska *et. al.* [181] shows that after 8 hours of constant irradiation of a glycerol droplet, the contact angle of the unfunctionalised chitosan surface, changed from 84.4° to 78.4° over 2 hours of constant UV irradiation. The photoisomerisation of the azobenzene on the surface that will be covered here, switches on a picosecond timescale, reducing the need for long UV exposures, thus negating any surface angle changes over time. Even though only a 6° change was observed, this could affect the results, so any photoisomerisation reactions on the surface would need to be very rapid.

Azobenzenes have been successfully incorporated into chitosan to create a biopolymer which was prepared using chitosan and methyl red (an azo dye). Characterisation using UV-Vis spectroscopy amongst other methods confirmed the product. However, the emphasis here is to graft to the surface of chitosan rather than blend a polymer using chitosan and azo compounds.[182] Chitosan contains functional amino groups which will couple to a triazinyl derivatised azobenzene group easily, as amino groups are highly reactive functional groups.

2.30 Photoinduced wettability changes on surfaces

In order to perform contact angle studies on the materials produced in this work, a review of some previous work on silica and on silicon wafers is required. This will form a guide as to the level of contact angle change expected to be observed on the surfaces produced here.

Interfacial phenomena such as wettability can be reversibly switched by photoisomerisation. A few studies report the photocontrol of wettability of LB films of azobenzene polymers containing fluorinated end chains,[183–186] whereupon isomerisation the contact angle decreases due to the formation of the polar the *cis*-isomer. Furthermore, Ichimura *et. al.*[187] used the photoinduced wettability changes of calix[4]resorcinarenes, cyclic bowl-shaped macromolecules.

Dipole moment changes can also induce changes in the surface potential of self assembled monolayer (SAM) films,[188,189] where the surface potential was observed to increase upon isomerisation due to the presence of the more polar *cis*-azobenzene. Perhaps one of the most striking effects of the azobenzene photoisomerisation is the controlled motion of a neighbouring photo inactive substance. Ichimura reported that spatial control of the UV-irradiation of a photoresponsive film of calix[4]resorcinarenes generates a gradient in the surface tension enabling the net mass transport of liquid drops on that surface.[190]

The first example demonstrating that the wetting of surfaces functionalised with photochromic spiropyran molecules can be tuned when irradiated with laser beams of the correct photon energy was demonstrated. The hydrophilicity increased upon irradiation with a UV laser as embedded non-polar spiropyran molecules were isomerised to the polar merocyanine form. The process is reversible upon irradiation with green light. In order to increase the hydrophobicity of the system, the photochromic polymeric surfaces were formed via soft lithography.[191]

Water droplets features interact with air molecules in the micro cavities, yielding superhydrophobic air–water contact angle changes. The light-induced wettability changes on the surfaces are increased 3 times compared to those on flat surfaces. This significant increase in contact angle is due to the photoinduced reversible volume changes of the surface

gratings, which in turn contribute to the wettability changes induced by irradiation. In this work, it was demonstrated how surface chemistry and structure can be combined to influence the wetting behaviour of polymeric surfaces. However, the contact angle values after irradiation are limited to only two UV–green irradiation cycles. The aging and degradation of the compounds upon multiple irradiation cycles is a major disadvantage of such a polymeric system.[191,192]

On the other hand, Lim *et. al*.[192] have reported a photoswitchable multilayer film with wettability that can be reversibly switched from superhydrophobicity to superhydrophilicity under UV/visible irradiation. A combination of surface roughness and a photoswitching of fluorinated azobenzene molecule (7-[(trifluoromethoxyphenylazo)phenoxy]pentanoic acid was used here. The surface roughness was created via the use of a layer-by-layer deposition technique of poly(allylamine hydrochloride (PAH)), which is a polyelectrolyte, and SiO_2 nanoparticles. This enables the formation of a porous organic–inorganic hybrid film on the surface of silicon. The surface roughness can be tuned by controlling the number of bilayers.

The film was further modified by the use of 3-(aminopropyl)triethoxysilane (APTS) to introduce amino groups serving as binding sites for the photoswitchable azobenzene based moiety. The wettability is caused by the change of dipole moment of the azobenzene molecule upon photoisomerisation. For example, in the *trans* state, the azobenzene molecules exhibit the fluorinated moiety leading to a lower surface energy. The *trans*-to-*cis* isomerisation of azobenzene is induced by UV light irradiation and leads to a large increase in the dipole moment of these molecules disrupting the chain packing in the azobenzene monolayer and a resulting in a lower contact angle as the fluorinated moiety was not present on the surface.

Several researchers have studied the photoswitchable wettability of SnO_2 nanorods by using SnO_2 seeds which can be spin coated onto substrates. The SnO_2 nanorod based films demonstrated superhydrophobic behaviour (contact angle of 154°), as compared to 20° displayed by a smooth SnO_2 surface. SnO_2 nanorod films changed to superhydrophilic state (0°) just by exposure to UV irradiation (254 nm) for 2 h. Then, the wettability changes back to its initial state by keeping the films in the dark for four weeks.[193]

The switchable wettability was explained by the generation of hole-electron pairs after UV-irradiation on the surface of the SnO_2 nanorods reacting with lattice oxygen to form surface oxygen vacancies. The defective sites are kinetically more favourable for hydroxyl adsorption than oxygen adsorption, leading to the superhydrophilic state. During dark storage, hydroxyls adsorbed on the defective sites can be gradually replaced by oxygen in the air, because oxygen adsorption is thermodynamically more stable and leads to a superhydrophobic state. Similar switchable wettability properties can also be obtained using ZnO nanorod films as oppose to SnO_2 nanorod films.[194]

In these cases, the reversible switching between superhydrophilicity and superhydrophobicity is related to the cooperation of the surface chemical composition and the surface roughness. The former provides a photosensitive surface, which can be switched between hydrophilicity and hydrophobicity, and the latter further enhances these properties.

The use of titanium dioxide instead of tin oxide and zinc oxide has been widely reported also. The examples given here are superhydrophobic surfaces produced on titania (TiO_2). By using titania nanoparticles, a patterning and tuning method of microchannel surface wettability was developed for microfluidic control.[195] Titania modification of a microchannel was achieved by introduction of titania solution inside pyrex microchannel providing a nanometer sized surface roughness. Subsequent hydrophobic treatment with ODS (octadecyl dichlorosilane) grafted to a superhydrophobic surface (contact angle of 150°). Photocatalytic decomposition of the coated hydrophobic molecules was used to pattern the surface wettability, which was tuned from superhydrophobic to superhydrophilic under controlled photoirradiation. Irradiation for 60 min gave a superhydrophilic surface (9°).

Self organised TiO_2 nanotubes grown on Ti by electrochemical anodisation was described by Balaur *et. al*.[196] The TiO_2 nanotubes display superhydrophilic wetting behaviour. Upon modification with organic molecules, the surfaces displayed superhydrophobic behaviour. UV induced decomposition of the organic molecules in the monolayer can be tuned to control the wetting properties of a surface of TiO_2.

Coffinier *et al*. presented a simple method for producing superhydrophobic surfaces based on chemical modification of silicon oxide nanowires.[197] The silicon nanowires were modified

by PFTS (perfluorodecyl trichlorosilane), resulting in a superhydrophobic surface with a contact angle of 152°, which is much higher than that of a smooth Si/SiO_2 surface modified with the same silane (109°). The contact angle of the unmodified surface was close to 0°, as expected for a surface terminated with polar hydroxyl (OH) groups. The surface wettability can be irreversibly tuned by controlling the UV-irradiation time, resulting in a partial or complete removal of the organic layer. The chemical modification and degradation of the organic layer was followed by XPS analysis.

2.31 Polymers containing the azobenzene moiety

Azobenzenes have been extensively studied as moieties in polymers and in liquid crystals. This work has lead to several conclusions; one of which is that the lifetime of the *cis* isomer can be altered using polymer chains as a hindrance, therefore enabling the control of the isomerisation reaction. The polymers used have included several alkyl branched chains, aryl rings and liquid crystals.[198-201] The effect of bulky substituents on the lifetime of azobenzenes has been widely studied, as the *cis* state could then be isolated and it would allow the two states to be selected without the unwanted conversion.

This has been achieved by using bulky substituents which hinder the thermal back reaction, like aryl groups and long polymer chains. The utilisation of a polyurethane molecule with a azo chromophore in the polymer chain gave a lifetime of approximately 4 days and a rate constant of approximately 3×10^{-6} s^{-1}.[202] The substitution of azo groups with bulky pendant molecules gave a lifetime of nearly 60 days and there have been other investigation using macrocycles which have provided *cis* lifetimes of 20 days,[203] 1 year,[204] and even 6 years.[205]

The *cis* form of the azobenzene molecule can be prevented from isomerisation completely by isolating it, affixing it to a surface or creating a ring like structure, however in the case of the surface work presented here, the *trans* isomer is used to affix the azo group to the surface.[206] The experiments shown above indicate that great geometrical changes are required in order to isomerise polymer based material. All of the above thermal relaxation reactions were found to be first order, however, polymer matrices can produce abnormally fast decay components. The higher the matrix crystallinity, the faster the decay component.[207,208]

As part of the work conducted here, the polymers were first dissolved into solutions of toluene and the lifetime was measured as with the Admat compounds. An attempt was then made to graft the azo polymers onto slides in order to see if photoisomerisation is present in the films on the surface of glass slides. The fact that the isomerisation reaction of azobenzene is associated with a large structural change in geometry and in the dipole moment has been exploited. The isomerisation reaction leads to a change in the distance of the *para* carbon atoms in azobenzene in the *trans* form of about 9.0Å to 5.5Å in the *cis* form. The dipole moment also changes, as the *trans* form has no dipole moment, whereas the *cis* form has a dipole moment of around 3.0 D. These properties manifest themselves in polymers and are useful in designing photoactive polymers.[209,210]

The investigation of physical and chemical behaviours of photochromic moieties in polymer backbones and the effect that polymers have on the isomerisation reaction has been investigated by Flory who observed that the attachment of an azobenzene moiety to a polymer does not lead to altered activity of a polymeric material however, there has been a number of interesting cases observed where the opposite is seen.[211]

Differences in the thermal relaxation reaction rate of different azo compounds with different moieties have been observed and the literature describes the essential influence that the nature and morphology of the polymer has on the photochromic and thermochromic isomerisation reactions of different moieties. The size, shape and conformation also play a key role in the amount of free volume available to the moiety.[212,213]

Several factors though have been thought to influence the isomerisation of azobenzene in polymers, i.e. the macroscopic and microscopic polarity values, the regional arrangement and the glass transition temperature have all been studied for their effects on isomerisation of a variety of different photochromic compounds and their results have been interpreted and the trends are discussed next.

2.3.2 Polymer backbones

Pioneering work by Kuhn *et. al.*[214] into the conformational changes in flexible chain molecules has led to the investigation of the dynamics of conformational changes within

polymers. The theory that is most popular states that long polymer chains are involved with two crank like hindered rotations. This has become known as the crankshaft motion. This avoids the requirement for a polymer to move through a viscous solvent medium. This would infer that the activation energy of the polymer isomerisation and thermal relaxation reactions should be substantially higher than for the molecule in a solution.

Work by Zimmerman [215] suggests that the isomerisation of the azobenzene moiety involves a thermal isomerisation reaction between excited *trans* and *cis* isomers separated by a low energy barrier. This postulate was then subsequently confirmed by Malkin *et. al*.[216] who said that temperature dependence of the quantum yield for *trans*/*cis* isomerisation reactions indicated that only a 2-3 kcal/mol activation energy barrier separated the two excited states.

The photochemistry of azobenzene based polymers was studied in order to investigate what effect, if any, the presence of an azo linkage would have on the ability of a polymer chain to photoisomerise compared with their low molecular weight analogues. The thermal isomerisation reaction was studied and the result found no difference between the rates of isomerisation of azo residues in the chain compared with lower molecular weight analogues. [217]

However, when Chen *et. al*.[218] studied the photoisomerisation of azo based polymers, it was found that when the polymer was diluted to low concentrations, it behaved the same as a low molecular weight analogue but the addition of polymer to both the low molecular weight analogue and the azobenzene based polymer, there was found to be marked difference in the rates of photoisomerisation, as the azo polymers had their thermal relaxation rates reduced by several orders of magnitude due to hindrance from the backbone of the polymer in thermal relaxation. There was found to be no evidence of a crank-shaft like motion in either of the experiments conducted, and this theory was later disproved by computer modelling.

Work by Kumar *et. al*.[219,220] also reported that the introduction of azo groups into polyureas does not hinder the photochemical reaction in dilute solution, and thus a series of polyaromatic ureas with pyridine moieties were synthesised and investigated for their photochemical properties. Activation energies for *cis*-*trans* thermal isomerisation of these polymers suggest similar energy barriers to lower molecular weight analogues and also polymers with different molecular weights and chain segments. Further work discovered that

azobenzenes are not directly influenced in dilute solution by the composition of the polymer chain, since the pre exponential factor did not vary much when particular novel diol based chains were used as the backbone of the polymer.[221]

Work by Irie *et. al*.[222] discovered that the much faster scale of azobenzene isomerisation compared with polymer backbone motion supported the theory, thus the above observations were not entirely unexpected, as work conducted by the Irie group also showed that the relaxation time due to a conformational change in the molecule after photoisomerisation (around 1 ms) was much slower than the photochemical isomerisations of azobenzenes which are around (100 ns).

2.3.3 Effects of side chain substitution.

The affect of side chain substitution were investigated by Kamogawa.[223-226] The azo compounds were studied in films and in solution. The azo bearing polymers and models were compared by measuring the half life of the recovery, and found that the thermal relaxation reaction was slower with co-monomers which increased chain rigidity, such as styrene and faster with less rigid moieties such as methyl methacrylate.

The main explanation proposed is that the photoisomerisation step from *trans* to *cis* induces steric strain and it is this strain which causes the increased rate of thermal recovery after isomerisation. The effect was noticed when a hindered polymer backbone was appended with azo moieties which caused a degree of strain and unusually high steric interference was found to thermally relax back much slower than other polymers.

The effect of the glass transition temperature (Tg) of the polymers has also been investigated and a fast component of the thermal isomerisation reaction was observed when the polymers were in a glass state. This effect has been seen previously for small azo compounds dissolved in glassy polymers, and was interpreted as evidence for non uniform distribution of free volume in the glassy state.

The size of the Tg depends on the way an azobenzene is attached to a polymer and the time dependence of the Tg for azobenzenes attached to polymers has been studied in relation to the changes in free volume during thermal relaxation.[227]

Similar behaviour was observed by Eisenbach[228-231] for *cis-trans* isomerisation of azobenzene residues attached to co-polymers and investigated below their glass transition temperatures. In solution and in a rubber-like state, the thermal recovery follows first order kinetics, but in a glassy state, some azo groups react anomalously fast while others isomerise at a much slower rate than can be observed in solution.

2.3.4 Cross Linkage

The process of thermal isomerisation in polymer gels and in matrices has been widely investigated. Kumar *et. al*.[232] investigated how photochromism of azo groups lodged in the cross linkers would be affected by the nature of a polymer matrix and by the presence of spacer groups separating them from the main chain. The main result of the investigation was that a bulky substituent next to the azobenzene functionality seems to retard the photoisomerisation process. The comparison of first order plots seems to infer that the thermal isomerisation reaction is not affected by the nature of the polymer matrix but by the orientation that the chromophore is fixed in.

Polyisobutylene swollen gels containing an azo moiety were prepared with the intention of studying the effects on the isomerisation. The rate constant of thermal relaxation was found to be dependent on the density of the cross-linked polymers. Measurements at various temperatures indicated that the activation energy remained unaltered and that the temperature dependence of the reaction rate constant is the result of the dependence on the activation entropy of the cross linked polymer. The isomerisation causes a decrease in the conformational entropy of the chains. The corresponding elastic retraction causes a faster *cis trans* isomerisation which contradicts work conducted by Eisenbach, who postulated that the cross linking was the cause of the slowing down of the thermal isomerisation process.[233-234]

2.3.5 Azobenzenes as trigger molecules.

Photoresponsive polymers are speciality polymers possessing photoreceptor chromophores which can transfer light energy into a conformational change in the polymer.[235] The light energy can be stored in the chemical structure and transferred into the polymer chain, causing reversible conformational changes. The conformational change is expected to produce a change in the physical and chemical properties of the polymer solutions and solids. The use of photoresponsive trigger molecules allows for control of the properties of the polymers by photoirradiation. Examples of photostimulated polymers having azobenzene moieties are described in this section. Some of the physical and chemical properties which can be reversibly controlled include

- Viscosity
- Conductivity
- pH
- solubility
- wettability
- mechanical properties

2.3.6 Photoviscous Polymers

The viscosity of a polymer depends largely upon the conformation of the polymer itself. Irradiation of these polymers leads to a conformational change in which the rod-like shape of the polymers is compacted into a smaller conformation when the polymer is isomerised from the *trans* to the *cis* form. This results in a change in viscosity of the solution and this term is the photoviscosity effect.[236]

Polyamides containing azobenzene have been developed which can photoisomerise upon irradiation and the intrinsic viscosity can be reduced from 1.22 to 0.5 upon UV irradiation and returned to the initial value in 30 hours in the dark at 20°C. Utilising UV and visible light irradiation the viscosity can be reversibly changed by anything up to 60%. With azobenzene units connected by a rigid phenyl group, the resulting viscosity change is large whereas in flexible groups, such as methylene groups, the viscosity changes are small. This has been

demonstrated by showing that there is no photoviscosity change when a long chain is used as the strain can be absorbed. Experiments involving azobenzene based polyamides showed no decrease in viscosity upon UV irradiation, however, upon irradiation at higher concentrations, a small decrease in the viscosity was detected.[237]

Further work conducted in this area shows that there is no effect of concentration on the viscosity of the sample and that a decrease in viscosity has to arise from a conformational change of the polymer chain and not from the interactions between chains.[238]

2.3.7 Photomechanical effects.

Photoisomerisable groups incorporated into polymer frameworks have been shown to cause reversible contraction or expansion of polymer samples upon irradiation. Polyimides containing azoaromatic groups in the backbone were prepared by Agolini and Gay.[239] The imide polymer was obtained in a film with predominantly *trans* azobenzene groups. Upon irradiation, these films contracted due to the isomerisation from *trans* to *cis* in the amorphous regions of the film. Studies of the contraction and the dilation showed that the rate of isomerisation did not control the rate of contraction and dilation. At lower temperatures in the dark, the films returned to the pre-irradiated form.

Contraction and dilation experiments were performed by Eisenbach on stretched polyethylamide networks which were cross-linked with 4,4-bis(dimetacryloylamino) azobenzene which upon irradiation the *trans cis* isomerisation reaction caused conformational changes of the network segments, though the observed contraction recorded here amounted to only about 0.20%.[240]

Riordan *et. al*.[241] also studied polyamide films in which an azo moiety was present on every monomer unit. Upon irradiation the measured stress increases, indications that a contraction has occurred, however in the dark, the stress can be seen to decrease, and thus the contraction ceases and the polymer returns to its pre-irradiation form. This cycle can be repeated many times over again, but the thermal relaxation from *cis* to *trans* in the dark is much faster than for other polymers in solution. This can be explained by the isomerisation of a small fraction of azo residues on the local strained non-equilibrium sites in the polymer matrix. Also,

similar effects were observed with Langmuir films, which are monolayers of photochromic polyamides. Upon irradiation, the contraction effect was observed, which can be monitored as an increase in the area per monomer unit. The thermal relaxation from *cis* to *trans* carried out in the dark shows also that the reaction in Langmuir films is reversible, as the contraction is reversed, i.e. the surface area per monomer unit increases.

2.3.8 Reversible solubility

The incorporation of photoisomerisable chromophores into a polymer chain allows photoisomerisation to occur. Upon isomerisation, the physical properties of the solution are affected, as the isomerisation involves a change of polarity. Changes in the dipole moment can expand or contract the polymer chain.

Much of the work in this area has been conducted by Irie *et. al.*[242,243] and the investigation centred on the reversible solubility of polystyrene in cyclohexane. Polystyrene with 5% of azobenzene pendant groups was dissolved in cyclohexane. Upon irradiation the polymer precipitates out of solution as it becomes insoluble upon irradiation with UV light. Lower weight polymers of azobenzene did not show any change upon irradiation. Upon irradiation with blue visible light, the polymer became soluble again.

The explanation of this is that in cyclohexane, there is intermolecular interactions between the polystyrene and the solvent molecules alongside inter polymer interactions. The increase in dipole moment brought about by UV irradiation is considered to alter the balance of polymer-solvent and polymer-polymer interactions. The amount of precipitation that occurred upon irradiation sharply increased upon increasing the azobenzene content from 5% of the monomer units, which indicated that isomerisation of only a few azobenzene moieties can bring about a solubility change in the polymer.

Further work by Irie *et. al.*[243] showed that a reversible change in the phase separation temperature can be observed in aqueous polymer solution upon irradiation. The use of copolymers of N-isopropylacrylamide with N-(4-(phenylazo)phenyl)acrylamide allowed for the photocontrol of the phase separation temperature of aqueous solutions of the co-polymer formed.

2.3.9 Reversible pH changes.

The control of pH using photoresponsive polymers has also been investigated. Photocontrol of the conformation of poly(methacrylic)acid (PMMA) in solution at varying degrees of ionisation where the polyelectrolyte molecules uncoil is possible by the use of cationic ligands based on azobenzene modified quaternary ammonium salts of co-polymers on cationic ligands. PMMA solutions exhibit a change of 0.2 in the pK_a on *trans* to *cis* photoisomerisation, caused by the change in the coiling of a photoelectrolyte molecule.[244]

Irie *et. al*. investigated the conductivity of dimethylacetamide solutions of a polymer which exhibited a response upon alternate UV and visible light irradiation. The response seen was found to correlate with the isomerisation of azo moieties on the backbone and the dissociation equilibrium of the acid residues in the polymer backbone is influenced by a change in the conformation of the polymer chain. The acid dissociation is greatest in the compact or shrunken form, but in the extended forms the dissociation decreases.[242,243]

2.3.10 Photoresponsive metal ion chelation.

The development of supramolecular chemistry has led to the development of ion sensors. These ion sensors, which are usually macrocycles, work by a change in the conformation brought about by a photoinduced trigger, which when isomerisation occurs, changes the binding ability of the macrocycle. Shinkai developed crown ethers functionalised with azobenzenes which can be controlled by photoisomerisation. It was found by the same group that *cis* crown ethers can bind alkali metal ions by forming a reversible complex with them, a 1:2 metal/ crown sandwich complex. Shinkai also synthesised a polystyrene derivative bearing the 4-azo(benzo-15-crown-5) as the monomeric model and investigated its photoresponsive affinity for alkali metal ions. This study demonstrated that the binding of the alkali metal ions to the functionalised crown ether molecules changes in response to changes in the conformation and side chain polymer configuration also. The activation energy of these polymers was investigated and similar energy barriers were found with low molecular weight analogues, but upon binding to metals, the activation energy increases along with the viscosity. This effect can be summarised as the change in conformational rearrangement of the ligand prior to complexation with the metal ion.[245-247]

2.3.11 Reversible surface energy

The surface energy of a solid is important for functions such as printing and adhesion. If control over the surface energy is obtained and the surface energy can be controlled by external physical stimuli such as light, the material can have numerous applications.

Work by the group of Ishihara[248] into photoresponsive polymers on surfaces showed that using azobenzene modified polymers as thin films gave a change in the water contact angle due to the change in surface free energy upon irradiation with light. The polymers used here were poly(HEMA) and p-(phenylazo)acrylanilide and 2 hydroxyethyl methacrylate co polymers which upon exposure to light exhibit a decrease in water contact angle. If irradiation by visible light followed, the absorbance of the *trans* form returned to the original value before irradiation. This shows that the wettability of a surface can be regulated by the photoisomerisation of the azobenzene moiety.

Work by Irie [249] also showed that the contact angle on a polymer surface could be decreased upon photoisomerisation with UV light, and that the contact angle returned to its pre-irradiation level after being left in the dark overnight.

This investigation of surface energy changes upon photoisomerisation is crucial to the work reported in this thesis on two levels. The first is that to control a large assembly of azo based molecules on a surface, the fundamental study of the isomerisation in solution and in polymers must be carried out first. One of the main aims of this work is to create photoisomerisable surfaces which can be used as a model to apply to fabric coatings.

3.0 Experimental

3.1 Solvents and Reagents

All reagents were purchased as described below. No further purification was attempted on any purchased reagent. Where distilled water is used, MilliQ distilled water (18.0 MΩ/cm is used.

Reagent	Purchased	Purity
Methanol	Fisher	99.9 % HPLC grade
p-Xylene	Aldrich	99% Spec grade
Acetonitrile	Fisher	99.9% HPLC grade
Acetone	Aldrich	99.5% Spec grade
Cyclohexane	Aldrich	99% Spec grade
Dichloromethane (DCM)	Aldrich	99.9% HPLC Grade
Cyanuric Chloride	Aldrich	99% Aldrich technical grade
Aminoazobenzene	Aldrich	98+% Aldrich reagent grade
Chitosan	Aldrich	From Crab shells ~75 % deacetylated
PVA	Aldrich	89000-98000 av mol weight 99% hydrolysed
Sodium Carbonate	Fisher	Reagent grade (99%)
Acetic Acid	Fisher	Reagent grade (98%)
Microcrystalline Cellulose	Aldrich	20µm diameter powder
9-Anthracene-carboxylic acid	Aldrich	99% Aldrich reagent grade

3.2 Compounds Studied.

Both the Admat 1, Admat 2 and Cfam 29 and Cfam 23 were prepared on site at DSTL. The synthesis of these compounds is reported in section 3.23.

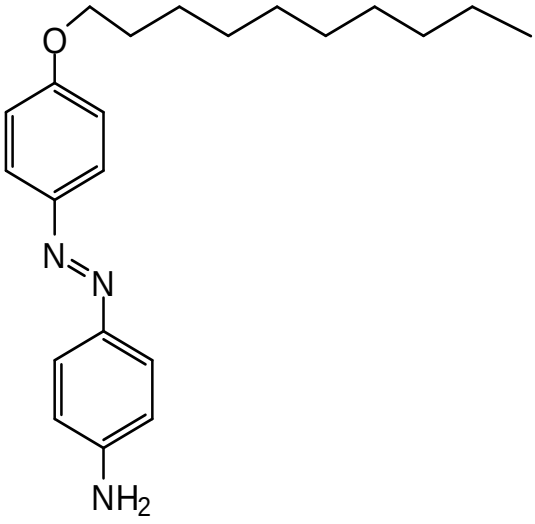

Cfam 29

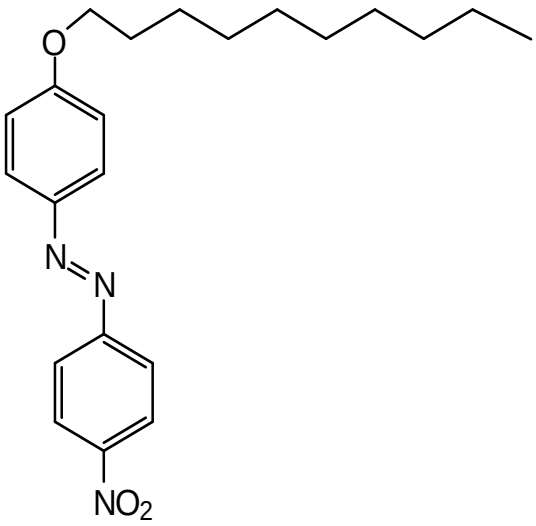

Cfam 23

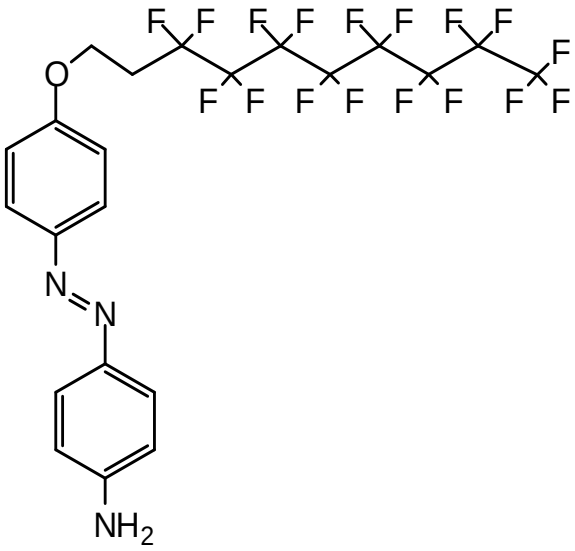

Admat 1

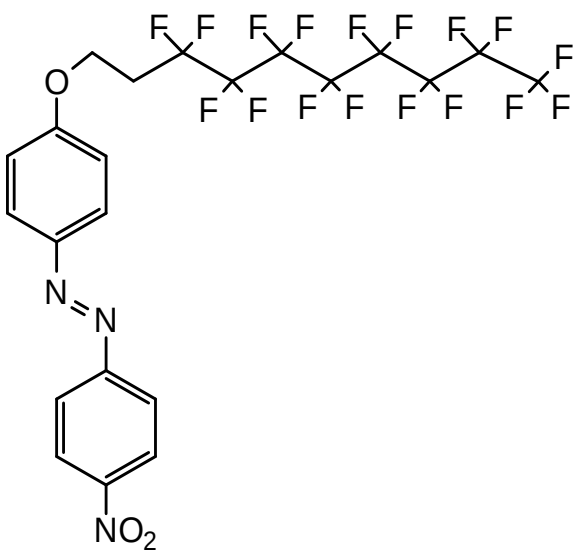

Admat 2

Figure 13: Azobenzene compounds studied

3.3 Ground State Absorbance Spectra

For this procedure, a Hewlett Packard diode array spectrophotometer (Model No: HP8453) was used. All wavelengths of light from 190nm to 1100nm were measured simultaneously. This system also uses a low power light, composed of two lamps, a tungsten and a deuterium lamp.

The sample is placed in a fused silica cuvette (path length 1cm) and is then placed between the light source and the detector. The amount of light transmitted through the sample can then be measured. The machine must first be blanked, using a sample of the solvent, giving the I_0 value, and the absorbance and transmission at all wavelengths can then be measured. The computer which is attached to the spectrophotometer displays the spectra as either absorbance or transmission.

3.4 Ground state Fluorescence Spectra

Fluorescence measurements were measured using a Spex Fluoromax spectrofluorimeter using right angle geometry. Fused 1 cm path silica glass cuvettes were used, the aperture slit width was 1mm and excitation was accomplished at 350nm unless otherwise stated.

3.5 Deoxygenation of samples

All samples were purged of oxygen by nitrogen bubbling prior to fluorescence studies. The solution in a cuvette was fitted with a rubber septum. A tube from a nitrogen cylinder fitted with a needle is placed in the rubber septum and another needle is placed in the rubber septum to act as an exit for displaced gases. The solutions were purged with nitrogen for 10 minutes prior to fluorescence measurements.

3.6 Drying of microcrystalline cellulose

All microcrystalline cellulose samples were dried at 70°C for 24 hrs *in vacuo* before use.

3.7 Direct Dyeing

Direct dyeing of a compound to cellulose is reliant upon the formation of van der Waals forces to bind the fibres and also upon hydrogen bonding between the dye and the cellulose OH groups. The procedure for direct dyeing is dissolving a known concentration of a compound into a volatile solvent, adding the solution to 3 g of cellulose and allowing the solvent to evaporate, followed by drying *in vacuo* at 70°C overnight.

3.8.0 Reactive Dyeing

The dye is attached to the cellulose surface via a triazinyl coupling reaction. This procedure requires a reactive group, in this case a triazinyl derivative, to bind to both the dye and the cellulose. The chosen reagent for this procedure was cyanuric chloride, which consists of a trichlorotriazinyl ring. The scheme for the reaction is outlined below. (Figure 14)

3.8.1 Procedure for preparing triazinyl aminoazobenzene [250]

To a cooled biphasic solution of cyanuric chloride (4 mmol,0.74 g) in dichloromethane (50 ml) and sodium carbonate (4 mmol, 0.44 g) in water (50ml) was added 4-aminoazobenzene (4 mmol, 0.79 g) in 10 ml of dichloromethane. The reaction was stirred at 0°C for 1 hour before the mixture was separated, the organic layer washed with water (50 ml) and dried over anhydrous magnesium sulphate for 15 minutes. The organic layer was concentrated to afford triazinyl coupled 4- aminoazobenzene as a light brown solid. The crude solid was then dissolved in dichloromethane and petroleum ether 40/60 was added until the triazinyl compound precipitated out. The precipitate was removed via filtration and dried in a vacuum dessicator overnight. (1.22 g, 88% yield) MS FAB^+ *m/z* 345.202. (Calculated 345.19)

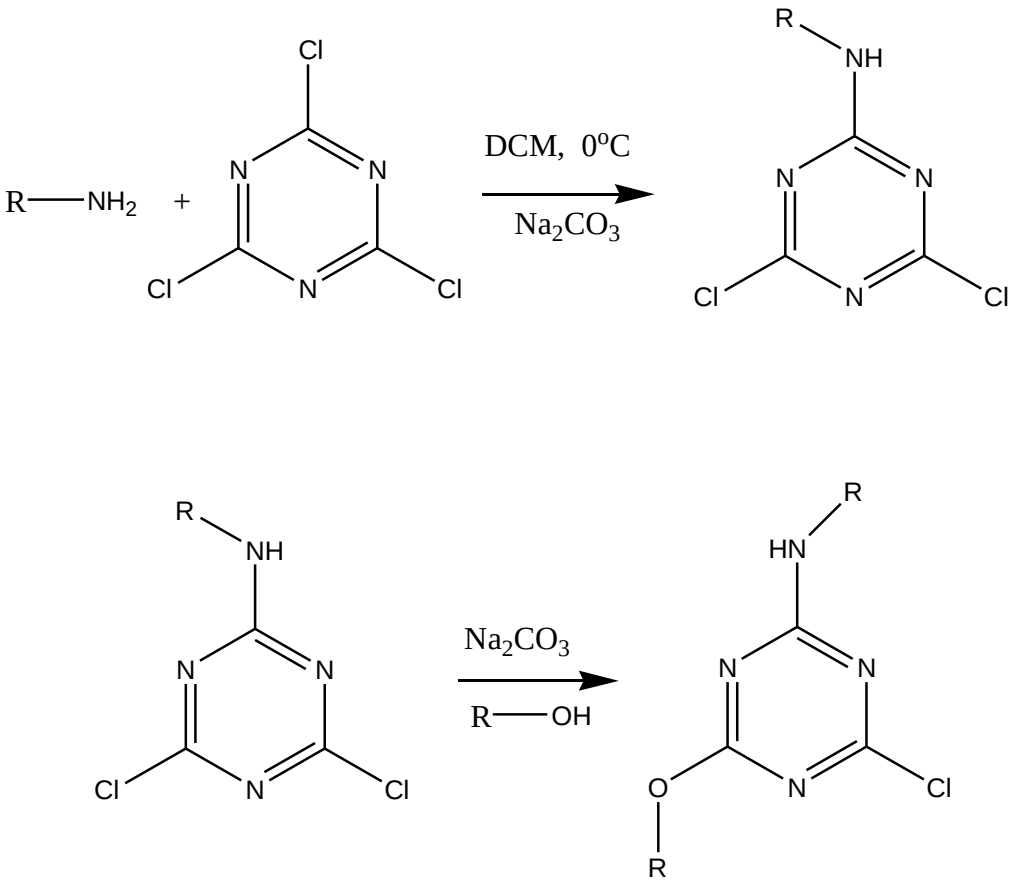

Figure 14: Synthesis of triazinyl coupled derivatives

3.9 Diffuse Reflectance

Diffuse reflectance measurements were carried out using a Perkin Elmer Lambda Bio 40 spectrophotometer. An integrating sphere is used to ensure all the diffusely reflected light is collected. The apparatus contains a low intensity light source. The percentage intensity of light reflected from a white surface is the reflectance. The standard chosen was barium sulphate in a 10mm path length fused silica cuvette, in order to conduct measurements below 300nm, as glass absorbs light below this wavelength.

The remission function is determined according to the Kubelka Munk equation

F(R) = K/S = $(1 - R\infty)2/\ 2R\infty$ (Eqn 1.6) [251]

K is the Absorption Coefficient = the limiting fraction of absorption of light energy per unit thickness, as thickness becomes very small.

S is the Scattering Coefficient = the limiting fraction of light energy scattered backwards per unit thickness as thickness tends to zero.

The molar absorption coefficient of the absorbing substance can be found via the utilisation of the remission function F(R). There should be a linear relationship between the concentration of the adsorbed compound and the remission function if no aggregation is present.

3.10 Diffuse reflectance at a single wavelength.

The spectrophotometer is set to record the reflectance at 380 nm overnight (12 hours, 720 mins), a blank is taken (barium sulphate) and the reflectance before irradiation is taken. The sample is irradiated for 10 minutes in a 150W Xenon arc lamp and the reflectance measured as the *cis* isomer recovers to the *trans* isomer. The reflectance of the sample before irradiation is subtracted from the values for the reflectance after irradiation in order to obtain the percentage change in reflectance which is then plotted as a function of time.

3.11 Preparation of 9-anthracene carboxylic acid on cellulose samples

Samples were prepared by drying 3 g of cellulose (surface area estimated at 100 $m^2 g^{-1}$) at 70°C under full vacuum. The anthracene-9- carboxylic acid was dissolved in HPLC methanol (25 ml) and added to the dried cellulose samples.

Amounts of anthracene-9-carboxylic acid were calculated as below:

Estimated Surface area of cellulose: 100 $m^2 g^{-1}$
Estimated surface area of molecule of 9-anthracene carboxylic acid 64 x 10^{-20} m^2
100/64 x 10^{-20} = 1.56 x 10^{20} molecules for a monolayer

1.56 x 10^{20} / N_A (6.022 x10^{23}) = 2.59x10^{-4} moles for a monolayer.
Mr 9-anthracene-carboxylic acid = 222.24 = 0.058g for 100% monolayer

3.12 Synthetic procedure for triazinyl coupling of Admat 1 [250]

To a cooled biphasic solution of cyanuric chloride (0.23 mmol, 41 mg) in dichloromethane (50 ml) and sodium carbonate (16 mg, 0.15 mmol) in water (50 ml) was added Admat 1 (0.1 g, 0.15 mmol) in 10 ml of dichloromethane. The reaction was monitored by TLC and stirred at 0°C for 1 hour before the mixture was separated, the organic layer washed with water (50 ml) and dried over anhydrous magnesium sulphate for 15 minutes. The organic layer was concentrated to afford crude triazinyl coupled Admat 1 as a light brown solid. The crude triazinyl derivative was dissolved in dichloromethane and petroleum ether (40/60) was added dropwise until the triazinyl derivative precipitated out. The precipitate was removed via filtration and dried in a vacuum dessicator overnight. (97 mg, 80% yield) MS FAB^+ *m/z* 806.543. (Calculated: 806.53)

3.13 Adsorbing aminoazobenzene to cellulose surface

The procedure for adsorbing the aminoazobenzene to the surface is as follows.

The cellulose was dried overnight for 24 hours under full vacuum. The required amount of aminoazobenzene was added to 25 ml of methanol and allowed to dissolve. The methanol solution was added to the dried cellulose and the methanol allowed to evaporate. The resulting yellow mixture was dried at full vacuum at room temperature for 24 hours. Diffuse Reflectance was carried out on all samples produced

3.14 Coupling aminoazobenzene to cellulose [250]

The aminoazobenzene coupled to cellulose was prepared via triazinyl coupling the aminoazobenzene compound and then coupling it to cellulose. This method is also suitable for coupling the Admat 1 triazinyl derivative to the surface of cellulose and silica.

The solution of triazinyl coupled 4-aminoazobenzene in 1:3 water acetone mixture was added to a suspension of 3 g of cellulose in sodium carbonate solution (20 g/dm^3).
The mixture was left to react for 1 hour. The reaction mixture was filtered, the solid washed with acetone/water mixture (1:3) and dried under vacuum at room temperature for 24 hours.

3.15 Chitosan Films

Prepared according to Chen *et al* [252]

Chitosan powder (2.5 g) was added to 100 ml of 0.1 M acetic acid solution and stirred to form a clear amber-coloured liquid. PVA (polyvinyl alcohol) (2.5 g) was added to 100 ml of 80°C hot water and stirred until it dissolved to form a clear solution. In order to form films, 5 ml of the chitosan solution and 5 ml of the PVA solution were mixed together in a 50 ml beaker to form 10 ml of a 50/50 mixture of chitosan and PVA and stirred for 10 minutes at room temperature. A microscope slide was then added to the mixture and allowed to drip free of solution. The slide was then dried in an oven at 100°C overnight under vacuum.

3.16 Coupling the aminoazobenzene to the surface of chitosan via triazinyl derivative.

Chemically coupling the aminoazobenzene compound to the surface was accomplished via the use of the triazinyl derivative of aminoazobenzene, a solvent (THF) and a base (sodium carbonate).

The chemical coupling reaction was accomplished in THF using a base (sodium carbonate), with stirring to afford a chemically coupled slide for comparison to the adsorbed slides as described above. This reaction was previously tried in DCM but did not appear to work.

Triazinyl coupled aminoazobenzene (2 mg) was dissolved in 50 ml of THF and 1 equivalent of sodium carbonate was added to the solution. The mixture was stirred for 10 minutes in order for all of the triazinyl coupled compound to dissolve in the THF. The chitosan coated microscope slide was then placed in the reaction mixture with gentle stirring, and left to react for 1 hour, in order to ensure enough time for the coupling reaction to take place. The absorbance of the slide was then measured after 1 hour and then replaced into the reaction mixture. The absorbance was then measured every hour for a further three hours.

3.17 Adsorbing azobenzene compounds to the surface of chitosan slides

The microscope slides coated in chitosan/PVA mixture, were then used in experiments to determine the adsorption of aminoazobenzene to the surface. It was decided to adsorb

aminoazobenzene to the surface by dissolving the compound in chloroform and dripping it on, leaving it to evaporate and then measuring the absorbance.

Initially a solution of aminoazobenzene in chloroform (1 mg /25 ml) was prepared and 0.1 ml was dripped onto the slide via a pipette and allowed to evaporate. The absorption of the slide was then measured and compared to the blank slide without any aminoazobenzene on the surface. The formation of crystals on the surface of the slide suggested that the concentration was too high, so a lower concentration was tried.

The 1 mg/25 ml solution was diluted 10 times (1 ml in 10 ml of chloroform) and 1 ml was dripped onto the slide, the solvent was left to evaporate and the absorbance was measured again, and both the higher concentration and lower concentration slides were examined via UV-Vis spectroscopy.

3.18 Activation energies of thermal relaxation reaction in solution

Measurement of the activation energies in solution was accomplished via measuring the rate of thermal relaxation in solution at a range of temperatures, 20°C, 30°C, 40°C and 50°C. The Arrhenius Equation was then utilised to work out activation energy by plotting ln(k) against 1/T

$k = Ae^{-Ea/RT}$ Equation 1.7

$\ln k = \ln A - E_a/RT$

Where k = rate constant (s^{-1}), A = pre-exponential factor, (maximum rate constant), E_a is the activation energy R=universal gas constant and T = absolute temperature (K)

Thus the plot of lnk against 1/T gives the gradient as $-E_a/R$. As the value of R is known (universal gas constant), E_a can be calculated.

3.19 Functionalising the surface of silica with Aminopropyltriethoxysilane

Silica gel (60Å 3 g) was added to a 100 ml round bottom flask along with 30 ml of toluene. The solution was heated to reflux and then APTS (0.57 ml, 2 mmol) was added to the solution and the mixture was refluxed for 6 hours. The toluene was removed under vacuum and the resulting slurry stirred with methanol water mixture (1:1, 30 ml) for 2 hours to removes any excess, unreacted APTS. The mixture was filtered and washed with methanol (30 ml) and dried in an oven at 50°C for 3 hours

3.20 Coupling the triazinyl azobenzene derivates to the silica surface

The required amount of triazinyl Admat 1 or aminoazobenzene was dissolved in acetone (30 ml) and added to 3 g of silica gel and dried at 100°C overnight in an oven. Sodium carbonate (2eqv) in water (15 ml) was added in order to raise the pH to 10.9 to deprotonate the hydroxyl groups on the surface. The reaction mixture was stirred at room temperature for 2 hours, then the mixture was filtered and the solid silica was then washed with acetone and the concentration on the surface was calculated via the absorbance of the solution before and after the filtration process.

3.21 Contact angle studies

Contact angle measurements are most commonly used to determine surface wettability. The contact angle for a liquid on a flat surface is defined as the co-operative result of three different types of surface tension at the solid/liquid/gas interface. The basis of Youngs' equation is that hydrophilicity is defined as a contact angle of less than 90° on a solid surface, whereas hydrophobicity refers to a contact angle of greater than 90° (see Figure 15). This equation reflects some aspects of surface wettability, however, the definition of hydrophilicity should be able to reflect the chemical and physical characteristics of the solid/liquid/gas interface.

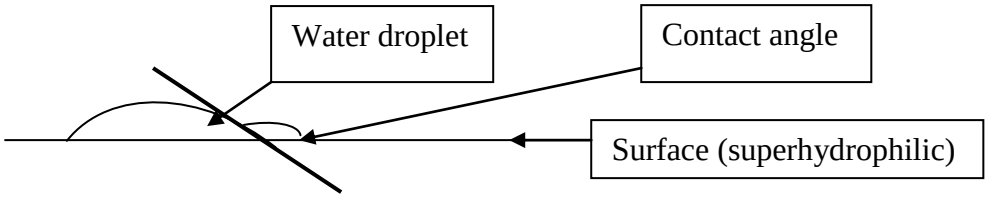

Superhydrophilic surface, almost totally wet.

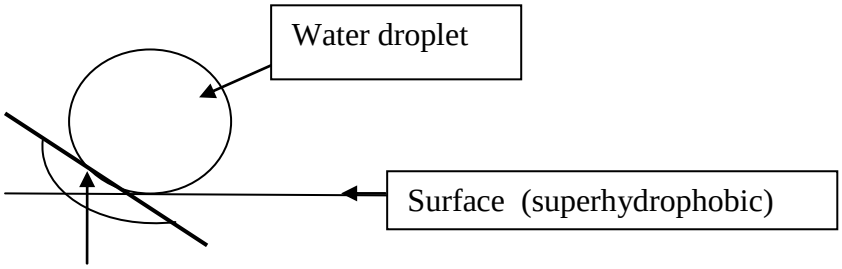

Superhydrophobic surface, no wetting present.

Figure 15. Contact angle diagram.

Vogler *et al.* defined a hydrophilic surface as having a contact angle greater than 65° and a hydrophilic surface having a contact angle of less than 65°.[254]

This definition is clearly different from the classical 90° definition as given above by Young. There still remains continuous debate in the literature, even with an abundance of experimental evidence which has assisted in the understanding of the properties of surface wettability, such as surface roughness and contact angle hysteresis. For example, Feng showed that a polyvinyl alcohol (PVA) nanofibre film shows a contact angle of 171°, whereas on a smooth PVA surface the contact angle was only 72°.[255]

X. Feng demonstrated that on a rough titanium dioxide nanostructure film, the contact angle is 154°, whereas on a smooth titanium dioxide surface, the contact angle is 74°.[255] The presence of phenomena such as this make the dividing line between hydrophilic and hydrophobic proposed by Young (90°) seem ambiguous, as a hydrophilic surface should become more hydrophilic with the introduction of surface roughness, as grooves within the surface allow liquid to spread out, as surface area is increased.

Solid surfaces which are defined a ‘flat’ are in fact not perfectly flat, but possess roughness. This effect of surface roughness has to be taken into account when considering surface

wettability. This factor is represented by the term r, or the surface roughness factor, which is the ratio of the actual area to the projected area. The Wenzels[257] equation and Cassies[258] equation are the principal theories which account for the relationship between surface roughness, (defined as r on solid surfaces) and contact angle.

In the model proposed by Wenzel,[257] an assumption has been made that the liquid can enter completely and contact the concave regions upon the solid surface with the equation:

$\cos\theta_r = r\cos\theta$

Where θ_r is the contact angle on a rough surface

Where air is trapped by a liquid to give a composite surface, then Cassies[258] model can be applied and therefore the apparent contact angle is described in the following equation

$\cos\theta_r = rf_1\cos\theta - f_2$

Where f1 and f2 are the area fractions of the projection solid and vapour on the surface, respectively, and f1 + f2 =1.

The two theories described above demonstrate that surface roughness can increase the surface wettability on solid surfaces either hydrophobic or hydrophilic. The models above allow tuning of the surface wettability by controlling surface structure independently of chemical composition.

3.22 Laser Flash Photolysis Experiments

Laser flash photolysis investigations were conducted using azobenzene compounds coupled and adsorbed to the chitosan coated slides. Flash photolysis was conducted using a Neodymium YAG laser (Photonics Limited), frequency doubled at 355 nm and a timebase of 0.1ms. The fundamental operating wavelength of the Neodymium YAG laser is 1064 nm.

3.23 Fitting of exponential data

The fitting of data in chapters 4, 5, 6 and 7 was fitted using the first order rate parameter in Microcal Origin version 6.1 i.e. ($[A] = [A]_0 \exp^{(-kt)} + y_0$) unless otherwise stated.

3.24 Contact angle measurements and wettability

Contact angle measurements were made by placing a 2 µl droplet of either water or hexadecane on the surface of the slides. An image of the drop, which is magnified, is taken and the contact angle is calculated by measuring the angle at the solid/ liquid interface. The process is repeated in other areas of the slide and an average of these results is taken.

3.25 Synthesis of the Azo-benzene compounds [259]

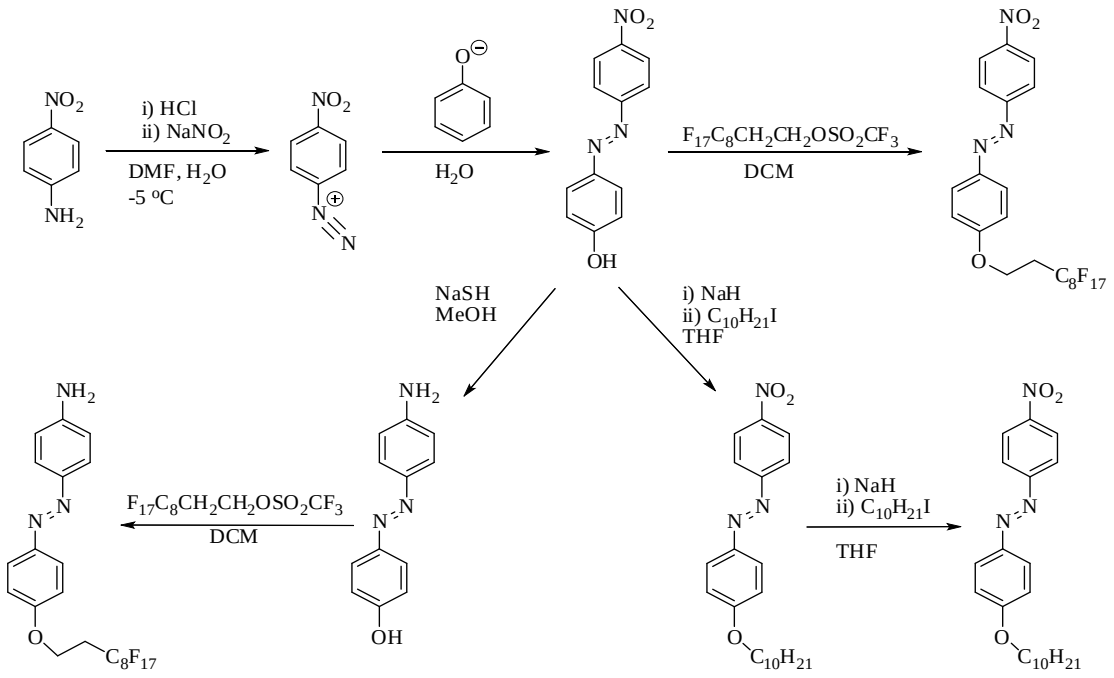

Figure 15: Synthesis of Admat 1 and Cfam hydrocarbon analogues

Synthesis of 4-Hydroxy-4′-nitroazobenzene

To a stirred solution of 4-nitroaniline (145 mmol, 20 g) in 60 ml DMF hydrochloric acid (363 mmol, 5 M, 72.5 ml) was added slowly, ensuring the temperature remained below 5 ^{O}C. This was treated with sodium nitrite (145 mmol, 10.0 g) in 60 ml water, ensuring the temperature was kept below 5 ^{O}C, to form the yellow diazonium salt which was added to a solution of phenol (145 mmol, 13.65 g) and sodium hydroxide (752 mmol, 29.0 g) in 500 ml water to

form a dark purple solution. Acidification with 5 M hydrochloric acid (479 mmol, 96 ml) formed orange 4-Hydroxy-4′-nitroazobenzene. This was isolated, washed with water (2 x 150 ml), re-dissolved in ethyl acetate, dried, filtered and stripped to yield a dark orange solid purified by Soxhlet extraction in methanol and recrystallised to yield 24.16 g (68.5 %).

^{1}H NMR (300.53 MHz, CD_3CN): δ 6.99 (m 2H), 7.89 (m 2H), 7.97 (m 2H), 8.34 (m 2H).
^{13}C-{^{1}H} NMR (75.57 MHz, CD_3CN): δ 117.0, 123.9, 125.7, 126.7 (all s, C_{Ar}) δ 162.9 (all s, C_{ipso})
MS ESI: *m/z* 288 [MH^+]

Synthesis of 4-Hydroxy-4′-aminoazobenzene
4-Hydroxy-4′-nitroazobenzene was reduced to 4-hydroxy-4′-aminoazobenzene by the method described in Vogel. [182]

To sodium sulphite nonahydrate (74.8 mmol, 16.76 g) dissolved in 50 ml water, solid sodium hydrogen carbonate (71.0 mmol, 5.97 g) was added portion-wise. Methanol (50 ml) was added to the solution and cooled to 15 °C. The precipitated sodium carbonate was removed by filtration and washed with methanol (3 x 15 ml). The filtrate and washings were added to a hot methanol (50 ml) solution containing 4-hydroxy-4’-aminoazobenzene (41.1 mmol, 10.0 g). This was refluxed for 20 minutes and most of the methanol was removed by distillation. The reaction mixture was poured into 200 ml cold water and storage in the fridge produced dark crystals 2.45 g.

^{1}H NMR (300.53 MHz, CD_3CN): δ 4.69 (br NH_2), 6.72 (m 2H), 6.91 (m 2H), 7.66 (m 2H), 7.71 (m 2H).
MS ESI: *m/z* 214 [MH^+]

Triflate Synthesis
To trifluoromethanesulphonic anhydride (70.9 mmol, 23.7 ml) in 200 ml dichloromethane at 0 °C, 1H, 1′H, 2H, 2′H-perfluorodecan-1-ol (142 mmol, 32.9 g) and pyridine (142 mmol, 11.4 ml) in 100 ml dichloromethane was added. Upon addition a white precipitate formed. The reaction mixture was stirred for 16 hours, washed with water (3 x 200 ml), dried over

magnesium sulphate, filtered and solvent removed under reduced pressure to yield a white solid 35.9 g, 85%.

^{1}H NMR (300.53 MHz, $CDCl_3$): δ 4.78 (t, $^{3}J_{(HH)}$ 6 Hz, 2H), 2.67 ppm (tt, $^{3}J_{(HH)}$ 6 Hz $^{3}J_{(HF)}$ 17 Hz 2H)

^{19}F-{^{1}H} NMR (282.78 MHz, $CDCl_3$): δ -74.5 (s, CF_3), -80.6 (t, $^{3}J_{(FF)}$ 10 Hz), -113.4 (br, CF_2CH_2), 121.5 (br, $2CF_2$), 121.7 (br, CF_2), 122.6 (br, CF_2), 123.3 (br, CF_2), -125.9 (br, CF_2)

GC-MS: m/z 427 [M^+ -$OSOCF_3$ and –HF]

mp: 43.4 - 44.4 °C

Synthesis of 4-(1H, 1′H, 2H, 2′H-perfluorodecan-1-one)-4′-aminoazobenzene

To sodium (12.6 mmol, 0.29 g) dissolved in 50 ml ethanol solid 4-hydroxy-4'-aminoazobenzene (12.6 mmol, 2.7 g) was added portion-wise and stirred for 30 mins to form a dark coloured, basic solution. 1H,1′H, 2H,2′H-perfluorodecane triflate (12.6 mmol, 7.5 g) in 40 ml ethanol was added. An orange precipitate formed upon addition. The reaction mixture was stirred for 10 mins before adding water (100 ml). A brown solid was isolated and washed with 0.5 M sodium hydroxide solution and then water until the eluent was neutral to yield 4-(1H, 1’H, 2H, 2’H-perfluorodecan-1-one)-4’-aminoazobenzene, 2.68 g, 32.3 %.

^{1}H NMR (500.16 MHz, $CDCl_3$): δ 2.66, (tt, $^{3}J_{(HH)}$ 7 Hz $^{3}J_{(HF)}$ 18 Hz), 4.35 (t, $^{3}J_{(HH)}$ 7 Hz, 2H), 6.74 (m, 2H), 6.99 (m, 2H), 7.77 (m, 2H), 7.84 (m, 2H)

^{13}C-{^{1}H} NMR (125.77 MHz, $CDCl_3$): δ 114.8, 116.4, 124.1, 124.8 (s, CH-Ar)

MS FAB$^+$: m/z 659.08730 (calc. 659.088135) [M^+]

Synthesis of 4-(1H, 1′H, 2H, 2′H-perfluorodecan-1-one)-4′-nitroazobenzene

To sodium (12.6 mmol, 0.29 g) dissolved in 50 ml absolute ethanol solid 4-hydroxy-4′-nitroazobenzene (12.6 mmol, 2.7 g) was added portionwise to form a dark coloured, basic solution followed by 1H,1′H, 2H,2′H-perfluorodecane triflate (12.6 mmol, 7.5 g) in 40 ml ethanol was added dropwise to the stirred solution. An orange precipitate formed upon addition. The reaction mixture was stirred for 10 mins. Water (100 ml) was added to the solution and the solid was isolated in a sinter funnel. The solid was washed with 0.5 M sodium hydroxide solution and then water until the eluent was neutral. Yield 2.68 g, 32.3 %.

^{1}H NMR (300.53 MHz, $CDCl_3$): δ 2.70 (tt 18, 7 Hz, 2H CH_2), 4.39 (t, 7 Hz, 2H, CH_2), 7.05 (m, 2H, CH), 7.99 (m, 4H, CH), 8.37 ppm (m, 2H, CH)

^{19}F-{^{1}H} NMR (282.78 MHz, $CDCl_3$): δ -113.1 (m, 3F, CF_3), -121.5 (br, 2F, CF_2), -121.8 (br, 4F, CF_2), -122.6 (br, 2F, CF_2), -122.9 (br, 2F, CF_2), -123.3 (br, 2F, CF_2), -125.9 ppm (br, 2F, CF_2)

MS FAB^{+}: m/z 689.06140 (calc 689.062012) [M^{+}]

Synthesis of 4-(decan-1-one)-4′-nitroazobenzene

To a stirred solution of sodium hydride in and 4-nitro-4'-hydroxy azobenzene in DMF (10 ml) iodomethane (2 eqv) was added drop wise. The reaction mixture was stirred for 14 hours. 100 ml water was added to the reaction mixture and the product was extracted into hexane, dried with magnesium sulphate and stripped to yield an orange solid. Chromatography on silica gel eluted with ethyl acetate:hexane 1:4 yielded 0.61 g, 67 % product.

^{1}H NMR (300.53 MHz, $CDCl_3$): δ 0.86 (t, 3H, CH_3), 1.26 – 1.51 (m, 14H, CH_2), 1.81 (tt, 7, 15 Hz, CH_2), 4.05 (t, 7Hz, CH_2), 7.01 (m, 2H, CH_2), 7.96 (m, 4H, CH_2), 8.35 ppm (m, 2H, CH_2)

MS FAB^{+}: m/z 384.22938 (calc 384.229060) [MH^{+}]

Synthesis of 4-(decan-1-one)-4′-aminoazobenzene

4-(decan-1-one)-4′-nitroazobenzene was reduced to 4-(1H, 1′H, 2H, 2′H-decan-1-one)-4′-aminoazobenzene by the method described in Vogel.[260]

To sodium sulphite nonahydrate (3.04 mmol, 0.75 g), dissolved in 20 ml water, solid sodium hydrogen carbonate (3.0 mmol, 0.25 g) was added portion-wise. Methanol (15 ml) was added to the solution and cooled to 15 °C. The precipitated sodium carbonate was removed by filtration and washed with methanol (3 x 15 ml). The filtrate and washings were added to a hot methanol (20 ml) solution containing 4-(1H, 1′H, 2H, 2′H-decan-1-one)-4′-nitroazobenzene (1.3 mmol, 0.5 g). The reaction mixture was refluxed for 20 minutes and 50 ml of the methanol was removed by distillation. The reaction mixture was then poured into 200 ml cold water and storage in the fridge produced an orange solid yield 0.53 g.

Chromatography, on silica gel, eluted with ethyl acetate:hexane 1:4 yielded product 0.26g, 33 %.

^{1}H NMR (300 MHz, $CDCl_3$): δ 0.88 (t, 7 Hz, 3H, CH_3), 1.23 – 1.49 (m, 14 H, CH_2), 1.81 (tt, 7, 15 Hz, 2H, CH_2), 3.98 (br, 2H, NH_2), 4.01 (t, 2H, CH_2), 6.74 (m, 2H, CH), 6.97 (m, 2H, CH), 7.76 (m, 2H, CH), 7.83 ppm (m, 2H, CH)
MS FAB$^+$: m/z 353.24625 (calc 353.24671) [MH^+]

Chapter 4.0: Solution studies

4.1 Overview of solution studies

The emission and absorption properties of the adaptive materials supplied were studied in order to gain information regarding the processes these compounds undergo when excited. The absorption spectra in solution at room temperature were studied in order to obtain extinction coefficients in different solvents. Further to those studies, the activation energies for the thermal *cis-trans* isomerisation processes in different solvents were then studied. Understanding of the molecular processes that occur in solution is fundamental to any work with photoisomerisable molecules. There is a fundamental requirement to understand what occurs at a molecular level in solution as this will help to make a comparison between molecules of azobenzene in solution and immobilised on surfaces, which as they are immobilised are possibly hindered by torsional strain.

4.2 Absorbance spectra in the Ground State

The azobenzene derivatives **1** and **2** were dissolved in a variety of solvents listed below in order to measure ground state absorbance and photoisomerisation in solution. Quantitative measurements (molar absorption coefficients) were made using the Beer-Lamberts law as previously described in section 1.3.1. The absorption spectra of Admat 1 in acetone is shown in Figure 17. The dyes are insoluble in water, but are soluble in acetonitrile, p-xylene, cyclohexane and acetone.

The absorption spectra shown do obey the Beer-Lambert law at given concentrations from 2 x 10^{-6} mol dm^{-3} to 5x10^{-5} mol dm^{-3}. The shape of the spectra do not change over this chosen concentration range, indicating that aggregation does not occur.

As the azobenzene derivatives used here are substituted, the absorption spectrum shifts to longer wavelengths (365 nm for Admat 2 and 380 nm for Admat 1 in acetone solution, see figure 17). In aminoazobenzene compounds, the effect is more pronounced on the π-π* absorption than on the n-π* absorption. This results in closer proximity of the n-π* and π-π* states, transition to the n-π* not being resolved in these spectra (as stated previously, the

molar absorption coefficient for the n-π* transition is larger in the *cis* than the *trans* form, although is still some 20 times lower than for the π-π* absorption.

For example in acetonitrile, there is a second π-π* absorption at shorter wavelengths corresponding to excitation to S_3 (around 275nm), although this is obscured by solvent absorption in acetone. The amino substitution is found to shift the absorption to longer wavelengths than is seen for the nitro substitution.

Most transitions result in an excited state, which is more polar than the ground state. Therefore the energy of the excited state is higher than the ground state. Thus it can be observed that alcohol solutions give longer wavelength maxima than hydrocarbon solutions, which translates to a red shift in the peak maxima of about 5 nm-10 nm when changing solvent from hydrocarbons (such as cyclohexane) to alcohols such as methanol.

This is due to the Franck-Condon principle. However, the Franck-Condon principle dictates that, upon excitation of a chromophore, the molecule is excited to a higher electronic energy level in a far shorter timeframe than it takes for the chromophore and solvent molecules to re-orient themselves within the solvent-solute interactive environment. As a result, there is a time delay between the excitation event and the re-ordering of solvent molecules around the solvated chromophore, which generally has a much larger dipole moment in the excited state than in the ground state.

After the chromophore has been excited to higher vibrational levels of the first excited singlet state (S_1), excess vibrational energy is rapidly lost to surrounding solvent molecules as the chromophore slowly relaxes to the lowest vibrational energy level (occurring in the picosecond time scale). Solvent molecules assist in stabilizing and further lowering the energy level of the excited state by re-orienting (termed solvent relaxation) around the excited chromophore in a slower process that requires picoseconds. This has the effect of reducing the energy separation between the ground and excited states, which results in a red shift (to longer wavelengths) of the absorbance emission. Increasing the solvent polarity produces a correspondingly larger reduction in the energy level of the excited state, while decreasing the solvent polarity reduces the solvent effect on the excited state energy level.

The polarity of the chromophore also determines the sensitivity of the excited state to solvent effect.

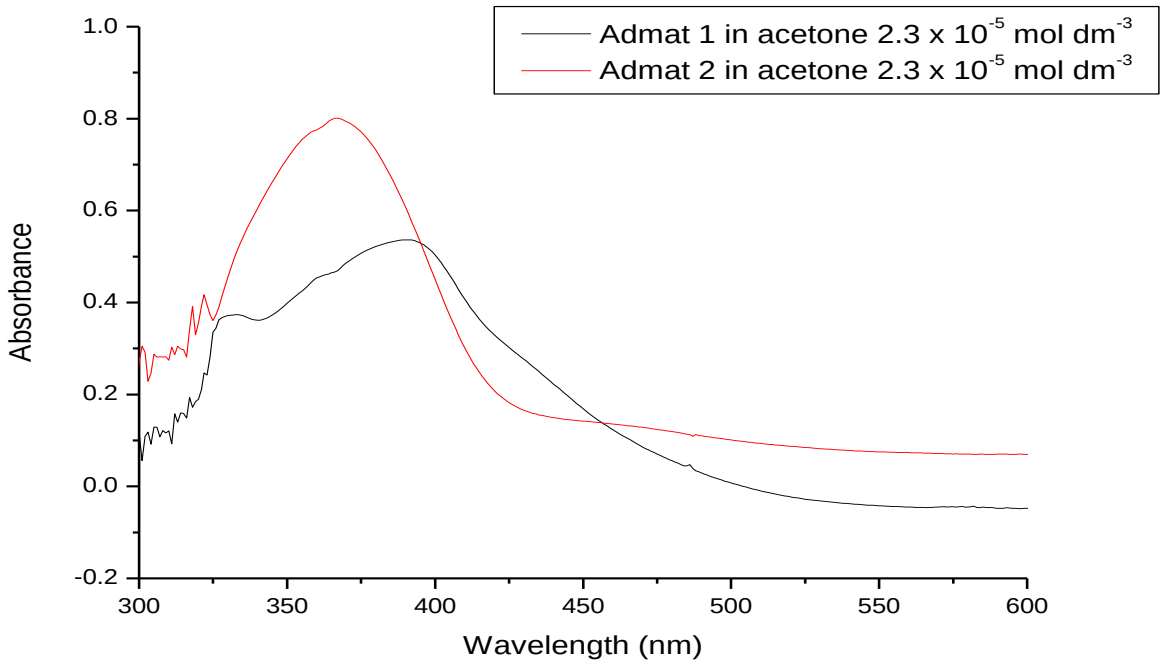

Figure 17: Absorption spectra of Admat 1 and Admat 2 in acetone

4.3 Fluorescence

An unsuccessful attempt to detect emission from both Admat 1 and Admat 2 in solution was made. Concentration ranges from $1x10^{-6}$ mol dm^{-3} to $1x10^{-5}$ mol dm^{-3} were used in order to detect fluorescence. Radiative transitions are less likely to happen as the movement of the molecule is unrestricted. This has also been found from previous investigations which were mentioned in the introduction section, that fluorescence is only detectable from azobenzene molecules in a rigid glass at low temperatures. If a molecule can move around freely then radiative transitions occur less frequently, as energy is lost via torsional and rotational motion as oppose to transitions.

In order to possibly enhance their fluorescence, both compounds were adsorbed onto microcrystalline cellulose, as the movement of the molecules becomes more restricted but

isomerisation still occurs, making non-radiative transitions less efficient and therefore unlikely to happen, whereas radiative transitions, such as fluorescence are more likely to occur. Emission was subsequently not detected from Admat 1 and Admat 2 on cellulose. The scattering from the cellulose was too high and possible weak emission from the dyes was lost in noise. The fluorescence spectrum of microcrystalline cellulose does not differ from that of the adsorbed compounds indicating that they do no fluoresce on microcrystalline cellulose.

4.4 Photoisomerisation of fluorinated azobenzene derivatives in solution

Solutions of the azobenzene compounds Admat 1 and Admat 2 were irradiated using the unfiltered output of a xenon arc lamp. The photobleaching was conducted in order to ascertain the lifetime of the *cis* isomer in solution. The rapid photobleaching in the peak at 380nm (Fig 18) and the relative increase in the absorption at 470nm is relative to *cis* to *trans* isomerisation. The presence of an isosbestic point at 460nm and at 325 indicates the presence on two isomers. The lifetime of the *cis* state was monitored in several solvents in order to ascertain if the solvent had any effect on the lifetime of the *cis* isomer.

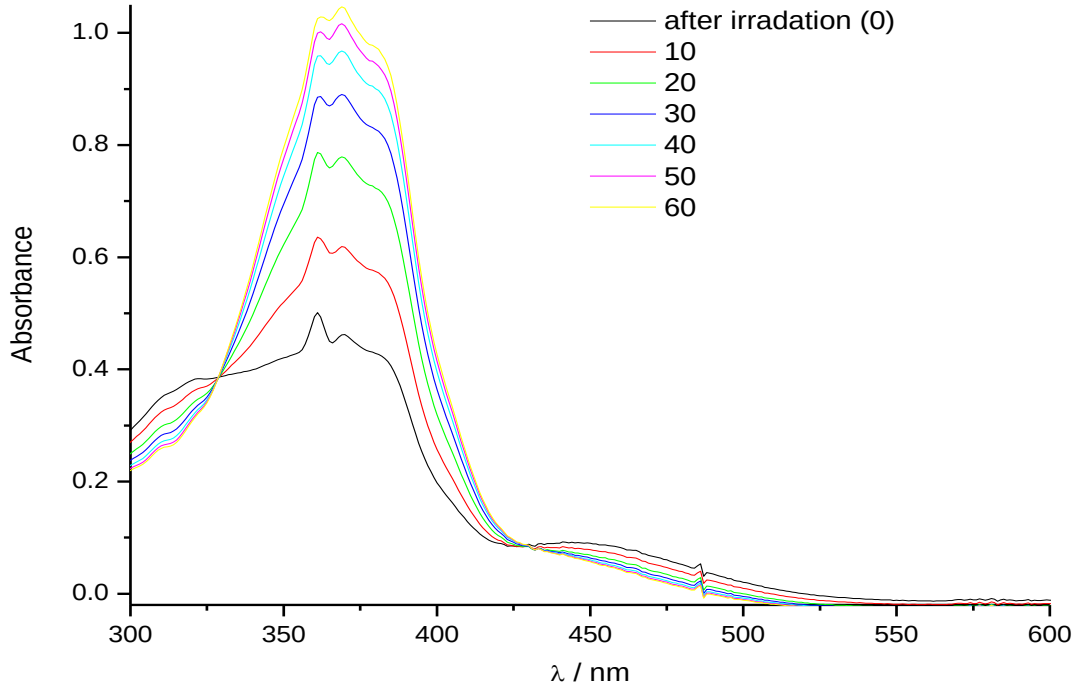

Figure 18: Admat 1 in cyclohexane solution following steady state irradiation (peak 370nm, absorbance of solution 1.0, concentration 7.7 x 10^{-5} mol dm^{-3})

Absorbance versus time graphs were also plotted in order to determine the rate constant and lifetime of the *cis* isomer. First order kinetics was observed for all of the relaxation reactions. The first order kinetics observed concur with other photoisomerisation studies conducted for similar azobenzene molecules.[261]

The half life of Admat 1 in methanol and xylene is much shorter than Admat 2. The increase in the size of the π-π* peak and decrease in the size of the n-π* peak shows the gradual recovery of the *trans* state. The presence of an isosbestic point indicates two isomers are present at around 425nm in figure 18.

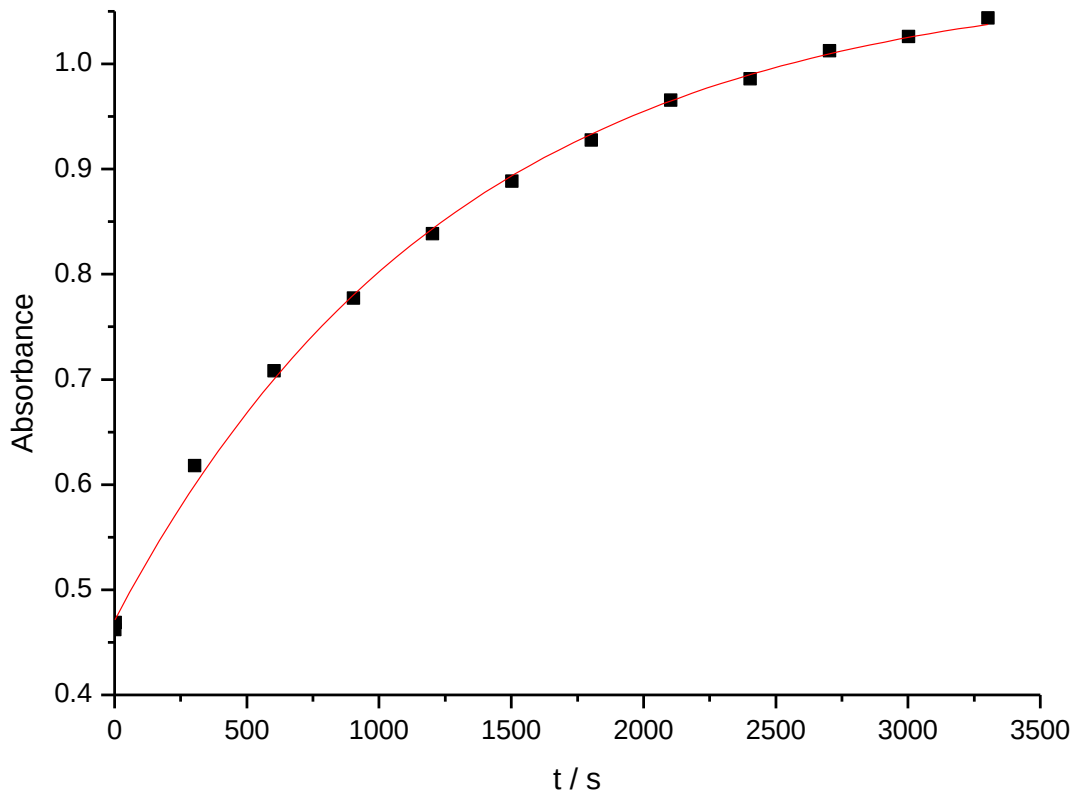

Figure 19: Kinetics rate plot of Admat 1 in cyclohexane (peak 370 nm) for cis to trans thermal isomerisation.

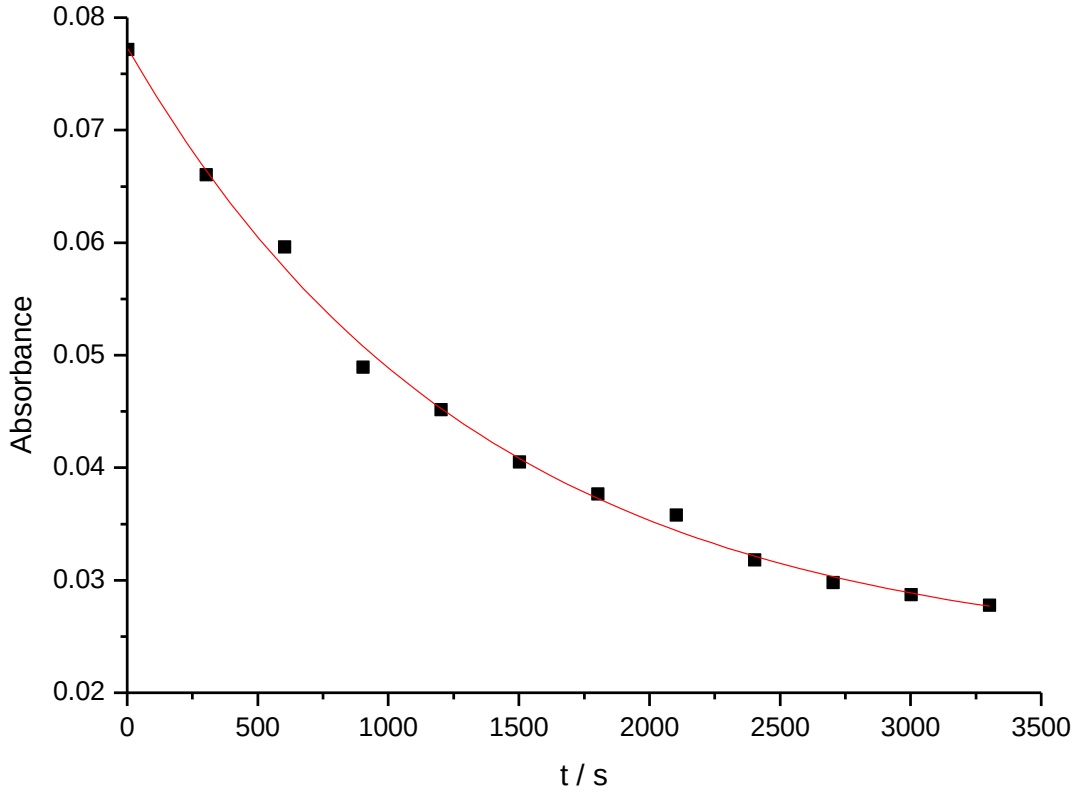

Figure 20: Trans isomer to cis form for Admat 1 in cyclohexane measured at 480nm.

4.5 Hydrocarbon derivatives photoswitching in solution

Kinetics studies were conducted on the hydrocarbon derivatives of Admat 1 and Admat 2 in various solvents to measure the *cis* state lifetime and thermal relaxation. First order kinetics was also observed for the hydrocarbon derivatives of the Admat compounds, Cfam 23 and Cfam 29 (Fig. 21 and 22). Similar values for the amino functionalised hydrocarbon derivative and the fluoroalkyl functionalised group were found in cyclohexane and in acetone. However, the thermal relaxation of Cfam 23 in methanol appears much slower than that of its fluorinated analogue, Admat 2. This would lead to the conclusion that the electronegativity of the fluoroalkyl chain is somehow influencing the thermal relaxation rate from *cis* to *trans*. The presence of the fluoroalkyl chain in the Admat derivatives also appears to affect the thermal isomerisation reaction in acetonitrile, as the hydrocarbon derivatives, Cfam 29 and Cfam 23 thermally relax much faster than the fluorinated analogues, Admat 1 and Admat 2.

Also in xylene, the thermal relaxation reaction appears to be affected by the amino and nitro substituent, regardless of the presence of the long hydrocarbon or fluoroalkyl chain.

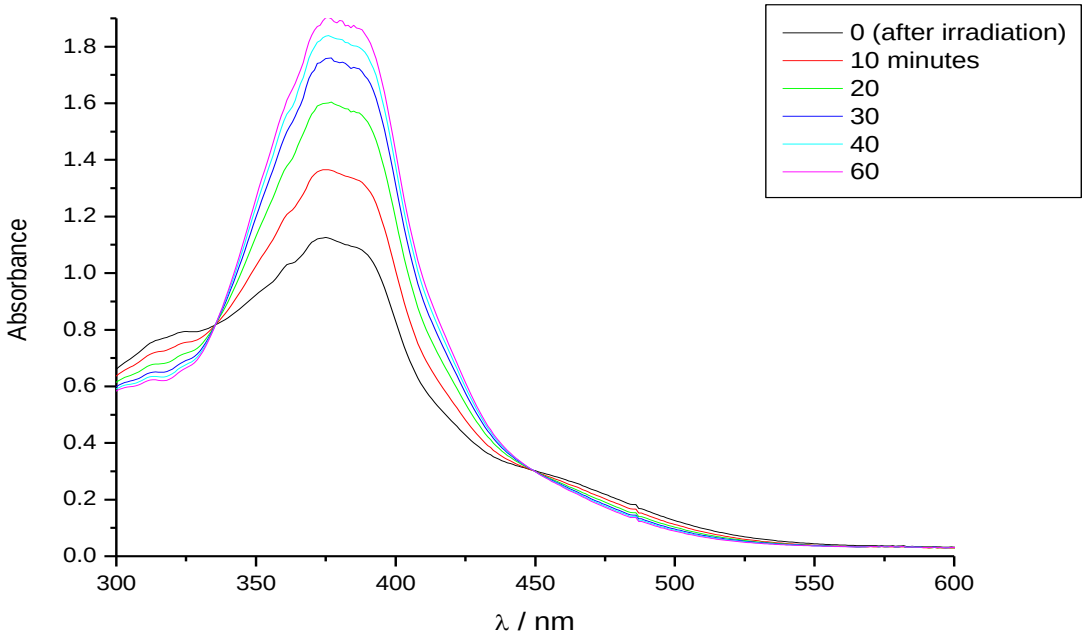

Figure 21: Thermal relaxation of Cfam 29 in p-xylene from cis state to trans state. Initial absorbance 1.41, wavelength 375nm.

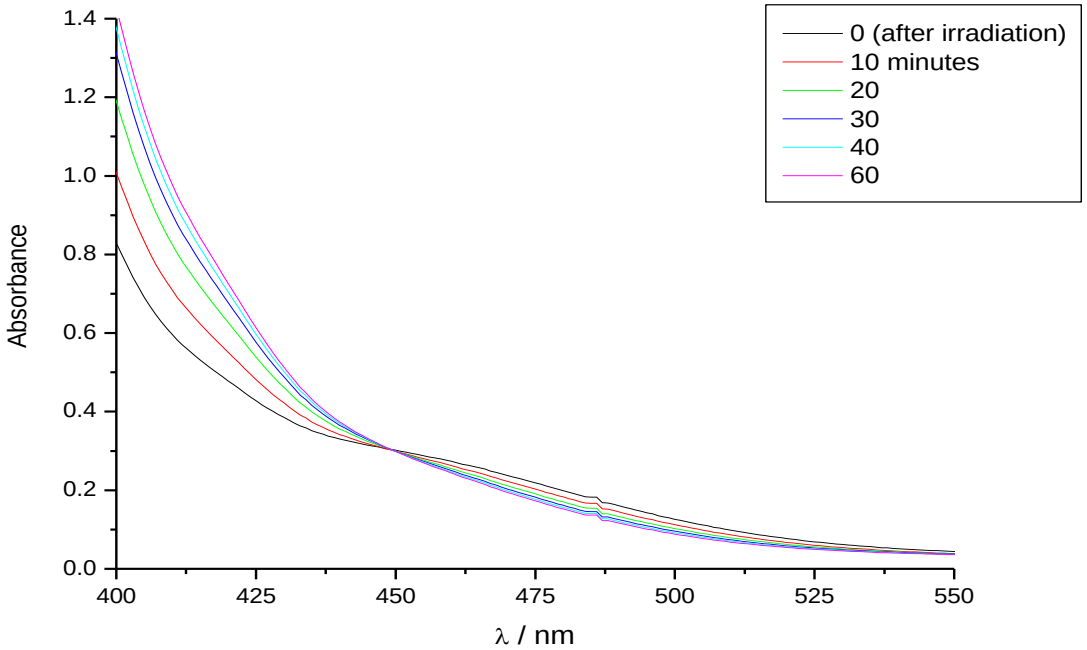

Figure 22a: Thermal relaxation of Cfam 29 in p-xylene from cis state to trans state. Initial absorbance 1.41, wavelength 375nm (relaxation of trans to cis isomer)

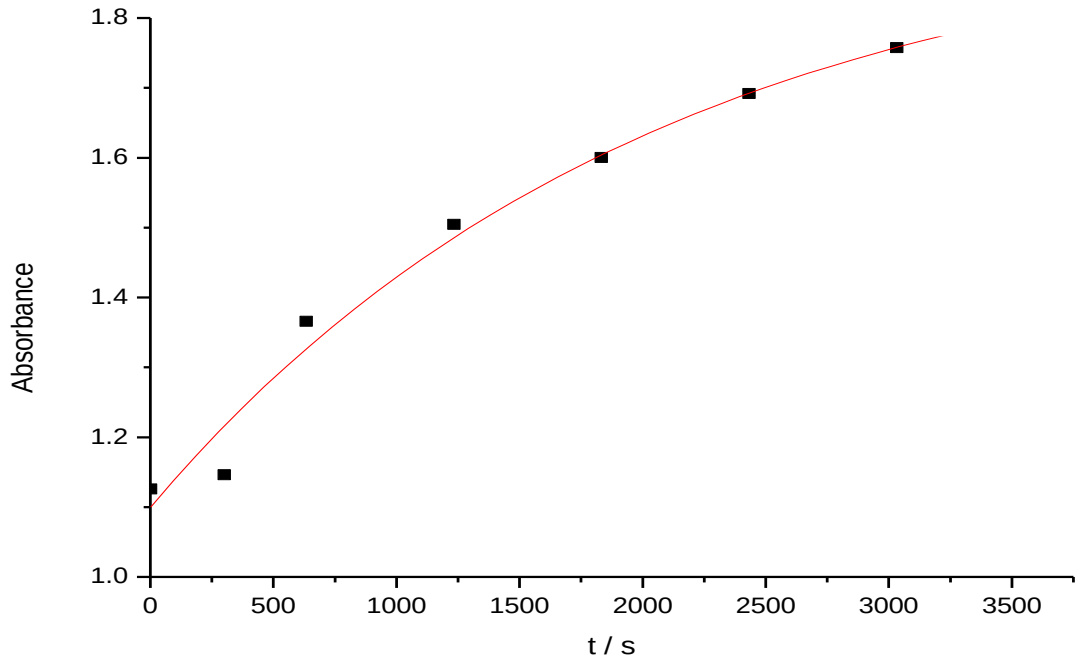

Figure 22b: First order rate plot for thermal relaxation of Cfam 29 in p-xylene.

4.6 Activation energies of thermal relaxation reaction in solution

In order to compare the activation energies of the thermal relaxation reaction of Admat 1 and Admat 2 with that of the literature value of 88.4 kJ mol^{-1} in *n*-heptanes[(262)], the rate of the thermal relaxation of *cis* to *trans* reaction was measured at different temperatures, ranging from 20 °C to 60°C and Arrhenius graphs were plotted (Figs 23 and 24)

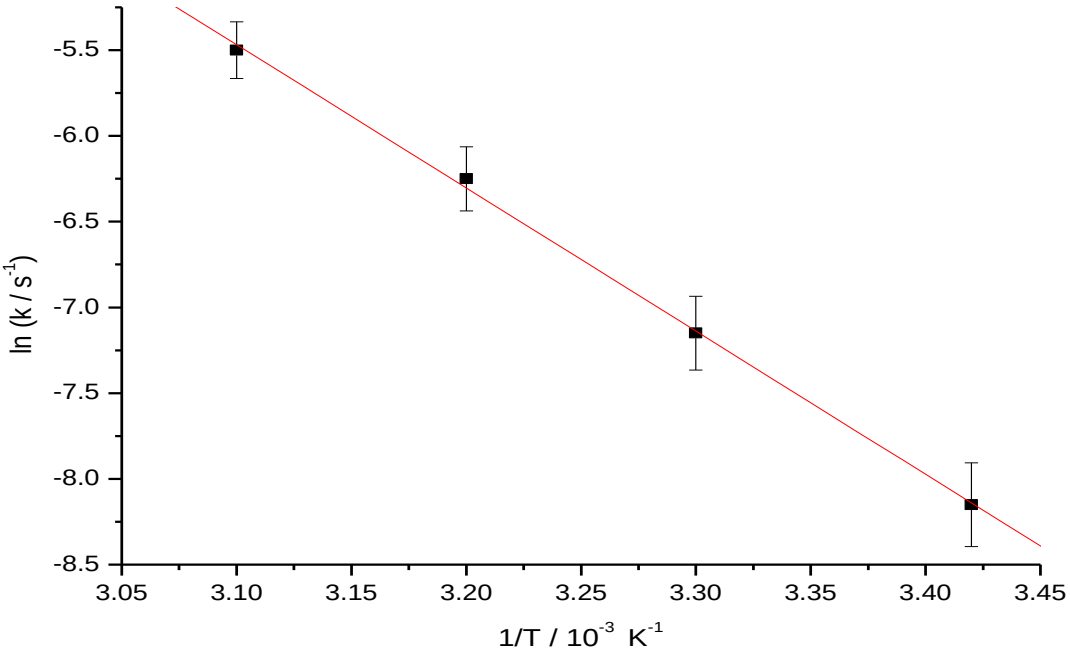

Figure 23: Plot of ln(rate) versus 1/T for Admat 2 in acetonitrile

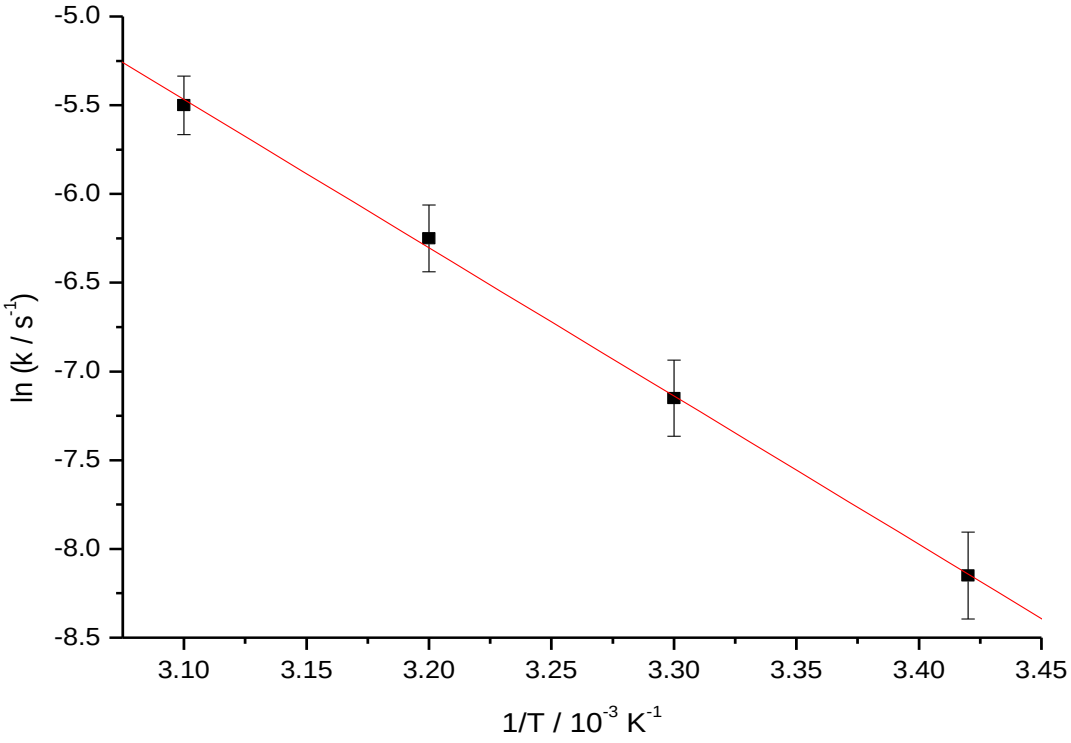

Figures 24: Plot of ln (rate) versus 1/T for Admat 2 in p-xylene

A table of data was complied for Admat 1 and Admat 2 compounds as well as the Cfam compounds in various solvents (Table 1)

It was found that for the perfluoroalkyl, amino-substituted derivative, there is a large variation in the rate for the process with change in solvent. In solvents such as xylene the amino compounds have faster relaxation rates and lower activation energies than the nitro derivatives, independent of fluorination.

In cyclohexane, a non-polar solvent, the thermal relaxation rate is relatively independent of substitution with the amino-substituted compounds showing only slightly faster relaxation rates (Table 1). Literature values for the thermal relaxation of azobenzene in heptanes is around 88-90 kJ mol^{-1}.[262] The fact that the activation energies are lower in the fluoro and alkyl chain derivatives is an indication that the thermal relaxation rate is affected by the substitution of the molecules, and, the amino and nitro groups present of the molecule, of which, the amino group can engage in hydrogen bonding with polar solvents.

In polar solvents, hydrogen bonding ability clearly plays an important role in determining isomerisation rates, alongside the fluorination of the alkyl chain. The relationship between the pre-exponential factors and the activation energy was investigated, and apart from methanol, the pre exponential factors decrease when the activation energy decreases, this is evidence for solvent dependence on the rate of reaction. Studies by Asano elucidated that the thermal relaxation proceeds via a highly polar transition state and the possibility that the rotational mechanism predominates here, and not the inversion mechanism.[264]

Compound	Methanol					p-Xylene				
	Peak / nm	**ε +/- 500 /mol^{-1} dm^3 cm^{-1}**	**k +/- 0.2 /10^{-4} s^{-1}**	**E_A/ +/- 2.2 kJ mol^{-1}**	**Pre exponential values (A) / +/- 2.3 s^{-1}**	**Peak / nm**	**ε +/- 500 /mol^{-1} dm^3 cm^{-1}**	**k +/- 0.2 /10^{-4} s^{-1}**	**E_A /+/- 2.2 kJ mol^{-1}**	**Pre exponential values (A) / +/- 2.3 s^{-1}**
Admat 1	385	-------	------	---------	----------	375	14000	42.70	23.7	4.3
Admat 2	365	18000	42.0	63.3	20.2	370	19000	3.00	63.5	17.5
Cfam 29	385	-------	------	---------	----------	375	18000	39.70	30.2	5.3
Cfam 23	375	22000	9.05	34.5	14.6	377	21000	4.37	59.6	18.1
	Acetonitrile					**Acetone**				
Admat 1	380	18000	5.30	54.9	13.8	385	13000	3.90	63.2	15.1
Admat 2	367	24000	2.90	68.8	10.1	365	25000	3.60	64.3	15.8
Cfam 29	385	19000	67.80	55.2	19.8	380	16000	5.90	58.6	13.5
Cfam 23	373	27000	65.60	64.1	21.4	375	17000	5.20	54.2	15.2
	Cyclohexane									
Admat 1	370	13000	7.80	41.2	15.3					
Admat 2	360	28000	4.00	50.6	13.1					
Cfam 29	375	26000	5.80	56.4	15.9					
Cfam 23	375	19000	4.68	58.1	17.3					

Table 1: Summary of absorbance and photoisomerisation reactions of Admat and Cfam compounds and activation energies in various solvents NB: k is measured at 22°C (295 K)

The relationship between π* solvent parameters in various solvent was investigated in relation to the solution work conducted. The π* parameters were obtained from published literature.[263] The π* parameter is so named as it derives from and best correlates solvatochromic effects on n-π* and π-π* electronic spectral transitions. Solvent effects on the v max values of seven primary indicator compounds are used in the construction of the π* scale and correlations with 40 spectral indicators are used to expand and refine the data base. There was found to be only mild relationship between the parameters and the rate constant and only for one compound in particular, in the various solvents (Figure 25a). This would indicate that the isomerisation process observed here is dependent on the solvent used. This would support previous literature that states that there is heavy solvent dependency in isomerisation; however, there is no change in the spectra in this section that would indicate a ground state complex with the solvent is formed here.

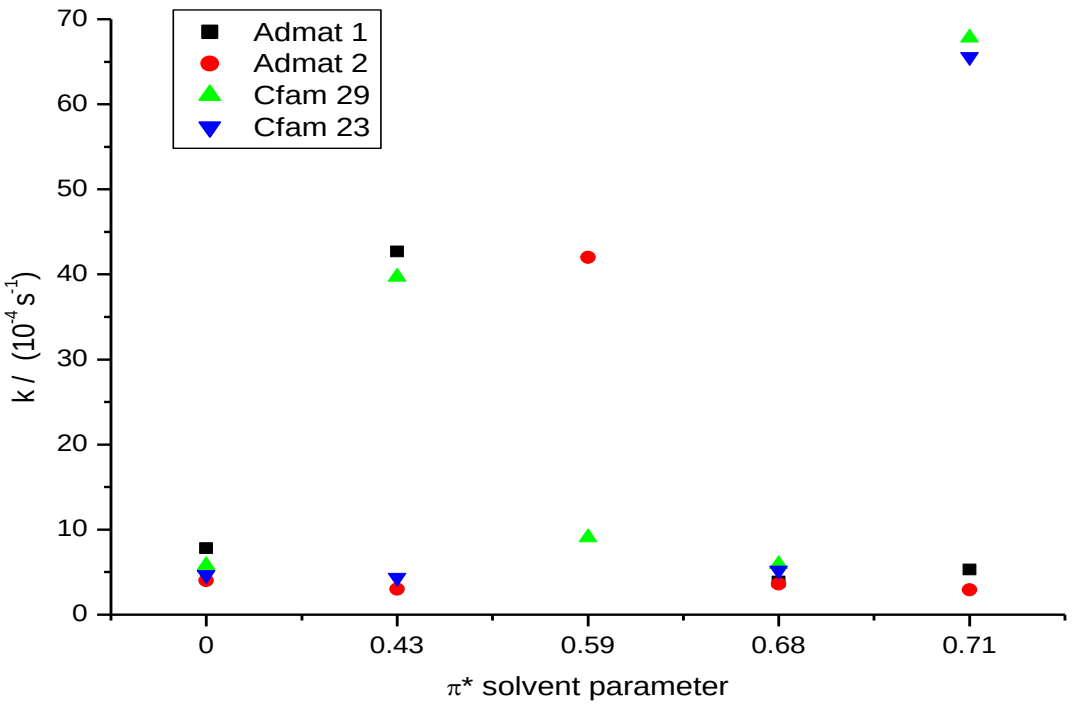

Figure 25a: Rate versus π solvent parameter for Admat and Cfam derivatives in various solvents. 0.0 = cyclohexane, 0.43 = p-xylene, 0.59 = methanol, 0.68 = acetone, 0.71 = acetonitrile.*

There is an interest point to be observed from the π* data, in the fact that a linear relationship (apart from the acetone value) can be found from the π* solvent parameter and Cfam 29. This

is not seen with any of the other compound, which elucidated to the fact the perfluoroalkyl chain and the amino moiety must be a significant factor in the isomerisation process in solution. Cfam 23 shows some relationship to the π* solvent parameters until acetonitrile, where the rate increases almost seven fold. Also an important comparison is that aminoazobenzene showed the fast kinetics in methanol shown in table 1, which, as an amino substituted azobenzene, is a useful indication that the amino group interacts with the solvent to increase the rate of the thermal relaxation reaction. Aminoazobenzene also, in common with the amino functionalised derivatives studied here shows almost tenfold increase in the thermal relaxation rate in xylene. One possibility for the sudden increase in rate in xylene is that a change in the isomerisation mechanism is responsible, though this would require much further investigation. Work by Asano *et. al*. showed that the rate constant in polar solvents increases. This was thought to be as a result of the rotational isomerisation thermal relaxation reaction proceeding via a higher polar transition state. Also it was found that the nitro group increases the stability of the inversion state as oppose to the polar state, which would explain the fact that with Admat 2, the rate constant is much slower than with the amino derived Admat 1.[186]

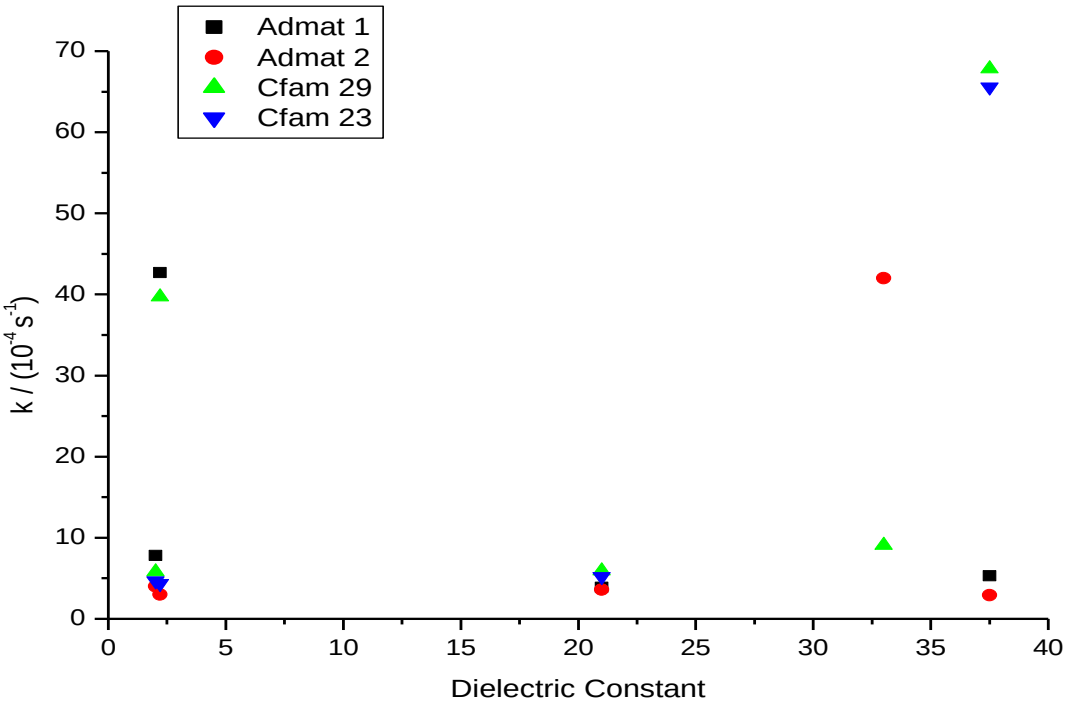

Figure 25b: Rate versus dielectric constants for all Admat and Cfam derivatives. 2.02 = cyclohexane, 2.20 = p-xylene, 21.0= acetone, 33.0 = methanol, 37.5 = acetonitrile.

The π* values and the dielectric constant appear to show some similarities for the data obtained in methanol and in acetonitrile (Figure 25b), i.e. the fast thermal relaxation reactions of the fluorinated Admat 1 and Cfam 29 in p-xylene and the Cfam derivatives in acetonitrile are faster. Interestingly, aminoazobenzene also shows similar fast kinetics in xylene and in methanol, (table 6 and 7). The relationships between activation energy and dielectric constants and solvent parameters were also investigated by plotting data from table 1 against the values of the π* parameter and dielectric constant given in the literature.

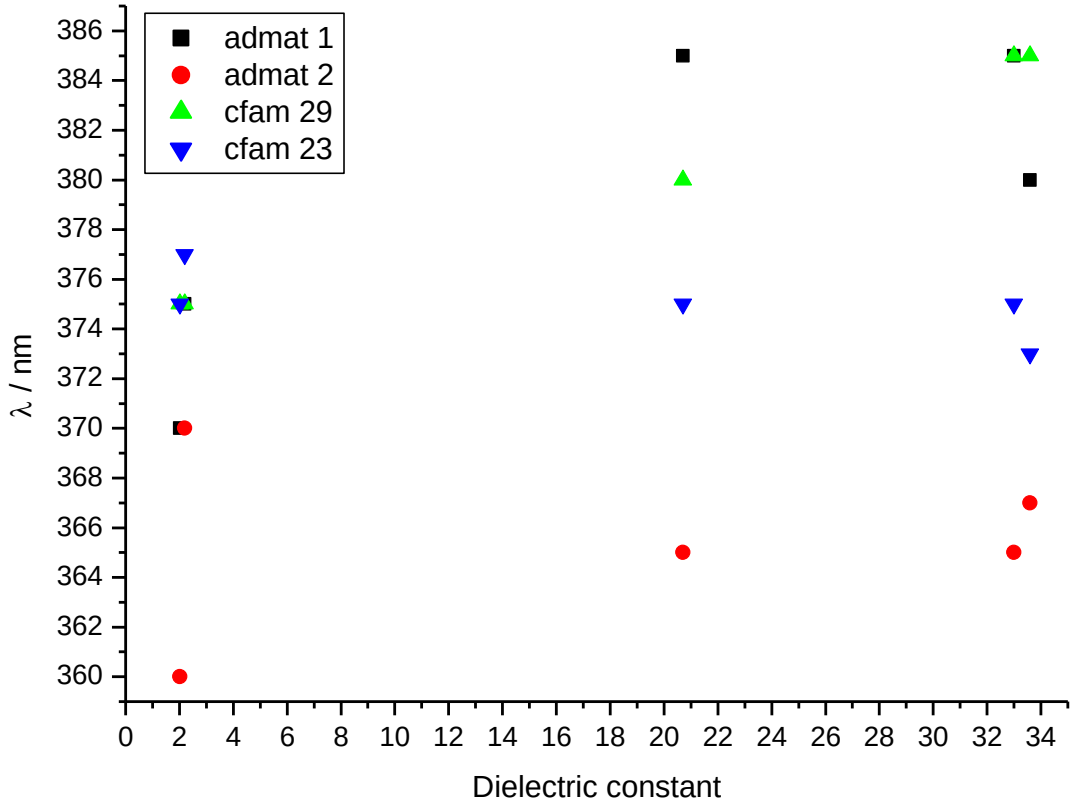

Figure 25c: Wavelength versus dielectric constant for Admat and Cfam derivatives. 2.02 = cyclohexane, 2.20 = p-xylene, 21.0= acetone, 33.0 = methanol, 37.5 = acetonitrile.

The relationship between wavelength and dielectric constant was investigated and although no real linear trends were found, several interesting relationships were discovered. The amino substituted Cfam 29 and Admat 1 were both found to have larger peak wavelengths (λ max) in more polar solvents, regardless of the fluoroalkyl or alkyl chain presence, see the figure

above (Figure 25c) as the dielectric constant increases, the wavelength increases, which ties in with the discussion of the Franck Condon factors in more polar solvents mentioned earlier. There is a slight increase in the wavelength for Admat 2 as the dielectric increases; however, the Cfam 23 compound appears unaffected by change in the dielectric constant.

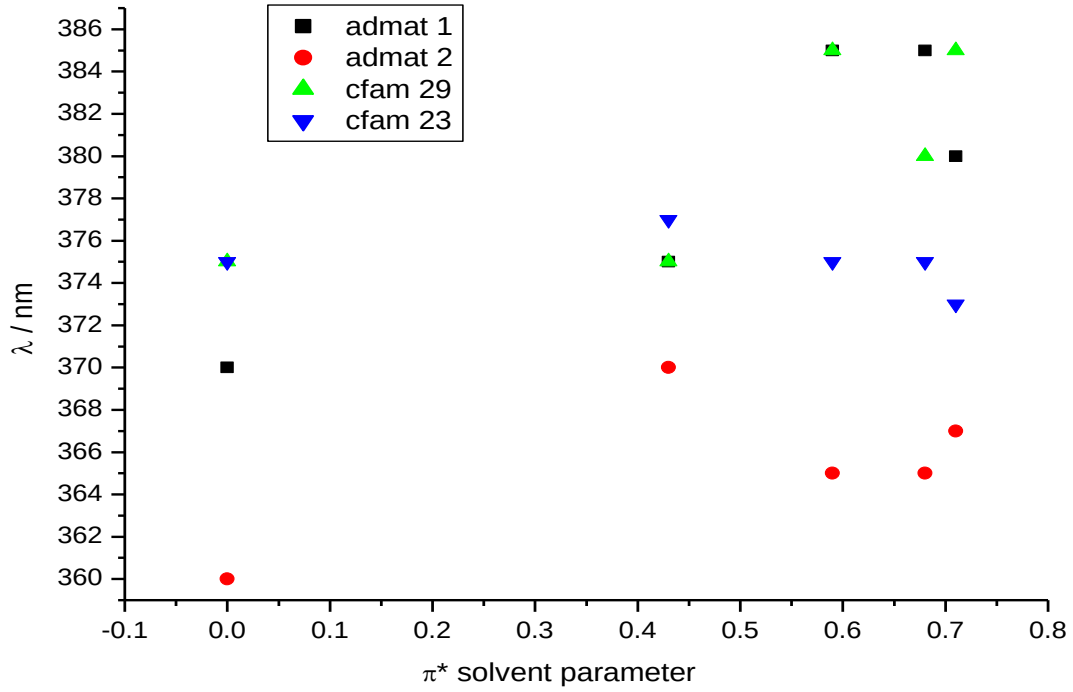

Figure 25d: Wavelength versus π parameters for all compounds both Admat and Cfam derivatives. 0.0 = cyclohexane, 0.43 = p-xylene, 0.59 = methanol, 0.68 = acetone, 0.71 = acetonitrile.*

There is also a similar relationship between the wavelengths and the π* parameters, as can be seen from the figure above (Figure 25d), the wavelength gets longer for the amino derivatives Admat 1 and Cfam 29 as the solvent becomes more polar. The nitro groups on Admat 2 and Cfam 23 show no significant affects on the wavelength between each solvent, though a general increase for Admat 2 is observed, apart from in *p*-xylene. The amino group can undergo hydrogen bonding with the more polar solvents, which would explain the increase in the wavelength.

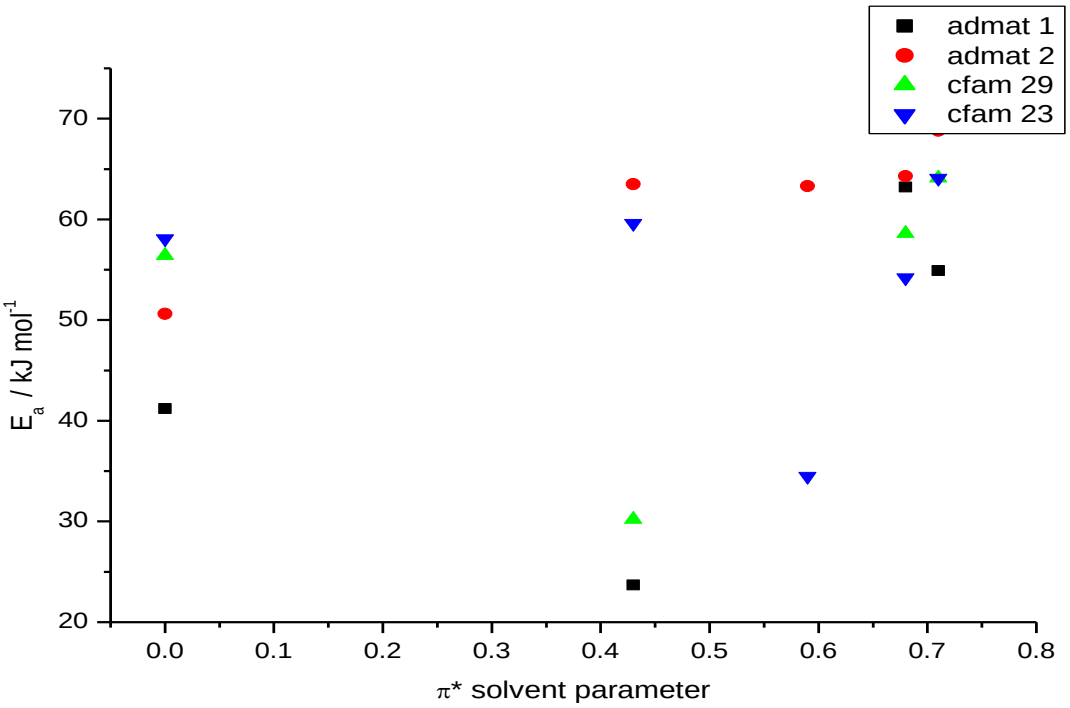

Figure 25e: Activation energy versus π solvent parameter graph. 0.0 = cyclohexane, 0.43 = p-xylene, 0.59 = methanol, 0.68 = acetone, 0.71 = acetonitrile.*

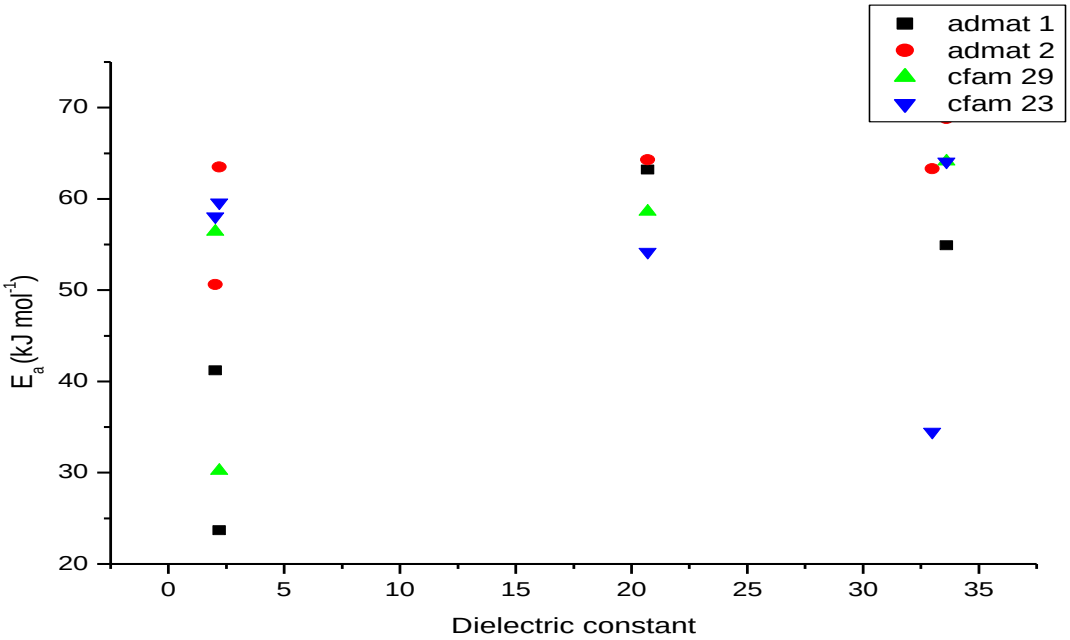

Figure 25f: Activation energy versus dielectric constant for all azo derivatives. 2.02 = cyclohexane, 2.20 = p-xylene, 21.0= acetone, 33.0 = methanol, 37.5 = acetonitrile.

There appears to be very little relationship between the activation energies and the dielectric constant (Figure 25f), this suggests that the polarity of the solvent is not a factor in the activation energy of the thermal relaxation reaction. Similar trends can be observed for the π* versus activation energy plot (Figure 25e), which backs up the theory that the polarity of the solvent does not affect the activation energy. There was also found to be no relationship between the maximum wavelength and the activation energy. The activation energies were largely independent of the solvent, however, k was found to have some relationship to the functional groups on the azobenzene moiety. For example the amine functionalised Cfam29 an Admat 1 in xylene showed a marked 10 fold increase in the rate constant, whereas the same effect for the nitro groups was not observed. However, the Cfam 29 and Cfam 23 alkyl derivatives were much faster than the fluoroalkyl chain derivatives (Admat 1 and Admat 2) in acetonitrile, indicating that the fluoro chain was somehow hindering isomerisation in acetonitrile. Further to activation energy and π* parameters, the relationship between the molar absorption coefficient and the wavelength was investigated.

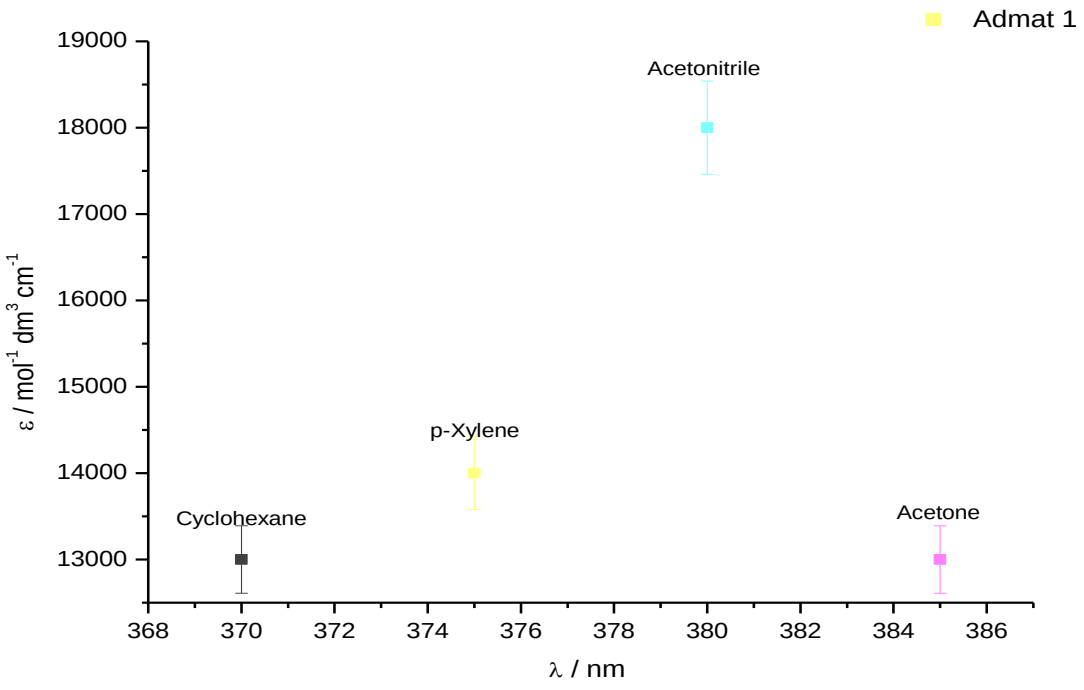

Figure 25g: Molar absorption coefficient versus maximum wavelength of absorption for Admat 1

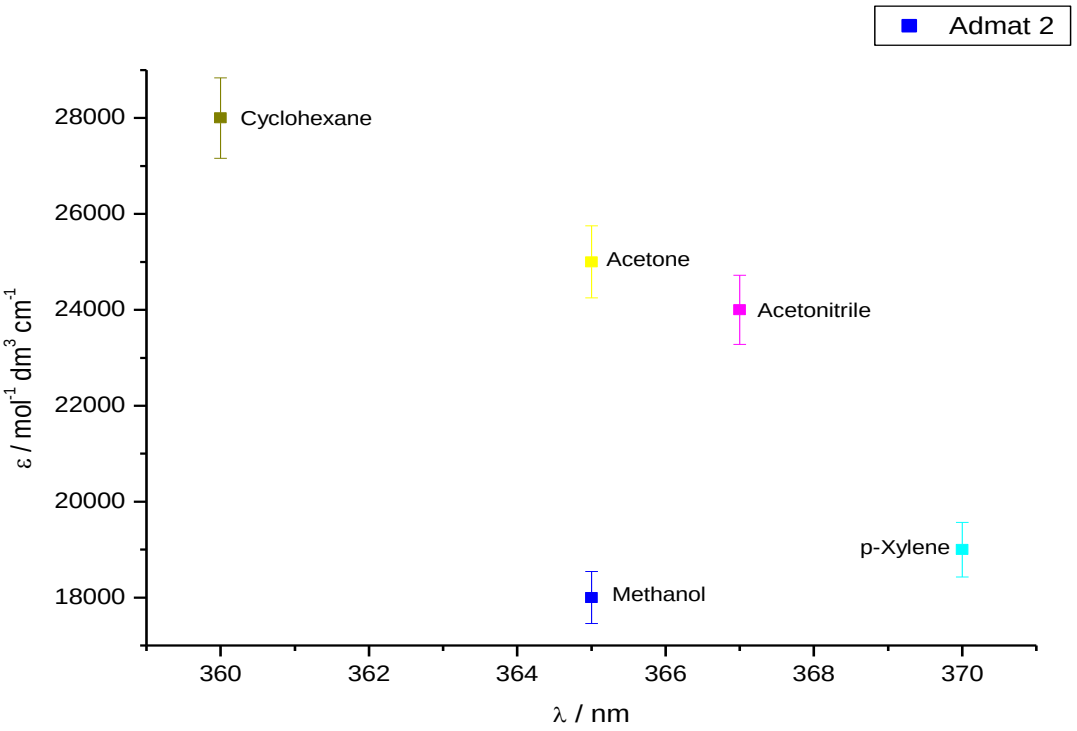

Figure 25h: Molar absorption coefficient versus maximum wavelength of absorption for Admat 2 in various solvents.

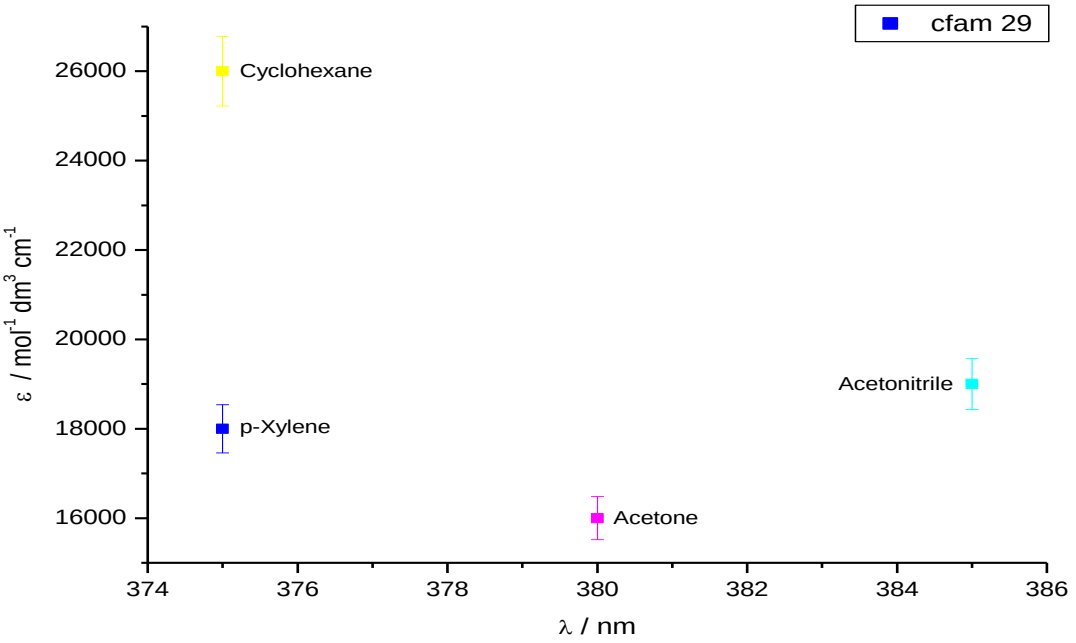

Figure 25i: Molar absorption coefficient versus maximum wavelength of absorption for Cfam 29 in various solvents.

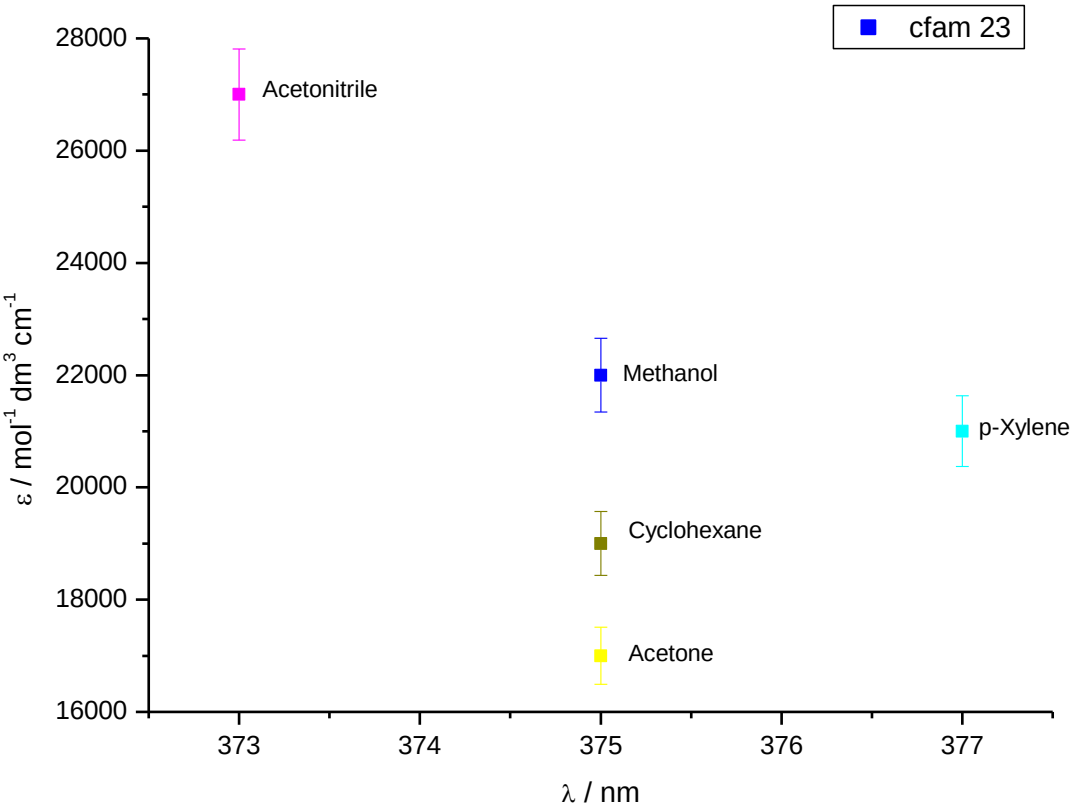

Figure 25j: Molar absorption coefficient versus maximum wavelength of absorption for Cfam 23

The relationship between the molar absorption coefficient and the wavelength (Figure 25g-j) shows some interesting results for Admat 1 and Cfam 29 (the amine functionalised derivatives) as it shows, apart from one anomaly (Cfam 23 in acetone) that the peak maximum of the absorbance spectra is largely blue shifted in non polar solvents such as cyclohexane and p-xylene than in methanol. A proposed reason for this is the possibility of hydrogen bonding occurring between the amino groups and methanol, however, the same is seen in acetonitrile, which is further proof of the solvent dependency on the absorption spectrum of the molecule. The solvent dependence has also been seen in the previous data for the dielectric constant and solvent parameter.

4.7 Thermal relaxation kinetics in polar solvents

Admat1 displayed very fast thermal relaxation in methanol. Work was conducted using other short chain alcohols in order to ascertain if a trend was present. Mixed solvents were also attempted in order to investigate if addition of solvent had any effect on the thermal relaxation rate.

Alcohol	**λ_{max} / nm**	**k / 10^{-4} s^{-1}**	**Dielectric Constant**
Ethanol	387	905	24.3
Propanol	385	9.49	20.1
Isopropanol	385	9.47	18.2

Table 2: Rate constants for thermal relaxation of Admat 1 in three different alcohols, ethanol, 2-propanol and 1-propanol.

There appears to be no relationship between the dielectric constant here and the rate constant observed for thermal relaxation (Table 2). The dielectric constant is a measure of polarity, so the higher the dielectric constant, the higher the polarity. The reason for investigating this, as the initial thought was that as methanol is more polar than most other solvents, that somehow the rate constant was affected by solvent polarity.

The thermal relaxation of Admat 1 in ethanol was approximately 100 times faster than in propanol; however, it was still slower than in methanol. Flash photolysis was used to investigate the thermal relaxation reaction for Admat 1 in methanol and in ethanol, however this proved futile. The activation energy of the Admat compounds in table 2 show little relationship with the dielectric constant. The activation energies in propanol and methanol were measured to investigate further this relationship.

A mixture of solvents was then chosen, methanol and propanol, to find out if the addition of a more polar solvent would affect the rate of thermal relaxation of Admat 1.

The table of rate constants for the addition of methanol is shown below. (Table 3)

Alcohol mixture	**λ / nm**	**k / 10^{-3} s^{-1}**
20% methanol in 1-propanol	385	1.32
40% methanol in 1-propanol	385	15.13
55% methanol in 1-propanol	385	47.36
60% methanol in 1-propanol	385	92.43

Table 3: Table of solvent mixtures and corresponding rates of reaction.

With regards to Admat 1 in propanol, addition of a polar solvent affects the rate, (Table 3), however above a certain concentration the thermal relaxation from *cis* to *trans* speeds up almost 10 times. Early indications are that there is a point between 50% and 60% methanol where the mechanism of thermal relaxation changes. The graph (Figure 26) of rate versus % methanol shows a sharp increase between 40% methanol and 60% methanol. 80% methanol and propanol mixture was also tried, but the thermal relaxation reaction was far too fast to be measured via ground state spectroscopy.

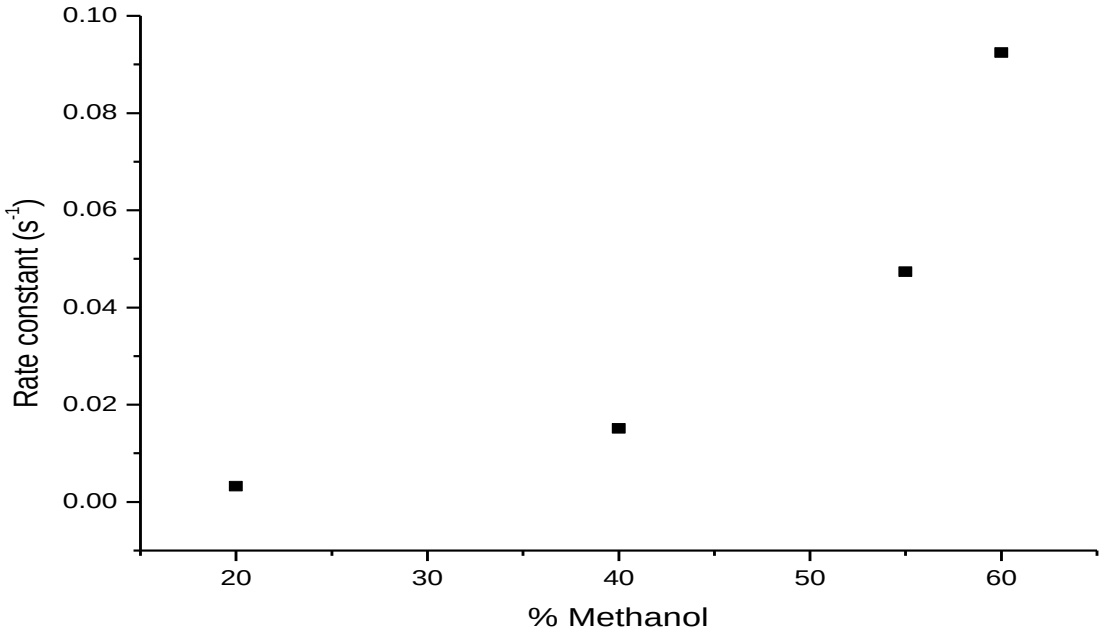

Figure 26: Graph of rate constant versus % methanol in 1-propanol for Admat 1.

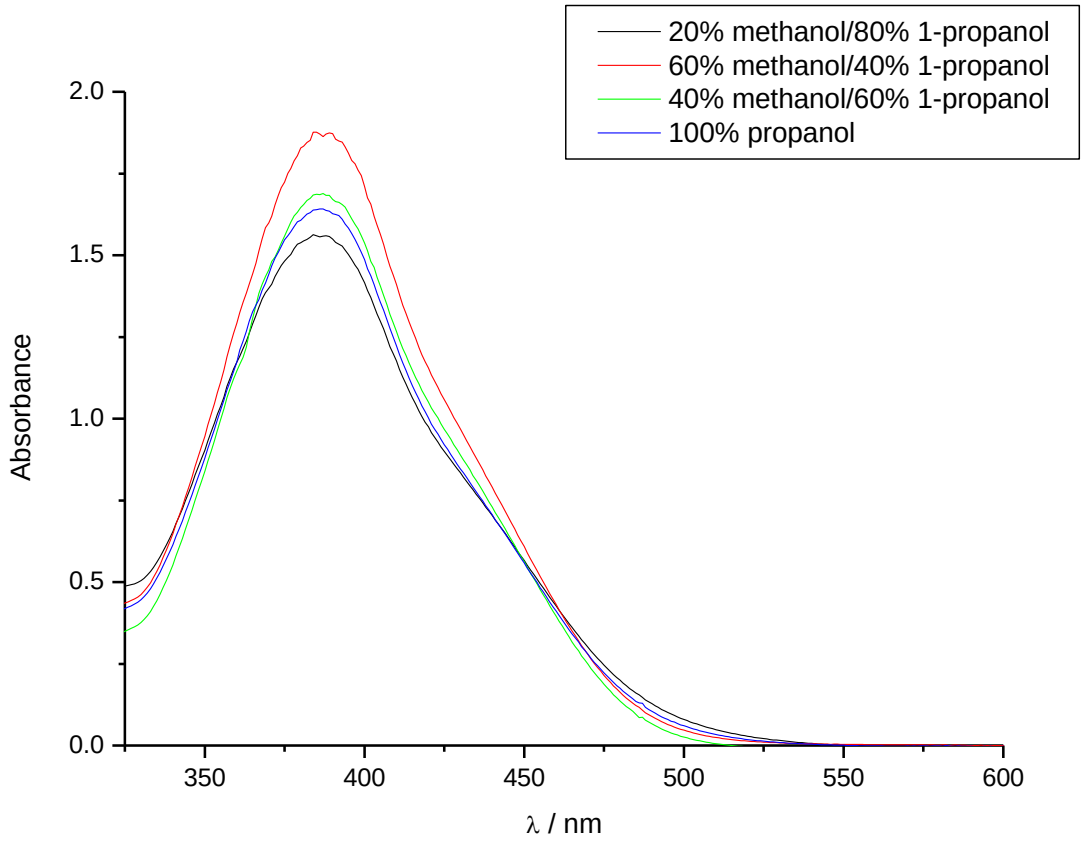

Figure 27: Absorbance of alcohol mixtures for aminoazobenzene.

As can be observed from Table 4, a rapid increase in rate constant is observed upon addition of methanol to THF solutions. An experiment in which 5 drops of water was added to a solution of aminoazobenzene in acetone resulted in a very rapid thermal relaxation which was too fast to measure on a spectrophotometer.

This investigation concurs with previous literature,[264] [265] as the rate of azo isomerisation can be influenced by water concentration. Water concentration in THF was found to give rise to measureable differences in the isomerisation reaction in THF solution, as water is miscible with both methanol and ethanol, and with THF, the water effect within the solution is certainly marked in the work seen thus far. The aggregates in the studies previously conducted show that upon addition of water, the thermal isomerisation reaction from *cis* to *trans* after irradiation was hindered, however here the reaction is observed to increase, leading to the conclusion that possibly the long chains present there affect the aggregation and that the aggregation displayed here is different due to influence of the fluoroalkyl groups. Figure 27 shows the absorbance spectrum of the alcohol mixtures, which change upon addition of methanol to the 1-propanol. The formation of aggregates upon addition is suspected here due to the slight shift in the absorbance spectra between 480nm and 520nm.

4.8 Rate of thermal relaxation of Admat 1 in THF solution with the addition of methanol

Further to previous work, which involved the addition of methanol to a solution of aminoazobenzene in acetonitrile, it was decided to investigate if the increase in the rate was observed in other solvents. Tetrahydrofuran (THF) was chosen as the azobenzene derivatives are soluble in it at higher concentrations than in acetone or in xylene. A solution of known concentration of Admat 1 in THF was prepared in order to keep the concentration of Admat 1 in the solutions constant.

The addition of larger amounts of methanol than was used before was required, as adding small amounts (0.1 ml-0.5 ml) had little effect upon the rate constant for thermal relaxation of the solution in THF. The sample was irradiated in a Xenon arc lamp for 10 seconds. The rate constant was measured by monitoring absorbance versus time at 385 nm, the peak of the

absorbance spectra. The amounts of methanol added, the concentration obtained and the rate constant for thermal relaxation are all shown in the table below (Table 4).

Amount of methanol added / cm^3	Concentration of methanol in the solution / mol dm^{-3}	Rate of thermal relaxation / 10^{-4} s^{-1}
0	0	3.14
1	0.98	6.52
2	1.96	8.41
3	2.94	9.32
4	3.92	10.3
5	4.88	30.0
6	5.88	32.3

Table 4: Data obtained from thermal relaxation experiments of Admat 1 in THF with the addition of Methanol. Final volume 25 cm^3.

The rate calculation was obtained by fitting the data with a first order exponential curve as below.

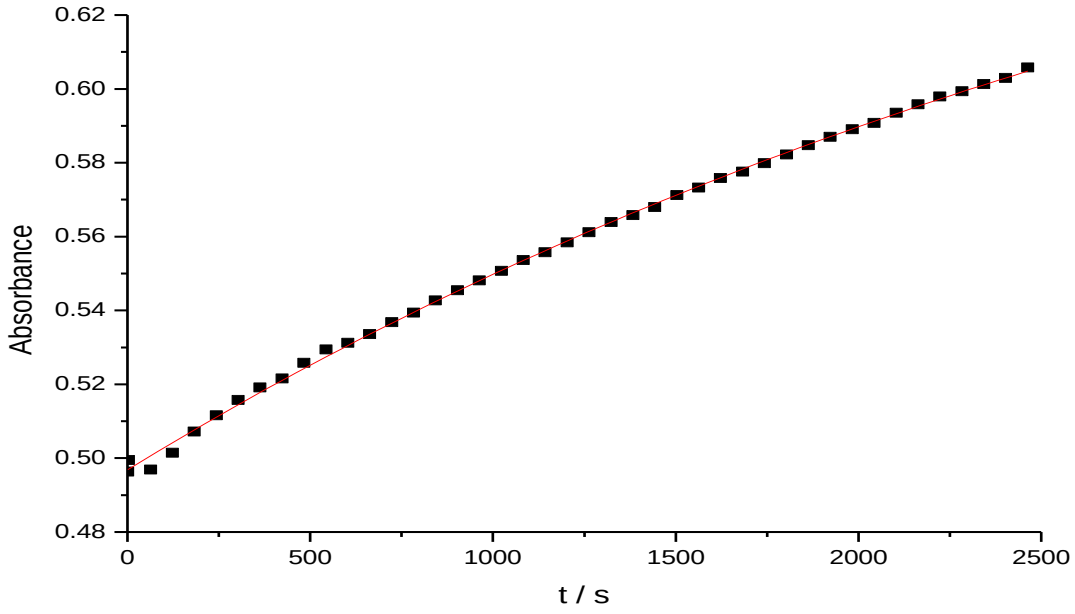

Figure 28a: Absorbance versus time plot for Admat 1 in THF with added methanol

The data obtained for the thermal relaxation is consistent with first order kinetics (Figure 28a). A rate constant versus [MeOH] graph was then plotted so see the effects observed upon adding methanol to the Admat 1 solution in THF (Figure 28b).

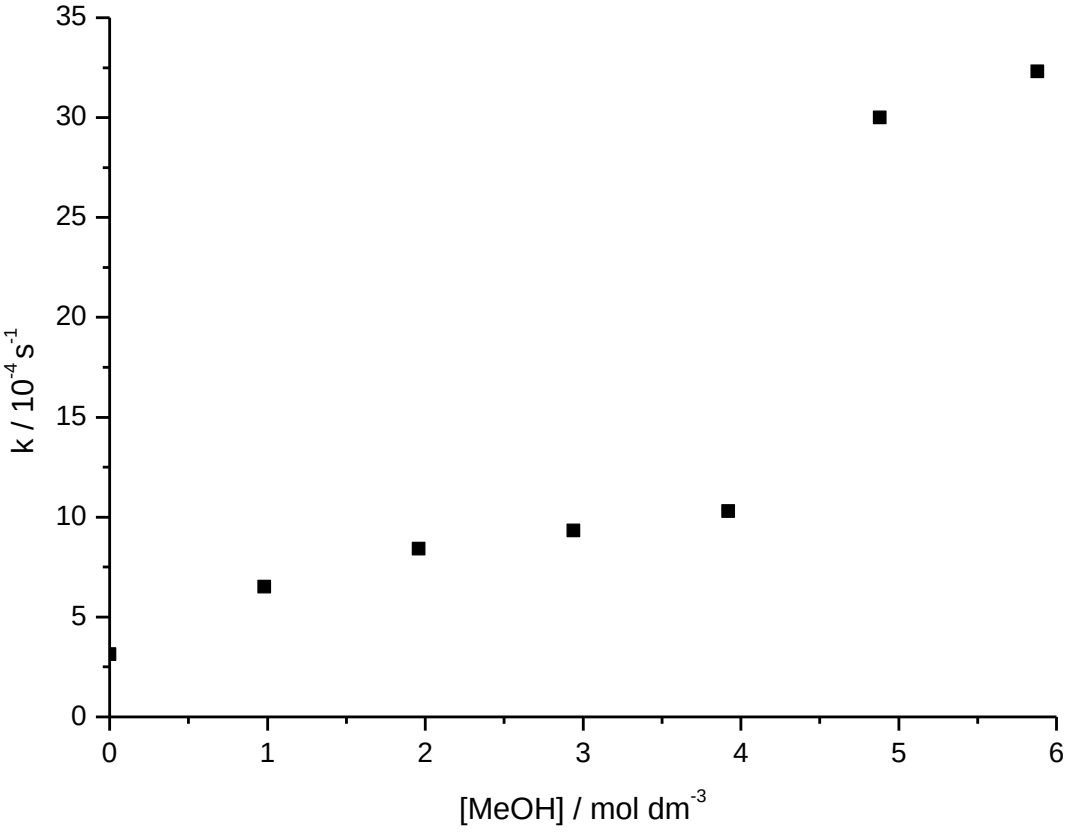

Figure 28b: Graph of addition of methanol to THF solution of Admat 1.

The data obtained (Figure 28b) shows that upon addition of methanol, the rate of thermal relaxation increases, however, upon addition of larger amounts the rate increases dramatically, in a non linear relationship. This is due to precipitation of the compound from solution upon adding higher concentrations of methanol, as Admat 1 is not particularly soluble in methanol. The fact that aggregates can form from precipitation means that the rate constant for thermal relaxation will increase as observed, as the presence of aggregates appears to increase the rate of thermal relaxation with these particular azo compounds.

4.9 Rate constant for thermal relaxation reaction of Admat 1 with the addition of dimethylaniline

Further to work completed earlier concerning the addition of methanol to a solution of Admat 1 in THF, the same experiment was carried out using THF as the solvent with the addition of dimethylaniline. A known concentration of Admat 1 in THF was prepared and known amounts of dimethylaniline were added to the solution, and the solution was irradiated using a 150 W Xenon arc lamp for 10 seconds.

The absorbance spectra were measured (Figure 29) thermal relaxation rate constants were measured for each concentration and then the rate constant was calculated via fitting with a first order exponential. The data obtained is displayed in table 5 below

Amount of dimethylaniline added / cm^3	Concentration of dimethylaniline in solution / mol dm^{-3}	Rate of thermal relaxation / 10^{-4} s^{-1}
0	0	3.14
1	0.315	8.57
2	0.63	18.4
3	0.94	38.1
4	1.26	49.3
5	1.57	69.8

Table 5: Concentration of dimethylaniline and rate constant for thermal relaxation data for Admat 1 in THF with added dimethylaniline. Final total volume = 25 cm^3.

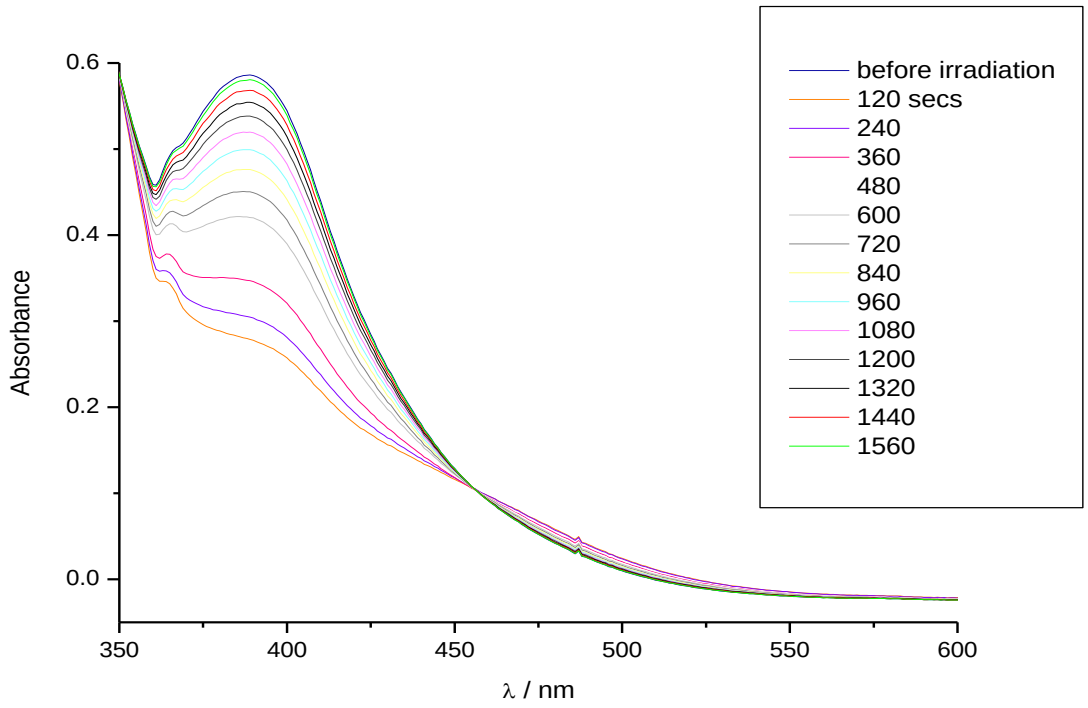

Figure 29: Absorption spectra of Admat 1 with dimethylaniline added.

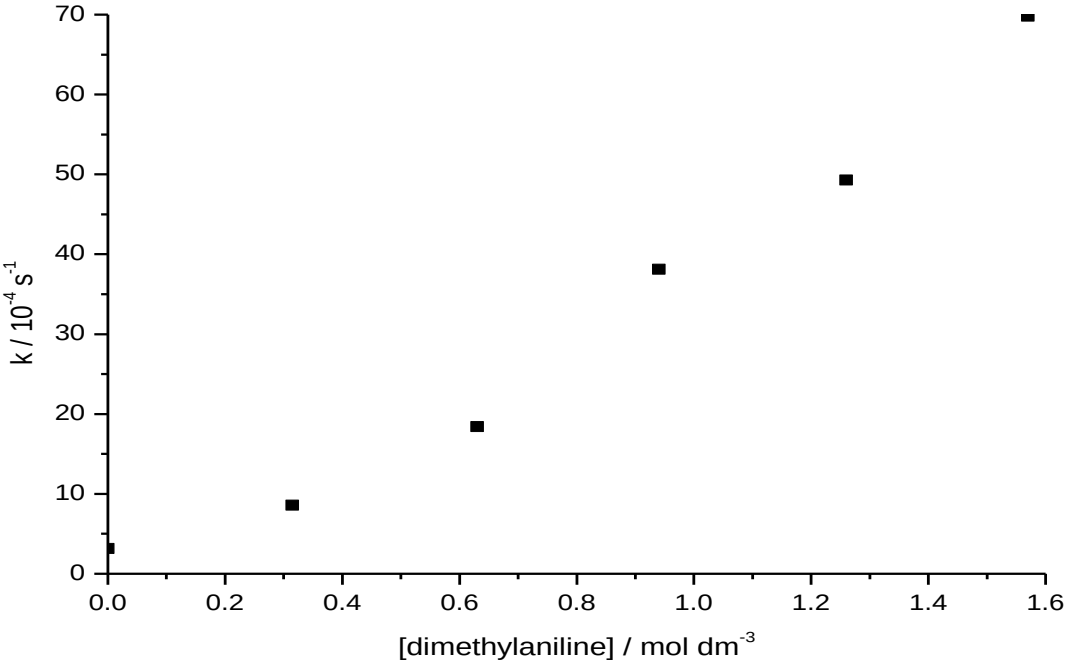

Figure 29: Rate constant versus concentration graph for dimethylaniline added to Admat 1 in THF solution.

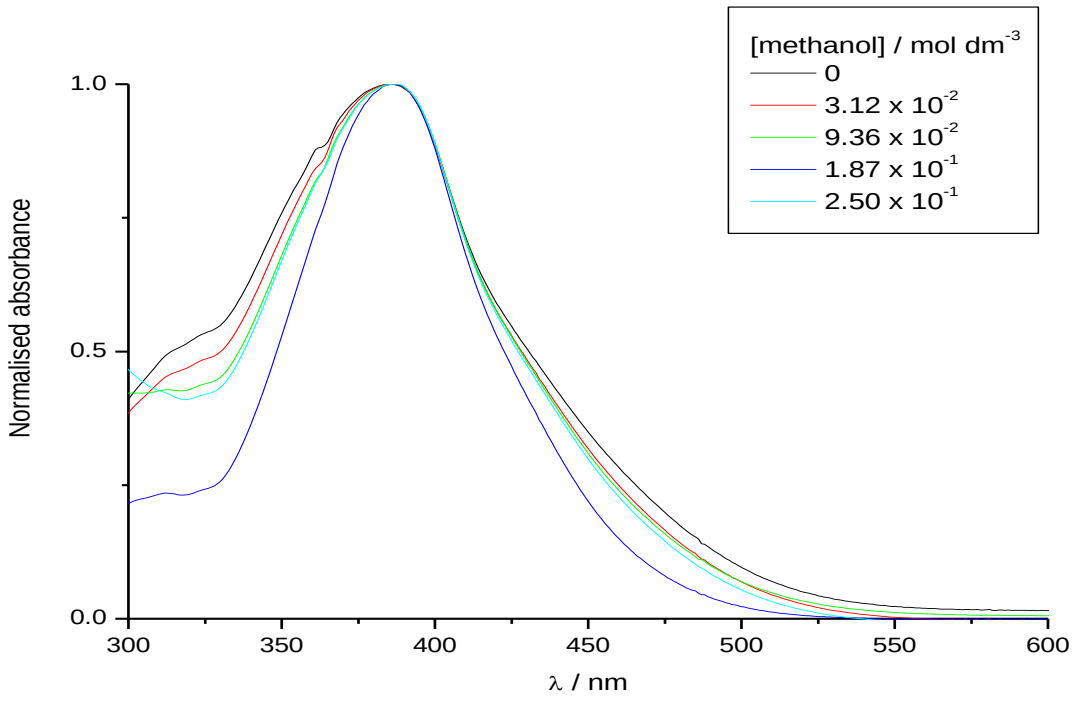

Figure 30: Spectra of Admat 1 in THF solution upon addition of increasing amounts of methanol.

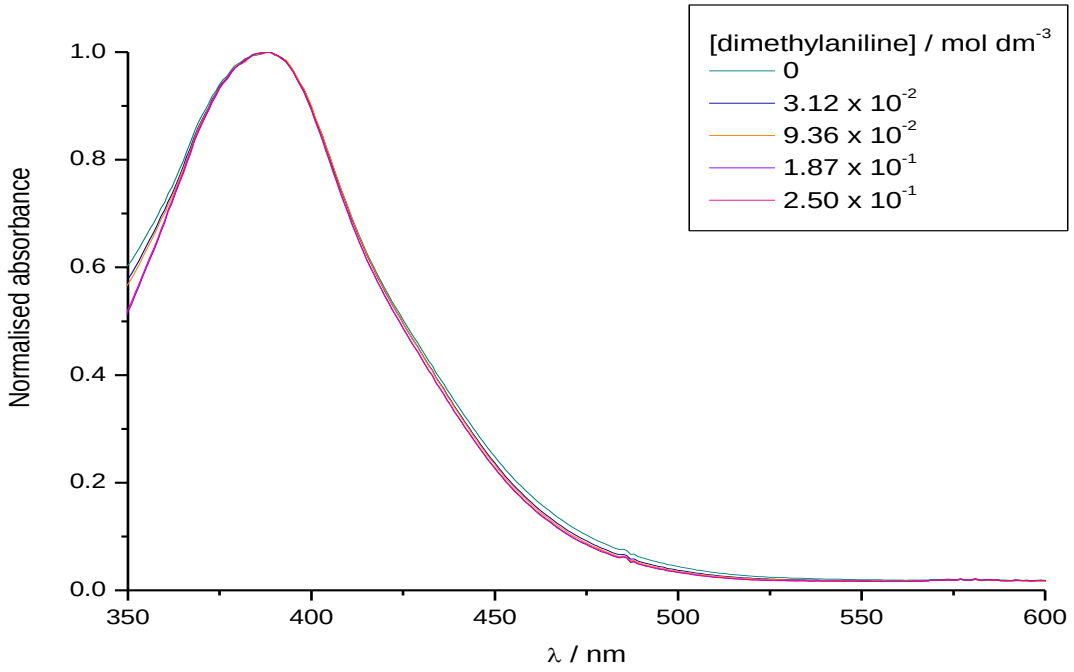

Figure 31: Spectra of Admat 1 in THF solution upon addition of increasing amounts of dimethylaniline.

The absorbance spectra were measured upon addition of dimethylaniline in order to check for molecular interaction in the ground state. As with methanol, it can be seen that in figure 31 there is a slight shift in the peak at around 340 nm, as the absorbance at 340 nm appears to decrease upon addition of dimethylaniline to the solution (Figure 32). This could be due to the solubility issue of the azo compound itself which could precipitate from the solution, hence lowering the absorbance value.

Several interesting points have been observed in the solution work, and these deserve a further discussion. The first order rate constant observed is consistent with the literature observations, that azobenzene compounds in solution thermally relax back via a first order process.[261] No attempt was made to investigate the azo compounds within in a rigid glass, due to the fact that for isomerisation on the surface of materials for everyday use, the use of a rigid glass would be both impractical and expensive.

The suggestion from previous literature is that the formation of aggregates in the presence of water and of polar protic solvents such as methanol afford a slower, hindered thermal relaxation rate is not what was seen here, however the possibility of some of the molecules isomerising, which are not in an aggregate form upon addition of water, is a factor which must be considered. The increase in the thermal relaxation rate upon addition of methanol and dimethylaniline to a solution of Admat 1 in dry THF is suggestive of other interactions at a molecular level occurring.

The work conducted using isopropanol as the solvent with addition of methanol shows a marked increase in the thermal relaxation rate constant after isomerisation from the *trans* to the *cis* isomer. The *cis* isomer can therefore be assumed to be less thermodyamically stable in polar aprotic solvents than in non polar solvents. The stacking of the π-π units in azobenzene has been observed previously to be influenced heavily by solvent, which is the trend observed here. The influence of polar groups on surfaces needs to be explored also, in order to make a comparison between solution and surface chemistry of these molecules, as attachment to surfaces is the priority for adaptive materials projects, understanding what happens in solution at a molecular level is helpful.

Azobenzene units are extremely sensitive to packing and aggregation, with π–π stacking causing shifts in the absorption spectra, and changes in photophysical properties. When the azobenzenes are aligned in a parallel fashion (head-to-head), they are called J aggregates, and give rise to a red-shift (bathochromic) compared to the well-isolated chromophore spectrum. If the dipoles are instead antiparallel (head-to-tail), they are called H-aggregates, then blue shift is observed.[264,265] Possible aggregation could result in the slower thermal relaxation of the triazinyl aminoazobenzene to the *trans* state. The relaxation could also be hindered due to the large triazinyl group, which appears to shift the absorption quite considerably from 374 nm to 355 nm, as any form of steric hindrance could affect the thermal relaxation rate

The rate of thermal relaxation from *cis t*o *trans* with dimethylaniline was plotted against concentration and found to give a curved graph (Figure 30). The rate does not dramatically increase was with the methanol. This could be due to less aggregation upon addition of dimethylaniline to the THF solution, also the possibility that upon addition of dimethylaniline, the mechanism of thermal relaxation does not change. The fact that precipitation is observed upon adding concentrations of dimethylaniline over 2 mol dm^{-3}, is the main reason why larger concentrations were not attempted.

4.10 Photoswitching of triazinyl coupled 4-aminoazobenzene and Admat 1 in solution

Aminoazobenzene was dissolved in various solvents to give an absorbance of 1. These solutions were then irradiated for 10 second in a 150 W xenon arc lamp. The thermal relaxation from *cis* to *trans* was then measured.

Solvent	λ / nm	k /(+/- 0.07) / 10^{-4} s^{-1}	ε / dm^3 mol^{-1} cm^{-1} (+/- 500)
Acetone	370	4.56	19000
cyclohexane	360	3.19	16400
acetonitrile	370	4.67	19500
Xylene	360	39.8	21000
Methanol	385	----------	----------

Table 6: Rate constants for thermal relaxation of aminoazobenzene in various solvents

Solvent	λ / nm	k /(+/- 0.06)10^{-4} s^{-1}	ε / dm^3 mol^{-1} cm^{-1} (+/- 500)
Acetone	375	5.16	23000
Cyclohexane	363	3.29	18500
Acetonitrile	375	4.81	17400
Xylene	370	35.6	23500
Methanol	385	----------	----------

Table 7: Rate constants for thermal relaxation for triazinyl coupled aminoazobenzene in various solvents

4.11 Summary of solution work.

The solution work carried out here has yielded some interesting results. The first and most important result is that of the solvent dependence upon the thermal isomerisation reaction in solution. The second is the behaviour of the amino functionalised azobenzene in methanol and higher alcohols. To summarise, it is important to consider all of the aspects of table 1 individually.

Firstly the peak shift that is found in polar protic solvents such as methanol, which was discussed in the introduction section, has been found here. The peak of Admat 1 in methanol is at 385 nm, whereas the peak of Admat 2 is at 365 nm. The Franck Condon interactions which produce this shift, due to reordering of solvent molecules are clearly seen here, this correlated with known literature of substituted azobenzenes in alcohol based solvents, and the explanation for this shift is found in the introduction to the solution work.

The fact that the kinetics in methanol were too fast to measure on the UV-Vis spectrophotometer has been further investigated in this section via the addition of polar alcohols to solutions of Admat 1 in THF. The results appear to indicate that solubility of the compound in methanol is a major factor here, as the Admat 1 compound precipitates out of solution upon addition of methanol, as it is poorly soluble in methanol initially.

As has been discussed earlier in this section, there is also a large variation for the perfluoroalkyl compounds and the rate constants for the thermal relaxation change with

solvent. The larger values for the rate constants in xylene for the perfluoroalkyl amino azobenzene (Admat 1) and the alkyl chain are interesting, as xylene is a non polar solvent where hydrogen bonding cannot occur, therefore the explanation of hydrogen bonding as a factor in the rate of thermal relaxation in xylene can be discounted. Interestingly, in xylene the aminoazobenzene and triazinyl aminoazobenzene compounds (tables 6 and 7) also show a marked increase in rate, similar to the Admat and Cfam compound.

In polar solvents such as cyclohexane, the fluoroalkyl and hydrocarbon chain azobenzenes (Admat 1 and Admat 2) have rate constants with the same order of magnitude as each other, indicating that non polar solvents such as cyclohexane do not affect the thermal relaxation rate as much as methanol or polar solvents. This has been seen previously with the addition of more polar solvents (water) to solutions of azo compounds in THF.

The relationship between the rate and solvent parameters has been investigated and no convincing relationship has been found suggesting, as mentioned earlier in this section that the solvent dependence on the rate of reaction is high. The dielectric constant has also been investigated and no discernable relationship was found here either, so the fact that hydrogen bonding can occur with methanol (but not with non-protic solvents) is a factor in the fast kinetics observed with methanol.

Chapter 5.0 Cellulose functionalised with azobenzene based molecules

5.1 Introduction

Cellulose has been discussed in the literature review as a possible substrate to couple to azo compounds. Cellulose has been chosen as the substrate due to its structural similarity to cotton, which is the basis of most natural fabrics.

The whole aim of this research is to create a photoisomerisable surface on a fabric coating for protection against liquids. This coating must be photoisomerisable, meaning that upon irradiation the coating can photoisomerise and upon further irradiation with the correct wavelength of light, it can photoisomerise back to its original state.

The aim here is to utilise the fluoroalkyl chain to create a photoisomerisable surface with superhydrophobicity which, upon irradiation changes to superhydrophilic. To control these properties, one must understand the functions of the azo molecules on the surface of the cellulose itself, hence copious amounts of preliminary studies are required before actually attaching the compound to the surface of the cellulose directly.

Having characterised the solution photochemistry and photophysics of the azo compounds in the previous chapter, there is a need to ascertain if these effects are similar or if they differ when azobenzene based molecules are affixed to surfaces and this is the objective of this chapter.

The work carried out here includes determining the amount of compound required to form a monolayer, the fractional coverage of the cellulose needed to form a monolayer, photoswitching studies and activation energy studies, which can then be compared with the values obtained for similar processes in solution.

5.2 Cellulose fractional coverage

In order to assess loading on cellulose, a series of samples were prepared with a variety of fractional monolayer coverage in order to ascertain the amount of Admat 1 that will be

required to obtain 100% monolayer coverage. Diffuse reflectance, UV-Vis spectroscopy and fluorescence were carried out on each of the samples.

The number of molecules needed to form a monolayer was calculated in section 3.11. The fluorescence peak of the monomer when excited a 375 nm was observed at 425 nm, the dimer peak at 475 nm. The ratio of estimated percentage loading to dimer concentration was plotted to obtain an estimate of the percentage of the 9-anthracene carboxylic acid required to obtain 100% monolayer coverage.

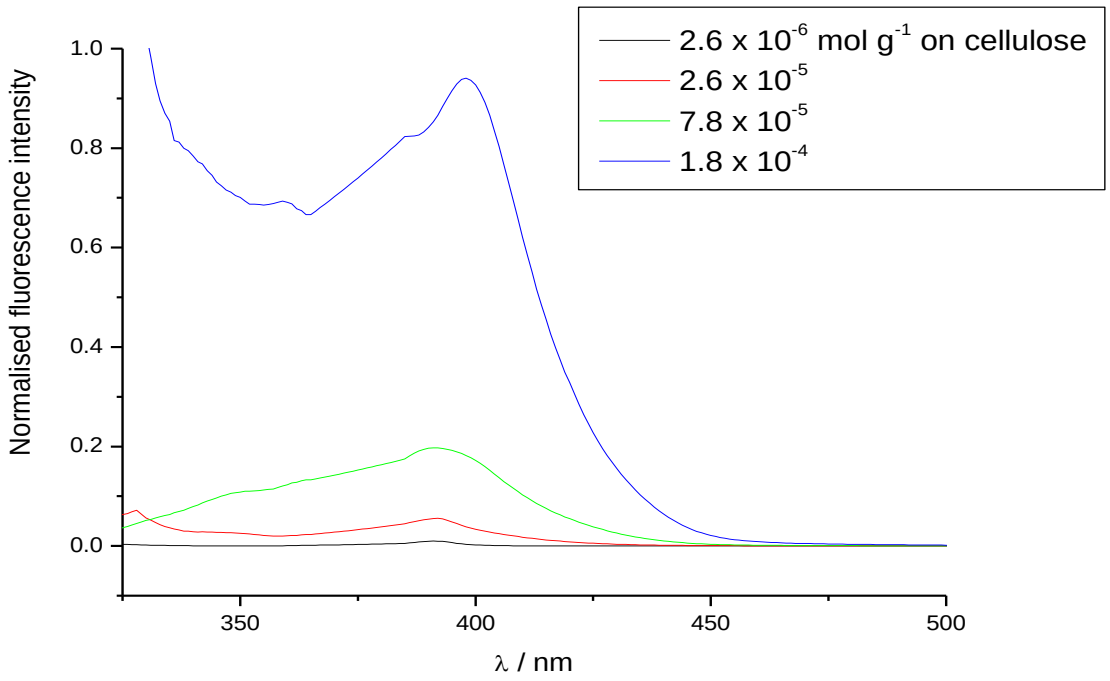

Figure 33: Graph of remission function versus wavelength (nm) for 9-anthracene carboxylic acid adsorbed onto cellulose at the concentrations shown.

The assumption made here is that the Admat 1 molecule and 9-anthracene carboxylic acid are around the same size, and that significant aggregation occurs only upon formation of a monolayer. F(R) was found to increase with concentration of compound, as expected. (See Figure 33)

Remission function increases with concentration as can be seen from the graph, indicating that surface coverage at low concentrations was successful. Fluorescence of the samples that were prepared was carried out in order to investigate emission properties.

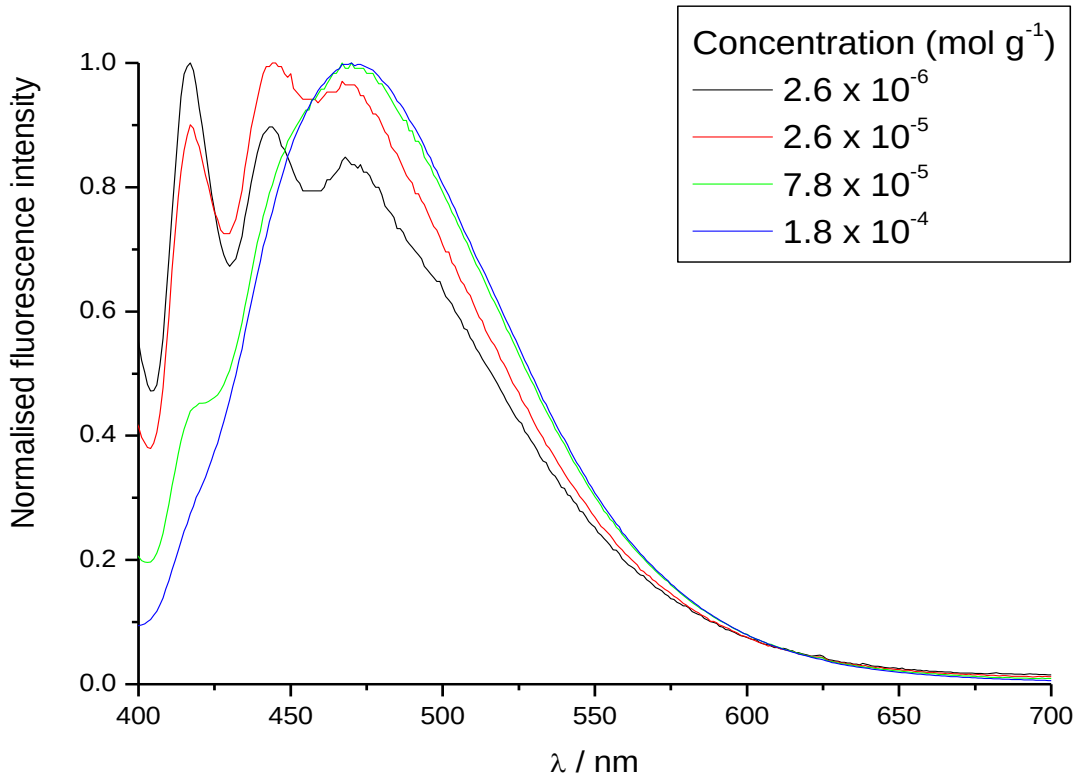

Fig 34: Normalised Fluorescence as a function of wavelength for different concentrations of 9-anthracene carboxylic acid on cellulose

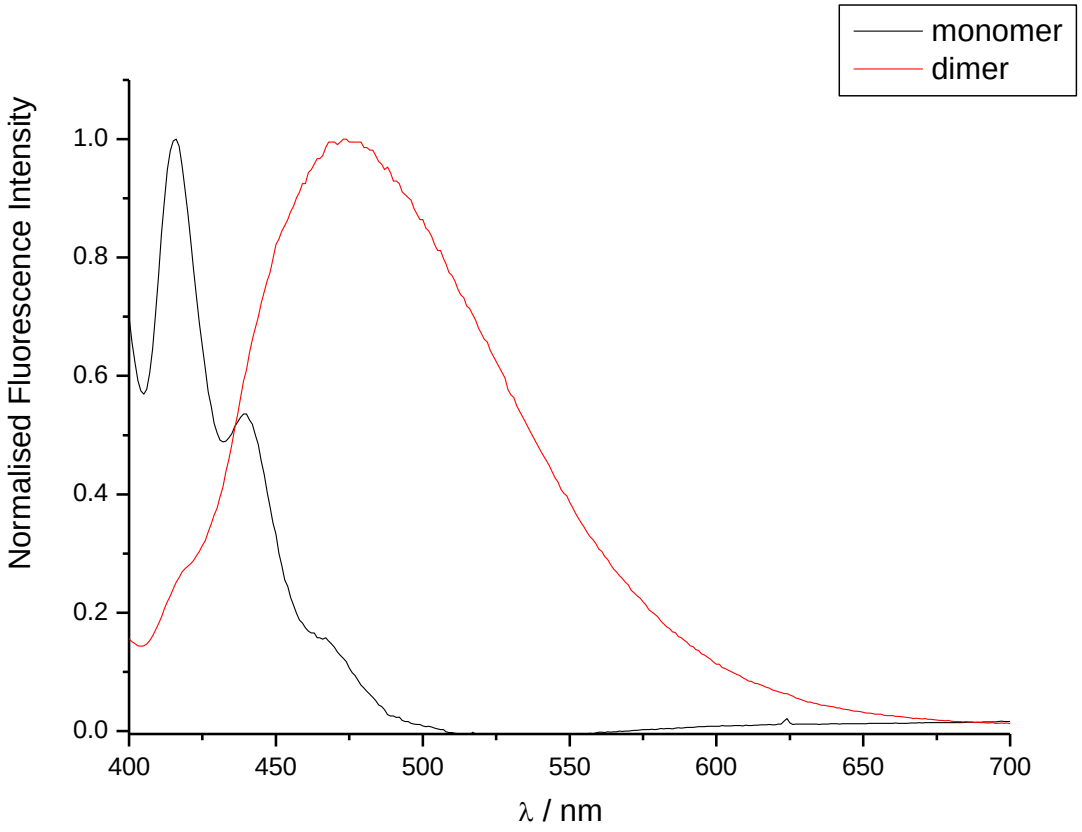

Figure 35: Pure monomer and dimer spectra of 9-anthracene carboxylic acid. Peaks for the monomer at 425 nm and for the dimer at 475 nm can be clearly seen.

The presence of two peaks in the spectra (Fig 34) indicates the presence of a monomer and a dimer of the 9-anthracene carboxylic acid. The peak at 425 nm is the monomer, whereas the peak at 475 nm is the dimer. The pure monomer and dimer spectra can then be combined in different amounts, i.e. 10% monomer, 90% dimer, etc until a variety of calculated spectra have been produced.

The pure monomer and dimer spectra were obtained by diluting the anthracene carboxylic acid until no spectral change was observed (for the monomer) and increasing the concentration until no further change in the spectra was observed (for the dimer) (Figure 35)

These spectra were then combined in different ratios to produce a series of calculated spectra from which comparisons to the fluorescence spectra of the samples of 9-anthracene

carboxylic acid could be made (Fig 36 and 37). The spectra were combined with each other in ratios i.e. 10% monomer/90% dimer based on the pure monomer and pure dimer spectra obtained. This would give a rough indication of surface coverage in terms of the percentage of a monolayer.

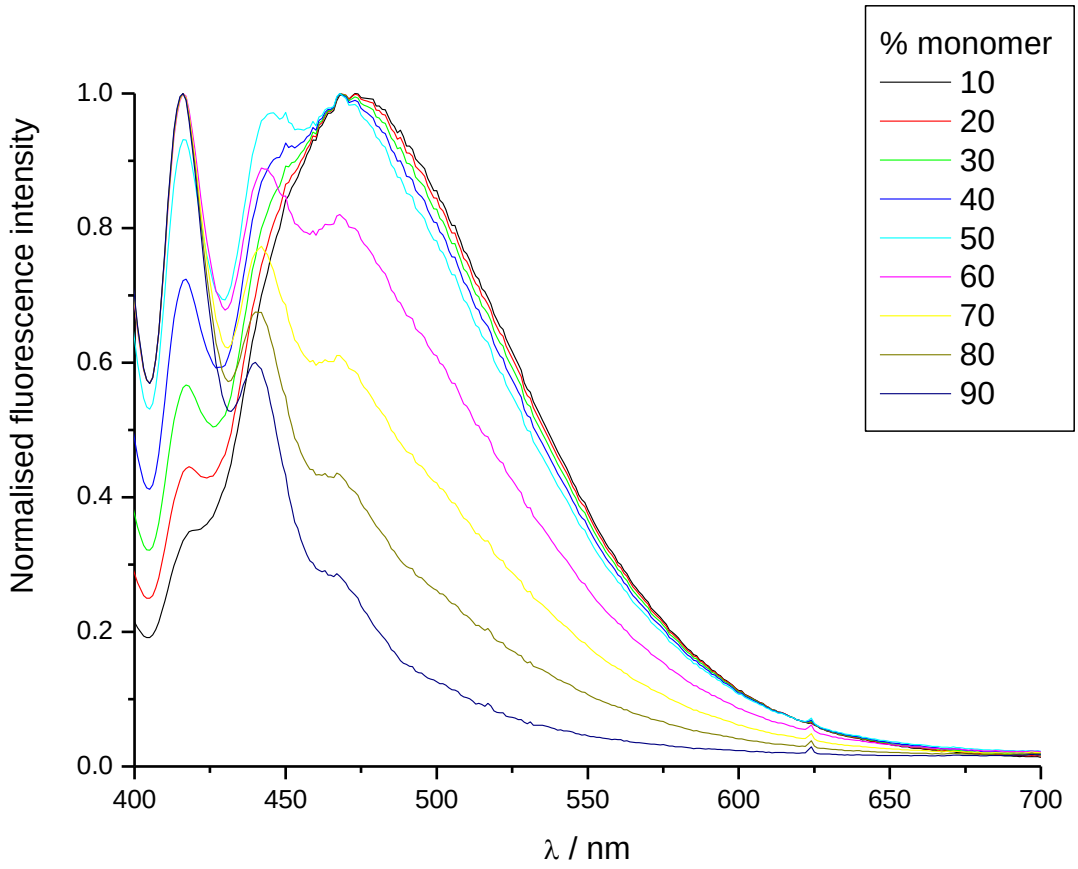

Figure 36: Calculated spectra for monomer:dimer mixtures.

The fluorescence emission from the samples prepared was measured (excitation at 375nm). The monomer dimer combinations were then compared with spectra obtained for different concentrations of 9-anthracene carboxylic acid on cellulose and were matched up to the monomer dimer plots.

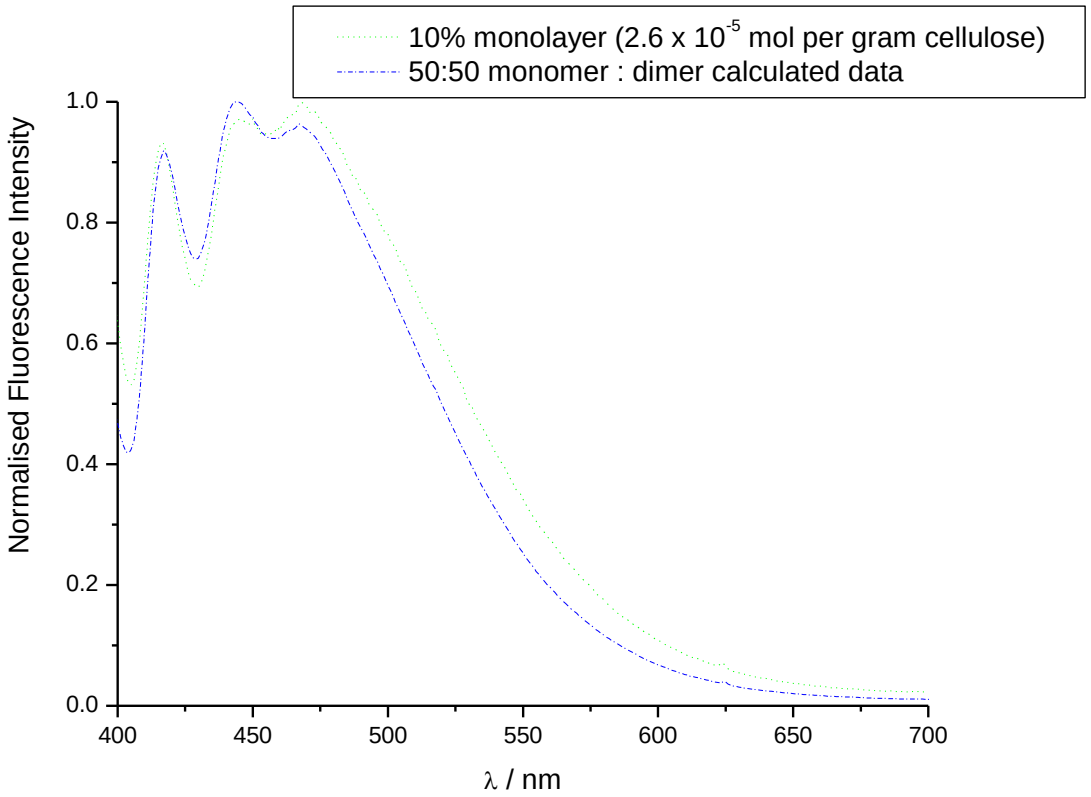

Figure 37: Normalised fluorescence as a function of wavelength data for 10% monolayer of 9-anthracene carboxylic acid and the calculated 50:50 monomer dimer spectrum.

From Figure 38, the close relationship between the 50:50 monomer dimer plot and the 10% monolayer plot can been seen. The other loadings on cellulose of 1%, 30% , 50%, 60% and 70% were treated in the same way, by looking at the spectra and finding out which calculated monomer dimer spectrum is the nearest to the actual fluorescence data obtained. The estimates for surface coverage were then used on a graph of percentage dimer versus concentration.

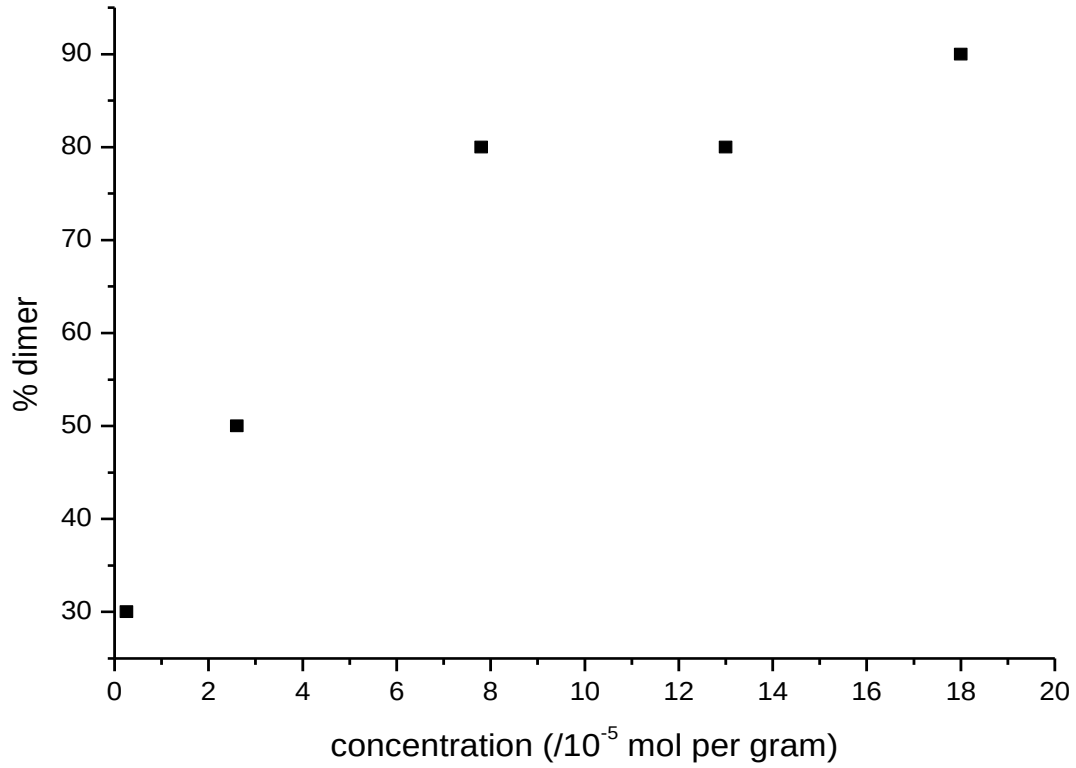

Figure 38: Plot of % dimer versus concentration for 9-anthracene carboxylic acid on cellulose.

From this graph, it can be estimated that monolayer coverage occurs at about 5 x 10^{-5} moles per gram of cellulose, which corresponds to about 65.9 mg g^{-1} of Admat 1 per gram of cellulose (see Figure 39). The assumption made here is that Admat 1 and 9-anthracene carboxylic acid are of the same size.

5.3 Admat 1 adsorbed to cellulose

Further to earlier work conducted with 9-anthracene carboxylic acid, Admat 1 was adsorbed to the surface of cellulose.

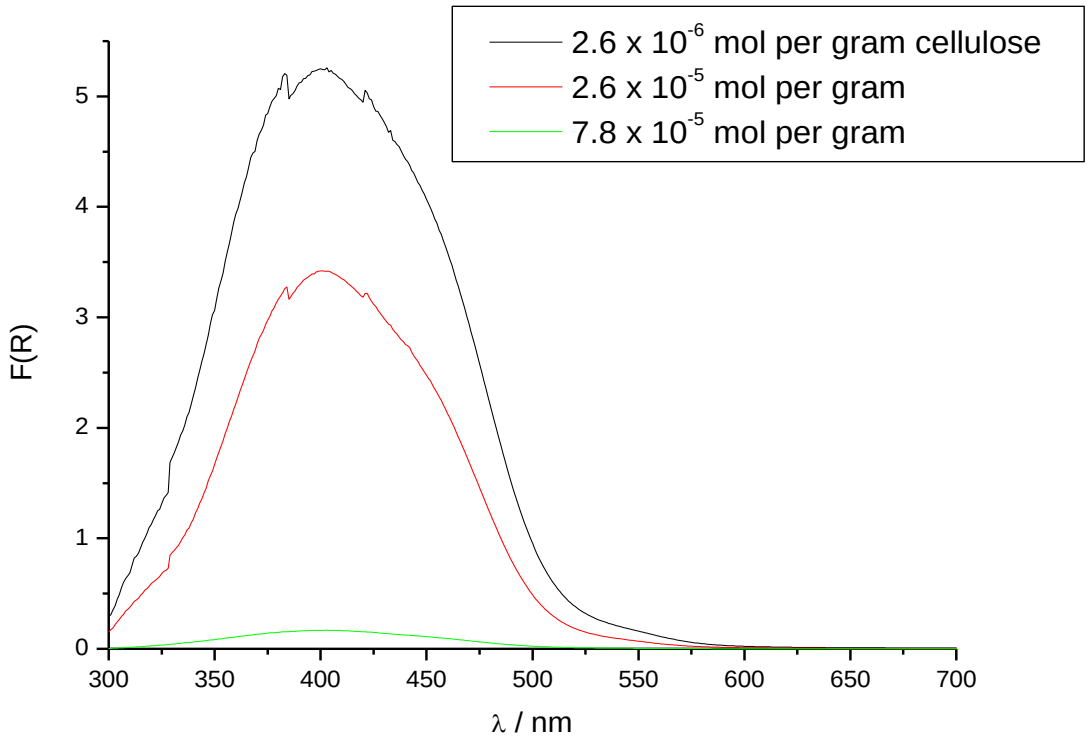

Figure 39: Diffuse reflectance of Admat 1 adsorbed onto cellulose at various concentrations.

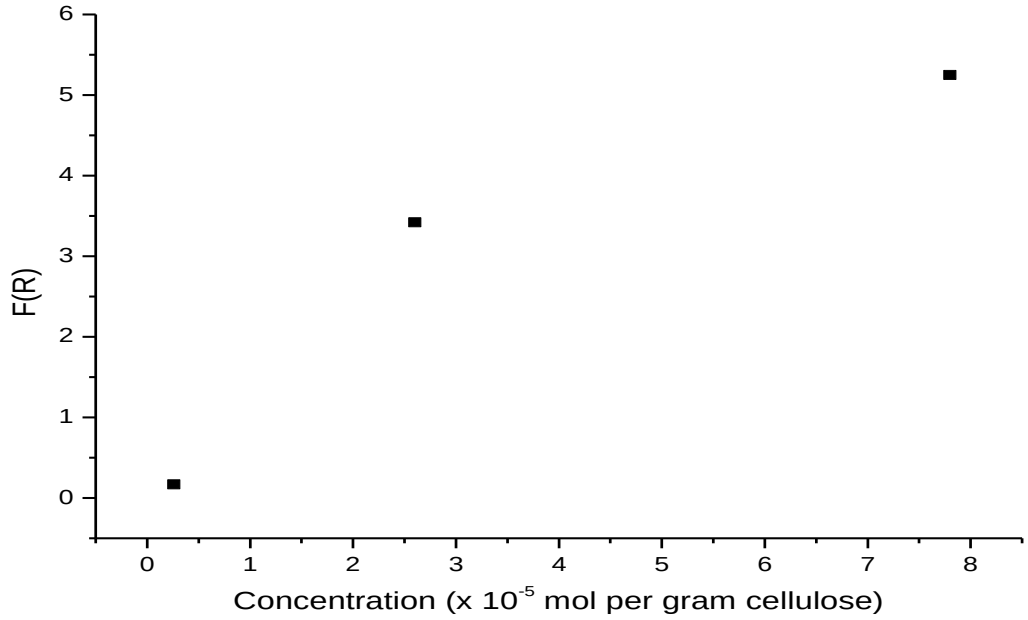

Figure 40: Graph of F(R) versus concentration for Admat 1 chemically onto cellulose.

The diffuse reflectance spectra (figure 39) shows that as the concentration of azobenzene increases, the F(R) increases also, which is indicative of the Admat 1 absorption to the surface. The F(R) is not exactly linear (figure 40), suggesting the formation of aggregates of the compound on the surface of the cellulose.

From figure 40, aggregation appears to occur after around 5 $x10^{-5}$ mol per gram of cellulose. The next stage is to ascertain if the azobenzene molecules on the surface can photoisomerise. Comparing figure 38 and figure 40, they both appear to show that aggregation occurs after around 3 x 10^{-5} mol per gram of cellulose.

The literature reports that Auramine O (a diarylmethane dye) did not aggregate until concentrations of 1 x 10^{-5} mol per gram were used on cellulose, which gives a good indication that the value obtained is of the correct order of magnitude. [267]

5.4 Admat 1 photoisomerisation on cellulose

A sample of Admat 1 of concentration 1 $x10^{-5}$ mol g^{-1} was produced by dissolving Admat 1 in a solution of methanol with sonication and then adding it to a sample of dry cellulose. Evaporation of the solvent yielded a sample of Admat 1 adsorbed to the surface of cellulose. The ability of this sample to photoisomerise successfully was assessed by irradiation of the sample for 10 seconds and then monitoring the reflectance change at 390 nm over 30 minutes (figure 41). This shows that the sample can photoisomerise, and after around 12 hours, returns to the initial value.

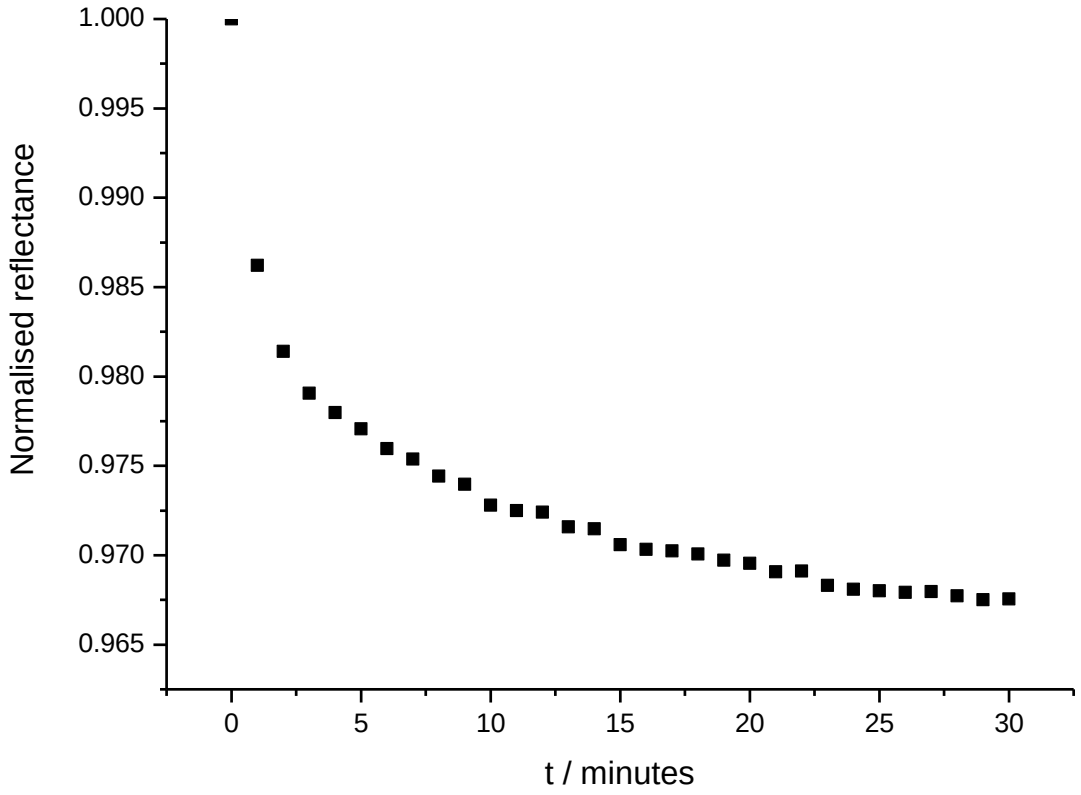

Figure 41: Thermal relaxation of Admat 1 sample 1 x 10^{-5} coupled onto cellulose surface.

The next stage of the process is to monitor this isomerisation process at different temperatures, in order to find the activation energy in order to compare this value with the solution data previously obtained.

5.5 Temperature dependence of the thermal relaxation process of Admat 1 coupled and adsorbed onto cellulose samples

The samples described here were prepared via the methods shown in the experimental section (sections 3.13 and 3.14).

The samples were heated using an electrically heated thermostat block. The temperatures studied ranged from 20°C to 65 °C. The samples were measured at a single wavelength (390 nm) over a period of 30 minutes. The samples were heated until the temperature was constant, then the samples were switched in a 150W xenon arc lamp for 1 minute. The

thermal relaxation was then measured. Figure 42 shows a temperature dependence plot obtained during the studies.

The data obtained from the thermal relaxation plots was then fitted with an exponential curve in order to obtain the time constant, which then is used to calculate the rate. The rates are then used in order to calculate the activation energy by means of the Arrhenius Equation.

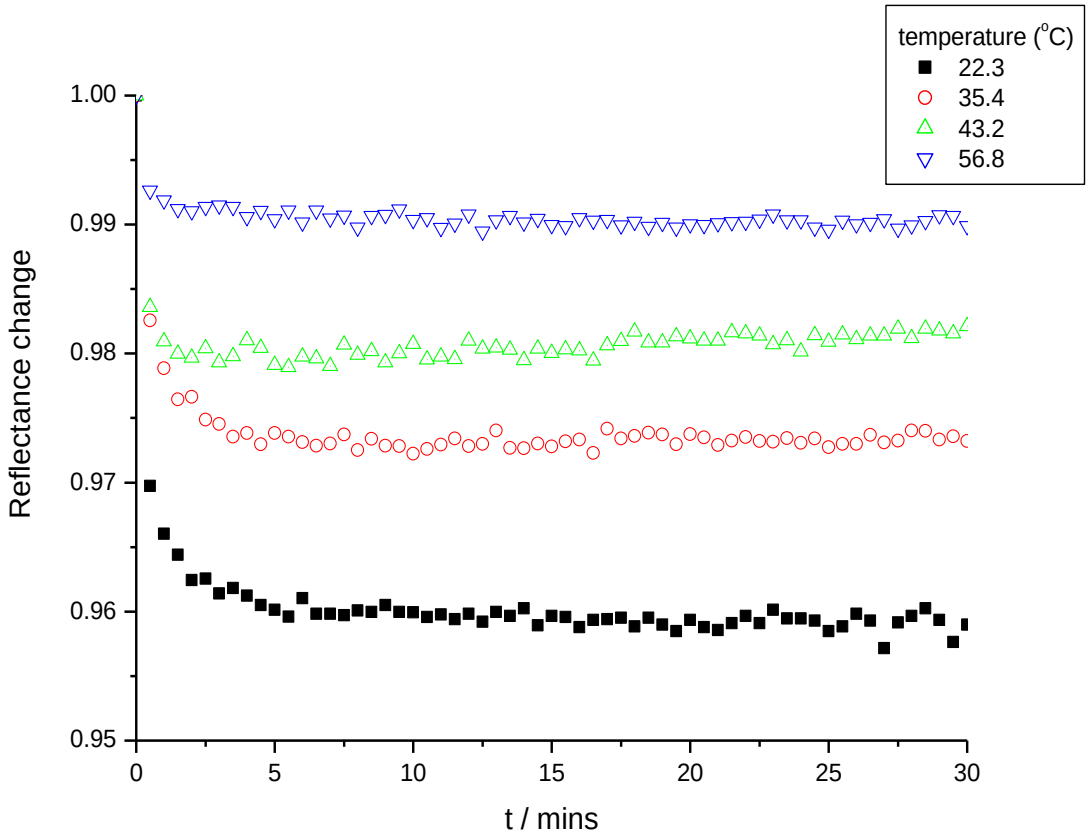

Figure 42: Temperature dependence of Admat 1 (2.6 x 10^{-5} mol g^{-1}) coupled to cellulose.

Analysis of the results from running temperature dependence experiments for 30 minutes showed that the thermal relaxation reaction occurred over a shorter time period, after around 5 minutes there is virtually no change in reflectance. Therefore, the experiments were repeated over a time period of 5 minutes. The graph below shows a dependence of thermal relaxation time with increasing temperature.

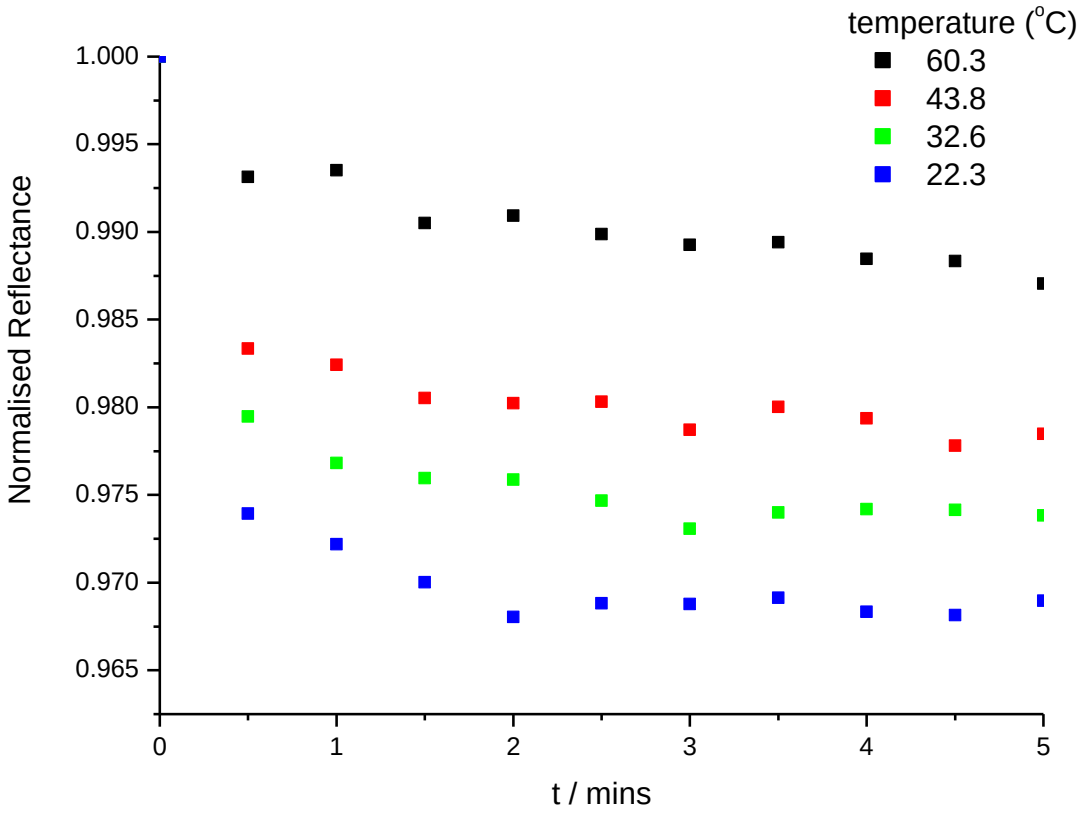

Figure 43: Temperature dependence of Admat 1 coupled to cellulose (7.12 x 10^{-8} mol g^{-1}).

At higher temperatures, running the experiment for 5 minutes appears to show that at lower temperatures, some relaxation is occurring, however, at higher temperatures, the thermal relaxation has finished even after 2 minutes, hinting that the reaction has ceased, and the compound has returned to its initial state before irradiation.

5.6 Rate calculations for Admat 1 coupled and adsorbed to cellulose and summary of results

The activation energies were calculated by fitting the graphs of temperature versus reflectance with a first order exponential curve. Arrhenius plots were then constructed.

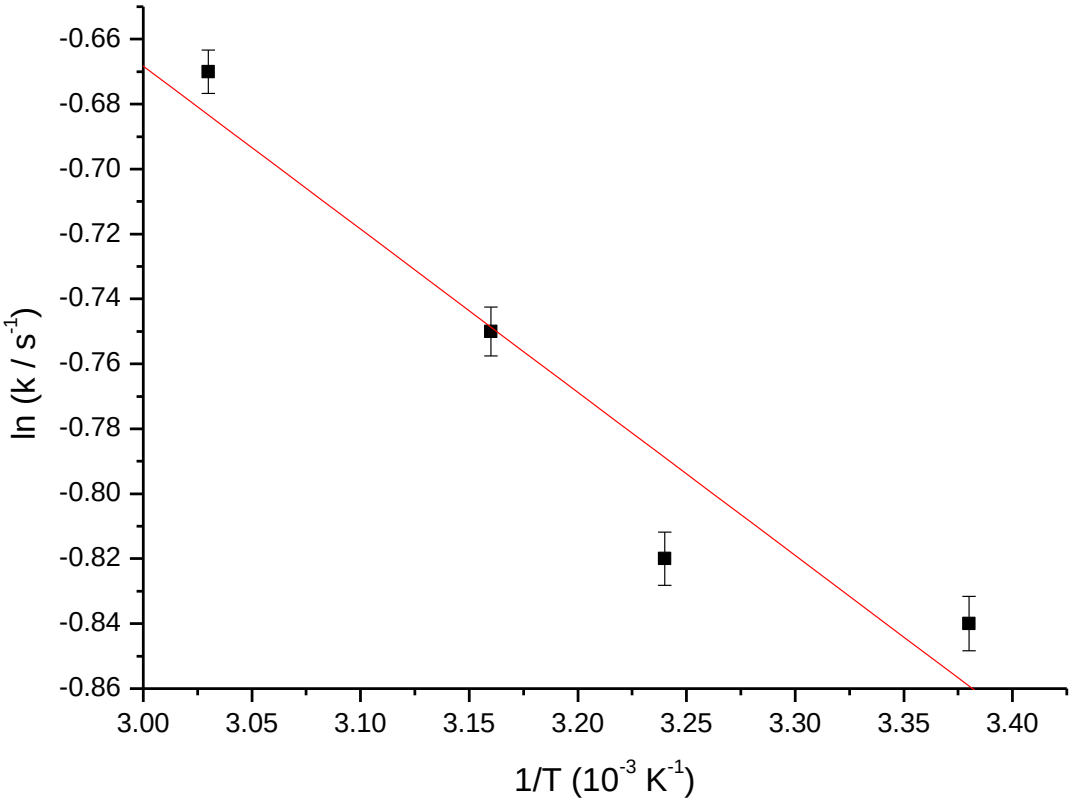

Figure 44: Arrhenius plot of Admat 1 chemisorbed to cellulose (7 x 10^{-8} mol g^{-1})

Admat 1 adsorbed to cellulose

Concentration / mol per gram	Activation energy / +/- 0.5 kJ mol^{-1}	Pre exponential factors /10^{-1} s^{-1}
1 x 10^{-7}	2.01	4.86
5 x 10^{-6}	2.36	3.36
1 x 10^{-5}	3.30	3.16
5 x 10^{-5}	3.85	3.01

Table 8: Activation energy of thermal relaxation reaction of Admat 1 adsorbed to cellulose

Admat 1 coupled to cellulose

Concentration mol per gram	Activation Energy / +/- 0.5 kJ mol^{-1}	Pre exponential factor $/10^{-1}$ s^{-1}
7×10^{-8}	4.04	7.91
2×10^{-6}	5.25	7.60
5×10^{-5}	8.15	5.06
1×10^{-4}	9.30	5.12

Tables 9: Activation energies for the thermal relaxation reaction of Admat 1 coupled to cellulose

From the data shown above (Tables 8 and 9), it is shown that the coupled samples have a slightly higher activation energy then the adsorbed samples. This could be due to the fact that the groups are actually anchored to the surface, so movement is hindered, leading to higher activation energy. The movement of the azobenzene molecule on the surface can also be hindered by the fluoroalkyl chains twisting, which creates a hindrance to the switching, leading to higher activation energies.

The activation energies seen here are much lower than in solution, this may be caused by the lack of hindrance from solution molecules, which hinder the isomerisation reaction. The lower values for the uncoupled compounds on cellulose is a result of the fact that the molecules on the surface are free to move as they are only held in place by hydrogen bonds between the OH groups of the cellulose and the NH_2 groups of the amine. This enables the molecules to move easily and therefore lowers the activation energy.

The shift in the peak on cellulose is similar to that of methanol (385 nm) for Admat 1. The presence of the hydroxyl group and the polarity of the surface, due to the presence of OH groups allows for the conclusion that the polarity is the cause of the peak shift to 390 nm here also.

Chapter 6.0: Azobenzene on a silica surface

6.1 Modification of the surface of silica with aminopropyltriethoxysilane

The hydroxyl groups on the surface of silica make it an interesting substrate to investigate as the triazinyl group can be made to attach to the surface. The decision to investigate silica was began by calculating the surface area of the silica used, coupling the azo dye to the surface and investigating the activation energy of the thermal relaxation reaction on the surface of the silica.

A known method of coupling the APTS (aminopropyltriethoxysilane) to silica was found. [267] The aminopropyltriethoxysilane is coupled to the surface of the silica, and then the triazinyl azobenzene derivative is then attached to the end of the APTS group.

Initially, the amount of APTS to form a monolayer was calculated, which was found to be 8.1 x 10^{-4} mol g^{-1} of silica (surface area of silica gel 60Å, 6 x 10^{-10} m is 490 m^2 g^{-1}). Therefore 8.1 x 10^{-4} x 221.37 (M_r of APTS) = 0.179g APTS per gram of silica gel.

The APTS was coupled to the silica gel according to the method described in the experimental section (section 3.19)

Reflectance of the sample was measured (Figure 45)

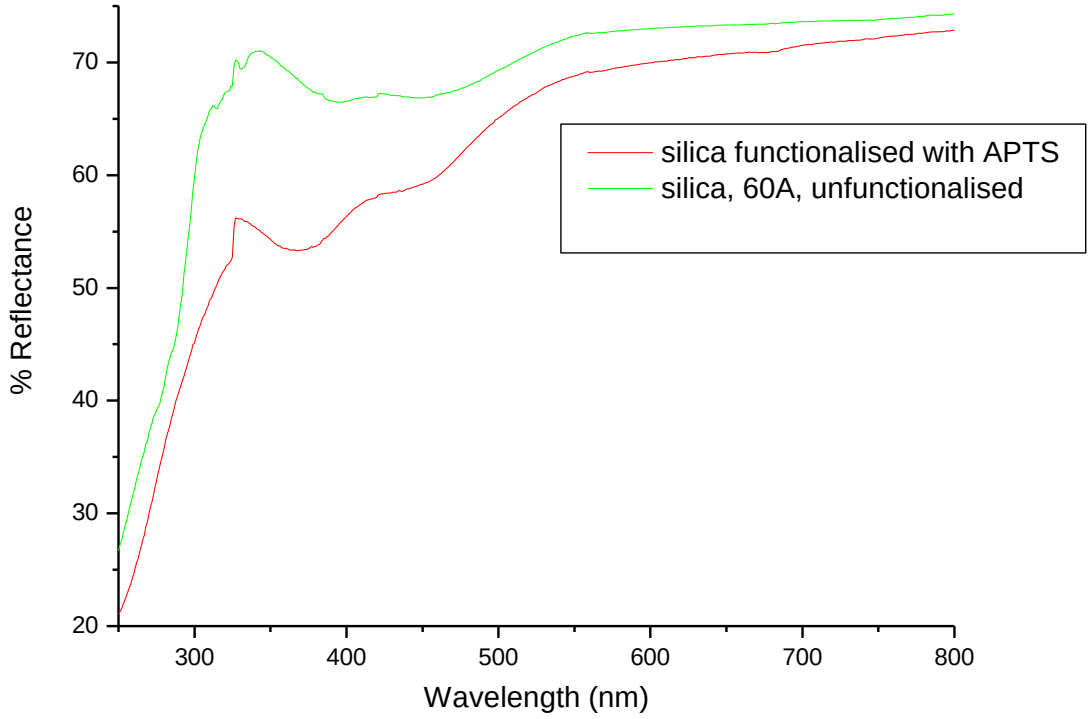

Figure 45: Reflectance spectra of unfunctionalised silica and functionalised silica (blanked to barium sulphate)

The reflectance of the silica functionalised with APTS (aminopropyltriethoxysilane) is less than the pure silica, indicating that the APTS is on the surface of the silica itself. ^{29}Si NMR was attempted on this sample in order to make a comparison between the sample produced and the literature data given. The ^{29}Si NMR (Figure 46) was concurrent with the literature data[(268)] showing peaks at around 70 and 110 ppm, which is comparable to the data given in the literature. Figure 45 shows that the reflectance increases from 250 nm to 300 nm as silica absorbs below around 220 nm. The decreases in reflectance between the functionalised silica gel and the unfunctionalised silica gel show that the bonding on the surface between the APTS groups and the OH groups on the silica affects the reflectance, as the more APTS groups are present, the greater the absorption of light, hence the lower reflectance.

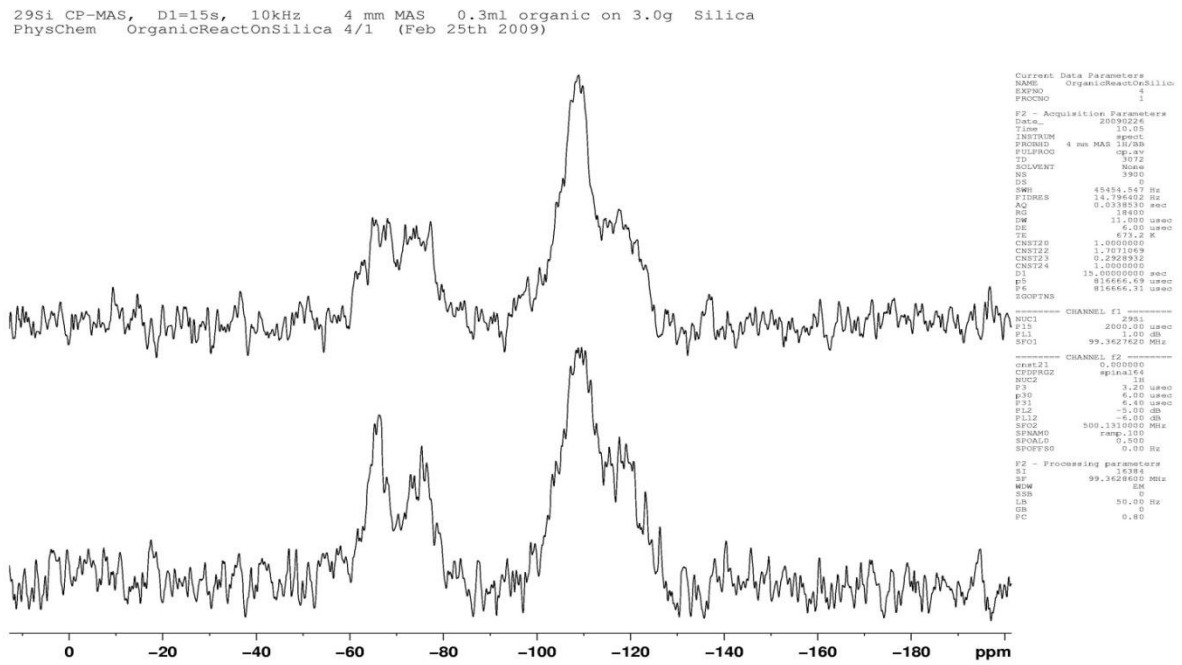

Figure 46: ^{29}Si NMR of functionalised silica samples. Peaks at 65 ppm and 75 ppm consistent with reported literature.[(268)]

6.2 Coupling triazinyl aminoazobenzene to APTS functionalised silica gel

Samples of functionalised silica with APTS were used as a substrate to couple to triazinyl aminoazobenzene. Samples of 2.89 x 10^{-6} mol g^{-1} (1mg/gram) and 2.89 x 10^{-7} mol g^{-1} (0.1 mg per gram) were prepared according to the method described in the experimental section.

An attempt was made to produce a sample of triazinyl coupled silica without the APTS linker group, but this was unsuccessful, as the triazinyl aminoazobenzene was washed off when the compound was filtered and washed with acetone. This is further proof that the coupling reaction between the triazinyl group and the APTS has worked, as without the APTS the triazinyl aminoazobenzene washes off, leaving the unfunctionalised silica in the filter paper.

The reflectance of the samples was measured between 250 and 800 nm using barium sulphate as a blank. Then the samples were irradiated and the reflectance measured in order to detect any photoisomerisation reaction which may occur.

6.3 Diffuse reflectance of coupled aminoazobenzene to APTS surface

The diffuse reflectance of both samples was measured (Figure 47) and, as expected, as the concentration increases, the reflectance decreases, due to an increase in the absorbance. The peak of the aminoazobenzene compound at around 370nm is present, showing coupling has occurred. The compounds were then irradiated to assess photoisomerisation.

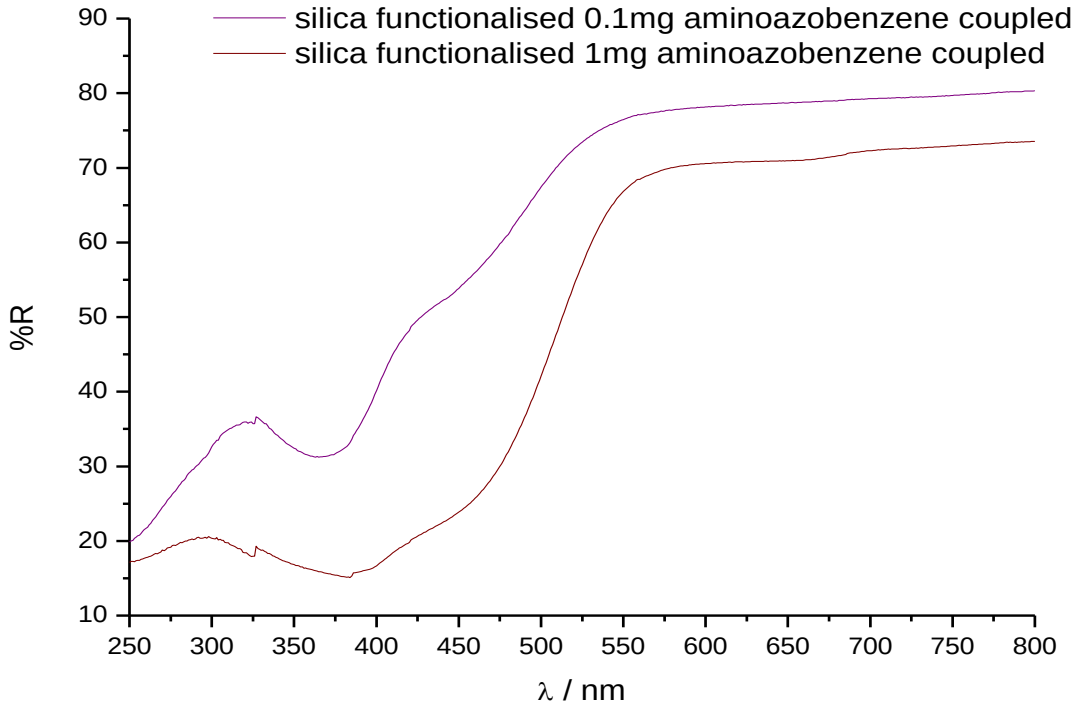

Figure 47: Diffuse reflectance of coupled silica samples (0.1mg g^{-1} and 1mg g^{-1})

The peak at around 380 nm which is characteristic of the azobenzene groups is present, indicating coupling to the surface of the silica gel. The peak at 380 nm is at the same wavelength seen when the compounds are dissolved in polar solvents. The presence of OH groups on the surface of silica as well as in methanol solution, the similarity of the wavelengths of the peaks would suggest the polar OH groups interact with the NH_2 moiety on the azobenzene surface possible through hydrogen bonding.

The loss of the structure of the peak at 1mg g^{-1} shows high aggregation and is a possible indication of overloading, i.e. too high concentration of compound on the surface. This is confirmed when the F(R) (Figure 48) is plotted as the line does not pass through the origin,

therefore indicating that aggregation is present. Aggregation is observed at 1 x 10^{-5} mol per gram using Auramine O as the dye, but aggregation is seen here at concentrations lower than with Auramine O and as the Admat and Cfam molecules are larger, which would be expected.[266]

The correlation with the cellulose, where aggregation occurred at around 1 x10^{-4} mol per gram, and in the case of silica, where aggregation is present at around 2 x10^{-7} mol per gram can be explained. The overall surface area of silica is lower than cellulose; therefore aggregation at lower concentrations of Admat compound would be expected.

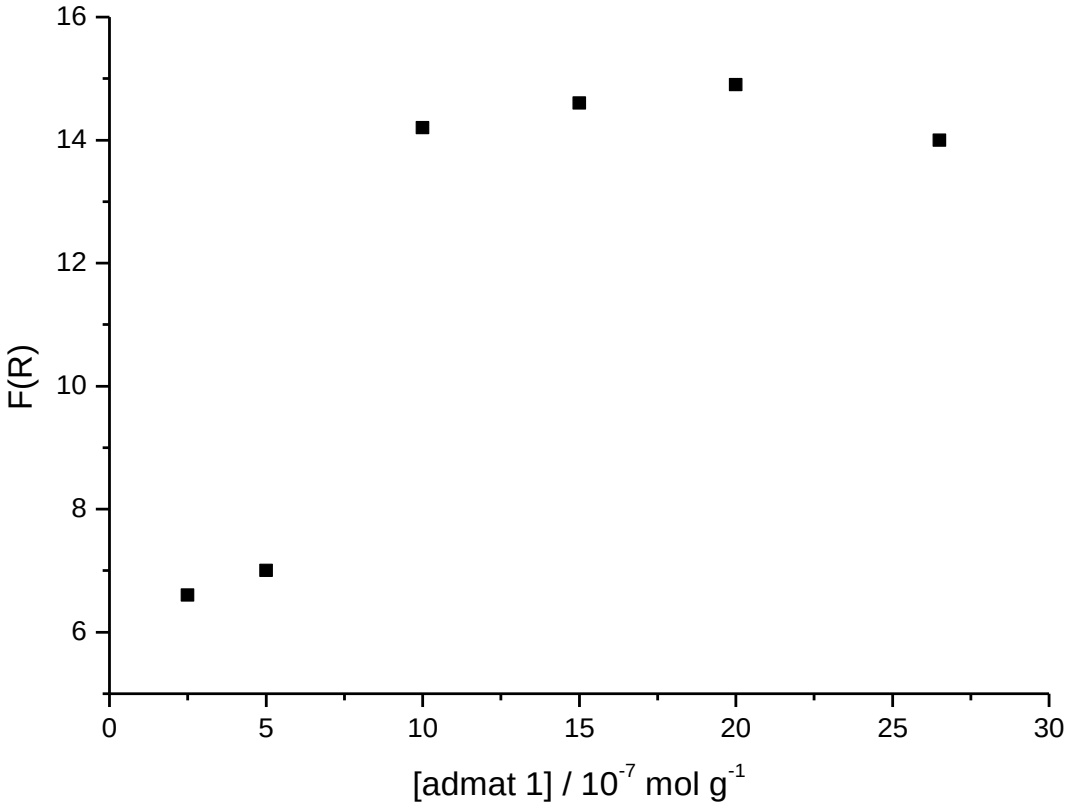

Figure 48: F(R) versus concentration of aminoazobenzene on the surface.

6.4 Switching of coupled aminoazobenzene on APTS functionalised silica

The samples 1 mg (1.2×10^{-6} mol g^{-1}) and 0.1 mg per gram (1.2×10^{-7} mol g^{-1}) were irradiated for 5 minutes using a 150W Xenon arc lamp; the change in reflectance was then measured.

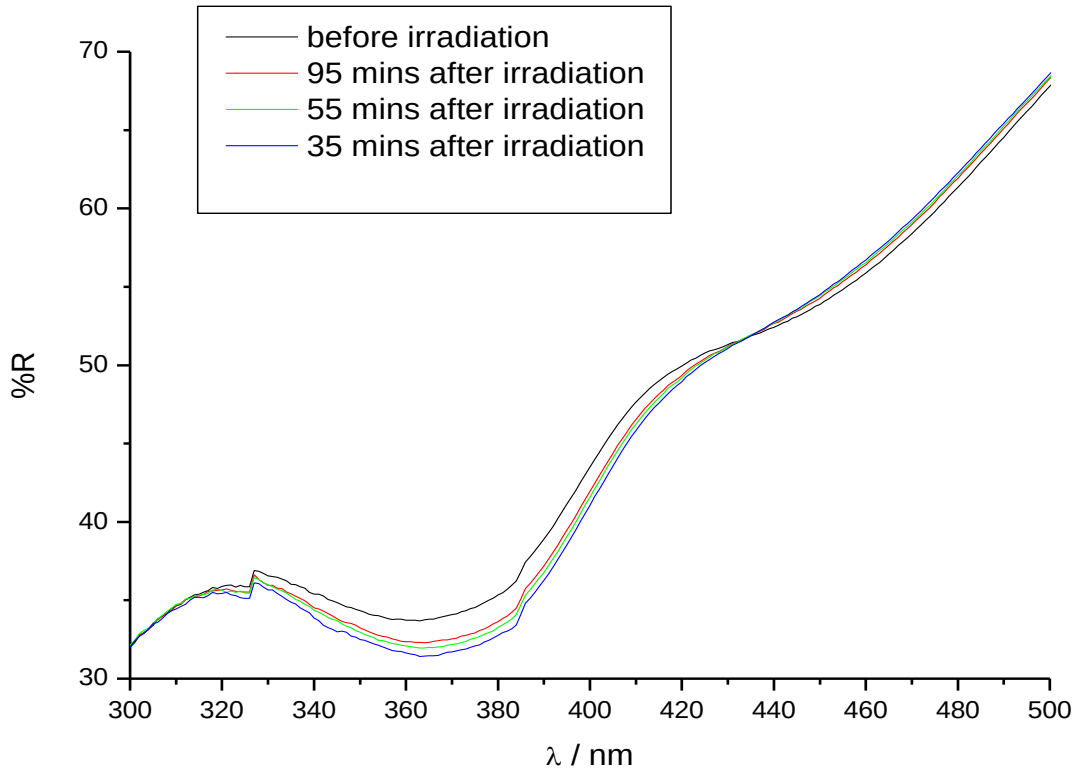

Figure 49: Reflectance change after irradiation for 0.1 mg g^{-1} (1.2×10^{-7} mol g^{-1}) coupled aminoazobenzene to silica using APTS

The results of the photoisomerisation experiments (Figs 47 and 49) show that upon irradiation with a 150 W Xenon arc lamp, *trans-cis* photoisomerisation occurs.

The *trans* peak (370 nm) can be seen to increase in reflectance (decrease in the absorbance) whilst the *cis* peak (at 480 nm) decreases in reflectance (increases in absorbance) at 480nm. Further work was carried out to ascertain the lifetime of the triazinyl aminoazobenzene on the silica surface.

The evidence provided in Figure 49 for photoisomerisation is important in the context of this work, as the process is reversible, as the *cis* isomer formed from irradiation thermally relaxed back to the *trans* isomer. This fact enabled the calculation of the activation energies using an Arrhenius Plot, which would allow a comparison to be made between silica surface activation energies and activation energies in solution.

6.5 Temperature dependence of the thermal relaxation process for Admat 1 coupled and adsorbed to silica

The coupled samples of aminoazobenzene produced were shown to photoisomerise. The next stage was to investigate the isomerisation of Admat 1 on the surface. This investigation was required in order to investigate the rate of thermal isomerisation from *cis* to *trans* so that the activation energy could be obtained. This enabled a comparison to be made between the activation energies on the different substrates studied.

The silica samples produced were irradiated for a period of 10 seconds using a 150 W Xenon Arc lamp and the change in reflectance was measured over 5 minutes (Figure 50). The temperature dependence investigations were carried out using the diffuse reflectance spectrophotometer as mentioned in the experimental section, fitted with a temperature controlled heating block.

From the temperature dependence data shown below, the activation energy was found in the same way as with the cellulose samples by fitting the data with a first order exponential curve, then calculating the rate constant and plotting the Arrhenius graph of the data. (Fig 51)

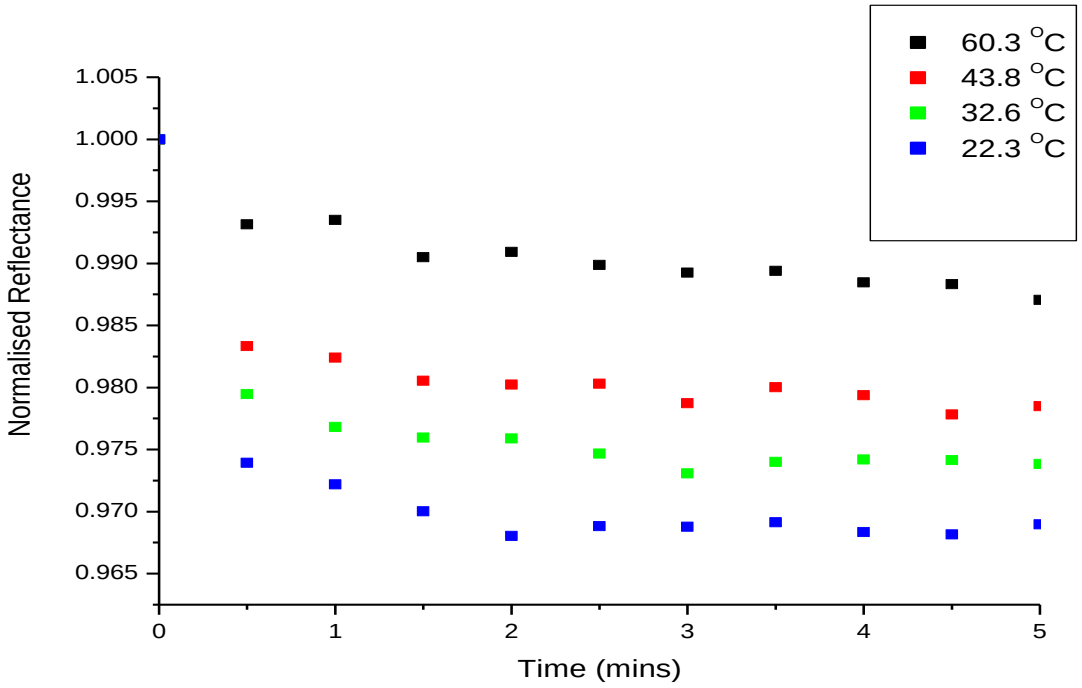

Figure 50: Temperature dependence of 1.2 x10^{-7} mol per gram Admat 1 coupled to silica.

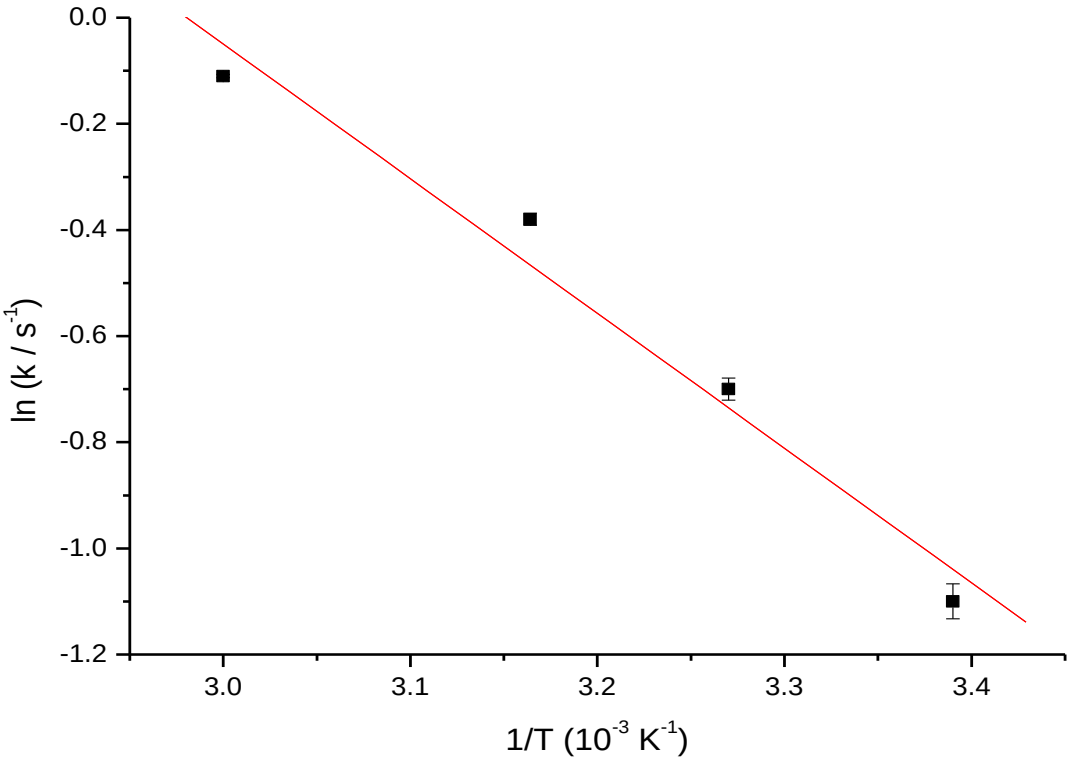

Figure 51: Arrhenius plot of 3.7 x 10^{-7} mol per gram Admat 1 coupled to silica.

In order to investigate how very high and low concentrations of Admat 1 affect the thermal relaxation rate on silica, it was decided to produce a high concentration and a low concentration of Admat 1 coupled and adsorbed to silica. The thermal relaxation of the Admat 1 on silica was determined for the concentrations prepared.

The samples were produced as described previously in the experimental section, by chemically coupling the Admat 1 to the surface and via the method of adsorption previously used. The concentrations prepared were 25 mg per gram (3.7×10^{-5} mol per gram), as a high concentration and 0.01mg per gram (1.5×10^{-8} mol per gram) as the low concentration samples. The samples were irradiated using a 150 W Xenon arc lamp for 10 seconds and them the reflectance change was measured using a solid state spectrometer. The rate is calculated via fitting the curve and then the activation energy calculated via the plotting of an Arrhenius plot.

The data obtained is shown in figures 52 and 53

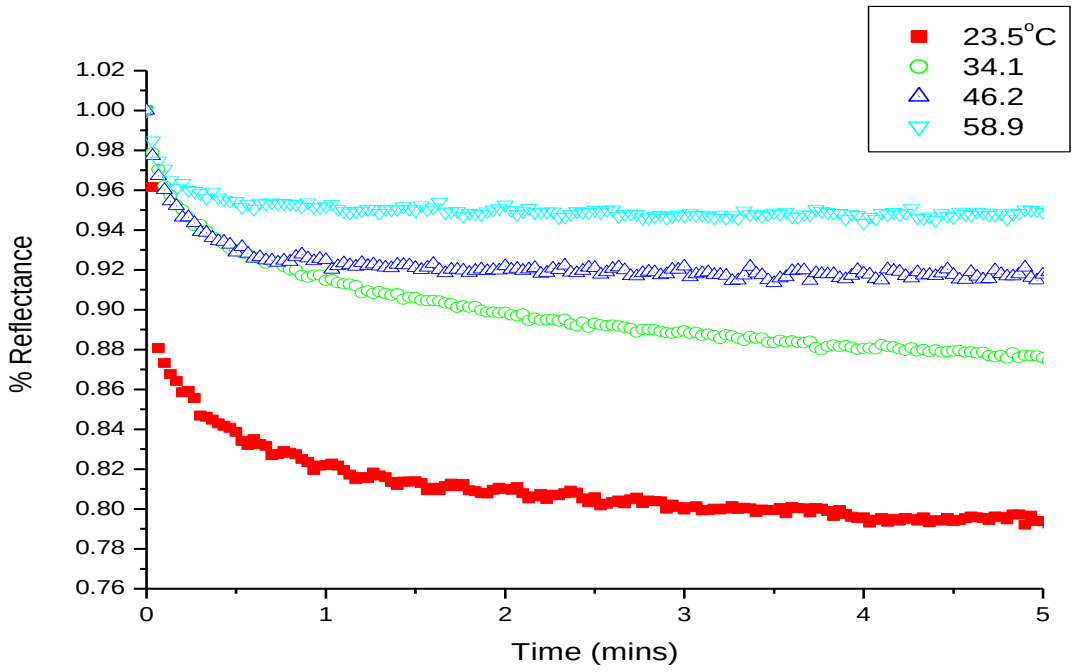

Figure 52: Temperature dependence of 0.01mg/ gram (1.5×10^{-8} mol per gram) Admat 1 coupled to silica

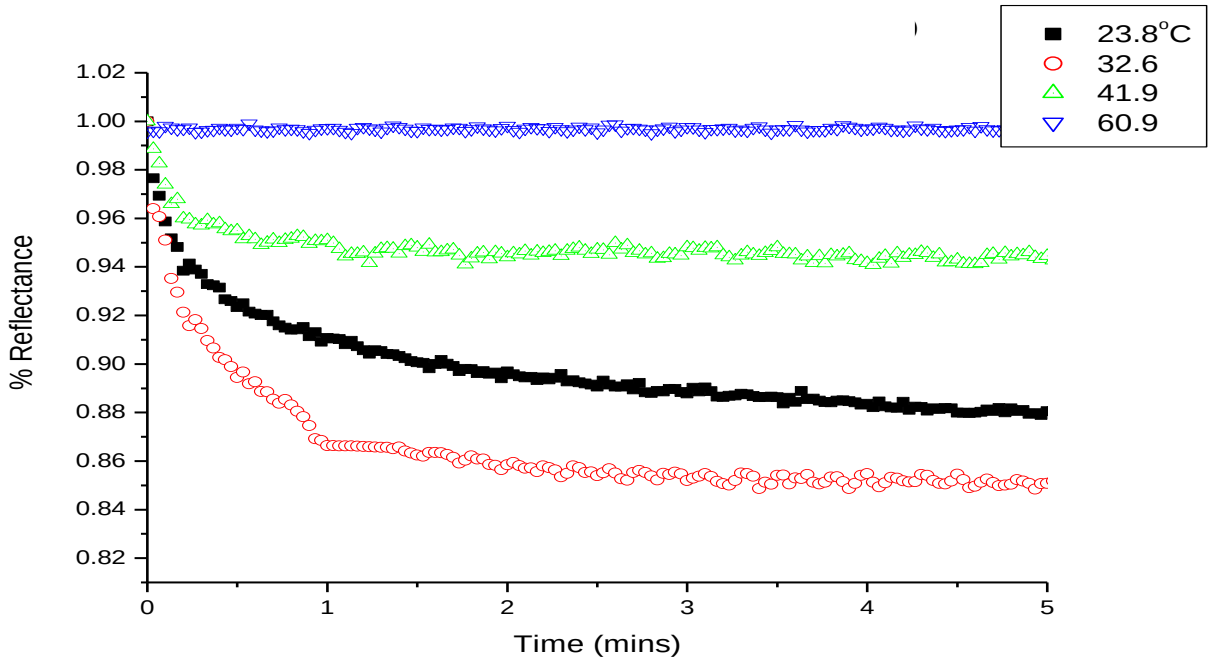

Figure 53: Temperature dependence of 25mg/ gram (3.7 x 10^{-5} mol per gram) Admat 1 coupled to silica

The data was fitted and the values obtained were added to the table from previous work.

Chemically coupled

Concentration / mol g^{-1}	E_A / +/- 0.5 kJ mol^{-1}	A / 10^{-2} s^{-1}
1.5 x 10^{-8}	5.2	3.46
1.2 x 10^{-7}	10.1	2.71
3.7 x 10^{-7}	12.9	1.43
1.2 x 10^{-6}	14.8	1.15
1.1 x10^{-4}	15.6	0.12

Table 10: Data obtained for thermal relaxation experiments on Admat 1 chemically coupled to silica samples.

Adsorbed

Concentration / mol g^{-1}	E_A / +/- 0.5 kJ mol^{-1}	A / 10^{-2} s^{-1}
1.5 x 10^{-8}	4.3	4.12
1.5 x 10^{-7}	9.1	4.28
4.6 x 10^{-7}	10.2	5.79
1.5 x 10^{-6}	11.3	5.90
1.1 x 10^{-4}	13.9	7.89

Table 11: Data obtained for thermal relaxation experiments on Admat 1 adsorbed to silica samples.

The trend observed here in table 10 is with increasing concentration, the activation energy increases. This is possibly due to steric hindrance from the fluoroalkyl chain which could possibly interlink and hinder the thermal relaxation from the *cis* isomer to the *trans* isomer. Investigation of the pre-exponential factors for the coupled and absorbed silica data was conducted.

The same trend in table 11 is observed, that the pre-exponential factors increase with increasing concentration, indicating that at higher concentrations the thermal relaxation reaction is hindered possibly as a result of surface aggregation and interlocking of fluoroalkyl chains on the surface. The activation energies on cellulose are less than is found here on silica, this is probably due to the fact that the large linker group used here on silica means that the triazinyl compound can attach to the surface without aggregating, hence the lower activation energies on cellulose than in silica. The activation energies in solution were found to be higher than on silica. The molecular motion of the azobenzene molecule can be hindered by solvent molecules, whereas there are no solvent molecules present here to hinder the movement of the molecules, therefore the activation energy is less than in solution.

6.6 Summary of silica studies

The data obtained shown in tables 10 and 11 indicates that as the concentration increases, then the activation energy increases, which can be explained as the more concentrated the sample, the more chances of molecules aggregating on the surface, leading to steric

hindrance, and thus leading to a higher activation energy, as more energy is required for the thermal isomerisation process.

The activation energy of the azobenzene compounds coupled to silica was higher than the activation energy on cellulose. The use of the spacer group, APTS, may interact with the large fluoro chain on the azobenzene causing steric hindrance. The activation energies are lower than that of the solutions, which would indicate that solvent dependence as well as the possibility that hydrogen bonding between the OH groups on silica and the amino groups on the azobenzene compound could also be present. The peak of the cellulose spectra is at around 380 nm, 10 nm less than on silica, the main reason being that the use of the spacer APTS group means that surface OH interaction, which causes the blue shift, is less than on cellulose, however, this value is similar to the polar solvents such as methanol, so this still suggests the surfaces are largely polar environment.

There is also a slightly larger change in absorbance after irradiation on silica than on cellulose, leading to the conclusion that a slightly larger degree of photoisomerisation occurs than with cellulose as a substrate. Larger activation energies with higher concentrations also would indicate that some steric factors, such as overcrowding or clustering of the azobenzene molecules on the surface is present, leading to aggregation, which hinders the thermal isomerisation process, leading to higher activation energies.

The similarity with solution of the compounds in alcohols and polar solvents was mentioned earlier as a possible cause of the higher activation energies seen, due to a large amount of hydrogen bonding present on the surface due to OH groups. Hydrogen bonds are stronger than van der Waals attractions, therefore more energy is required to break them and therefore higher activation energies will result from this process.

An increase in the pre-exponential factor between the chemically coupled and physisorbed samples suggests that the method of attachment to the surface plays an important role in the reaction, this could be due to the fact that physisorption of the substance onto the surface, which can orientate itself in different ways, whereas with chemisorption, the amino groups must couple to the APTS or they will be subsequently removed during the washing phase of the reaction to remove unreacted compounds from the surface of the substrate.

The activation energies for both the coupled cellulose samples and the coupled silica samples are both higher than their respective adsorbed samples. This is thought to be due to the fact that the azo molecules can only attach via the OH groups reacting with the triazinyl groups on the azobenzene molecules, therefore any unattached compound is washed off. This results in attached compounds having less freedom to move, versus the adsorbed molecules, as the attachment restricts the motion of the molecule. The adsorbed azobenzene can however move easier as only hydrogen bonding is holding the molecule to the surface, hence the lower activation energies.

All of the surface activation energies, i.e. cellulose and silica are lower than the activation energies in solution (around 30-60 kJ mol^{-1} for solutions) though solvent dependence is seen in the thermal relaxation reaction. The reason for the lower activation energies is thought to be that there are no solution molecules to hinder the thermal relaxation of the azo compound from *cis* to *trans.*

Chapter 7.0: Studies of azobenzene on chitosan films

As discussed in Chapter 2, chitosan can be easily cast into films which possess pendent amine groups on the surface, which are by nature more reactive than hydroxyl groups on the surface of silica and cellulose. The aim of this chapter is to produce thin chitosan films as described in Chapter 3 and chemically couple and adsorb azobenzene based dyes to the surface. The surface area was first ascertained and conditions for coupling were investigated. The investigation of the photochemical behaviour of the coupled and adsorbed slides was also investigated followed by investigation of any observable contact angle change, which is the overall aim of the thesis.

7.1 Investigating the surface area of chitosan

In order to ascertain at what concentration of azobenzene a monolayer is formed, a model using 9-anthracene carboxylic acid was used. Varying amounts of 9-anthracene carboxylic acid were adsorbed to the surface of chitosan coated slides that were prepared as in the experimental section 3.15.

A series of concentrations of 9-anthracene carboxylic acid were chosen to encompass 1×10^{-4} to 1×10^{-8} moles of 9-anthracene carboxylic acid on the surface of the chitosan slides. The solutions were prepared by dissolving the required amount of 9-anthracene carboxylic acid in methanol and dripping it onto the surface of chitosan coated slide, and allowing it to evaporate in a fume hood. A solution of 1×10^{-4} moles of 9-anthracene carboxylic acid was prepared in methanol, the subsequent solutions were prepared via serial dilution. Fluorescence spectra of solution samples were also recorded using the same instrument setting as used for the slides. Fluorescence measurements were then taken of the slides (Instrument parameters: slit width 1.00 mm, excitation at 375 nm).

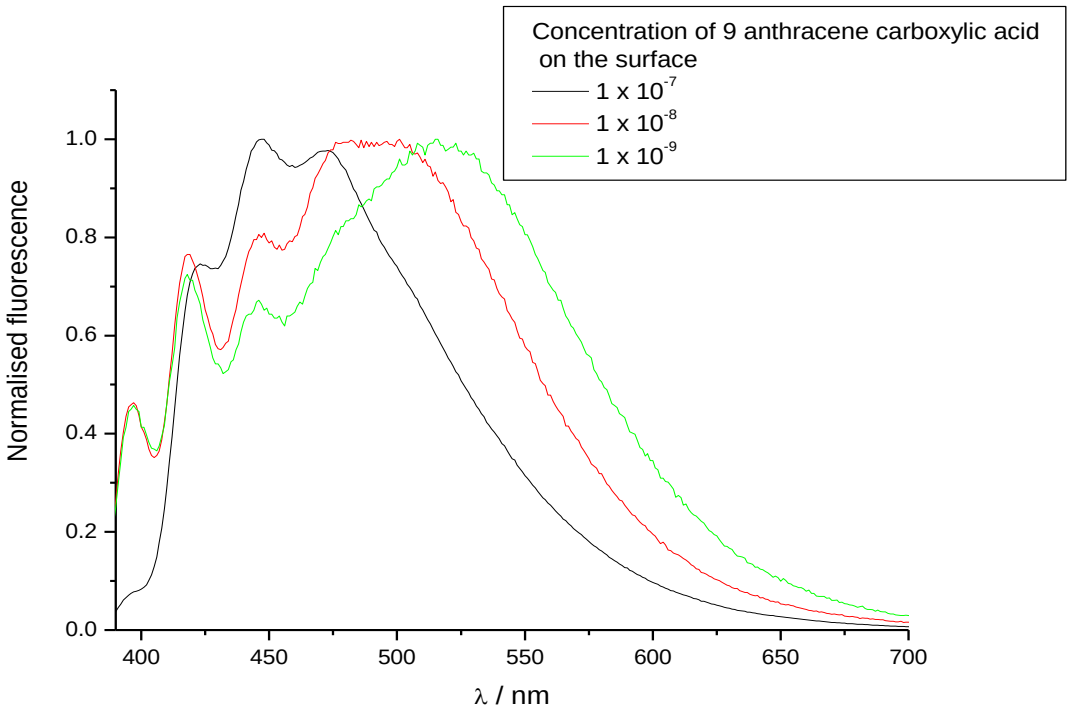

Figure 54: Graph of normalised fluorescence versus wavelength for 9-anthracene carboxylic acid adsorbed to chitosan.

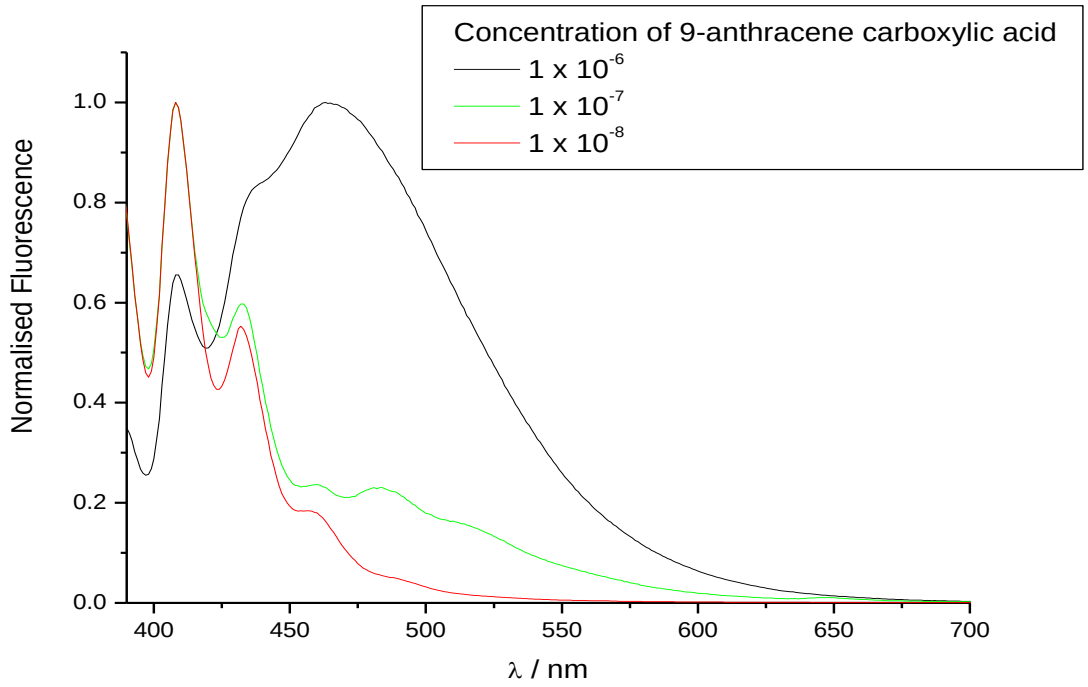

Figure 55a: Normalised solution fluorescence of 9-anthracene carboxylic acid in methanol.

The graph (Fig.54) shown above indicates that nanomole amounts of 9-anthracene carboxylic acid are required for a monolayer to be formed, as dimer is still present at 1 x 10^{-9} moles. The monomer in solution, (Fig.55a) can be seen at 10^{-7} and 10^{-8} moles, so this could indicate possible aggregation even at nanomolar concentrations is occurring on the slide surface. At higher concentrations (Fig 55a), the formation of higher aggregates can be seen as the peak shifts to the right. A monomer dimer graph (Figure 55b) plot was used (as for the cellulose data) in order to find the concentration of 9-anthracene carboxylic acid required to form a monolayer on the surface of the chitosan film.

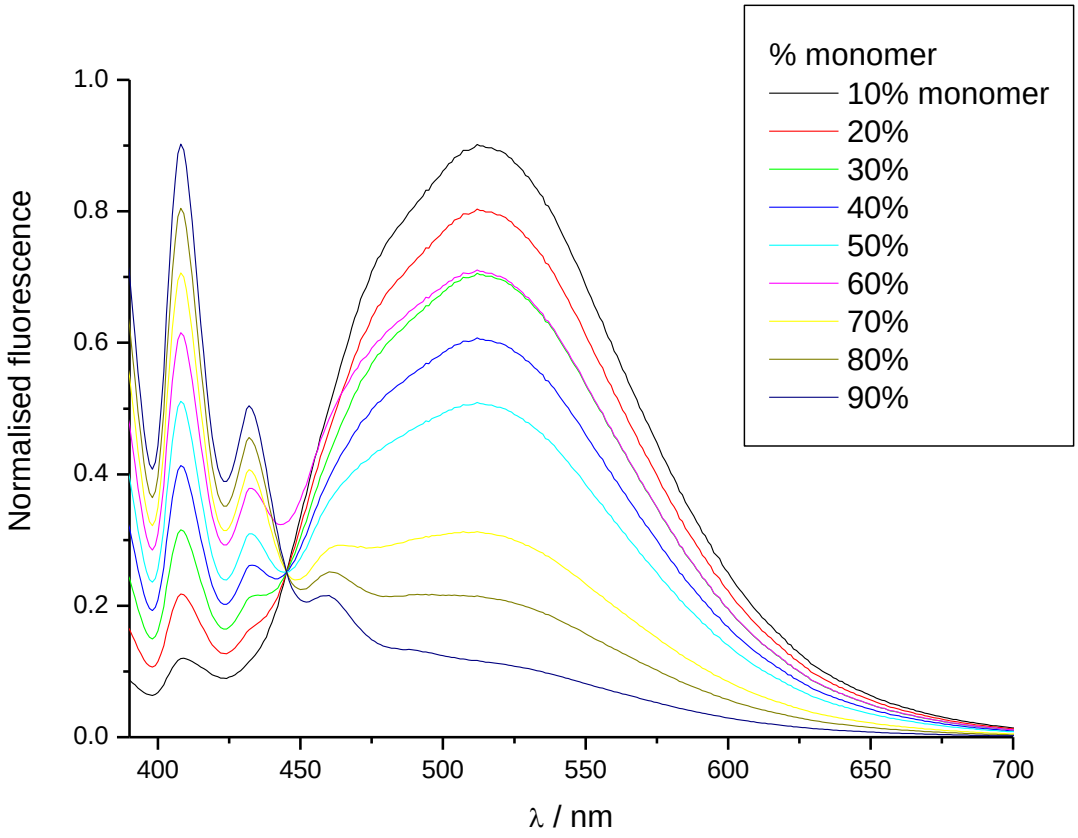

Figure 55b: Monomer dimer plot for 9-anthracene carboxylic acid on the surface of chitosan films.

The ability to couple triazinyl azobenzene derivatives to the surface of chitosan slides was investigated at higher concentrations than monolayer coverage in order to investigate if,

similarly to what was observed in silica or in solution, aggregation occurs with aminoazobenzene.

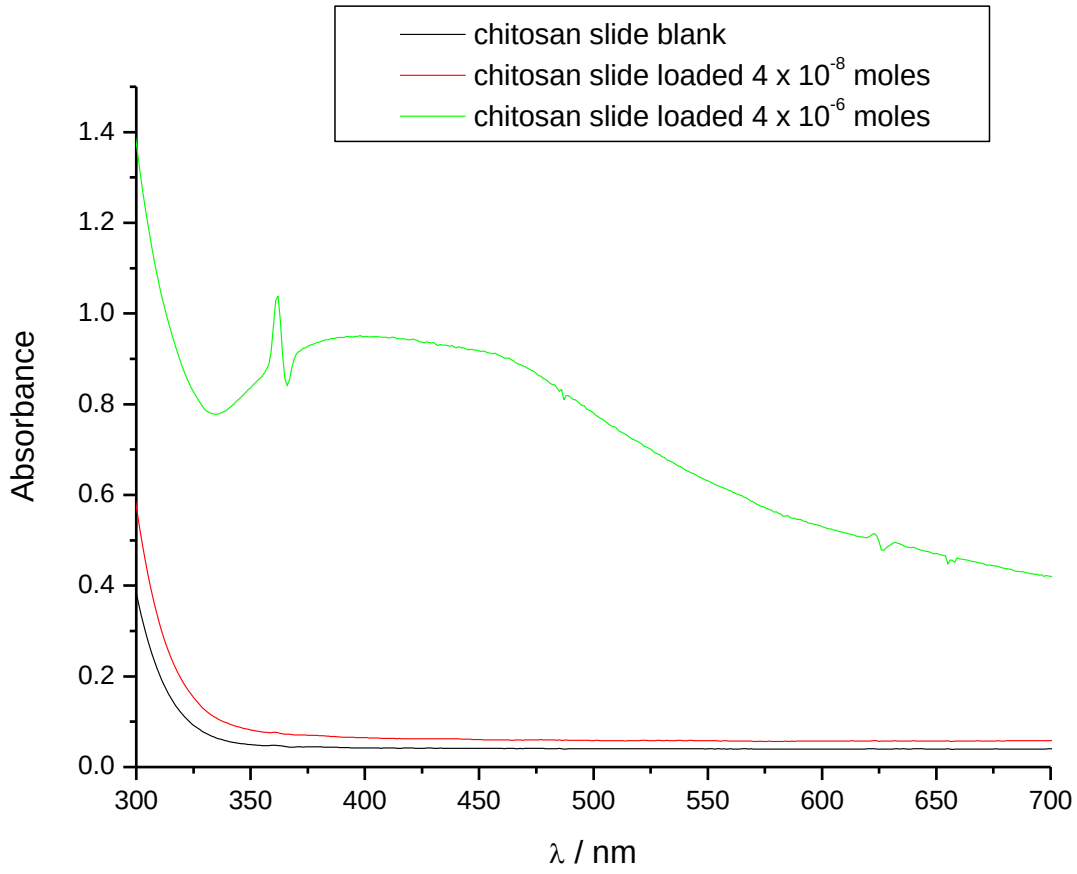

Figure 56: Absorbance of Aminoazobenzene at 8 x 10^{-6} mol and 8 x 10^{-5} mol on the surface of a chitosan slide.

Chitosan slides were prepared successfully via the method described in the experimental section. The slides produced varied in film thickness from about 1.6 x10^{-4} m to around 2.8 x 10^{-4} m measured using a micrometer. Adsorption and coupling of the azobenzene was also carried out according to the method described in the experimental section. The absorbance of the adsorbed slides showed the presence of aminoazobenzene on the surface of the slide (Fig 56). The coupling reaction appears to be complete within 1 hour, as little absorbance changes can be observed after measuring the absorbance for a further 3 hours (Figure 57). The shift of the baseline in Figure 1 is possibly the result of aggregation of azobenzene molecules on the surface which scatter the light.

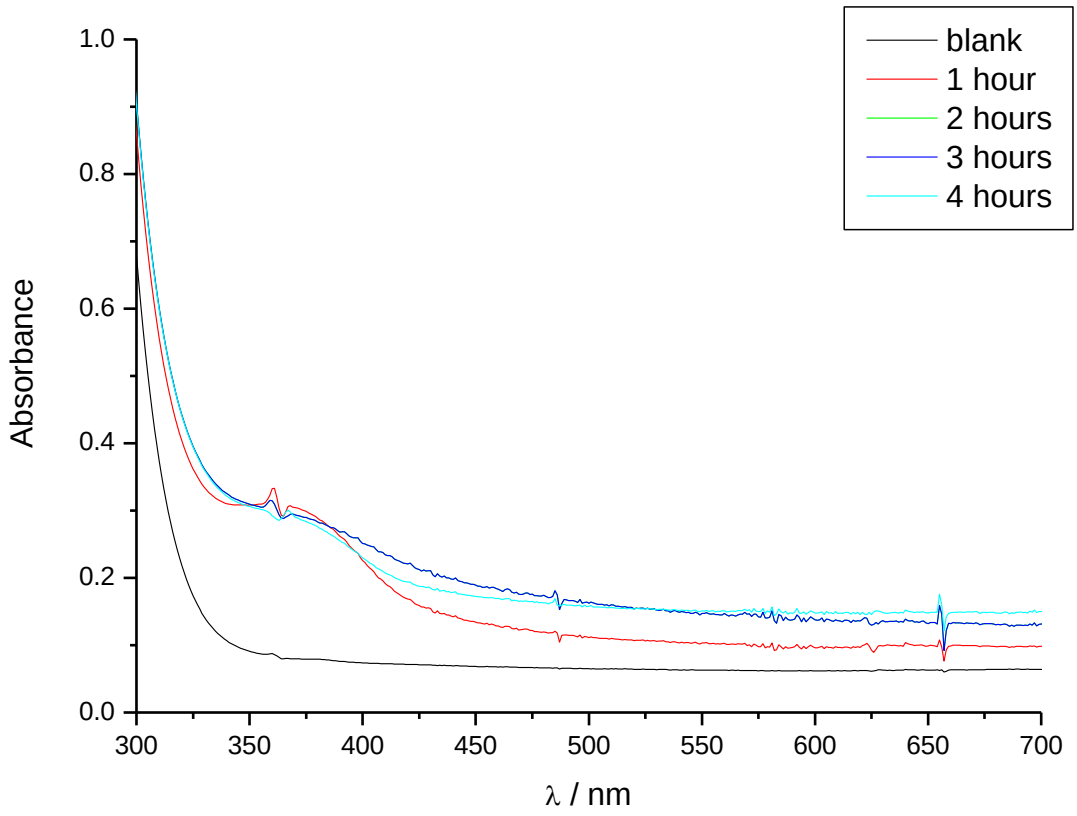

Figure 57: Absorbance of triazinyl aminoazobenzene coupled to chitosan slide 2mg, measured over 4 hours.

The fact that a large peak is observed at around 370nm is indicative that aminoazobenzene is on the surface of the chitosan slide and that the coupling reaction is successful. This is an important result as if the surface has now been modified; the photoisomerisation reaction can be investigated. Also, another crucial factor is that the compounds could not be washed off in either acetone or chloroform, indicating chemical attachment to the surface of the chitosan.

7.2 Photoisomerisation

The main aim of the project is to achieve photoisomerisation of the azobenzene group on the surface. With this in mind, an attempt was made to photoisomerise, the surface of the slide by irradiation with a 150W Xenon arc lamp.

The slide was placed in front of a 150 W Xenon arc lamp for 10 seconds. The absorbance after that 10 second irradiation was then measured. The subsequent absorbance after every 3 seconds post irradiation was measured in order to see if any thermal relaxation of the *cis* isomer of the aminoazobenzene was present (Figure 58).

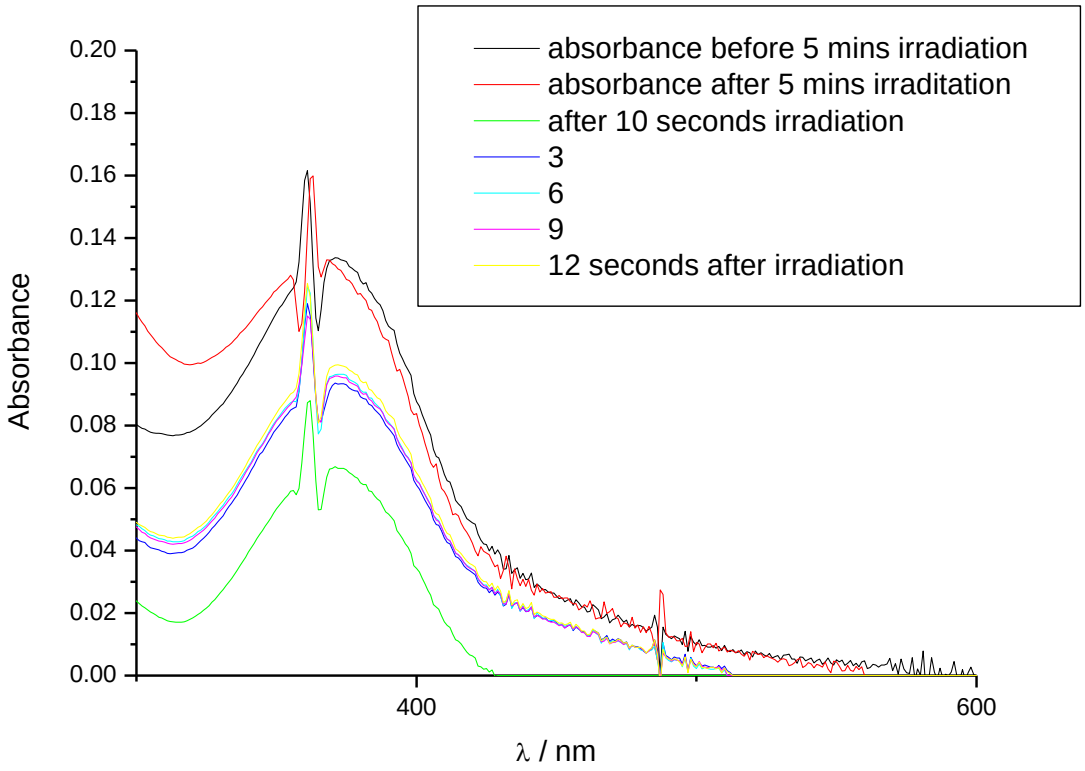

Figure 58: Thermal relaxation of aminoazobenzene coupled to chitosan slide after 10 seconds irradiation under a 150 W Xenon arc lamp.

The switching on chitosan films is much faster than on the cellulose surface (see Chapter 5). This is indicative that the thermal relaxation of the molecule from its *cis* form back to the *trans* state is surface dependent. The fact that the *cis* form does thermally relax back to the *trans* form on chitosan, shows that it is possible to observe a contact angle change upon isomerisation.

7.3 Adsorbing Admat 1 and aminoazobenzene to slides of chitosan

Several concentrations of aminoazobenzene and Admat 1 adsorbed to slides were prepared, 0.125 mg/cm^2, 0.25 mg/cm^2, 0.75 mg/cm^2 and 1.25 mg/cm^2. They were prepared by dissolving the required amount of compound in 1 ml of chloroform and dropping it onto the slide and allowing the chloroform to evaporate. Four slides were prepared of each compound, both adsorbed and coupled. Absorbance spectra were run on all slides produced and an increase in absorbance with amount of azobenzene compound on the surface was found as expected. The relationship of absorbance to surface concentration was also examined. A chitosan coated slide with no compound on the surface was used as a blank.

Admat 1	Amount (mg/cm^2)	Amount (mol)	Amount (mg)
	1.25	7.58×10^{-6}	5
	0.75	4.55×10^{-6}	3
	0.25	1.52×10^{-6}	1
	0.125	7.58×10^{-7}	0.5
Aminoazobenzene			
	1.25	2.53×10^{-5}	5
	0.75	1.52×10^{-5}	3
	0.25	5.06×10^{-6}	1
	0.125	2.53×10^{-6}	0.5

Table 12: List of concentrations of slides produced.

7.4 Coupling to slides

The triazinyl Admat 1 and aminoazobenzene compound was coupled to the slides via the use of THF as a solvent and sodium carbonate as a base (see Experimental, Chapter 3). The same amounts that were used to prepare the adsorbed slides were added to THF (50 ml) and sodium carbonate (1eq) was added and the mixture stirred for over 1 hour. An increase in the absorbance in relation to the surface concentration was found.

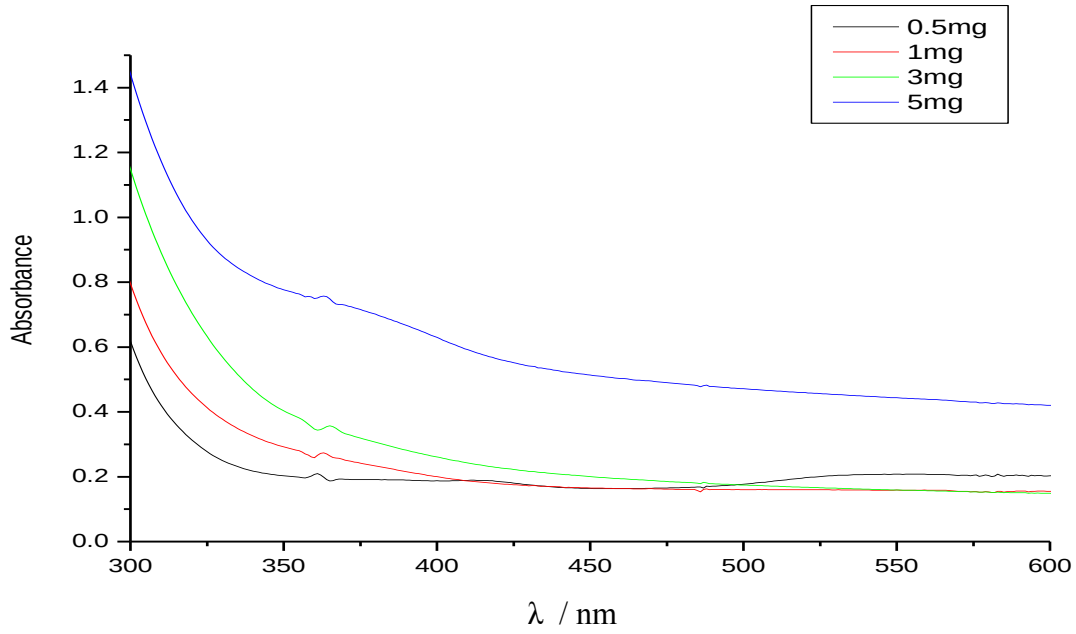

Figure 59: Absorbance spectra of Admat 1 coupled to chitosan slides.

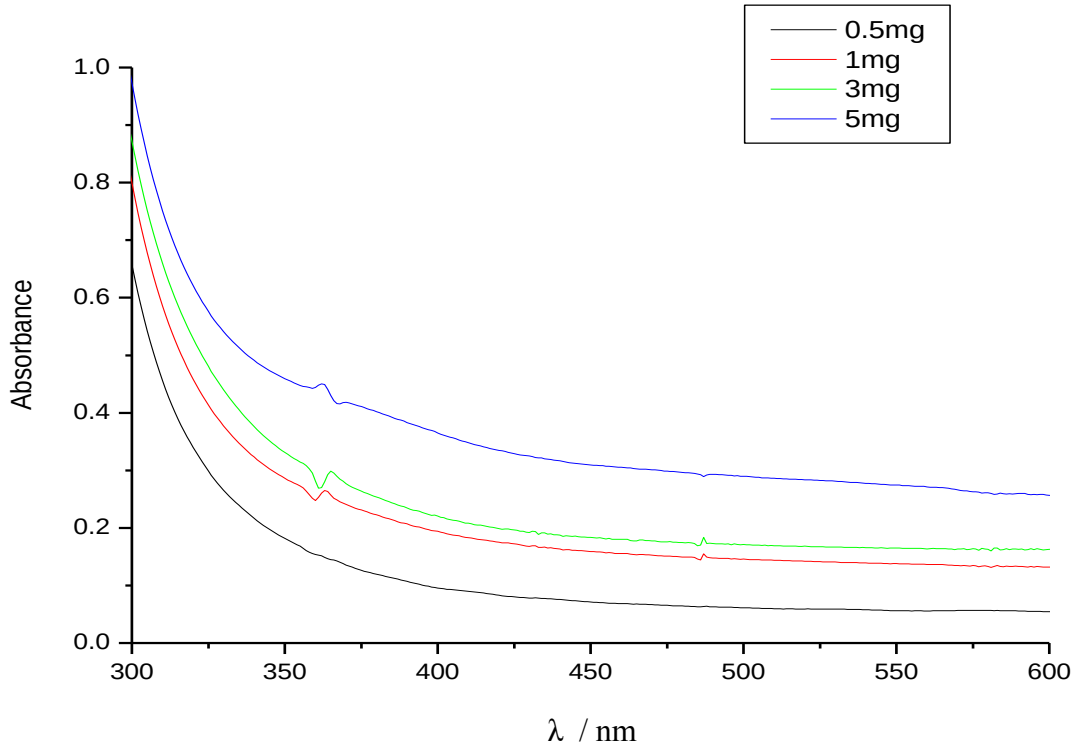

Figure 60: Absorbance spectra of aminoazobenzene coupled to chitosan slides.

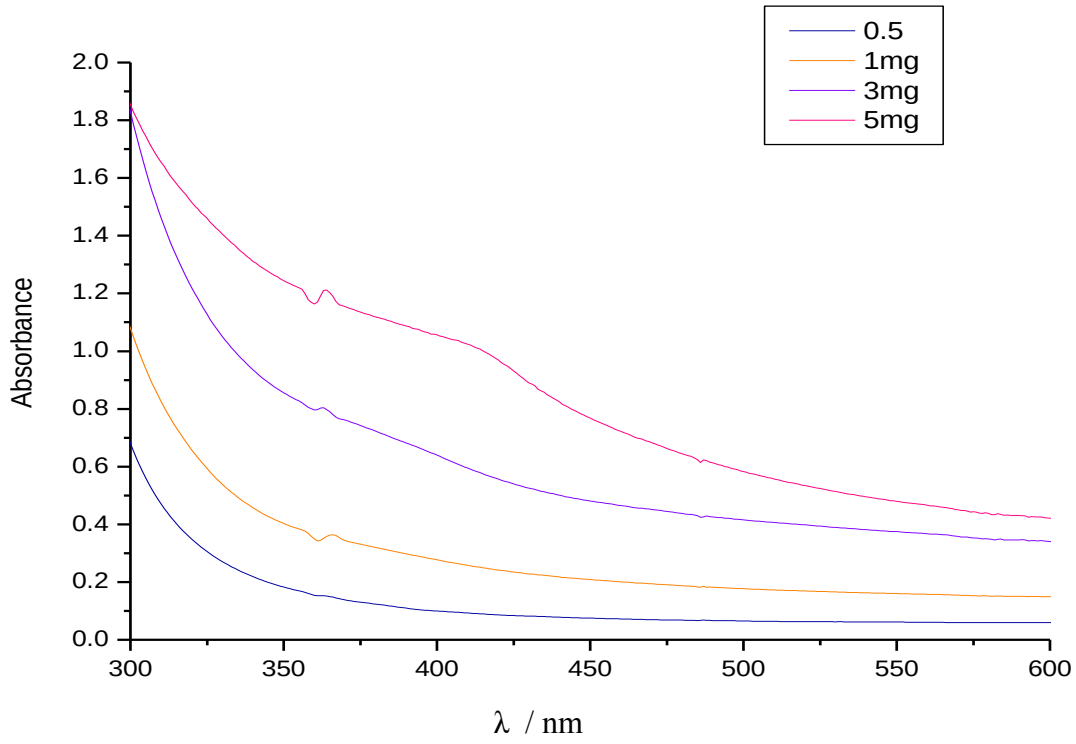

Figure 61: Absorbance spectra of Admat 1 adsorbed to chitosan slides.

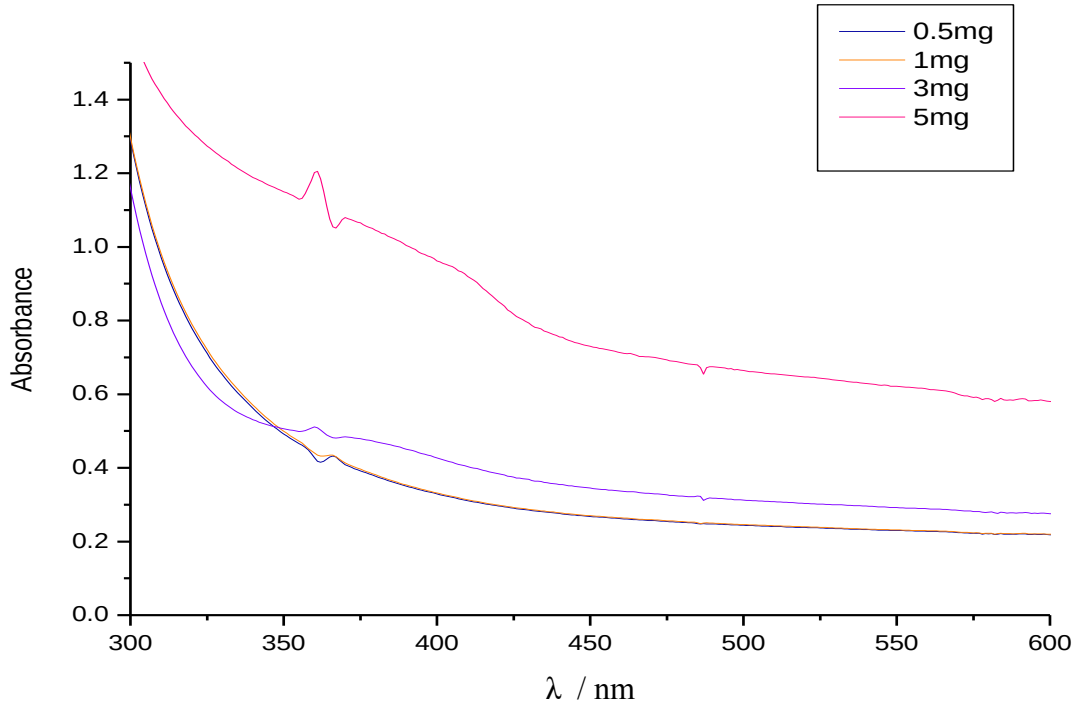

Figure 62: Absorbance spectra of aminoazobenzene adsorbed to chitosan slides.

The absorbance data (Figs 59-62) shows that with increasing concentration, there is an increase in absorbance. For the higher concentrations, the baseline shifts slightly, possible due to overloading. This baseline shift appears more prominent in the coupled samples, even though thorough washing with THF to remove unreacted compound was carried out, there is a possibility that not all the triazinyl compound was removed. Due to the baseline shift, which is an indication of possible aggregation and the fact that the aggregation could have affected the contact angle on the higher concentration slides due to surface bound aggregation, lower concentrations were investigated.

An attempt to prepare slides with 1×10^{-9} mol Admat 1 was made by coating two glass slides with chitosan. The chitosan was dried under vacuum and then a low concentration of Admat 1 solution in THF (1×10^{-7} mol dm^{-3}) was prepared. The slides were dipped into two portions of this solution (50mls) with sodium carbonate as a base and then left for 2 hours. The absorbance of the solution was measured and the amount on the surface could then be calculated. The amount of Admat 1 was found to be 3.29×10^{-10} moles on slide 1 and 5.48×10^{-8} moles on slide 2. The slides were rinsed thoroughly with THF to make sure any unreacted compound was removed. These slides were then subject to contact angle analysis (see section 7.7).

7.5 Summary

Chitosan slides were prepared successfully via the method described in the Experimental section. The absorbance spectrum of the adsorbed slides showed the presence of aminoazobenzene on the surface of the slide. The coupling reaction appears to be complete within 1 hour, as little absorbance changes can be observed after measuring the absorbance for a further 3 hours. At high concentrations, aggregation effects are again seen, as with silica and cellulose, however, the photoisomerisation reaction appears to be much faster than on either silica or cellulose, possibly due to less steric hindrance, as a flat surface is used rather than a fine powder, the azo groups can isomerise quickly due to less hindrance form the bulky substrate.

Contact angle work can then be carried out on the slides, as the main reason for doing this investigation as stated earlier, was to assess if the change in photoisomerisation occurs alongside any contact angle change that can be observed.

7.6 Contact angle work with azobenzene derivatives

The purpose of the previous chitosan section is to create thin films functionalised with azobenzene derivatives which can be studied for contact angle change upon irradiation with light. Several functionalised surfaces have already been prepared, as described earlier in Chapter 2. The focus of this work is azobenzene molecules which undergo isomerisation upon irradiation.

7.7 Photoinduced wettability changes on surfaces

The ability for the fluorinated azobenzene compounds to photoisomerise on surfaces is crucial to this project. In order to ascertain in any photoisomerisation occurs, the surfaces were subjected to irradiation and then contact angles changes were measured. A variety of concentrations of Admat 1 and Admat 2 were used in order to investigate the relationship between concentration of azobenzene compound on the surface and contact angle change.

7.8 Contact angles changes of slides of high concentration of Admat 1

Contact angle measurements were conducted on the slides produced as described above. Contact angle investigations were conducted on a VCA2500 Video contact angle system (AST Product) using 2 μl distilled water droplets (see Experimental section 3). Three contact angles were measured and an average value was taken. Control experiments were conducted using a blank chitosan coated slide.

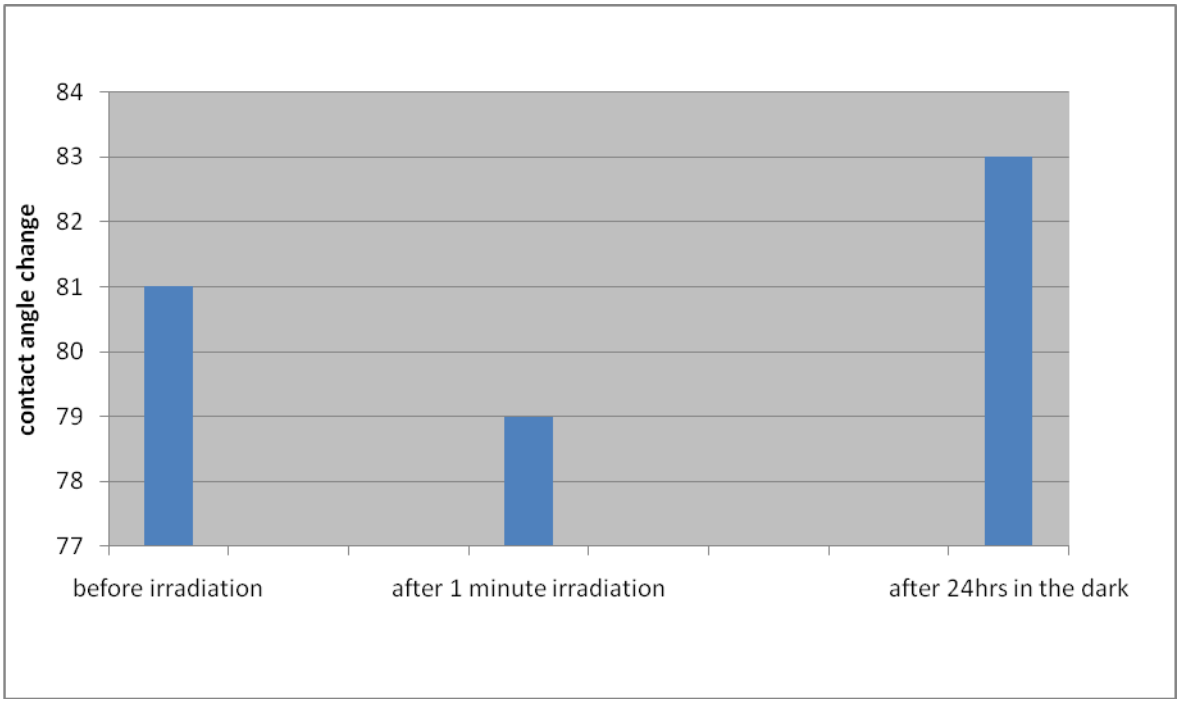

Figure 62: Blank slide irradiation (control experiment)

Slide (mg/cm^2)	Contact angle before Irradiation (+/- 2°)	Contact angle after irradiation for 2 mins (+/- 2°)	Contact angle change (+/- 4°)
0.125 (Coupled)	111	100	11
0.25 (Adsorbed)	129	119.5	9.5

Table 13: Admat 1 high concentration slides contact angle change.

Aminoazobenzene

Slide (mg/cm^2)	Contact angle before Irradiation (+/- 2 °)	Contact angle after irradiation for 2 mins (+/- 2 °)	Contact angle change (+/- 4°)
0.125 (Coupled)	81	69.5	11.5
0.25 (Adsorbed)	89	83	6

Table 14 Aminoazobenzene high concentration contact angle slides.

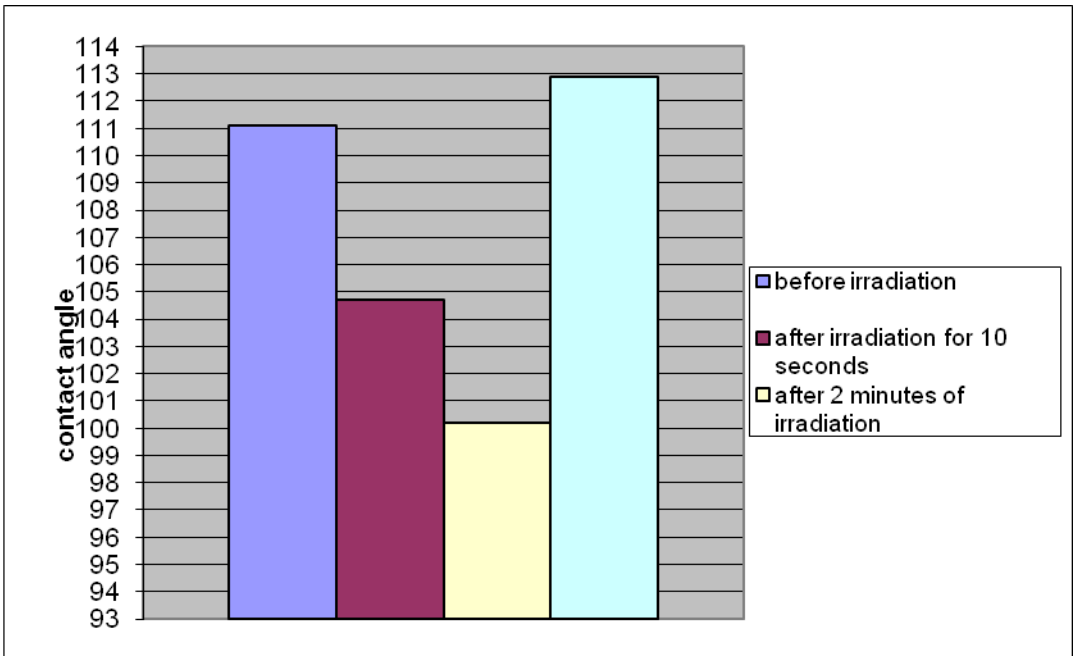

Figure 63: Contact angle change after irradiation for 0.125 mg/cm^2 Admat 1 coupled to chitosan.

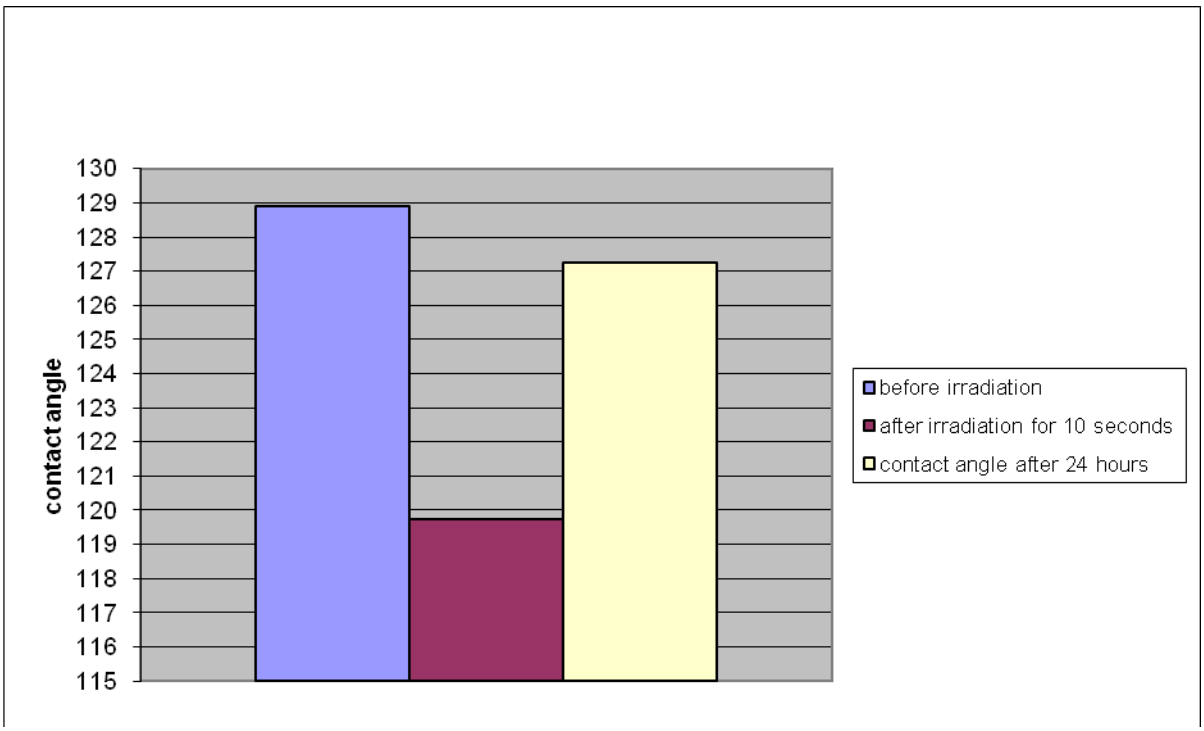

Figure 64: Contact angle change for 0.25 mg/cm^2 Admat 1 adsorbed to the surface of chitosan.

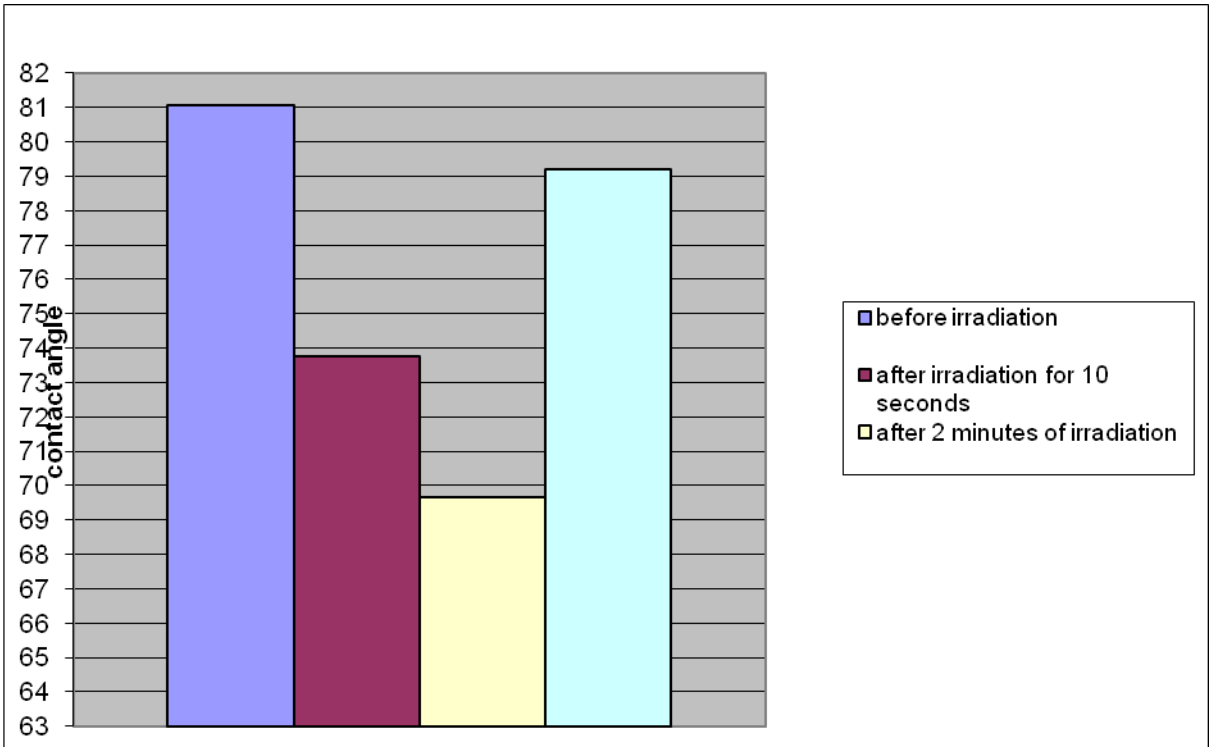

Figure 65: Contact angle change after irradiation for 0.125 mg/cm^2 aminoazobenzene coupled to chitosan slide.

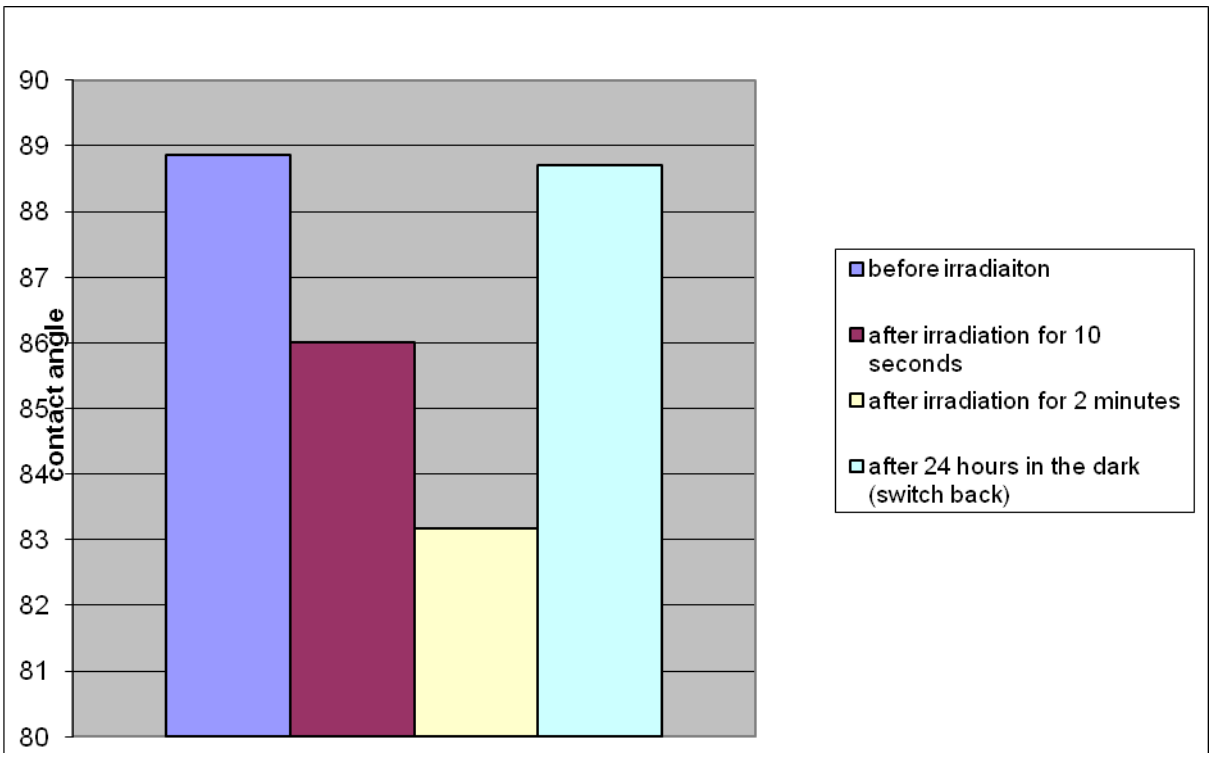

Figure 66: Contact angle change after irradiation for 0.25mg/cm^2 Admat 1 coupled to chitosan film

From the data shown (Figures 63-66), a change in contact angle upon irradiation of between 5° and 12° can be observed for 0.125 and 0.25 mg/cm^2 slides. No contact angle change was observed for the higher concentration slides, (5 mg and 3 mg) which is thought to be as a result of aggregation due to the very high concentrations. The contact angle changes as a result of the orientation of the azobenzene molecules on the surface, which results in an increase in polarity, which decreases the contact angle of the water droplet. This is a reversible change, as after 24 hours in the dark, the contact angle returns to the same value as before irradiation. The contact angle changes after switching were only observed at lower concentrations, suggesting that at the higher concentrations, aggregation occurred.

The baseline shift in the absorbance spectra is a good indication of aggregation, so this explanation is the most likely reason for there to be no observable contact angle change at higher concentrations. The small contact angle change is possibly due to aggregation as the aggregates cannot isomerise easily, therefore the change in surface energy required does not occur, hence the low contact angle change.

There is little difference in the contact angles of the perfluoroalkyl chains and the aminoazobenzene. This is thought to be due to the high concentration causing aggregation on the surface of the slides, and this causes the chains to interlock, which hinders isomerisation. The change in initial contact angle from an unfunctionalised chitosan slide (58.7°) shows that coating the slide with azobenzene derivatives on the whole increases the contact angle, which as they are non polar molecules, is expected.

7.9 Contact angle work with low concentration azobenzene derivatised chitosan coated slides

An attempt to prepare slides with 1 x 10^{-9} mol Admat 1 was completed by coating two glass slides with chitosan. The chitosan was dried under vacuum and then a very low concentration of Admat 1 solution in THF (1 x 10^{-7} mol dm^{-3}) was prepared. The slides were dipped into two portions of this solution (5 ml) with sodium carbonate as a base and then left for 2 hours. The absorbance of the solution was measured and the amount on the surface was then calculated. The amount of Admat 1 was found to be 3.29 x 10^{-10} mol cm^{-2} on slide 1 and 5.48

x 10^{-9} mol per cm^2 on slide 2. The slides were rinsed thoroughly with THF to make sure any unreacted compound was removed. Slides were produced in duplicate. The slides were dried and the contact angles were measured using a Data Physics OCA Contact angle device with 2µl of water droplet. Tables of data obtained are shown below.

Slide 1:

Mean contact angle before Irradiation +/- 2°	Mean contact angle after irradiation +/- 2 °	Contact angle change (+/- 4°)
122.71	84.52	38.19
123.03	51.41	71.62
121.48	54.12	67.36
123.77	64.81	58.96

Table 15: Mean contact angle change for slide 1 = 59.46°

Slide 2:

Mean contact angle before Irradiation +/- 2°	Mean contact angle after irradiation +/- 2°	Contact angle change (+/- 4°)
117.89	80.17	37.72
122.10	68.02	54.08
120.43	86.48	33.95
116.88	81.91	34.97

Table 16: Mean contact angle change for slide 2 = 40.18°

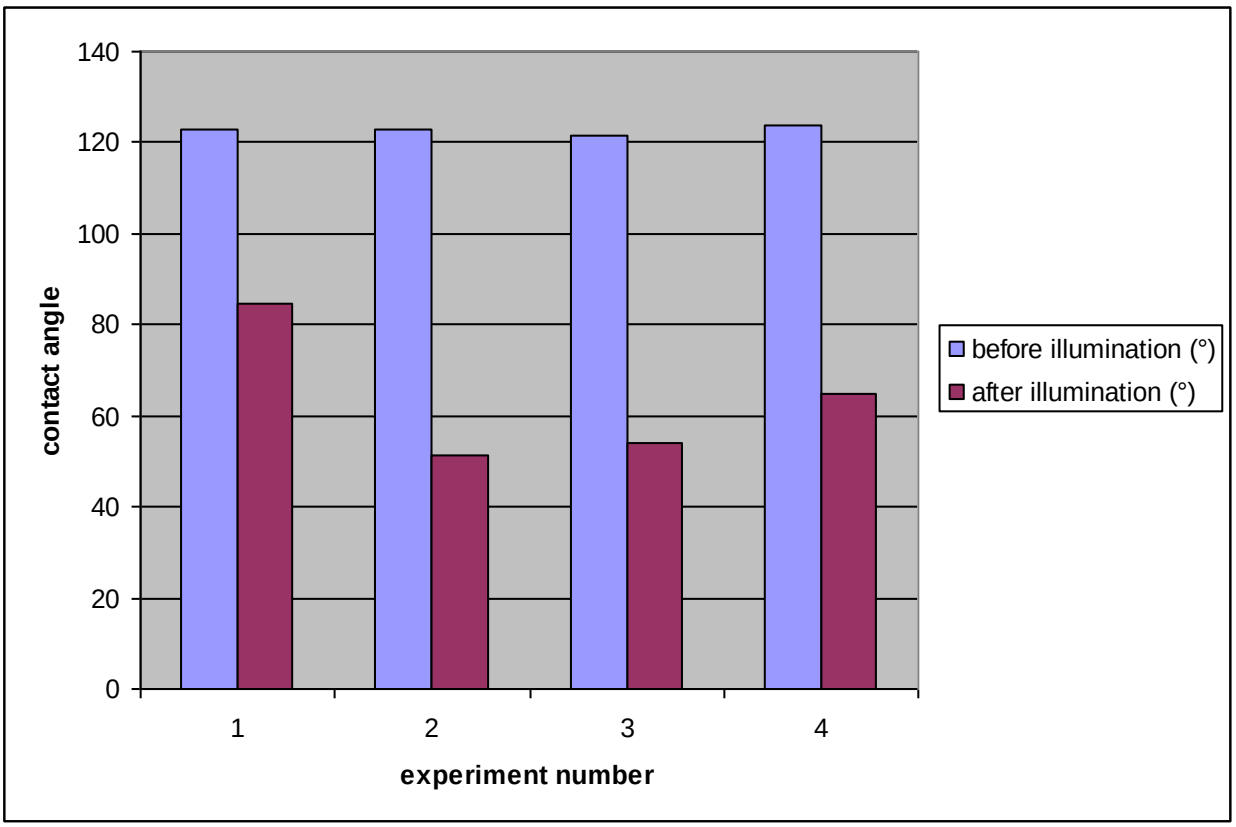

Figure 67a: Slide 1 contact angle changes upon irradiation (3.29×10^{-10} mol cm^{-2})

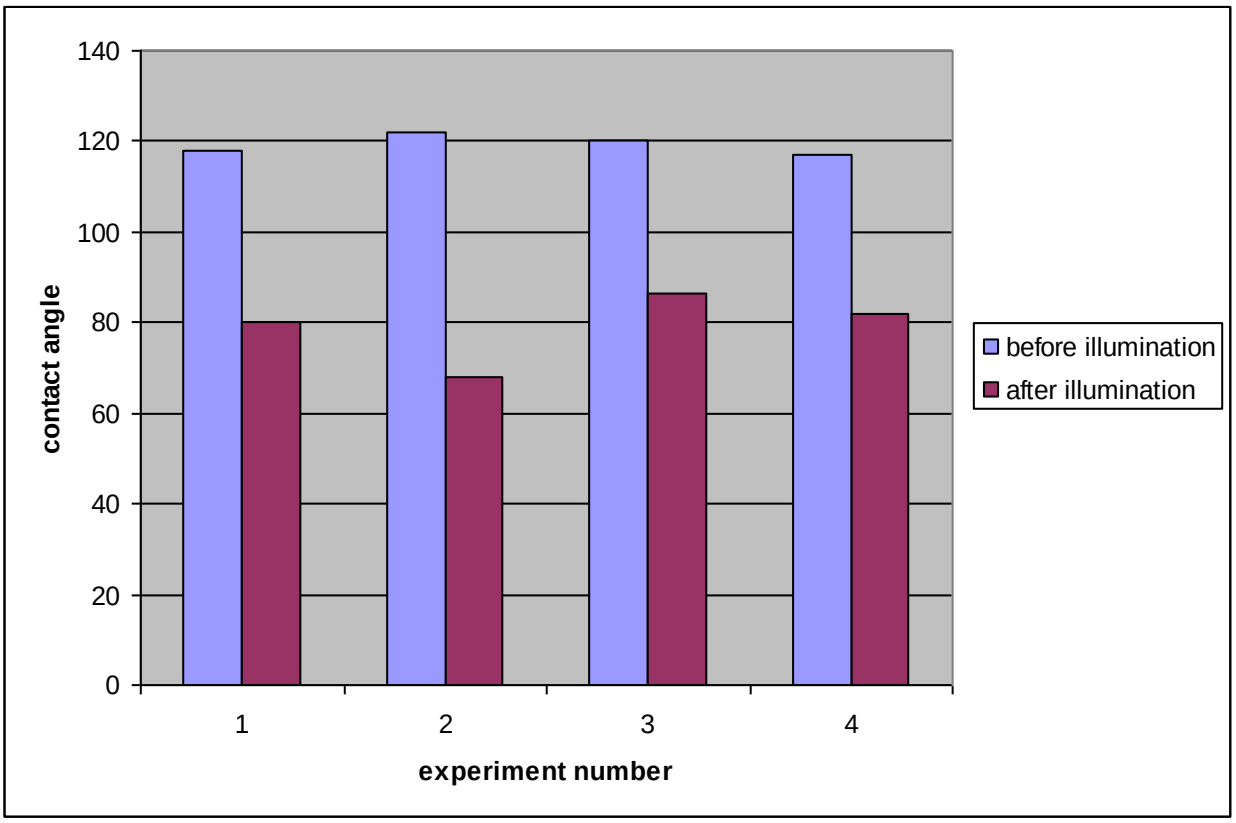

Figure 67b: Slide 2 contact angle changes upon irradiation (5.48×10^{-9} mol cm^{-2})

The higher contact angle changes shown for slide 1 (Figure 67a) corresponds with a lower amount of Admat 1 on the surface. This is an interesting result, as it seems to indicate that the lower the concentration, the easier it is for isomerisation to occur. This is possible due to less aggregation of Admat 1 on the surface, allowing the molecule to isomerise effectively.

The lower the concentration of Admat 1, the higher the contact angle change, and the explanation that there is no aggregation on the surface is plausible, as there would be little hindrance for isomerisation on the surface of the chitosan slides. The superhydrophobicity presented earlier in the review, i.e. greater than 150° is not present here. The larger amount of Admat 1 present on slide 2 (figure 67b) corresponds to a higher surface concentration which would explain the lower contact angle change due to hindered isomerisation.

The initial contact angles shown for the perfluoroalkyl derivatives correlate to hydrophobic surfaces, as the contact angle given is around 120°. The contact angles for aminoazobenzene are much lower than the perfluoroalkyl Admat 1, which can be explained as the absence of a superhydrophobic fluoroalkyl chain means the contact angle will be much lower. The surface energy is higher on the aminoazobenzene surface, hence the lower initial contact angles. The perfluoroalkyl chain lowers the surface energy of the surface, hence larger contact angles. The use of the perfluoroalkyl chains as a method to lower surface energy and increase contact angle has been widely reported.[198]

The changes noticed in both sets of data in tables 15 and 16 show a slight change in contact angle. The coupled samples of both Admat 1 and aminoazobenzene display slightly higher contact angles, mainly due the fact that any excess triazinyl compound that has not attached to the surface is washed off, therefore the only compound that can isomerise is the compound that is attached to the surface, therefore little if any hindrance due to aggregation is seen, unlike with the adsorbed samples. The fact that this reaction is reversible means that a key objective in this project has been achieved.

The difference between the high and lower concentration slides in terms of the initial contact angles is worthy of note. The higher initial contact angles present for the lower concentration is suggestive of their being very little aggregation present as the surface energy is lower. For the higher concentration slides the initial contact angle is lower as the surface energy

increases due to aggregation. This is the most interesting result as far as the contact angle work goes, as the contact angle changes on the lower concentration slides are the largest seen here at between 40° and 50° on the surfaces of chitosan functionalised with Admat 1. The contact angle values seen here are large and compare favourably with other literature discussed in the introduction.

The peak maximum wavelength in solution is very solvent dependent, however the peak maximum on cellulose, silica and on chitosan, are largely similar at 380-385 nm. The similarity with polar solvents observed here can be easily explained, as the presence of OH groups on the surface of cellulose, silica and chitosan make the surface very polar. This would lead to the red shift in the wavelength that is seen in the surfaces and in methanol also.

The activation energies and pre-exponential factors of the thermal relaxation rate in solution must also be considered. The main conclusion that can be reached is that all of the surface activation energies are lower than those observed in solution. The activation energies on silica are higher than on cellulose. This is thought to be due to the presence of the APTS linker group, which mean that the azobenzene group is further away from the surface on the silica than on the cellulose, so the influence of the hydroxyl groups on the surface of the silica is not as strong as it is on cellulose. On cellulose, the azobenzene molecules are closer to the surface, which means that influence of the OH groups is stronger, therefore, as seen with polar solvents such as methanol, the rate increases.

The activation energies displayed by the cellulose and silica are interesting, as there is an increase in the activation energies on silica surface and on the cellulose surface with concentration. The activation energies increase with the concentration due to the amount of azo compound on the surface, the increase in concentration is thought to lead to aggregation which hinders the thermal relaxation energy on the surface. The pre-exponential factors also increase with concentration, although there is not the large variation in pre-exponential factors and activation energies on the surfaces as there are in solution. The solution studies, in comparison, show almost tenfold increase in thermal relaxation in solution, but the activation energies are all fairly similar for the surfaces. The increase in pre-exponential factor in the case of the surfaces, cellulose and silica, is supportive of the conclusion that an increase in

concentration hinders the thermal relaxation process and hence the activation energies are higher on the surfaces.

The fact that the activation energies on cellulose and on silica are lower ties in with previous literature on azobenzene anchored to surfaces. Hagen *et. al*. reported that azobenzene on gold gave a pronounced reduction in the activation energy compared to the free molecule, which is largely what is seen with activation energies in the solvent solutions around 60 kJ mol^{-1} and here, the activation energies on the surface were found to be between 5-10 kJ mol^{-1}.[199]

7.10 Summary of chitosan studies

The rate of thermal relaxation of the Admat 1 on chitosan was much faster than on silica, in solution or on cellulose. The slides show that the azo compounds thermal recovery is around 30 seconds on the surface of the chitosan. This is interesting, and the reason for this is thought to be an increase in local viscosity on the slides, which in turn can cause an increase in the relaxation rate, which is seen here. The fact that the lower concentrations give larger contact angle changes is due to the effect of aggregation on the higher concentration slides, hindering the isomerisation process, which lowers the contact angle change, as the surface energy does not change as much as with the lower concentration slides, where aggregation is thought to be absent.

Chapter 8.0: Studies of perfluoroalkyl azobenzene containing polymers

Azobenzenes have been extensively studied as moieties in polymers and in liquid crystals. This work has lead to several conclusions; one of which is that the lifetime of the *cis* isomer can be altered using polymer chains as a hindrance, therefore enabling the control of the isomerisation reaction. The polymers used have included several alkyl branched chains, aryl rings and liquid crystals. For this work, we only focus on branched chain polymers in solution.[200,201] The *cis* form of the azobenzene molecule can be prevented from isomerisation completely by isolating it, affixing it to a surface or creating a ring like structure, however in the case of the surface work shown here, the *trans* isomer is used to affix the azo group to the surface.[206] The experiments shown above indicate that great geometrical changes are required in order to isomerise polymer based material. All of the above thermal relaxation reactions were found to be first order, however, polymer matrices can produce abnormally fast decay components. The higher the matrix crystallinity, the faster the decay component.[207,208]

As part of the work conducted here, the polymers were first dissolved into solutions of toluene and the lifetime was measured as with the Admat compounds. An attempt was then made to graft the fluorinated azobenzene polymers onto slides in order to ascertain if any photoisomerisation is present in the films on the surface of glass slides.

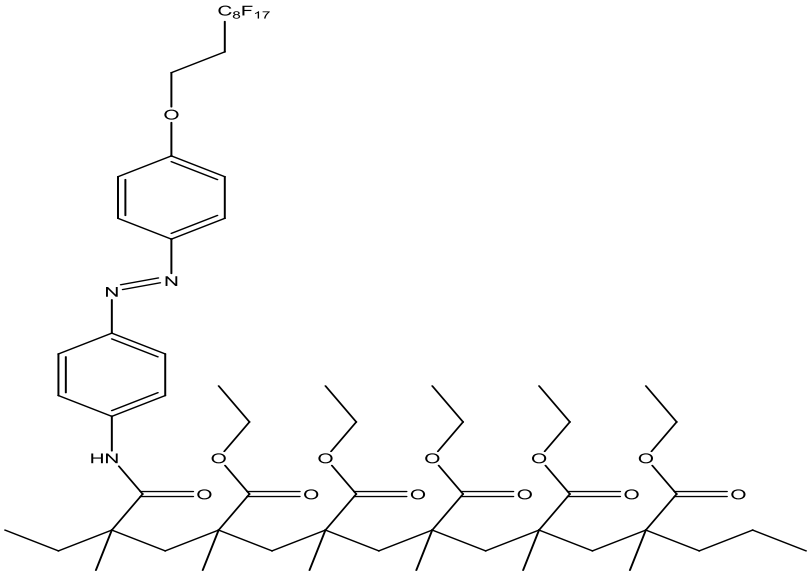

Figure 68: Structure of the polymers used in these studies.

8.1 Investigations with novel perfluoroalkyl based azobenzene polymers

The polymers supplied by DSTL were investigated via UV-Vis spectroscopy both in solution and on glass slides. The polymers were dissolved in toluene solution, which required sonication in order for them to fully dissolve.

Concentration of solutions prepared

F1R001 = 3.85 x 10^{-6} mol dm^{-3} (0.58% azobenzene)
COR001= 1.99 x 10^{-5} mol dm^{-3} (0.15% azobenzene)
FOR001 = 2.30 x 10^{-6} mol dm^{-3} (0.76% azobenzene)

The solution were irradiated in a glass cuvette using a 150 W arc lamp and the thermal relaxation rate of the *cis* to *trans* isomerisation was measured (Figures 69,70 and 71). The rate constants were measured for the thermal relaxation reaction of all the polymers supplied. (Table 17)

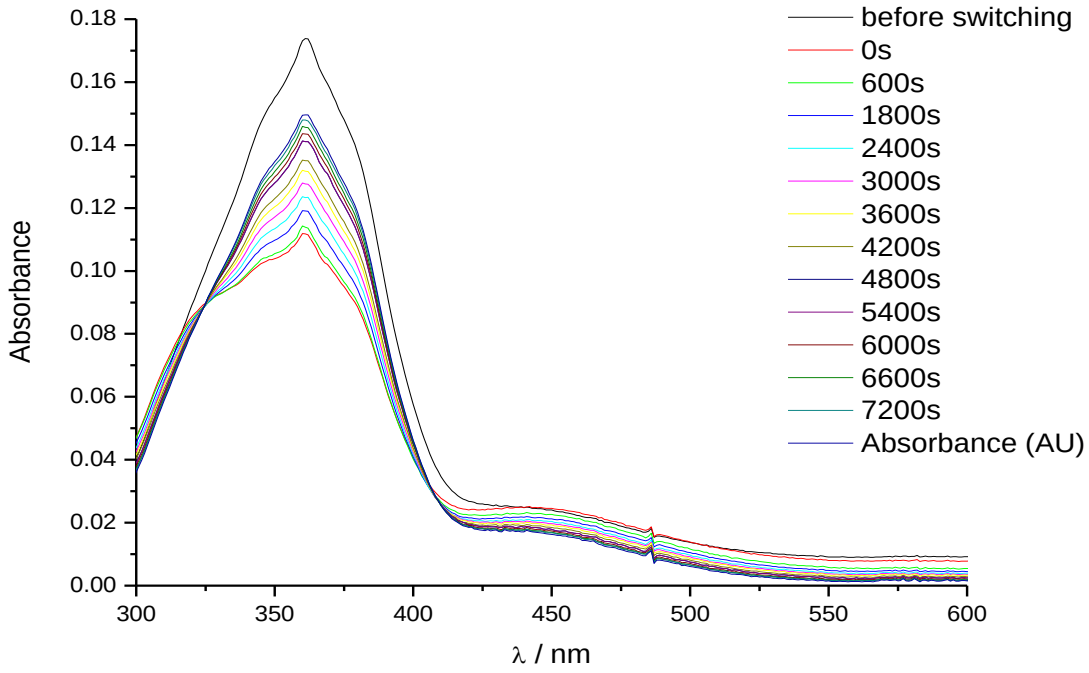

Figure 69a: Thermal relaxation of polymer COR001 in toluene solution. [COR001] = 1.99 x 10^{-5} mol dm^{-3}

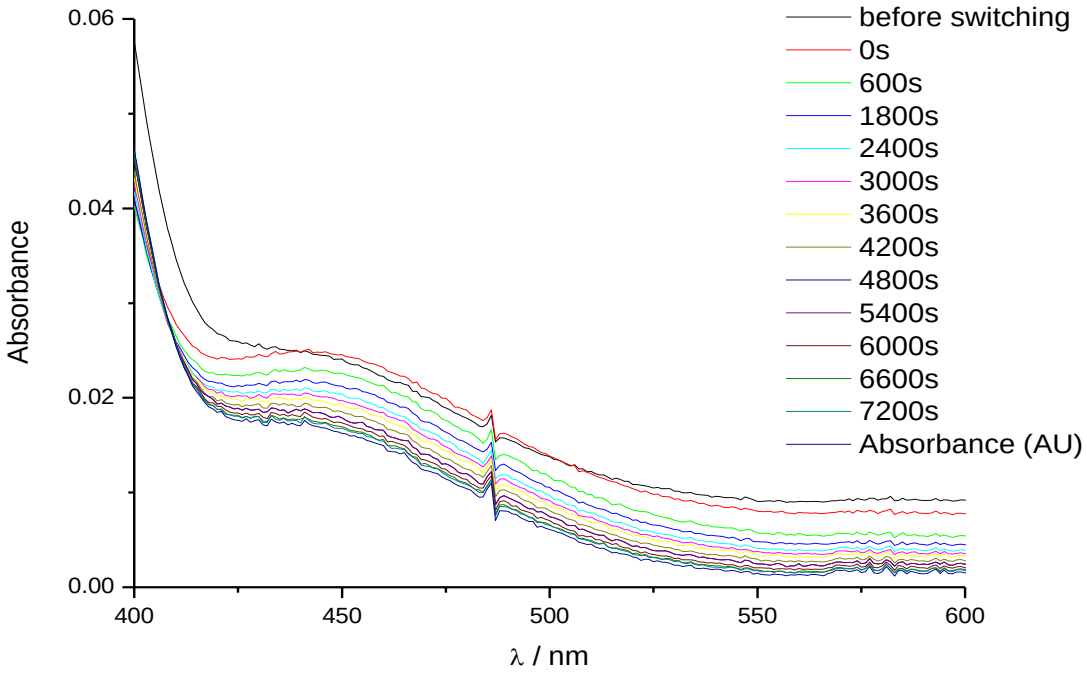

Figure 69b: Enlarged view of cis to trans thermal relaxation of COR001.

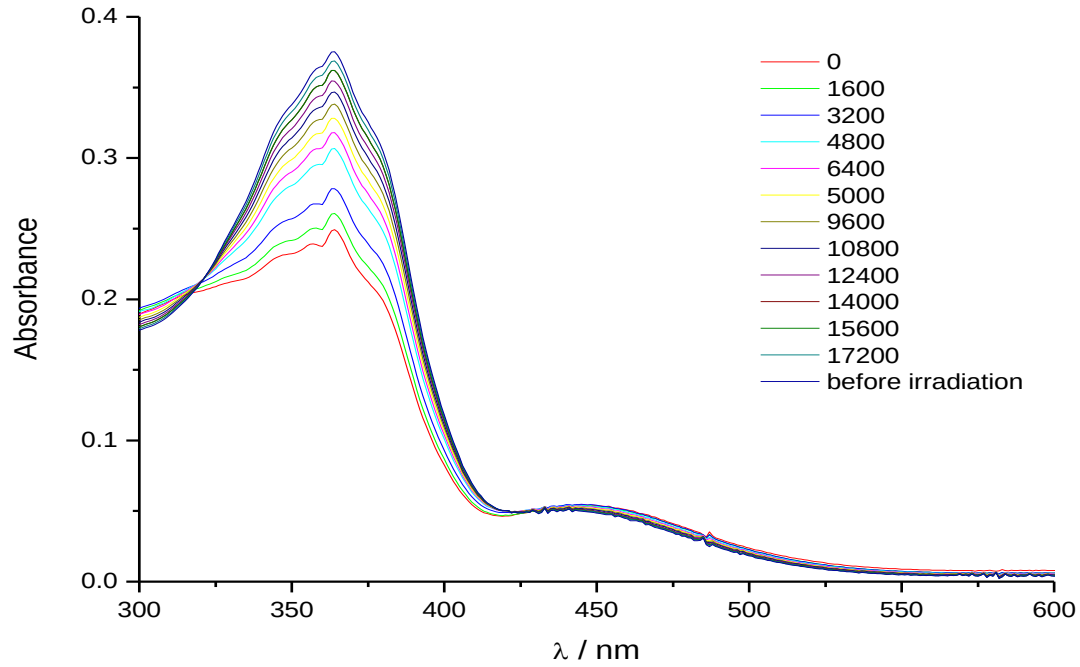

Figure 70: Thermal relaxation of FOR001 in toluene solution, 1mg/ml solution in toluene, Concentration 2.36 x 10^{-6} mol dm^{-3}.

The rate of thermal relaxation was measured by fitting the absorbance versus time plots with a first order exponential curve (Figures 72 and 73). The calculated rates are tabulated below.

Name	% Azobenzene	Concentration (mol dm^{-3})	k / $10^{-4}s^{-1}$ (+/- 0.05)
COR001	0.15	1.99 x 10^{-5}	1.96
F1R001	0.58	3.85 x 10^{-6}	1.62
F0R001	0.76	2.30 x 10^{-6}	1.84
Admat 1	----------	2.60 x 10^{-5}	42.0

Table 17: Thermal relaxation rate of polymers in toluene solution

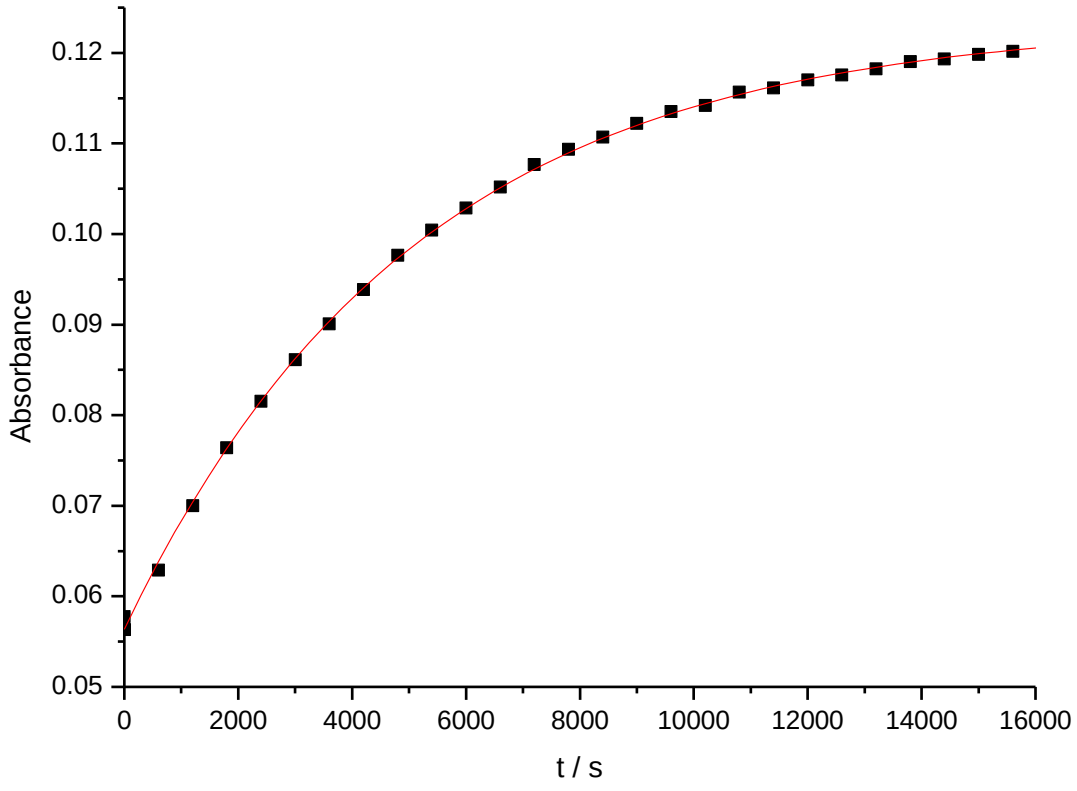

Figure 72: Absorbance time plot of COR001 in toluene solution k =1.96 x 10^{-4} s^{-1}.

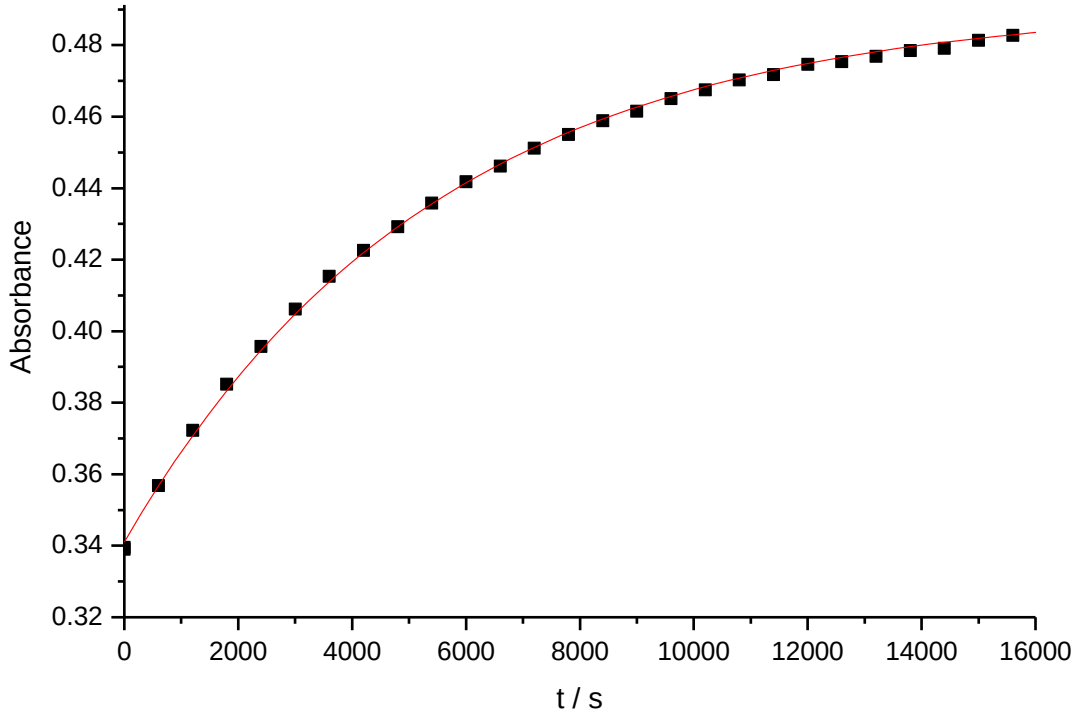

Figure 73: Absorbance versus time plot of FOR001 in toluene solution, k=1.84 x 10^{-4} s^{-1}.

The data obtained show that the thermal relaxation reaction of the polymer is over in around 4.5 hours. This is in contrast to Admat 1 unpolymerised in toluene, where the rate constant is 4.2 x 10^{-3} s^{-1}, and the thermal relaxation reaction is over in around 1.5 hours. The reason for the slower rate of thermal relaxation in the polymer could be due to hindrance from the polymer chain itself, as the chain is bulky and therefore requiring more energy for it to become mobile.

The possibility of a change in viscosity upon isomerisation has to be considered, although this was not investigated here, which could hinder the rate of thermal relaxation of azobenzene in polymer solution. There was no correlation noticed here for the rate of thermal relaxation and the different amount of azobenzene present in the polymer chain.[217]

8.2 Polymers on glass slides

In order to investigate if the polymers switched when immobilised onto a glass surface, 1mg of each polymer was dissolved in 1ml of toluene and dropped onto an untreated glass slide. The solvent was allowed to evaporate. The glass slides were examined by UV-Vis spectroscopy (Figure 74) in order to examine if any polymer was present on the surface and if any photoisomerisation occurred.

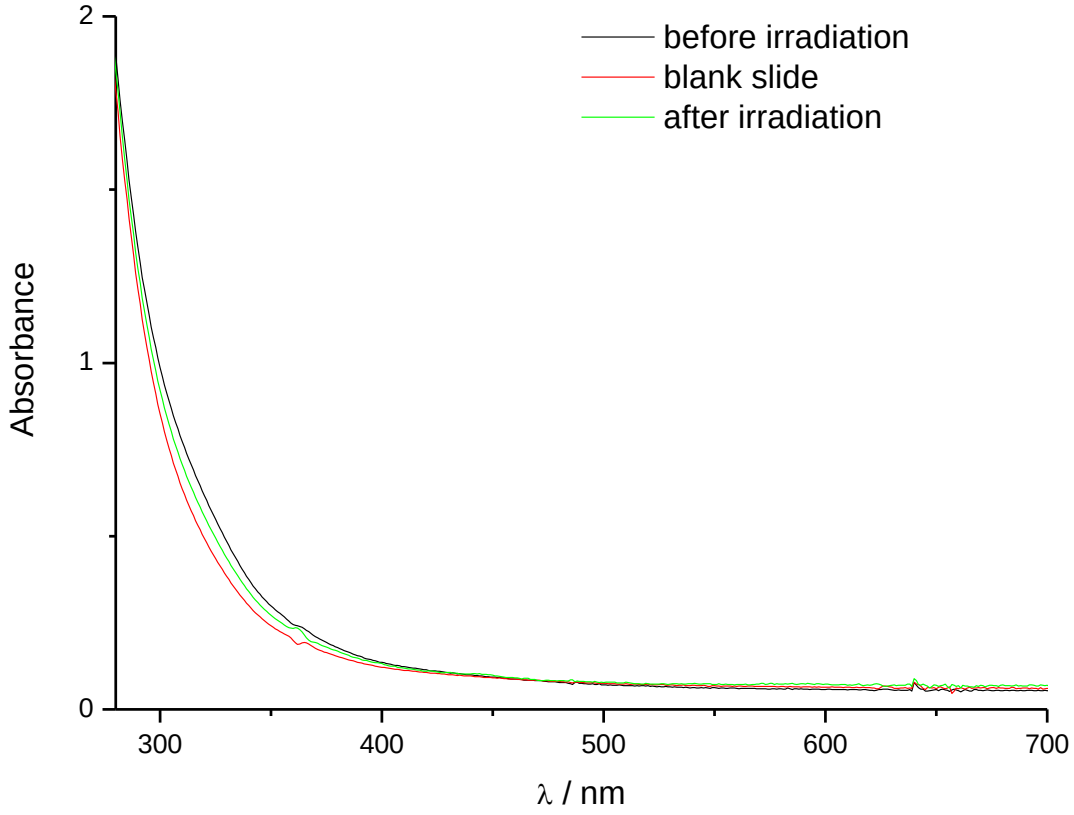

Figure 74: 1mg/ml FOR001 polymer on glass slide. After 1 minute irradiation in 150W Xenon Arc lamp.

From this experiment, it was decided that too little polymer was on the surface for any switching to be observed, and that there was an uneven coating of the polymer on the glass slides. This could be overcome by dipping the glass slides into a solution of the polymer in toluene.

The polymers were then cast as films on glass slides via dipping the untreated glass microscope slide into a solution of the polymer in toluene. A glass vial was filled with 3mg/ml solution of FOR001 in toluene and the slide dipped in and the solvent allowed to evaporate. This process was repeated 5 times. The absorbance of the slide was measured when all the toluene had evaporated and then the slide was switched using a 150W Xenon arc lamp. The absorbance after switching was then measured (Figure 75).

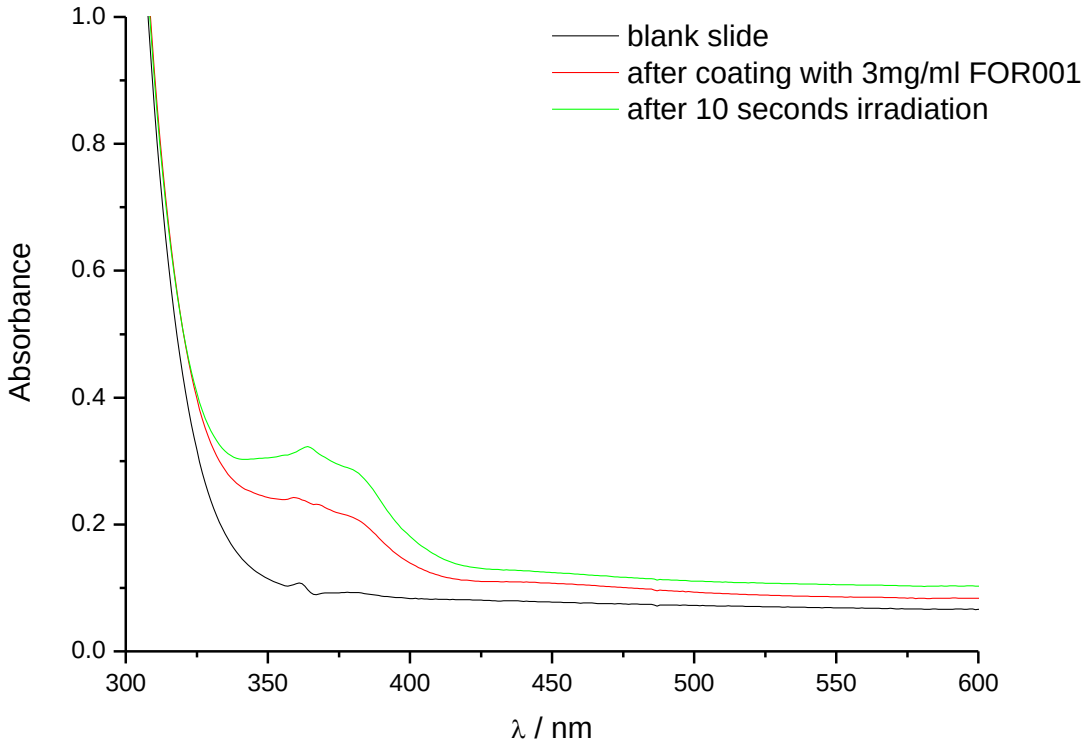

Figure 75: 3mg/ml FOR001 polymer on glass slide.

The switching can be observed from the plot above, however, the polymer did not switch back within 30 minutes, indicating that monitoring the thermal relaxation reaction of the polymer over a period of 6-8 hours may be required in order to obtain a rate constant for the relaxation of the polymer film on glass slides.

8.3 Summary of polymers investigation

The conclusions of this investigation thus far with polymers can be summarised through the consideration of several facts elucidated from this work.

The first is that the thermal relaxation in toluene solution after switching is reversible and somewhat slower than the azobenzene based molecule Admat 1 in toluene solution. This ties in with previous data reporting that the thermal relaxation rate of polymers in solution is slower than that of parent azo molecules due to steric hindrance from the polymer backbone. (200,268)

The second is that the polymers can be dissolved in solution and a thin film can be formed on a glass slide, which also exhibits photoisomerisation. This is interesting, as the motion of the polymers when fixed on a surface is usually hindered, however, these polymers are able to move and a slight absorption change is seen indicating that the isomerisation reaction has occurred.

Chapter 9: Conclusions and Further Work

9.0 Conclusions

The aims of this thesis have, for the most part been fulfilled. The development of a photoswitchable surface, the main reason for this investigation has been developed affording contact angle changes of over 40°. There have, however, been other significant findings from this work which are described below.

The solution studies of the perfluoroalkyl compounds in methanol showed significant acceleration of the thermal relaxation reaction relative to other solvents. The main reason for this was thought to be a solubility issue, as the perfluoroalkyl compound was found to precipitate out of the methanol solution. This is supported by results from studies adding water and other compounds to induce aggregation in other solvents. Some interesting findings were made in acetonitrile and in xylene which was possibly due to the amino group and perfluoroalkyl chain interacting with the solvent.

The thermal relaxation in several solvents was measured and found to be a first order process. The activation energies were measured for the thermal relaxation reaction in solution, and were found to be between 25 and 65 kJ mol^{-1} depending upon the solvent. The surface chemistry of the azo derivatives proved interesting. The photoisomerisation was measured on the surface of cellulose and the activation energy for the thermal relaxation process was measured. The activation energies were found to be smaller than those found in solution, at between 2 and 15 kJ mol^{-1}.

This large increase in the rate of thermal relaxation is due to the presence of hydrogen bonding on the surface, which can be compared to methanol solution, where there is hydrogen bonding present and where aggregates have been observed which increase the rate of the thermal relaxation reaction.

The surface chemistry of the compounds on silica was also investigated, similar results to cellulose were found, except that the activation energies were found to be larger on silica than on cellulose. The possibility of the APTS linker group influencing the hydrogen bonding and

the chains interlocking on the surface of the silica cannot be ruled out and this is an interesting comparison with cellulose, as with silica the linker group appears to exert influence on the thermal isomerisation process on the surface.

The desire to measure contact angles on a flat surface lead to the development of chitosan-coated slides functionalised with fluoroalkyl derived azobenzene compounds. The attachment of the fluoroalkyl azobenzenes resulted in the production of a hydrophobic surface, with contact angles of around 120° on the chitosan slides compared to the unfunctionalised chitosan coated slide contact angle of 57°.

The ability of the azo molecules on the surface to photoisomerise was noted and the change in contact angle was investigated. The overall change in contact angle on the higher concentration slides, was measured to be around 15° overall. This was less than expected and the thought that the higher concentrations caused aggregation lead to the development of slides of lower concentration, at 1 $x10^{-9}$ and 1 $x10^{-10}$ mol per cm^2. The initial contact angle on the less concentrated slides was higher than on the higher concentration slides and the change in contact angle upon irradiation was much higher, at between 40-50°. This was in effect proof that the theory of aggregation on the surfaces was concordant with data obtained here.

The investigation of the polymers yielded interesting results. The thermal relaxation rate in solutions of the polymers was found to be slower in solution than the free azobenzene molecules themselves. This is due to the hindrance of long polymer chain in the thermal relaxation reaction which is expected here. However, the photoisomerisation of the surface of glass slides appeared to occur quickly, which is in common with other surface data collected here.

Overall, azobenzene based molecules on several surfaces were studied here. All of the surfaces showed some degree of photoisomerisability. The rate constants, activation energies were obtained for all of the surfaces investigated and for the chitosan slides, the contact angle changes were observed. The aim to create a photoisomerisable surface with photoisomerisable wettability has been achieved, and furthermore, that contact angle data obtained showed promise.

9.1 Further Work

Overall, there are opportunities to expand each section of this work with further study. There is also the scope with the surface work to try new surfaces in order to make a comparison. Several key points require further investigation.

The interesting kinetics in methanol observed here require further investigation in order to providence credence to the theory postulated here that aggregation is responsible for the fast kinetics observed. The observation of precipitates could be backed up by absorbance spectroscopy studies, which would indicate scattering of the light from the precipitate particles, and also deviation from the Beer-Lambert Law, which would be observed.

The possibility to investigate the activation energy in a wider range of solvents must also be considered, as to be able to compare more than five solvents would give even more of an idea of the phenomenon observed in the solution work. The use of a series of polar aprotic solvents, such as dimethylformamide, (DMF) and dimethyl sulphoxide (DMSO) would provide a useful comparison to the polar protic solvents studied in this work.

The surface work warrants further investigation amongst a larger range of concentrations and comparison with other azobenzene derivatives in order to asses if the results shown here are particular to the novel fluoroalkyl compounds or to azobenzene compounds in general. There is scope here also to try a new, better characterised surface, possibly either gold, or couple compounds directly to a fabric substrate, i.e. cotton.

The cellulose data obtained needs to be compared with other cellulose derivatives in order to make a comparison of the rate constants and activation energies on a wide range of substrates based on cellulose, as all have varying pore sizes and structures. This is the main reason for the desire to conduct isomerisation studies of cotton fibres and on other textile material as cellulose was used in this work as a possible probe for studies on fabric.

The chitosan films requires further investigation by producing a range of films of varying thickness to compare with the data here, and also a variety of other concentrations, possibly

below 1 x 10^{-10} mol per cm^2 in order to ascertain if the contact angle change seen here is even greater at lower concentrations.

The studies on chitosan films themselves could be further expanded to incorporate azobenzene polymers directly into the chitosan films, by dissolving the azobenzene into the chitosan mixture via the use of an appropriate solvent and by studying the effects of the amount of the azobenzene present in the film and the thermal relaxation reaction, in order to compare with the polymer work conducted in this section. The possibility of obtaining activation energies for the thermal relaxation reaction on the surface of the chitosan film is another interesting avenue for research. This would then allow for the comparison of the cellulose and silica activation energies with that of those on the surface of chitosan.

The polymers study conducted as part of this work was brief, but the study of the polymer on films showed promise. The production of a variety of concentrations of polymer films and the investigation of their switching would also be a useful addition to this work. The measurement of activation energies in the polymer form would be useful information to obtain, as this would provide a comparison between the surfaces studied throughout this work. The activation energies of polymers in a wide variety of solvents would be useful, as a comparison to the solution work.

Overall, there are aspects of each are of study that required further expansion, and they have been listed in this section, however, the need to utilise other substrates in addition to the substrates studied here is an area of great importance. The ability of azobenzene to photoisomerise on surfaces has been established, therefore the main focus of further study needs to include other surfaces. These surfaces could be well characterised surfaces like gold or silicon wafers, or on the other hand, the application of which these novel azobenzenes were designed for, which is the photoisomerisation on the surface of fabrics.

Chapter 10: References

(1) Gilbert and Baggot *'Introducton to photochemistry'* CRC Press, New York, July 1991.

(2) Kasha, M. *D Faraday Disc. Chem. Soc*., 1950, 9, 14.

(3) H Zolliger "*Azo and Dye Chemistry*", Wiley Interscience, New York, 1961.

(4) P.Kwolek, J. Morgan, J. Schaefgen. '*Encyclopaedia of Polymer Science and Engineering'* John Wiley, New York, 1985.

(5) G.S.Hartley, *Nature*, 1937, 140, 281.

(6) R.F.Hutton, C.Steel, *J. Am. Chem. Soc*, 1964, 86, 745

(7) G. Mohlmann, C. van der Worst, '*Side Chain and liquid crystal polymers'*, Plenum and Hall, Glasgow, 1980.

(8) S. Yitzchaik and T. Marks., *J. Acc. Chem. Res*. 1996, 29, 197.

(9) D. Levy and L. Esquivias., *Adv. Mater*., 1995, 7, 120.

(10) I. Willner and S. Rubin., *Angew. Chem., Int. Ed. Engl*., 1996, 35, 367.

(11) J. Jung, C. Takehisa, Y. Sakata, T. Kaneda., *Chem. Let.*, 1996, 2, 147.

(12,13) H. Yamamura, H. Kawai, T. Yotsuya, T. Higuchi, Y. Butsugan, S. Araki, M. Kawai, K. Fujita. *Chem. Lett*., 1996, 25, 799.

(14) X. Liu, D. Bruce, I. Manners. *Chem. Commun*., 1997, 548, 289.

(15) H. Mekelburger, K. Rissanen, F. Vögtle. *Chem. Ber*., 1993, 126, 1161.

(16) D. Junge and D. McGrath. *Chem. Commun*., 1997, 9, 857.

(17) S. Chen, J. Mastrangelo, H. Shi, T. Blanton, A. Bashir-Hashemi, *Macromolecules*, 1997, 30, 93.

(18) S. Chen, J. C. Mastrangelo, A. Bashir-Hashemi, J. Li, N. Gelber., *Macromolecules*, 1995 28, 7775.

(19) A. Singh, J. Das, N. Majumdar., *J. Am. Chem. Soc*. 1996, 118, 6185.

(20) W. Andreoni, A. Curioni, K. Holczer, K. Prassides, M. Keshavarz-K., J. Hummelen, F. Wudl., *J. Am. Chem. Soc*., 1996, 118, 113335.

(21) H.Rau in "*Photochromism, Molecules and Systems*", Elsevier, New York, 1990.

(22) DMS UV atlas, Verlag, Chemie. Wienheim, (1967) spectra 7/5 c7/17.

(23) D.Georgiou, K.A.Muzkat, E Fisher, *J. Am. Chem. Soc*., 1986, 90, 12.

(24) F.Gerson, E.Heilbronner, *Helv. Chem. Acta*., 1962, 25, 51.

(25) H.Bisle, M.Romer, H.Rau, *Ber. Bunsenges. Physik. Chem*., 1976, 80, 301.

(26) H. Rau. *Ber. Bunsenges. Physik. Chem*., 1971, 75, 1343.

(27) S. Monti, S.Dellonte, P.Bortulus, *J. Photochem*., 1983, 23, 249.

(29) G.E.Lewis, *J. Org. Chem*., 1960, 25, 2193.

(29) G.M.Badger, R.J.Drewer, G.E.Lewis, *Aust. J. Chem*., 1963, 16, 1042.

(30) H.Rau, *Ber. Bunsenges. Physik. Chem*., 1967, 71, 48.

(31) J.L.Magee, W.Shand Jr, H. Eyring, *J. Am. Chem. Soc*., 1941, 63, 677.

(32) D.Y.Curtin, E.J.Grubbs, and C.G.McCarthy, *J. Am. Chem. Soc*., 1966, 88, 2775.

(33) D.L.Ross, J.Blanc, *Photochromism*, Wiley Interscience, New York, 1971.

(34) H.Rau, E.Ludekker, *J. Am. Chem. Soc.*, 1982, 104, 1616.

(35) H.Rau, *J. Photochem*., 1984, 26, 221

(36) C. Raduge, G.Papastavrou, H. Motschmann *Eur. Pys. J*., 2003, 10, 103.

(37) Ying-Chih Lu, Eric Wei-Guang Diau, H. Rau, *J. Phys Chem.*, 2005, 109, 2090.

(38) E. W.G. Diau, *J. Phys. Chem. A.*, 2004, 108, 950.

(39) D.A.Sandford, A.Stinnes, *'Biomedical Applications of High Purity Chitosan — Physical, Chemical and Bioactive Properties'* ACS Symposium Series, **1991,** 467**,** 430**.**

(39) K.E. Uhrich, S.M. Cannizzaro, R.S. Langer and K.M. Shakesheff, *Chem. Rev.,* 1999, 99, 3181.

(40) K. Matsuda, M. Irie, *J. Photochem. Photobiol. C: Photochem. Rev*., 2004, 5, 169.

(41) A. Fujishima, T.N. Rao, D.A. Tryk, *J. Photochem. Photobiol. C: Photochem. Rev.* 2000, 1, 1.

(42) K. Ichimura, S.K. Oh, M. Nakagawa, *Science*. 2000, 288, 1624.

(43) J.A. Delaire, K. Nakatani, *Chem. Rev.*, 2000, 100, 1817.

(44) N. Tamai, H. Miyasaka, *Chem. Rev*., 2000, 100, 1875.

(45) K. Ichimura, *Chem. Rev*., 2000, 100, 1847.

(46) A. Natansohn, P. Rochon, *Chem. Rev.*, 2002, 102, 4139.

(47) V. Shibaev, A. Bobrovsky, N. Boiko, *Prog. Polym. Sci*., 28 (2003) 729.

(48) T. Ikeda, O. Tsutsumi, *Science,* 1995, 268, 1873.

(49) T. Yamase, *Chem. Rev*., 1998, 98, 307.

(50) R.J. Colton, A.M. Guzman, J.W. Rabalais, *Acc. Chem. Res*. 1978, 11, 170.

(51) T. He, J.N. Yao, *J. Photochem. Photobiol. C: Photochem. Rev*., 2003, 4, 125.

(52) O. Sato, *J. Photochem. Photobiol. C: Photochem. Rev*., 2004, 5, 203.

(53) I. Willner, S. Rubin, A. Riklin, *J. Am. Chem. Soc*., 1991, 113, 3321.

(54) P. Aussillous and D. Quéré, *Nature,* 2001, 411, 924.

(55) W. Barthlott and C. Neinhuis, *Planta,* 1997, 202, 1.

(56) L. Feng, S. Li, Y. Li, H. Li, L. Zhang, J. Zhai, Y. Song, B. Liu, L. Jiang, D. Zhu, *Adv. Mater.*, 2002, 14, 1857.

(57) Q. Xie, J. Xu, L. Feng, L. Jiang, W. Tang, X. Luo ,C. Han, *Adv. Mater.*, 2004, 16, 302.

(58) L. Jiang, Y. Zhao and J. Zhai, *Angew. Chem. Int. Ed*., 2004, 43, 4338.

(59) X. Zhang, F. Shi, X. Yu, H. Liu, Y. Fu, L. Jiang, X. Li, *J. Am. Chem. Soc.*, 2004, 126, 3064.

(60) S. Wang, L. Feng and L. Jiang, *Adv. Mater*., 2006, 18, 767.

(61) C. Feng, Y. Zhang, J. Jin, Y. Song, L. Xie, G. Qu, L. Jiang , D. Zhu, *Langmuir*, 2001, 17, 4593.

(62) D. Crevoisier, P. Fabre, J. Corpart ,L. Leibler, *Science*, 1999, 285, 1246.

(63) T.N. Krupenkin, J.A. Taylor, T.M. Schneider and S. Yang, *Langmuir*, 2004, 20, 3824.

(64) X. Yu, Z. Wang, Y. Jiang, F. Shi, X. Zhang, *Adv. Mater*., 2005, 17, 1289.

(65) S. Minko, M. Muller, M. Motornov, M. Nitschke, K. Grundke , M. Stamm, *J. Am. Chem. Soc.*, 2003, 125, 3896.

(66) D.O.H. Teare, C.G. Spanos, P. Ridley, E.J. Kinmond, V. Roucoules, J.P.S. Badyal, S.A. Brewer, S. Coulson, C. Willis, *Chem. Mater*., 2002, 14, 4566.

(67) G. Decker, *Science*, 1997, 277, 1232.

(68) X. Zhang and J.C. Shen, *Adv. Mater*., 11 (1999), 1139

(69) A. Ulman, *Chem. Rev*., 1996, 96, 1533.

(70) L.M. Siewierski, W.J. Brittain, S. Petrash, M.D. Foster, *Langmuir*, 1996, 12, 5838.

(71) N. Delorme, J. Bardeau, A. Bulou, F. Poncin-Epaillard, *Langmuir*, 2005, 21, 12278.

(72) C. Feng, Y. Zhang, J. Jin, Y. Song, L. Xie, G. Qu, L. Jiang, D. Zhu, *Langmuir*, 2001, 17, 4593.

(73) G.S.Hartley, *Nature*, 1937, 140, 281.

(74) W. Jiang, G. Wang, Y. He, X. Wang, Y. An, Y. Song, L. Jiang, *Chem. Commun.*, 2005, 28, 3550.

(75) G. Berkovic, V. Krongauz, V. Weiss, *Chem. Rev.*, 2000, 100, 1741.

(76) R. Rosario, D. Gust, A.A. Garcia, M. Hayes, J.L. Taraci, J.W. Dailey, S.T. Picraux, *J. Phys. Chem. B*., 2004, 108, 12640.

(77) A. Athanassiou, M.I. Lygeraki, D. Pisignano, K. Lakiotaki, M. Varda, E. Mele, C. Fotakis, R. Cingolani, S.H. Anastasiadis, *Langmuir, 2006*, 22, 2329.

(78) E. Mele, D. Pisignano, M. Varda, M. Farsari, G. Filippidis, C. Fotakis, A. Athanassiou, R. Cingolani, *Appl. Phys. Lett*., 2006, 88, 2329.

(79) A. Nayak, H. Liu, G. Belfort, *Angew. Chem. Int. Ed*., 2006, 45, 4094.

(80) I. Vlassiouk, C.D. Park, S.A. Vail, D. Gust, S. Smirnov, *Nano Lett*., 2006, 6, 1013.

(81) S. Abbott, J. Ralston, G. Reynolds, R. Hayes, *Langmuir*, 1999, 15, 8923.

(82) N. Lake, J. Ralston, G. Reynolds, *Langmuir*, 2005, 21, 11922.

(83) K. Uchida, N. Izumi, S. Sukata, Y. Kojima, S. Nakamura, M. Irie, *Angew. Chem. Int. Ed*., 2006, 45, 6470.

(84) T. Kawai, T. Kunitake, M. Irie, *Chem. Lett*., 1999, 9, 905.

(85) K. Matsuda, M. Irie, *J. Am. Chem. Soc*., 2000, 122, 7195.

(86) T. Yamamoto, Y. Umemura, O. Sato, Y. Einaga, *J. Am. Chem. Soc*., 2005, 127, 16065.

(87) R. Mikami, M. Taguchi, K. Yamada, K. Suzuki, O. Sato, Y. Einaga, *Angew. Chem. Int. Ed*., 2004, 43, 6135.

(88,111,112) R. P. Feynman, *Eng. Sci.*, 1960, 23, 22.

(89) J.-M. Lehn, *Angew. Chem. Int. Ed. Engl.*, 1988, 27, 89.

(90) N. Koumura,R. W. J. Zijlstra, R. A. van Delden, N. Harada and B. L. Feringa, *Nature,* 1999, 401, 152.

(91) S. Shinkai, *Pure & App. Chem.*, 1987, 59, 425.

(92) A. Satake, M. Yamamura, M. Oda and Y. Kobuke *J. Am. Chem. Soc.*, 2008, 130, 6314.

(93)T.Minami, K. Yoneda, R. Kishi, H. Takahashi M. Nakano, *J. Phys. Chem C.*, 2010, 114l 6067.

(94) N. Nagata, Y. Kuramochi Y. Kobuke, *J. Am. Chem. Soc.*, 2009, 131, 10.

(95) A. J. Helsel, A. L. Brown, K. Yamato, W. Feng, L. Yuan, A. J. Clements, S. V. Harding, G. Szabo, Z. Shao B. Gong, *J. Am. Chem Soc*., 2008, 130**,** 1578.

(96) F. Hamada, M. Fukushima,T. Osa, H. Ikeda, F. Toda, A. Ueno, *J. Am Chem Soc.*, 1978, 101, 2780.

(97) Y. Inoue, M. Miyauchi, H. Nakajima, Y. Takashima, H. Yamaguchi, and A. Harada, *Macromolecules*, 2007, 40. 3256.

(98) A. A. Mart and J. L. Coln, *Inorganic Chemistry*, 2010, 49, 7298.

(99) J. Park, J. Yi, T. Tachikawa, T. Majima W. Choi, *J. Phys. Chem. Lett.*, 2010, 1, 1351.

(100) D. Zhang, Z. Wu, J. Xu, J. Liang, J. Li W. Yang, *Langmuir*, 2010 , 26, 6657-6662

(101) D. Ma, A. J. Kell, S. Tan, Z. J. Jakubek, B.Simard, *J. Phys. Chem. C.*, 2009, 113, 15974.

(102) M. Liu, X. Yan, M. Hu, X. Chen, M. Zhang, B. Zheng, X. Hu, S. Shao F. Huang *Org. Lett.*, 2010, 12, 2558.

(103) W. Zhou, H. Zheng, Y. Li, H. Liu, Y. Li, *Organic Letters*., 2010, 18, 4078.

(104) Y. Wang, F. Bie H. Jiang, *Organic Letters.*, 2010, 16, 3630.

(105) J.D. Badjic, V. Balzani, A. Credi, S. Silvi, J. F. Stoddart, *Science*, 204, 303, 1845.

(106) V. Balzani, A. Credi, M. Venturi, *Chem. Phys. Chem.*, 2008, 9, 202.

(107) V. Balzani, *Pure Appl. Chem*., 2008, 80, 1631.

(108) V. Balzani, A. Credi, M. Venturi *Chem. Sus .Chem*., 2008, 1, 26.

(109) A. Archut, G. C. Azzellini, V. Balzani, L. De Cola, F. Vögtle, *J. Am. Chem. Soc*., 1998, 120, 12187.

(110) V. Balzani, A. Credi, F.M. Raymo, J.F. Stoddart, *Angew. Chem. Int. Ed*., 2000, 39 3348.

(111,112) see ref 88. R. P. Feynman, *Eng. Sci.*, 1960, 23, 22.

(113) Y. Nishiyama, P. Langan, H.Chanzy, *J. Am. Chem. Soc.*, 2002, 124, 9074.

(114,115,116,) D. Klemm, B. Phillip, T. Heinze, U. Heinze, W. Wagenknecht, '*Comprehensive Cellulose Chemistry, Fundamentals and Analytical Methods'* Wiley Science, New York, 1993.

(117) S. Deguchi, K. Tsujii and K. Horikoshi, *Chem. Commun*., 2006, 10, 3293.

(118,119,120) D. Klemm, B. Phillip, T. Heinze, U. Heinze, W. Wagenknecht, '*Comprehensive Cellulose Chemistry, Fundamentals and Analytical Methods'* Wiley Science, New York, 1993.

(121) L.F.V. Ferriera, A.S.Oliveira, F.Wilkinson, D.R.Worrall., *J. Chem. Soc, Faraday Trans*., 1996, 92, 1225.

(122) L.F.V. Ferriera, A.S.Oliveira, F.Wilkinson, D.R.Worrall *J. Chem. Soc. Faraday Trans*. 1996, 92, 4814.

(123,124) F Wilkinson, PA Leicester, LFV Ferreira, V Freire, *J. Photochem. Photobiol.*, 1991 54, 599.

(125) M. G. Lagorio, L. E. Dicelio, M. I. Litter and E. San Román, *J. Chem. Soc., Faraday Trans*., 1998, 94, 419.

(126) G.Irick, J. Pacifi, *Textile Res. J.*, 1971, 41, 255.

(127) S.Sidikov, O.N.Bozov, R.S.Safutdinov, G.R.Rakhmanberdiev, T.M.Mirkamilov, *Chem. Nat. Comp.*, 2000, 36, 6.

(128) D. R. Lide, *'Handbook of Chemistry and Physics'*, CRC Press, Boca Raton, USA, 2000.

(129) D.N.S.Hon, *J. Polymer Sci. Polymer. Chem. Edt.*, 1979, 17, 441.

(130) I.A.Shkrob, M.C.Depew, J.K.S.Wan, *Chem. Phys. Lett*., 1993, 202, 133.

(131,132)K.J.Sribiladzey I.Roznak, A.Vig, G.E.Krichevsky, O.M.Anysimova, V.M.Anysimova, *Dye. Pigments*, 1992, 19, 235.

(133) I.B.Ranby, J.F.Rabek, *'Photodegradation, photoxidation and photostabilisation of polymers*' Wiley Interscience, 1975.

(134) A.H.M.Renfrew, M.Clarkson, *Coloration Technology* , 2008, 115, 280.

(135) Mansoor Iqbal, "*Dyes and Pigments*" Rahber Publishers, Karachi, 2008

(136) L.C.T Shoute, R.E, Huie, *J. Phys Chem A.*, 1997, 101, 3467.

(137) O. Meth-Cohn, M.J.Smith, J. *Chem. Soc. Perkin Trans*., 1994, 1, 5.

(138) H. Gorner, H.Gruen, D. Schulte-Frohilnde, *J. Phys Chem.*, 1980, 84, 3031.

(139) B.S.Solomon, T.F. Thomas, C. Steele, *J. Am. Chem. Soc.*, 1968 90 2249.

(140) J.Griffiths, *J. Dye. Colourists.*, 1972, 88, 106.

(141) P. Jaques, *Dye. Pigments.*, 1984, 5, 351.

(142) G. Gabor, E.Fischer, *J. Phys. Chem*., 1962, 66, 2478.

(143) G.Gabor, Y.F. Frei, *J. Phys. Chem.*, 1968, 72, 9.

(144) M. Sahu, S. Bikhash, S. Chandra Bera, *J. Photochem. Photobiol. Sci. A.*, 1995, 89, 19.

(145) H.CA. Van Beek, P.M.Heertjes, *J. Phys. Chem.*, 1966, 70, 1704.

(146) K.J.Sirbiladze A.Vig, V.M.Anysimov, O.M.Anysimova, G.E Krichevskiy Ruznak I, *Dye. Pigments.*, 1990, 14, 23.

(147) C.H.Giles, R.B. McKay, *J. Text. Res.*, 1963, 33, 527.

(148) F.Okada, F. Kukuko, Z Morita, *Dye. Pigments.*, 1997, 35, 311.

(149) Y Honma, N Choji, M Karasawa, *J. Text. Res.*, 1990, 63, 433.

(150) N.S.Allen, J.P. Binkley, B.J.Parsons, G.O Philips, N.H Tennant, *J. Polymer. Photochem.*, 1984, 5, 411.

(151) K Bredereck, C Schumacher, *Dye. Pigments.*, 1993, 23, 135.

(152) M. Kamel S. Sharif, F.I.Abdel-Hey, *J. Prak. Chemichte.*, 1973, 315, 236.

(153) E.Kissa, *J. Text. Res*., 1971, 41, 715.

(154) C.H.Giles S.M.K Rahman, *J. Text. Res*., 1961, 31, 1012.

(155) G.S.Egerton A.G.Roach, *J. Dye. Colour.*, 1971, 1, 268.

(156) K. Yamada H. Shoshenji Y.Nakano M.Uemura, S.Uto, M.Fukushima, *Dye. Pigments.*, 1981, 2, 21.

(157) N.R.Ayyangar, K.V.Srinivasa, *Colour.*, 1989, 36, 47.

(158) P.Ball, C.H.Nicholls, *Dye. Pigments.*, 1984,5,437.

(159) L.M.G. Jansen, I.P Wilkes, F.Wilkinson, D.R.Worrall, *J. Photochem. Photobiol. A.*, 1999, 125, 99.

(160) N.S.Allen, J.P.Binkley, B.J.Parsons, G.O.Philips, N.H.Tennant, *Dye. Pigments.*, 1984, 5, 209.

(161) N. G. Liu, Z. Chen, D.R. Dunphy, Y.-B. Jiang, R.A. Assink, and C.J. Brinker, *Angew. Chem. Int. Ed*., 2003, 42, 1731.

(162) N. Delorme, J.-F. Bardeau, A. Bulou, F. Poncin-Epillarde, *Langmuir*, 2005, 21, 12278.

(163) K. Maeda, T. Nishiyama, T. Yamazaki, T. Suzuki, T. Seki, *Chem. Lett*., 2006, 35, 736.

(164)Y. Wen, W. Yi, L. Meng, M. Feng, G. Jiang, W. Yuan, Y. Zhang, H. Gao, L. Jiang, Y. Song *J. Phys. Chem. B.,* 2005, 109, 14465..

(165) I. Vlassiouk, C.D. Park, S.A. Vail, D. Gust, S. Smirnov, *Nano Lett.* 2006, 6, 1013.

(166) S. Abbott, J. Ralston, G. Reynolds, R. Hayes, *Langmuir*, 1999, 15, 8923.

(167) N. Lake, J. Ralston, G. Reynolds, *Langmuir* 2005, 21, 11922.

(168) H. Sasaki, M. Shouji, *Chem. Lett*., 1998, 27, 293.

(169) R.A.A. Muzzarelli, '*Natural Chelating Polymers'*, Pergamon Press, New York, 1973.

(170) W.A. Mass, A. Mass and B. Tighe, *Polym. Int.*, 1998, 47, 89.

(171) L. Illum, *Pharm. Res.*, 1998, 15, 1326.

(172) J.Z. Knaul and K.A.M. Creber, *J. Applied. Polym. Sci.*, 1997, 66, 117.

(173) K. Kurita, H. Yoshino, K. Yokota, M. Ando, S. Inoue, S. Ishii and S. Nishimura, *Macromolecules*, 1992, 25, 3786.

(174) K.R. Holme and L.D. Hall, *Macromolecules*, 1991, 24, 3828.

(175) A.C.M. Wu, *Methods. Enzymol*., 1998, 161, 447.

(176) V.F. Lee, '*Solution and shear properties of chitin and chitosan'* Ph.D. Dissertation, University of Washington, 1974, 446.

(177) D. Rathke and S.M. Hodson, *Rev. Macromol. Chem*., 1994, 34, 375.

(178) R.A.A. Muzzarelli, *Cell Mol. Life Sci*., 1997, 53, 131.

(179) H.F. Mark, N.M. Bikales, C.G. Overberger and G. Menges, '*Encyclopedia of Polymer Science and Engineering'* Wiley, New York, 1985.

(180) M.N.V.R.Kumar, *Reactive. Function. Polymers.* 2000, 46, 1.

(181) A. Sionkowska, H. Kaczmarek, M. Wisniewski, J. Skopinska, S. Lazare and V. Tokarev, *Surface Sci., 2006,* 600, 3775.

(182) S. Kumar, N. Nigam, T. Ghosh, P. K. Dutta' , S.P. Singh, P. K. Datta, L. An, T. F. Shi. *Materials Chem. Phys.* 2010, 120, 361.

(183) C.H.Chen, F.Y. Wang, C.F. Mao, C.H. Yang., *J.Applied. Poly. Sci.*, 2007, 105, 1086.

(184) C. L. Feng, J. Jin, Y. J. Zhang, Y. L. Song, L. Y. Xie, G. R. Qu, D. B. Zhu, L. Jiang, *Langmuir*, 2001, 17, 4593.

(185) C. L. Feng, J. Jin, Y. J. Zhang, Y. L. Song, L. Y. Xie, G. R. Qu, Y. Xu, L. Jiang, *Surf. Interface Anal*., 2001, 32, 121.

(186) G. Muller, M. Harke, H. Mostchamann, *Langmuir*, 1998, 14, 4955.

(187) S. Oh, O. Nakagawa, K. Ichimura, *J. Mater. Chem*., 2001, 11, 1563.

(188) B. Stiller, E. Markava, D. Gustina, I. Muzikante, L. Brehmer. *Adv. Mater. Opt. Electron*., 1999, 9, 245.

(189) B. Stiller, G. Knochenhauer, E. Markava, D. Gustina, I. Muzikante, P. Karageogiev, L. Brehmer., *Mater. Sci. Eng. C 1999*, 8, 385.

(190) K. Ichimura, S. Oh, M. Nakagawa. *Science*, 2000, 288, 1624.

(191) T. Seki, R. Fukuda, M. Yokoi, T. Tamaki, K. Ichimura. *Bull. Chem. Soc. Jpn.* 1996, 69, 2375.

(192) H.S. Lim, J.T. Han, D. Kwak, M. Jin, K. Cho, *J. Am. Chem. Soc*., 2006, 128, 14458.

(193) W. Zhu, X. Feng, L. Feng, L. Jiang, *Chem. Commun*. 2753 (2007)

(194) X. Feng, L. Feng, M. Jin, J. Zhai, L. Jiang, D. Zhu, *J. Am. Chem. Soc*., 2004, 126, 62.

(195) C. Takei, M. Nonogi, A. Hibara, T. Kitamori, H.B. Kim, *Lab on a Chip*, 2007, 7, 596.

(196) E. Balaur, J.M. Macak, L. Taveira, P. Schmuki, *Electrochem.Commun*., 2005, 7, 1066.

(197) Y. Coffinier, S. Janel, A. Addad, R. Blossey, L. Gengembre, E. Payen, R. Boukherroub, *Langmuir*, 2007, 23, 1608.

(198) T. Sato, T.Tsugaru, J. Yamauchi, T.Okaya, *Polymer.*, 1992, 33, 5066.

(199) S.Hagen, P.Kate, M.V.Peters, S.Hecht, M.Wolf, P.Tegeder, *Appl. Phys. A*, 2008, 93, 253.

(200) G. Smets, *Adv. Polym. Sci*., 1983, 50, 17.

(201) J.L .Williams, R.C.Daly, *Prog. Polym. Sci.*, 1977, 5, 61.

(202) L.Lamarre, C.S.P.Sung, *Macromoleules*, 1983, 16, 1729.

(203) Y. Norikane, K. Kitamoto, N. Tamaoki, *J. Org. Chem*., 2003, 68, 8291.

(204) H. Rau, D. Roettger, *Mol. Cryst. Liq. Cryst. Sci. Tech. A.*, 1994, 246, 143

(205) S.A. Nagamani, Y. Norikane, N. Tamaoki, *J. Org. Chem*., 2005, 70, 9304.

(206) B.K. Kerzhner, V.I. Kofanov, T.L. Vrubel, *Zhurnal Obshchei Khimii*., 1983, 53, 2303.

(207) W.J. Priest, M.M. Sifain, *J. Polym. Sci. Part A: Polymer. Chem*. 1971, 9, 3161.

(208) C.S. Paik, H. Morawetz, *Macromolecules* 1972, 5, 171.

(209,210) J.J DeLang, J.M. Robertson, I Woodward,. *Proc. R. Soc. London, Sect. A.,* 1939, 171, 398.

(211) P.J Flory, *J. Am. Chem. Soc*.**,** 1939, 61, 3334.

(212) G. Smets, *Adv. Polym. Sci*., 1983, 50, 17.

(213) J.L.R Williams, R.C. Daly, *Prog. Polym. Sci*., 1977, 5, 61

(214) W.Kuhn, *Kolloid.*, 1934, 68, 2.

(215) G. Zimmerman. L.Y.Chow, U.I. Paik, *J. Am. Chem. Soc., 1958,* 80, 3528.

(216) S.Malkin, E. Fischer, *J. Phys. Chem*., 1962, 66, 2482.

(217) D.Tabak, H. Morawetz, *Macromolecules,* 1970, 3, 403.

(218) D.T.L.Chen, H. Morawetz, *Macromolecules,* 1976, 9, 463.

(219) G.S.Kumar, P. Depra, D.C. Neckers, *Macromolecules,* 1984, 17, 1912.

(220) G.S.Kumar, P. Depra, K. Zhang, D.C. Neckers, *Macromolecules,* 1984, 17, 2463.

(221) L.Lamarre, C.S.P Sung, *Macromolecules*, 1983, 16, 1729.

(222) M.Irie, W. Schnabel, *Macromolecules,* 1985, 18, 394.

(223) H.J.Kamogawa. *J. Polym. Sci. Polym. Chem. Ed*., 1969, 7, 725.

(224) H. Kamogawa,M. Kato, M.J Sugiyama, *J. Polym. Sci. Part A.*, 1968, 6, 2967.

(225) H.Kamogawa,. *J. Polym. Sci*., 1971, 9, 335.

(226) H.Kamogawa, H Hasegawa,. *J. Applied. Polym. Sci*., 1973, 17, 745.

(227) W.J.Priest, M. M. Sifain, *J. Polym. Sci., Polym. Chem. Ed.*, 1971, 9, 316.

(228) C.D.Eisenbach, *Makromol. Chem*., 1978, 179, 2489.

(229) C.D.Eisenbach, *Makromol. Chem*., 1979, 180, 565.

(230) C.D.Eisenbach. *Makromol. Chem., Rapid Commun*. 1980, 1, 287.

(231) W Gronski, D. Emis, A.M.M Bruderlin, M.M. Jacobi, K Stadler, C.D.Eisenbach, *Br. Polym. J*., 1985, 17, 103.

(232) G. Kumar, C. Savariar, M. Saffran, D.C. Neckers., *Macromolecules*, 1985, 18, 1525.

(233) R Stadler, M. Webe, *Polymer.*, 1986, 27, 1254.

(234) W Gronski, .R Stadler, M.M. Jacobi, *Macromolecules*, 1984, 17, 741.

(235) G., Erlanger, B. F., *NATO AS1 Series, Section A*, 1982, 68, 291.

(236) R.C Bertelson, '*Photochromism. (Techniques in Chemistry),'* Wiley Interscience, New York, 1971.

(237) M.Irie, A. Menju, K. Hayashi, *Macromolecules*, 1979, 12, 1176.

(238) H.S.Blair, H.I Pogue, E. Riordan, *Polymer.*, 1980, 21, 1195.

(239) F. Agolini, F.P. Gay, *Macromolecules*, 1970, 3, 349.

(240) C.D. Eisenbach, *Polymer.*, 1980, 21, 1175.

(241) H. Blair, H.I Pogue, E. Riordan, *Polymer.*, 1980, 21, 1195.

(242) M. Irie, H. Tanaka, *Macromolecules*, 1983, 16, 210.

(243) D. Kumvatchakun. M. Irie. *Makromol. Chem, Rapid Commun*., 1988, 9, 243.

(244) V.D. Ermakova, VD. Arsenov M.I.Cherkashin, P.P.Kisilitsa, *Russ Chem Rev. (Engl. Trans.),* 1977, 46. 145.

(245) S.Shinkai, T. Nakaji, T. Ogawa, M. Shimomura, M.Mauabe,. *J. Am. Chem. Soc.,* 1981 103, 111.

(246) S.Shinkai, T. Ogawa, T; Kusano, O. Hauabe, K. Kikukawa, T. Goto, T. Matsuda, *J. Am. Chem. Soc.,* 1982, 104, 1960.

(247) S.Shinkai, T. Nakaji, Y. Nishida, T. Ogawa, O. Hauabe, ***J. Am. Chem. Soc.,*** 1980, 102, 5860.

(248) K. Isihara N. Hawada, S.Kato, I. Shinohara, *J. Polymer. Sci.,* 1982, 27, 1897.

(249) M.Irie, R. Iga,. *Makromol. Chem., Rapid. Commun.,* 1987, 8, 569.

(250) Personal communication from Colin Willis at DSTL

(251) P.Kubelka, F. Munk, *Zeit. Für Tekn. Physik*., 1931, 12, 593.

(252) C.H.Chen, F.Y. Wang, C.F. Mao, C.H. Yang., *J. App. Poly. Sci*., 2007, 105, 1086.

(253) A.W. Adamson and A.P. Gast, '*Physical Chemistry of Surfaces',* John Wiley, New York, 1997.

(254) E.Vogler, *Adv. Colloid Interface Sci*., 1998, 74, 69.

(255) L. Feng, Y. Song, J. Zhai, B. Liu, J. Xu, L. Jiang and D. Zhu, *Angew. Chem. Int. Ed*., 2003, 42, 800.

(256) X. Feng, J. Zhai, L. Jiang, *Angew. Chem. Int. Ed*., 2005, 44, 5115.

(257) R.N. Wenzel, *Ind. Eng. Chem*., 1936, 28, 988.

(258) A.B.D. Cassie, S. Baxter, *J. Chem. Soc., Faraday Trans*., 1944, 40, 546.

(259) Personal communication from Cheryl Fish at DSTL

(260) B. S. Furniss, A. J. Hannaford, P. E. G. Smith, A. R. Tatchell *'Vogel's Textbook of Practical Inorganic Chemistry'*, Pearson Education Ltd, 1989.

(261) B.Serra S.Terentjev, *Macromolecules,* 2008, 41, 3.

(262) E. V. Brown, G. R. Granneman, *J. Am. Chem. Soc.*, 1975, 97, 621.

(263) M.J.Kamlet, J.LAbboud, R.W.Taft, *J. Am. Chem. Soc*., 1977, 99, 18.

(264) T. Asano, T. Okada, *J. Org. Chem*., 1984, 49, 487.

(265) Y. Li, Y. Deng, X.Tong, X. Wang, *Macromoleucles*, 2006, 39, 1108.

(266) L.L Norman, C.J.Barret, *J. Phys. Chem B,* 2002, *106,* 8499.

(267) L F. Vieira Ferreira, M. Rosário Freixo, A.R. Garcia, F. Wilkinson, *J. Chem. Soc., Faraday Trans.*, 1992, 88, 15.

(268) I. Shimizu, A. Yoshino, H. Okabayashi, E. Nishio, C. J. O'Connor, *J. Chem. Soc., Faraday Trans*., 1997, 93, 1971.

Professional Development hours and conferences attended.

DSTL meetings (sponsors) 2 days
Demonstrating 3 days
Safety Lecture 1 day
MC8 (London) 5 days
Power Point: An Introduction ½ day
Postgraduate Research Students Induction 1 day
Excel – Part A ½ day
Excel- Part B ½ day
Teaching Skills for postgraduates and research assistants with supervising practical activities ½ day
Keeping your research up to date for postgraduates ½ day
Working effectively with outside organisations for PGR's and RA's ½ day
Plagiarism, Citation and managing your references ½ day
Personal organisation and time management for PGR'S ½ day
Respecting Diversity ½ day
Conference Presentation skills Part A ½ day
Conference Presentation skills Part B ½ day
What is a literature review? ½ day
Photocatalysis conference at Loughborough University 1 day
Young Photochemistry Researchers Conference, Loughborough University 1 day
IUPAC Conference on Photochemistry, Gothenburg, Sweden 28th July to 1st August 5 days
Advanced Refworks ½ day
Fire Extinguisher Course ½ day
Getting articles published for post graduate students ½ day
SOMS workshop (Self organisation in molecular systems), January 6th 2008 2 days
Creating posters for conferences ½ day
Gratzel Cell workshops ½ day
Report Writing ½ day
Proofreading for postgraduate students ½ day
Total: 30 ½ days